Hyperspectral Data Analysis of Typical Surface Covers in Hong Kong

MA Fung-yan

A Thesis Submitted in Partial Fulfilment

of the Requirements for the Degree of

Master of Philosophy

in

Geography

June 1999

ABSTRACT

"Hyperspectral Data Analysis of Typical Surface Covers in Hong Kong"

Submitted by MA Fung-yan
for the degree of Master of Philosophy
at the Chinese University of Hong Kong in June, 1999

Subtropical environment is characterized by a great diversity of flora that is increasingly vulnerable to human impact. It is hoped that hyperspectral data which have been extensively studied for environmental monitoring in other areas will insert new insight to this environment.

In this study, a high resolution spectrometer was available for taking hyperspectral reflectances of a selected number of surface covers. Spectra of 25 tree species were measured in the laboratory for four seasons. 138 bands of the original spectra from 400 nm to 900 nm together with their first and second derivatives were used for tree species recognition. *In situ* spectral reflectance were also taken for ten surface covers including several tree species, grass, fern, water and concrete. A hyperspectral database was then set up.

Identification of the 25 tree species using linear discriminant analysis and artificial neural network yielded satisfactory results with overall accuracy of more than 70% using original spectra. Both classifiers generated similar results using the original spectra. For the first and the second derivatives data, neural network yielded better results than linear discriminant analysis which generated very poor results with overall accuracy under 26%. However, linear discriminant analysis was still recommended for classification of hyperspectral data as neural networks were

inefficiently slow and difficult to use.

Results also showed that the use of derivatives spectra could not improve tree species recognition in this study. Using the original spectra produced better classification results compared with using either the first or the second derivatives spectra. Meanwhile, using the first derivatives spectra performed better than using the second derivatives spectra. Seasonal comparison of 21 tree species indicated that seasonal variability affected the results of tree species recognition significantly. Autumn and winter data outperformed those in spring and summer.

Principal components analysis was applied to both the *in situ* data and the laboratory data. It was shown that hyperspectral data possess extra information which traditional broadband multispectral data do not have. PC3 and PC4 contained useful information for understanding and interpretation of hyperspectral data.

Results of band selection indicated the redundant nature of hyperspectral data. Appropriate band selection was essential for tree species recognition and improved the classification results significantly. It was found that the spectral bands along the edges including two edges before and after the green peak as well as the red edge which were neglected in traditional broadband multispectral sensors tended to contain useful information for tree species recognition.

摘要

香港典型地表物之高光譜數據分析

本研究利用一高分辨率光譜儀收集香港典型地表物之高光譜反射波譜數據，並建立一高光譜數據庫。數據收集分兩部份：一部份於實驗室內量度四季中二十五種樹木品種的光譜，以進行樹木判別；另一部份於野外收集十個典型地表物的光譜，包括五個樹木品種、草地、蕨類、水體及石屎地。

樹木判別利用在 400 nm 至 900 nm 光譜範圍內 138 波段的反射光譜、一階導數光譜及二階導數光譜，以線性判別分析和神經網絡系統進行分類，兩者均能利用反射光譜獲得總體精度超過 70%的滿意結果，而對於導數光譜，神經網絡系統就比線性判別分析優勝，但因爲神經網絡系統分析時間長及操作困難，線性判別分析仍是較爲適合作高光譜數據分析的分類研究。

研究結果發現反射光譜對於樹木判別較一階導數光譜爲佳，而一階導數光譜又較二階導數光譜爲佳。季節性因素也對識別結果有一定影響，在香港，秋冬兩季的數據，比春夏的數據較能獲得更好分類結果。

主成份分析的結果顯示，高光譜數據的第三成份及第四成份擁有一些傳統寬頻多光譜儀器未能得到的訊息。而波段選擇的結果發現高光譜數據包含很多剩餘訊息，適當的波段選擇可改良判別樹木的準確度，並發現於綠光峰值前後的波段及紅光邊沿之波段對樹木判別均有裨益。

ACKNOWLEDGEMENTS

I would like to express my sincere gratitude to my supervisor, Dr. Fung Tung, for his patient and painstaking guidance, support and help during the research.

Special thanks should also be given to Dr. Siu Wai-lok, for his enthusiastic participation in the whole research from the experimental design to the discussions on data analysis; Mr. Cheung Chun-man, for his assistance in data collection and data analysis; and Dr. Gong Peng and Mr. Pu Ruliang, for their help on solving the technical problems of instrumentation and advice on the implementation of the neural network program.

I would also like to thank my fellow colleagues, Miss Pauline Poon Mei-yan and Miss Chan Fong, and all the staffs in the Geography Department, for their help and support.

Lastly, I would like to acknowledge all the staffs who were responsible for the interesting and inspiring general education course "Earth as seen from space" in my final year undergraduate study. This course brought me into a new era of knowledge and gave me this invaluable opportunity to pursue further studies in a completely new field that I had never thought of.

TABLE OF CONTENTS

LIST OF TABLES

LIST OF FIGURES

CHAPTER ONE

INTRODUCTION

1.1. Introduction and background

In the past decade, hyperspectral data analysis has generated wide interest in the remote sensing community. From *in situ* measurement with imaging spectrometers to airborne hyperspectral imaging, studies have been undertaken covering a wide range of applications such as forest monitoring (Blackburn and Milton, 1997), vegetation biochemistry (Curran, 1989; Wessman *et al.*, 1989; Yoder *et al.*, 1995 and Zagolski *et al.*, 1996) and classification of soil spectra (Palacios-Orueta and Ustin, 1996). However, few hyperspectral studies have been done in the tropical and subtropical areas. Indeed, these areas comprise of a great variety of flora and fauna that cannot be found in other areas. Increasing population pressure and human activities have put tremendous pressure on these environments and has alerted increasing concern on the conservation and preservation of these resources. There is a great potential for using hyperspectral sensors in environmental monitoring and protection in the tropical and subtropical areas.

For the conservation and preservation of forest resources, it is essential to have effective forest management which depends greatly on correct recognition of tree species. Conventionally, reliable recognition of tree species is made by costly and labor intensive field surveys and interpretation of large-scale aerial photographs. Broadband multispectral images can successfully distinguish between broad-leaf and conifer trees (Nelson *et al.*, 1985 and Shen *et al.*, 1985). Other studies using broadband data can classify more detailed forest types (Frank, 1988; Skidmore,

1989; Franklin, 1994; Foody, 1994 and Schriever and Congalton, 1995). However, identification of individual tree species remains unresolved due to limitations of spatial and spectral resolution of the broadband multispectral sensors. If individual tree species can be successfully recognized by hyperspectral data analysis, it would have significant implications to the remote sensing community and to ecological and environmental researches. Recently, Gong *et al.* (1997) successfully identified six conifer tree species in Sierra Nevada, California using *in situ* hyperspectral data with high accuracy. It shows the potential of hyperspectral data for tree species recognition. It has significant implication to similar work in the identification of tropical and subtropical tree species. However, two difficulties exist.

First, tropical and subtropical forests are a mosaic of many different tree species and a pure stand of any one species seldom exists. In contrast, temperate and boreal forests are made up of relatively few tree species with a common occurrence of a pure stand of one species or a mix of few species. As a result, it is more difficult to thoroughly investigate the classification of individual tropical and subtropical tree species than temperate tree species with the limited spatial resolution of the currently operating airborne hyperspectral sensors or the developing spaceborne instruments. Martin *et al.* (1998) determined the forest species composition using AVIRIS data of which spatial resolution is 20 m. They can only classify the forest species into eleven categories which exhibits a general similarity in tree species composition. It indicates that spatial resolution is also an important factor for identification of individual tree species besides spectral resolution. It also shows that the nature of tropical and subtropical forest as a mixture of many different tree species may be a problem for the identification of individual tree species.

The second difficulty is a more crucial concern for tree species recognition. Tropical and subtropical forests typically contain a huge number of different tree species. It is not uncommon that more than hundreds of tree species are found in a tropical forest in a particular area. Although hyperspectral analysis has proved to recognize some individual tree species successfully in previous studies (Gong *et al.*, 1997), it is doubtful whether the spectral variations in the reflectance spectra of those hundreds or thousands of tree species can be detected and discriminated among one another by hyperspectral data. Thus, hyperspectral separability of tropical and subtropical tree species must be investigated.

Besides the ability of hyperspectral data for the identification of tree species, an understanding of the intrinsic properties of hyperspectral data in tropical and subtropical environment is also essential. Hyperspectral instruments can acquire data from hundreds to thousands of channels. However, some studies found that hyperspectral data contain a large number of redundant bands (Baret, 1995; Warner and Shank *et al.*, 1997 and Thenkabail *et al.*, 1999). For any particular applications, there should be an optimum set of wavebands, waveband centers and waveband widths required to maximize information. For vegetation, Curran (1989) found 42 bands from 400 nm to 2400 nm that are correlated with the concentration of organic compound such as cellulose, lignin and protein in leaves. Martin *et al.* (1998) selected nine AVIRIS bands which were closely correlated with field measured canopy nitrogen and lignin concentration to classify forest cover types. Thenkabail *et al.* (1999) recommended twelve bands along with their bandwidths in the visible and near-infrared spectral region as optimal number of wavebands required for

extracting agricultural crop biophysical information. The wave bands that were selected by the above three researchers are not consistent with each other. The only conclusion that can be drawn is that useful information of vegetation characteristics contains in several bands from the visible to the mid-infrared region. However, determining which wave bands are important still needs more study efforts.

1.2. Objectives

As few hyperspectral studies have been done in tropical and subtropical environments, hyperspectral data in the subtropical environment of Hong Kong are intended to study in this research. Hong Kong is located in the subtropical monsoon climate zone in South China with highly urbanized areas as well as non-agricultural mountainous areas. It has a relatively well-preserved natural environment with over 300 tree species although only 13% of the 1080 square kilometers territory is covered with woodland (Thrower, 1988). It is an excellent representative to South China areas.

This study aims at setting up a hyperspectral database of typical surface covers in Hong Kong. The database contains a selected number of surface cover types that commonly appear in an image scene if seen from satellites, with an emphasis in tree species. With the hyperspectral database, the spectral separability of subtropical tree species is studied to give insights to the problem of subtropical tree species recognition. Algorithms for tree species recognition are tested and compared in order to determine the most promising techniques for tree species recognition. The inherent hyperspectral data structure is then investigated with the help of principal components analysis and band selection to determine which spectral bands or regions

are useful for vegetation studies especially tree species recognition.

To summarize, the three objectives are

1. to measure hyperspectral reflectance of a selected number of surface covers, in particular tree species in the subtropical environment of Hong Kong and set up a hyperspectral database,
2. to examine the ability of hyperspectral data for identification of subtropical tree species and
3. to understand the inherent data structure through principal components analysis and band selection.

1.3. Significance

This research is the first hyperspectral study in Hong Kong. The hyperspectral database generated in this study can be used as a reference to the general remote sensing community and particularly to the users of hyperspectral data in Hong Kong and its surrounding areas. The results of band selection can help the design of the future generation of hyperspectral sensors to carry the optimal band set. It is hoped that the success of this pioneer research will lead to more applications of hyperspectral data in land use studies, forest management and environmental protection in Hong Kong as well as other areas particularly South China in the future.

1.4. Organization of the thesis

The thesis is divided into six chapters. Chapter One introduces the problem and background of this research. The objectives and the significance of this study are stated in this chapter. Chapter Two is the literature review. It briefly introduces what

hyperspectral remote sensing is all about and the current hyperspectral sensors available including airborne and spaceborne sensors and field spectrometers. The applications of hyperspectral remote sensing are also mentioned focusing on vegetation studies. Finally, previous studies and analytical techniques of tree species recognition, data compression and feature extraction are discussed and reviewed in detail. Then, Chapter Three goes into the details of the experimental design and methodology of this study. The study site, data collection and methods of data analysis will be described in detail in this chapter. Chapter Four presents the results and discussions for tree species recognition whereas Chapter Five covers the results and discussions for data compression and feature extraction. Finally, Chapter Six is the summary and conclusion of this study.

CHAPTER TWO

LITERATURE REVIEW

2.1. Introduction

This chapter presents a literature review for this study. The literature review is mainly divided into three parts: introduction to hyperspectral remote sensing, tree species recognition, and data compression and feature extraction. In the first part, hyperspectral remote sensing is introduced briefly explaining what hyperspectral remote sensing is. The current hyperspectral instruments available are mentioned. A brief review on the applications of hyperspectral remote sensing is presented with a focus on vegetation studies which include biochemistry of vegetation and spatial and temporal patterns of vegetation. In the second part, another application of hyperspectral remote sensing, tree species recognition is discussed in detail. The factors affecting the spectral reflectance of vegetation, the classification algorithms used for tree species recognition and a review on tree species recognition using hyperspectral data are described and discussed in this part. Finally, the analytical techniques used in data compression and band selection are reviewed in the third part.

2.2. Hyperspectral remote sensing

Hyperspectral remote sensing, or imaging spectrometry are techniques that acquire spectral data or images in many, very narrow, contiguous spectral bands throughout the ultraviolet, visible, near-infrared and mid-infrared regions of the electromagnetic spectrum (Lillesand and Kieffer, 1994). Typically, several hundreds channels of data can be collected for every pixel in the scene, thus, providing us a lot

more information than the conventional broad-band imagery such as Landsat or SPOT images. Hyperspectral imaging permits discrimination among earth surface features that have diagnostic absorption and reflectance characteristics over narrow wavelength intervals that are lost within the relatively coarse bandwidths of the various channels of a conventional multispectral scanner. Price (1994a) has analyzed the spectral properties of various materials and concluded that high spectral resolution, of the order of 10 nm, would permit unique discrimination of a wide range of surface types such as rocks, soils and vegetation. Therefore, hyperspectral imaging provides opportunities for us to improve our understanding of the Earth's surface.

2.2.1. Current imaging spectrometers available

Currently several airborne imaging spectrometers are operational and spaceborne systems are being developed and will be launched soon (Curran, 1994 and Kunkel *et al.*, 1997). The most commonly used and successful airborne imaging spectrometer is Airborne Visible/InfraRed Imaging Spectrometer (AVIRIS) developed by NASA (Green, 1994). The AVIRIS sensor acquires data in 224 contiguous spectral channels covering spectral region from 400 nm to 2500 nm of approximately 10-nm bandwidth. It became operational in 1989. Another one is Hyperspectral Digital Imagery Collection Experiment (HYDICE) which is in service since 1996. The HYDICE sensor acquires data in 210 channels from 400 nm to 2500 nm. Its spectral resolution ranges from 3 nm for the short wavelengths to 10-20 nm for the long wavelengths.

For the developing spaceborne imaging spectrometers, Moderate Resolution

Imaging Spectrometer (MODIS) developed by NASA is one of the instruments in Earth Observing System (EOS) sensor systems (Jensen, 1994). It will provide imagery in 36 bands from 0.4 μm to 15 μm. Another one is OrbView-4 which will be the first commercial satellite to acquire hyperspectral imagery (Orbital Imaging Co., 1998). It is scheduled to launch in 2000. It will provide 200-channel hyperspectral imagery from 450 nm to 2500 nm with eight-meter spatial resolution.

Despite airborne and spaceborne imaging spectrometry, field spectrometry also plays an important role in hyperspectral remote sensing. Milton *et al.* (1995) gave an outline of some field spectrometers being used and discussed thoroughly about field spectrometry. Point measurements in the field or from a low-level platform are more cost-effective and appropriate for some applications when image data are not necessary. Besides, field spectroscopy is used to characterize the reflectance of surfaces intended to be used for the in-flight calibration of airborne or spaceborne sensors.

2.2.2. Applications of hyperspectral remote sensing

A wide range of researches in hyperspectral remote sensing has been undertaken. Geological, ecological, aquatic and many other research topics have been conducted using either airborne sensors or taking measurements on ground with imaging spectrometers. High spectral resolution and rich information available allows questions that would not be answered using conventional remote sensing techniques ten years ago can now be addressed. In this review, applications of hyperspectral remote sensing will be discussed with a focus on vegetation studies: biochemistry of vegetation and spatial and temporal patterns of vegetation.

2.2.2.1. Biochemistry of vegetation

Biochemistry of vegetation has been widely investigated from leaf to canopy scales using hyperspectral data. The biochemical content of vegetation can provide us information of plant productivity, rate of litter decomposition and availability of nutrients in space and time (Curran, 1989). Hyperspectral data show promise of estimating biochemistry of vegetation globally and help us to understand ecosystem properties.

At the laboratory level, dried and powdered leaves are prepared for the reflectance spectra measurements. Correlation between chemical contents and spectral measurements is then obtained using stepwise multiple linear regression. This approach reveals the predictive relationships of the best linear combinations of wavelengths for assessing chemical concentrations. Curran (1989) gave a thorough review of foliar chemistry obtained from spectral data of vegetation at the laboratory level. Fourty-two minor absorption features were identified from the spectra of dried and ground leaves which were found to have correlation with the concentration of organic compounds such as cellulose, lignin and protein in dried leaves.

At the remote sensing level, chemical contents of vegetation covers at the canopy level are retrieved by either field or airborne hyperspectral remote sensing techniques combined with ground measurements of foliar and canopy chemical contents. Wessman *et al.* (1989) estimated forest canopy chemistry with Airborne Imaging Spectrometer (AIS) data over deciduous and coniferous forests. Ground measurements of foliar biomass and canopy nitrogen and lignin content were made. Strong correlations were found between AIS data and canopy lignin concentration in

both deciduous and coniferous forests. They also demonstrated that the canopy lignin content was strongly related to the measured annual nitrogen mineralization.

Yoder *et al.* (1995) predicted nitrogen and chlorophyll content and concentrations by field spectrometry. Reflectance spectra (R) of fresh leaves were obtained in the laboratory and canopy reflectance spectra were also measured in the field. They found that the best predictors for nitrogen and chlorophyll appeared with first-difference transformations of log (1/R) and the best predictors for nitrogen were shortwave infrared bands while that for chlorophyll were visible bands.

Zagolski *et al.* (1996) also studied forest canopy chemistry at two levels which included laboratory spectral measurements of dried ground leaves by two laboratory spectrometers and airborne measurements of forest canopy by two airborne sensors: AVIRIS and Infrared SpectroMeter (ISM). They aimed at establishing laboratory derived relationships between spectrometric information and concentrations of chemical compounds and validating these relationships with the airborne measurements. Results from these two airborne sensors were compared. They found that the laboratory derived predictive relationships were quite different depending on the laboratory spectrometers and the year of sampling. It revealed the difficulty to establish predictive relationships accurately. The application of laboratory derived predictive equations to airborne data suggested relatively strong correlation for nitrogen and cellulose but poor correlation for lignin. This result contradicted with that derived by Wessman *et al.* (1989). Better results were obtained with ISM spectra that had better signal-to-noise ratio.

2.2.2.2. Spatial and temporal patterns of vegetation

Spatial and temporal patterns of vegetation have been investigated widely using remote sensing techniques, from broadband to hyperspectral sensors. With the contiguous and high spectral resolution data, hyperspectral remote sensing has been applied to forest monitoring, vegetation mapping, change detection and seasonal variations monitoring with greater details and higher accuracy. These applications are important for ecological and environmental research. For example, Blackburn and Milton (1995) used a tower-mounted spectrometer to measure the seasonal changes in the reflectance properties of ash and beech canopies during an one-year experiment. Roberts *et al.* (1997) applied AVIRIS data to monitor the seasonal changes in atmospheric water vapor, liquid water, and green vegetated and nonphotosynthetic vegetated surface cover. Blackburn and Milton (1997) applied Compact Airborne Spectrographic Imager (CASI) data to create an accurate map of canopy gaps which were created by the death or destruction of trees within deciduous woodlands. Shaw *et al.* (1998) used field spectrometers to investigate the spectral properties of naturally regenerating Scots pine in relation to sapling cover and season.

2.3. Tree species recognition

Correct recognition of forest species is important in forest management, ecological and environmental research and biodiversity studies. In the past, tree species could only be classified by labor-intensive and time-consuming field surveys which cannot provide complete coverage of large areas. In contrast, remote sensing techniques are more effective that spectral data for large contiguous areas are provided. Remotely sensed data have long been used to recognize forest cover types

based on earlier photographic interpretation to more recently digital imaging processing. Satellite multispectral broadband sensors have been used to identify forest covers from which coniferous and deciduous tree stands can be successfully discriminated (Nelson *et al.*, 1985 and Shen *et al.*, 1985). Due to the relatively low spatial resolution of the satellite sensors, classification of a forest type refers to the classification of an area of forest which exhibits a general similarity in tree species composition and character instead of individual tree species. Other studies using broadband data to classify forest type achieved more detailed species resolution (Frank, 1988; Skidmore, 1989; Franklin, 1994; Foody, 1994 and Schriever and Congalton. 1995). For example, Frank (1988) used Landsat TM data combined with digital terrain data to classify sixteen dominant vegetation communities. Schriever and Congalton (1995) used also TM data to classify nine forest cover types. They collected the data in May (bud break), September (leaf on) and October (senescence) to explore whether different leaf phenology would improve the ability to generate forest-cover-type maps.

With the contiguous and high spectral resolution of hyperspectral sensors, classification of forest cover types should be improved with more precise identification. However, whether each tree species corresponds to a unique and diagnostic spectral reflectance signature is a fundamental problem for tree species recognition. Baret (1995) stated that the spectral signature of canopy reflectance was not strictly specific to a particular canopy. In other words, different canopies could have very similar reflectance spectra. Price (1994a) revealed that high spectral resolution data, on the order of 10 nm, offered unprecented opportunities for uniquely identifying a range of vegetation types. However, spectra from one species

might still match very closely spectra from another species, presenting the possibility of faulty identification. Thus, more research efforts should be made to identify unique tree species types. Recently, Gong *et al.* (1997) successfully used *in situ* hyperspectral data to classify six conifer tree species. It indicated the potential of hyperspectral data for tree species recognition.

Spectral reflectance of vegetation is a complex function of various factors and changes spatially and temporally. In order to understand those spectra, the factors affecting the spectral reflectance of vegetation should be first studied. Thus, the factors that affect spectral reflectance of vegetation are described in detail in this session. Then the classification methods for hyperspectral analysis of tree species recognition are discussed. Finally, previous studies in tree species recognition are reviewed.

2.3.1. Factors affecting spectral reflectance of vegetation

Factors affecting spectral reflectance of vegetation are categorized into five parts which are optical properties of leaf, canopy structure, canopy cover and background effects, illumination and viewing geometry and spatial and temporal dynamics of plants.

2.3.1.1. Optical properties of leaf

The dominant physical process at the visible wavelengths (400 to 700 nm) is the absorption by photosynthetic pigments such as chlorophyll, xanthophyll, and carotene (Wessman, 1991). These pigments have absorption maxima in the 300 to 500 nm region. Only chlorophyll absorbs in the red wavelengths. It has been shown

that changes in chlorophyll concentration produce apparent spectral shifts of the absorption edge near 700 nm.

High reflectance is characterized in the near-IR region (700 to 1300 nm). A steep rise in reflectance near 750 nm is exhibited and termed the vegetation red edge. The near infrared wavelengths are greatly influenced by the leaf internal structure and in particular the number of air spaces and their arrangement (Wessman, 1991). The mid-IR region (1300 to 2500 nm), on the other hand, is dominated by leaf water absorption (Wessman, 1991).

Beside the water absorption features in the short-wave infrared (SWIR) region, the spectra of organic compounds in this region are characterized by a mixture of harmonic overtones and combinations that are mainly caused by stretching and bending vibrations of strong molecular bonds between atoms of low weight (Wessman, 1991). Extractions of foliar constituents have been spectrally characterized by a number of researchers. Curran (1989) identified 42 absorption features in visible and near-IR wavebands that have been related to particular foliar chemical concentrations.

2.3.1.2. Canopy structure

Plant canopy reflectance is not only a simple function of the reflectance of the component leaves but also depends on the number and size of the foliage elements and their arrangement on individual plants. An important parameter accounting the factor of canopy structure is the Leaf Area Index (LAI) which is defined as the one-sided area of leaves per unit ground area (Peterson *et al.*, 1987 and Spanner *et al.*,

1990). It is a quantitative measure of the surface area available for the interception of photosynthetically active radiation and for transpiration. Thus, LAI has been referred to the most useful vegetation characteristic in ecological studies. Some preliminary researches show that there is a negative relationship between LAI and red reflectance but no relationship between LAI and near infrared reflectance (Peterson *et al.*, 1987 and Spanner *et al.*, 1990).

2.3.1.3. Canopy cover and background effects

Forest canopy cover is important in determining spectral response of forest canopies because it controls the amount of understory vegetation, soil and litter which is visible to the sensor. It was shown that canopy cover and background effects influenced LAI significantly (Spanner *et al.*, 1990 and Caetano and Pereira, 1996). The variation in canopy cover and background reflectance plays an important role in affecting the spectral variation in remotely sensed data instead of differences in species. Canopy cover varies both spatially and temporally in forest canopies and this effect, coupled with spatially, temporally and spectrally variable understory reflectance poses a significant problem on the remote estimation of forest biophysical variables.

2.3.1.4. Illumination and viewing geometry

In addition to the inherent properties of forest canopies, a set of independent parameters also affects the remotely sensed response of forest canopies (Danson, 1995). Different target illuminations and viewing conditions alter the spectral response considerably. The parameters include the solar zenith angle, the solar azimuth angle, the sensor zenith view angle and the sensor azimuth view angle.

2.3.1.5. Spatial and temporal dynamics of plants

It is a common sense that plants vary at a variety of spatial and temporal scales. Plant growth and reproductive patterns are responsive to seasonal fluctuations in climate (Hobbs, 1991). Many plant communities have distinct seasonal peaks of growth and flowering activity that can markedly affect spectral reflectance. Yearly climatic variations also account for differences in species growth and establishment patterns, leading to changes in species composition and distributions. Moreover, over long periods of time, directional vegetation changes may occur through succession.

2.3.2. Classification algorithms for hyperspectral analysis

2.3.2.1. Use of derivative spectra for tree species recognition

The derivative of a spectrum is actually its rate of change with respect to wavelength. There are several methods to generate derivative spectra. The simplest method is generating derivatives numerically by dividing the difference between successive spectral values by the wavelength interval separating them (Demetriades-Shah *et al.*, 1990). This gives an approximation of the first derivative at the midpoint between the values whose difference is used to compute the slope. Higher-order derivatives are obtained by repeating the process. If the differentiation interval is very small, then the differences between the successive values may be small in comparison to the random noise and a noisy derivative spectrum is obtained. A larger differentiating interval will reduce noise and maximize the signal but sharp spectral features may be lost. Another method involves fitting the spectra by various mathematical functions which are then differentiated (Cloutis, 1996). This method may introduce artifacts due to noise amplification. Some information may be lost during curve fitting.

The accuracy of derivative analysis can be affected by the signal to noise ratio. It is shown that some level of spectral preprocessing involving noise suppression is usually helpful prior to derivative analysis. It is also determined that lower order derivatives are less sensitive to noise and hence more useful in operational remote sensing (Cloutis, 1996). However, some information may be lost due to noise suppression.

The benefits of derivative analysis are its ability to eliminate background signals. In vegetation studies, this technique is often applied in order to suppress soil background reflectance. It is found that the spectral reflectance of most soils is an approximately linear function of wavelength. Thus, second order derivative analysis is in theory useful in eliminating the soil background (Demetriades-Shah *et al.*, 1990). Gong *et al.* (1997) used original reflectance spectra and first derivative spectra to classify six conifer tree species. They found that first derivative data produced better classification results than original reflectance spectra. The use of derivative data may help to improve tree species recognition accuracy.

2.3.2.2. Linear discriminant analysis

Linear discriminant analysis is commonly applied in classification of forest cover types (Nelson *et al.*, 1984; Frank, 1988; Franklin, 1994 and Gong *et al.*, 1997). It involves deriving a variate, the linear combination of the independent variables that will discriminate best between a priori defined groups (Hair *et al.*, 1995). Discrimination is achieved by setting the variate's weights for each variable to maximize the between-group variance relative to the within-group variance. The discriminant function, which is the linear combination for a discriminant analysis, is

derived from

$$Z = W_1X_1 + W_2X_2 + W_3X_3 + \ldots + W_nX_n$$

where Z is the discriminant score, W_i is the discriminant weight for variable i and X_i is the independent variable i. The absolute value of each discriminant weight represents the relative contribution of its associated variable to the discriminant function. In other words, independent variables with larger weights contribute more to the discriminating power of the function.

2.3.2.3. Artificial neural network

Neural networks are algorithms that caricature the way information is processed in biological networks of neurons. They are considered as a very powerful tool to discriminate between variables or to relate one set of variables to another. They are defined mainly by the type of neuron used, the way they are organized and connected (the network architecture) and the learning rule.

The most commonly used neural network is backpropagation feed-forward neural network. The network consists of one input layer, one or more hidden layers and one output layer (Openshaw *et al.*, 1997). The input nodes are fully connected to the nodes of the hidden layer(s) which in turn are fully connected to the output nodes. All signals flow from the input nodes through the hidden layers to the output nodes in one direction. The connections between neurons are weighted which represent the strength of connection through which knowledge or information is encoded. These weights determine the threshold level of the activation function of a node in the network, which in turn influences the level of activation of other nodes in the network and ultimately determines the network outputs. An iterative training

procedure determines the magnitude of the weights such that the network repeatedly tries to learn the correct output for each of the training samples. The error between the network output and the desired output is minimized in order to train the data. The procedure will modify the weights between units until the network is able to characterize the training data accurately. Once trained, the neural network may then be used to classify other data.

Though neural network methods have been widely applied in classification of remote sensing images (Paola and Schowengerdt, 1995), it is not commonly used in tree species recognition. Gong *et al.* (1997) used neural network methods to classify six conifer tree species. They found that neural networks worked superior to linear discriminant analysis.

There are several advantages of neural network methods compared with statistical methods (Openshaw *et al.*, 1997). Firstly, neural network technique is a distribution-free approach that the data are not necessary to satisfy a Gaussian normal distribution which is required by most statistical methods. Secondly, it can handle nonlinear data more efficiently. Thirdly, it can adapt to include multi-source or ancillary data more easily and to interpret texture of the data more easily. However, neural network has its own limitations. The training process is time and computational intensive. The optimal network size is difficult to determine. In addition, the network seems to be a black box that loses the interpretability of the information about the decision regions.

2.3.3. Tree species recognition using hyperspectral data

Not many studies have been reported in literature for tree species recognition using hyperspectral data. Martin *et al.* (1998) used airborne hyperspectral data from AVIRIS to classify eleven forest cover types, including pure and mixed stands of conifer and deciduous species. Multiple linear regression analysis was used to select eleven bands which were closely correlated with field measured canopy nitrogen and lignin concentration. Transformed divergence values were then calculated for all combinations of four to eleven of the selected bands to determine which band combinations would provide the best separability of signature classes. A maximum likelihood algorithm assigning all pixels in the image into one of the eleven categories was used to classify forest cover types with the selected bands from first difference reflectance spectra. An overall classification accuracy of 75% was yielded using nine of the selected bands when comparing with a random selection of validation pixels in the field.

Gong *et al.* (1997) used *in situ* hyperspectral data to identify six conifer tree species. The data were measured above sunlit and shaded sides of tree canopies from six study sites. Artificial neural network algorithm and linear discriminant analysis were used for species identification with original reflectance spectra and first derivatives of the spectra. They found that the six conifer species could be identified with high accuracy. The highest percentage of accuracy obtained was 91% when sunlit samples and first derivative spectra were used with neural network algorithms. This study provides us insights of the capability of tree species recognition by hyperspectral data. More analyses are necessary in terms of spectral measurements made from more tree species and in different places and seasons.

2.4. Data compression and feature extraction

For vegetation, the reflectance values in adjacent wavebands are often very strongly correlated because most absorption features are relatively broad with at least 40 nm (Baret, 1995). It was shown that the spectral information could be described by the reflectance observed in a small number of wavebands which is linked to the number of independent variables required to describe the various factors affecting the spectral reflectance of plant such as canopy structure and leaf optical properties. Thus, it is desirable to remove some of the information contents algorithmically before the data are analyzed.

The reasons for data compression as well as feature extraction are three-fold (Price, 1994b). First, a trade-off exists between the spectral resolution and the spatial resolution of the imagery acquired. The design of instruments is limited by cost, power and transmission rate. Thus, more spectral bands mean less spatial resolution though this factor may not be valid now as technologies are improving for more powerful and faster instruments. Second, signal-to-noise ratio of the data acquired trades off with the spectral resolution. Third, spectral information of the object of interest may be optimized in particular spectral regions, bandwidth and band number within each region. Therefore, data compression and feature extraction is recommended, especially extracting important bands that reduce the data volume without losing information. In this session, analytical techniques of data compression and feature extraction will be introduced and discussed.

2.4.1. Analytical techniques of data compression

The most obvious technique for data compression is selecting those spectral

bands for ranges which contain the most information for the specific application. It may also be possible to average the bands along the spectral regions of interest where the spectral information is expressed in the overall reflectance level rather than in small bandwidth features. Such averaging is particularly useful in low signal regions where the relative noise level will mask out spectral details (Mehl, 1994).

Another commonly used method for data compression is principal components analysis (PCA). PCA is an analytical technique based upon a transformation of spectral axes such as that spectral variability is maximized (Cloutis, 1996). This technique is found to be useful for analysis of remote sensing data for which certain channels exhibit high degrees of dependence. The greatest benefit of PCA is that spectral discrimination can be maximized from a large number of bands to the first few principal components. It makes PCA a useful tool for data compression. However, determining the physical significance of each principal component is sometimes difficult. Some information would be lost since the first few principal components can generally represent up to 95% of the spectral variation.

In the past two decades, PCA or tasseled cap transformation which is a technique similar to PCA for rotating data have been commonly applied in traditional multispectral broadband data for data compression. Kauth and Thomas (1976) rotated the Landsat MSS data by tasseled cap transformation such that the majority of the information is contained in two components. The first component is a weighted sum of all bands and is termed as brightness. It is defined in the direction of the principal variation in soil reflectance. The second component which is approximately orthogonal to brightness reveals contrast between the near-infrared

and visible bands. It is called greenness and strongly related to the amount of green vegetation. With the addition of two mid-infrared bands, TM data is found to have a third tasseled cap component called wetness which is related to moisture status of soil (Crist and Cicone, 1984).

For hyperspectral data analysis, few studies have been carried out using PCA. Blackburn and Milton (1997) surveyed deciduous woodlands using CASI with geobotany band setting which collects eight bands within the visible and near-infrared spectral regions and PCA is used for analysis. They found that the eigenvectors of the first component (PC1) reveal positive contributions from all spectral bands and that of the second component (PC2) are dependent upon the contrast between reflectance in visible and near infrared wavelengths. The third component loads on the bands which are located around the upper part of the red-edge. The first two eigenvectors were analogous to brightness and greenness respectively derived from tasseled cap transformation using broadband multispectral data. The images of the first three principal components are able to identify the canopy gaps created by the death or destruction of trees. They demonstrated that PCA remains to be an useful tool to interpret vegetation characteristics and conditions. However, more effort is needed when it is applied to hyperspectral data that have a much larger dimension than those studied.

2.4.2. Analytical techniques of feature extraction

Feature extraction is a more difficult and complicated process. It is a process to determine the bands that are most effective in discriminating each class from all others (Jensen, 1994). Three approaches for feature extraction will be explained in this section. The first approach is particularly used for vegetation studies. As the characteristics of spectral reflectance depend greatly on foliar biochemical concentrations and biophysical characteristics, correlation of the spectral bands with these parameters is a common tool to select useful spectral bands for vegetation studies. The other two methods which can be used for any applications are spatial autocorrelation-based approach and spectral autocorrelation-based approach (Petrie and Heasler, 1998).

2.4.2.1. Feature selection by correlation with biochemical and biophysical data

Selection of spectral bands that are closely correlated with biochemical and biophysical data has been done by various researchers (Curran, 1989; Martin *et al.*, 1998; Thenkabail *et al.* 1999). Reflectance spectra of vegetation are measured from dried and powdered leaves at the laboratory level or from canopies at the remote sensing level. Chemical contents or biophysical parameters are then obtained and correlated with the spectral measurements using stepwise multiple linear regression. The spectral bands that are closely correlated with the biochemical or biophysical data are selected.

Curran (1989) selected forty-two minor absorption features that were identified from the spectra of dried and ground leaves which were found to have correlation with the concentration of organic compounds such as cellulose, lignin and

Table 2.1. Wavelengths that are correlated with biochemical or biophysical information found by different researchers

	Curran, 1989	*Martin et al., 1998*	*Thenkabail et al., 1999*
Number of bands	42	9	12
Spectral range	400 – 2400 nm	400 – 2500 nm	350 – 1050 nm
Visible bands (400 – 700 nm)	430	627	495
	460		525
	640		550
	660		568
			668
			682
			696
Near-infrared bands (700 – 1300 nm)	910	750	720
	930	783	845
	970	822	920
	990		982
	1020		1025
	1040		
	1120		
	1200		
Mid-infrared bands (1300 – 2500 nm)	1400	1641	–
	1420	1660	
	1450	2140	
	1490	2280	
	1510	2290	
	1530		
	1540		
	1580		
	1690		
	1780		
	1820		
	1900		
	1940		
	1960		
	1980		
	2000		
	2060		
	2080		
	2100		
	2130		
	2180		
	2240		
	2250		
	2270		
	2280		
	2300		
	2310		
	2320		
	2340		
	2350		

protein in dried leaves (Table 2.1). Martin *et al.* (1998) selected nine AVIRIS spectral bands that were closely correlated with field measured canopy nitrogen and lignin concentration for forest classification (Table 2.1). Thenkabail *et al.* (1999) selected twelve spectral bands along with their bandwidths for extracting agricultural crop biophysical information such as wet biomass, leaf area index, plant height and yield (Table 2.1).

The spectral bands selected by the above researchers are not consistent with one another. The spectral bands selected by Curran (1989) and Martin *et al.* (1998) were mainly the near-infrared and mid-infrared bands in which 38 out of 42 and 8 out of 9 were found respectively. Among the selected near-infrared and mid-infrared bands, more mid-infrared bands were obtained. As the instrument used by Thenkabail *et al.* (1999) acquired wavebands between 350 nm and 1050 nm, no mid-infrared bands were found. However, Thenkabail *et al.* (1999) recommended more visible bands than the previous two researchers. Seven visible bands were selected while only five bands were near-infrared bands.

2.4.2.2. Spatial autocorrelation-based feature selection

Spatial autocorrelation-based feature selection methods are described in detail by Warner and Shank *et al.* (1997). Ratioing of each band with every other band is performed within a hyperspectral image. A noisy ratio image will be produced if the two bands are redundant and random spatial autocorrelation will be exhibited within the image. Thus, the resulting images are ranked according to their relative spatial autocorrelation. The best two bands are selected from the image with highest spatial autocorrelation. The third and the following bands are selected if highest spatial

autocorrelation is obtained when they are ratioed with all the previously selected bands. This feature selection process is termed narrow-band feature selection. Broad-band feature selection groups multiple adjacent bands. Bands can be grouped into the desired number of bands. Grouping is started from the identified best bands that are determined with the narrow-band feature selection technique. Adjacent bands are grouped into the identified best bands if the average spatial autocorrelation of the combined bands increases. Bands are rejected if the combination decreases the spatial autocorrelation. Nonadjacent multiple band feature selection is another method similar to the broad-band feature selection technique, except that groupings are allowed between nonadjacent bands.

Warner and Shank *et al.* (1997) used AVIRIS data to illustrate this method for feature selection. Twenty narrow bands are selected from the full 186 band set using narrow-band feature selection technique (Table 2.2). The bands that are identified as most valuable are clustered in the visible and near infrared region. It suggests that spectral and spatial information is not uniformly distributed throughout the spectral region over which data is collected. Moreover, broad-band feature selection technique identifies 20 broad bands, with an average width of 50 nm, that are broader than the spectral resolution of the AVIRIS sensor. The result does not deny the value of a narrow band sensor. Indeed, narrow band sensors are important to determine the spectral bounds of those broad band features.

Table 2.2. Twenty narrow band features selected from AVIRIS data using spatial autocorrelation feature selection (Source: Warner and Shank 1997)

Rank	*AVIRIS band number*	*Band center wavelength (nm)*
12	11	478
1	19	557
16	22	587
7	25	616
17	28	646
4	31	676
9	37	704
19	38	713
5	39	723
6	47	799
13	57	895
1	64	962
14	73	1048
20	81	1125
10	93	1240
15	117	1451
3	124	1521
18	130	1581
11	138	1660
8	186	2123

2.4.2.3. Spectral autocorrelation-based feature selection

Two algorithms are discussed for spectral autocorrelation-based feature selection, namely, optimization with distance metrics and linear stepwise discriminant analysis.

2.4.2.3.1. Optimization with distance metrics

Optimization with distance metrics often uses divergence as a means to measure the statistical separability of a pair of probability distributions that has its basis in their degree of overlap (Richards, 1993). In general, for selecting the best q feature subset out of n bands to discriminate between two classes, there exist ${}^{n}C_{q}$ combinations of the subset. Then the divergence values of the ${}^{n}C_{q}$ combinations have to be computed in order to identify the best q-band subset that results in the largest

divergence value. For the case where there are more than two classes, the average divergence which is computed by averaging over all possible pairs of classes while holding the q-band subset constant is implemented and the best q-band subset is identified by having the maximum average divergence values. (Jensen, 1994). Other distance matrices are also used such as transformed divergence and Jeffries-Matusita distance (Jensen, 1994 and Richards, 1993). This technique that has been applied to Landsat TM data (Jensen, 1994) seems to be impractical to hyperspectral data because the calculation of divergence is very computationally intensive with hyperspectral data which often possess over a hundred spectral bands.

2.4.2.3.2. Stepwise linear discriminant analysis

Linear discriminant analysis can also be used for band selection besides classification. The spectral bands which best differentiated between classes are selected in a stepwise way. It involves entering the independent variables (spectral bands) into the discriminant function one at a time on the basis of their discriminating power (Hair *et al.*, 1995). The stepwise approach begins by choosing the single best discriminating variable. The initial variable is then paired with each of the other independent variables one at a time, and the variable that is best able to improve the discriminating power of the function in combination with the first variable is chosen. The third and any subsequent variables are selected in a similar procedure. As additional variables are included, some previously selected variables may be removed if the information they contain about group differences is available in some combinations of the other variables included at later stages.

An additional means of interpreting the relative discriminating power of the

independent variables is using the partial F values which indicate the associated level of significance for each variable (Hair *et al.*, 1995). This is accomplished by examining the absolute sizes of the significant F values and ranking them. Large F values indicate greater discriminating power.

Nelson *et al.* (1984) used stepwise linear discriminant analysis to select Landsat TM bands determining which wavebands were most useful for delineating boreal forest cover types. They found that useful waveband combinations included at least one band from the visible, near-infrared and mid-infrared spectral regions.

2.5. Summary

Tree species recognition is improved with more precise identification of forest types using hyperpsectral data. Previous tree species recognition studies found that the use of derivatives spectra and artificial neural network algorithms outperformed the use of original reflectance spectra and statistical algorithms respectively. However, only few studies have been conducted for tree species recognition using hyperspectral data. More experiments should be performed to utilize hyperspectral data for tree species recognition.

With the redundancy of hyperspectral data, data compression and feature extraction are found to be essential for hyperspectral data analysis. Principal components analysis is a common tool for data compression. However, few studies have been applied this technique for hyperspectral data analysis.

In contrast, more studies have been conducted on feature extraction of

hyperspectral data. For vegetation studies, correlation of spectral bands with biochemical and biophysical parameters is a common tool for selecting useful bands. Other approaches are also used for band selection such as spatial autocorrelation, optimization with distance metrics and linear stepwise discriminant analysis. These studies reveal that hyperspectral data are highly redundant. It is essential to select the optimal band sets for different applications. However, the selected bands found by different researchers are not consistent with one another.

CHAPTER THREE

METHODOLOGY

3.1. Introduction

This chapter describes in detail the experimental design and methodology used in this study. The study site and the instruments used in this study are introduced. The procedures of data collection including laboratory measurement and *in situ* measurement are then described. Finally, methods of data analysis for tree species recognition, data compression and band selection are explained.

3.2. Study site

Hong Kong has a territory of over 1080 square kilometers which accommodates over six million population. It is located at a subtropical environment with an average temperature of 20°C and annual precipitation of 1600-2000 mm. It nourishes diverse types of flora with over 300 tree species which is quite a surprising number when only 13% of the total area is woodland (Thrower, 1988). The primary subtropical evergreen broadleaf forest and rainforest were destroyed by human activities and rapid urban development. Since the 1960s, there has been tremendous effect in tree plantation in both country parks and urban area using both indigenous and exotic species.

In this study, hyperspectral measurements were taken in the campus of the Chinese University of Hong Kong, located in Maliushui, Hong Kong. Maliushui was originally a rural village. For the past 30 years, most of the original vegetation cover were destroyed by construction and development of the campus. Meanwhile, tree

plantation similar to that in other areas of Hong Kong was carried out. Thus, trees that were commonly planted in Hong Kong were also found in the CUHK campus. As a result, the CUHK campus was selected as a primary study site in this research.

3.3. Instrumentation

A high spectral resolution spectrometer, S2000 fiber optic spectrometer (Ocean Optics, Inc., 1999), was available for taking hyperspectral data. The spectrometer is linked with a notebook computer for data acquisition and analysis. It is also connected with a single-strand optical fiber through which light energy transmits. Three optical fibers with fiber diameters of 50 μm, 100 μm and 400 μm are available. The effective range of the spectrometer is from 200 nm to 1100 nm. The spectral resolution is approximately 0.5 nm. It has a field of view of 22°.

During data collection, two references, a white and a dark, are used for calibration. The dark reference corresponds to the response of the system with no light being exposed to the detector whereas the white reference records the spectra from a standard white panel close to perfect diffusion. Based on the illumination condition, an integration time for collecting photons is selected to avoid saturation or shortage.

In a dark room with two 500 W tungsten lamps, light intensity is 190 W/m^2 as read from a pyranometer. An integration time of 80 ms is used with an optical fiber of 400 μm diameter. However, integration time varies remarkably when *in situ* measurements are made. For a sunny day with clear sky condition, the light intensity is greater than 500 W/m^2. Under this illumination condition, optical fiber of a

diameter of 50 μm, the smallest one, is used. The integration time is reduced to 7 ms and a cuvette holder is used to reduce light energy transmitted into the spectrometer to avoid saturation. However, when light intensity reduces to less than 50 W/m^2 for features lied under shadow, an integration time of more than 200 ms is used with an optical fiber of a diameter of 400 μm.

3.4. Data collection

Data collection was divided into two parts: laboratory measurement and *in situ* measurement. Laboratory measurement was carried out for leaf samples of selected tree species. The data collected from laboratory measurement were mainly used to test the separability of hyperspectral data of different tree species. *In situ* measurement was done for several selected surface covers in Hong Kong.

When the research project started in summer, 1997, all data were expected to be collected in the field. However, severe problems were encountered. Firstly, 1997 was a rainy year in Hong Kong. Few sunny days with cloudless skies were available for taking spectral data. Even on a sunny day, wind and cloud were still present leading to significant fluctuation in illumination. Secondly, the sensor of the spectrometer was difficult to be held steadily and the direction of the sensor could not be controlled precisely above the tree canopy due to technical difficulties. Other factors including the distance between the sensor and the canopy, the proportion of the leaves within the sampling area from which the sensor of the spectrometer read data could not be controlled during *in situ* measurement. As a result, fluctuation in spectral measurement was often recorded. Thirdly, trees in Hong Kong varies in heights and yet it is not uncommon to find trees exceeding five to ten meters which

poses difficulty for *in situ* measurement. It is advised to have a cherry picker truck for *in situ* measurement from tree canopy so that the sensor of the spectrometer could be held steadily while taking accounts for the factors mentioned above. Due to financial limitation, cherry picker truck was not available in this project.

3.4.1. Laboratory measurement

Laboratory measurements were made and twenty-five tree species (Table 3.1) were selected for tree species recognition. These tree species were selected so as to include species with a wide variety of different characteristics and they are commonly planted in Hong Kong. For example, these trees have obvious differences in the sizes of their leaves. Some trees are native species while some are exotic species which were introduced during the plantation campaign in Hong Kong. The general characteristics of these tree species were listed in Table 3.1. Tree samples were taken in the four seasons so that variation in different seasons can be traced. The four seasonal periods were April, 1998 (spring), July, 1998 (summer), October, 1998 (autumn) and January, 1999 (winter).

In autumn and winter, some tree species suffered from a decrease in foliage and no samples could be collected. Among the 25 tree species, no samples were obtained for *Firmiana simplex* in the autumn and winter seasons and for *Cratoxylum ligustrinum*, *Delonix regia* and *Firmiana simplex* in the winter season. Thus, the number of tree samples was reduced to 24 and 21 for autumn and winter respectively.

Table 3.1. The 25 tree species selected in this study

Species name	*Code*	*Descriptions (Thrower, 1988)*	*Remark*
Acacia confusa	ac	Evergreen, small-leaf, exotic	
Araucaria heterophylla	ah	Evergreen, coniferous, exotic	
Acacia mangium	am	Evergreen, broad-leaf, exotic	
Bauhinia variegata	bv	Deciduous, broad-leaf, native	
Cinnamomum camphora	cc	Evergreen, broad-leaf, native of Eastern Asia and widely cultivated in the tropics and subtropics	
Casuarina equisetifolia	ce	Evergreen, minute-leaf, exotic	
Castanopsis fissa	cf	Evergreen, broad-leaf, native	
Cratoxylum ligustrinum	cl	Deciduous, broad-leaf, native	Excluded from the winter data set
Aleurites moluccana	ct	Evergreen, broad-leaf, widely grown in the tropics	
Dimocarpus longan	dl	Evergreen, broad-leaf, native	
Delonix regia	dr	Deciduous, small-leaf, exotic	Excluded from the winter data set
Ficus microcarpa	fm	Evergreen, broad-leaf, native	
Firmiana simplex	fs	Deciduous, broad-leaf, native	Excluded from the autumn and winter data set
Ficus variegata	fv	Deciduous, broad-leaf, native	
Hibiscus tiliaceus	ht	Evergreen, broad-leaf, widely grown in the tropics	
Lophostemon conferta	lc	Evergreen, broad-leaf, exotic	
Liquidambar formosana	lf	Deciduous, broad-leaf, native	
Lagerstroemia speciosa	ls	Deciduous, broad-leaf, widely grown in the tropics	
Melaleuca quanqueenervia	mq	Evergreen, small-leaf, exotic	
Macaranga tanarius	mt	Evergreen, broad-leaf, widely grown from South Asia to Australia	
Pinus elliottii	pe	Evergreen, coniferous, exotic	
Thuja orientalis	pp	Evergreen, coniferous, native of North China	
Schima superba	sm	Evergreen, broad-leaf, native	
Sapium sebiferum	ss	Deciduous, broad-leaf, native	Excluded from the winter data set
Taxodium distichum	td	Deciduous, minute-leaf, exotic	

The experimental setup is shown systematically in Figure 3.1. The experiment was conducted in a dark room with constant illumination from two 500W tungsten lamps at a distance of 1.2 m apart. Both lamps were stationed with a height of 0.8 m. The light intensity is 190 W/m^2 as read from a pyranometer. The sensor of the spectrometer was pointed vertically downward and positioned at one meter from the ground. With an 22° field of view of the sensor, the sampling area from which the sensor read data should be a circle with diameter of 0.375 m on the ground. A black cloth was lied on the ground so as to minimize noise from the background.

Figure 3.1. The experimental setup

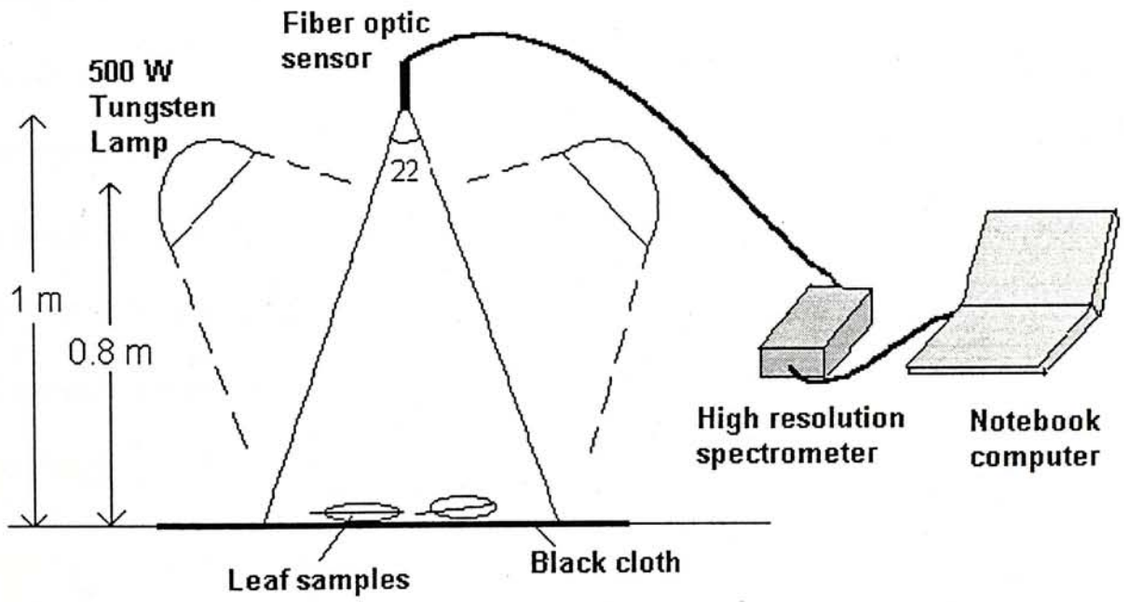

The procedures of the experiment were as followed. Five to six branches of leaves of sampled trees were first collected in the field and brought to the dark room for immediate data measurement. The leaves were then lied on the black cloth for taking spectral measurement. A digital photograph was taken for each sample. The proportion of leaves was measured later with image processing techniques. For each

type of tree species, three different levels of density were used so as to simulate the different densities of tree canopy. Under each density level, 12 samples are taken. Thus, a total of 36 samples were obtained for each tree species.

3.4.2. *In situ* measurement

Various types of surface cover were originally selected for *in situ* hyperspectral measurement to set up a hyperspectral database. The surface covers selected should be the typical surface covers observable from satellite sensors including various road pavement materials, various roof covering materials of buildings, sand, coastal and inland water, various species of grass, shrubs and trees, etc. Due to time limitation and restrictions in *in situ* measurement explained earlier, only ten surface covers were measured in the field. They were concrete, pond water, grass lawn, grass slope, fern (*Dicranopteris linearis*) and five tree species including *Acacia confusa*, *Castanopsis fissa*, *Dimocarpus longan*, *Ficus microcarpa* and *Taxodium distichum*. The height of all five tree species were over four meters. Measurements could not be made vertically above their canopies without the aid of a cherry picker truck which was expensive and unavailable for this study. Instead, measurements were taken at breast height (1 – 1.3 m) obliquely 10 – 20 cm from the canopies.

In situ measurement was done in November, 1998 which was late autumn in Hong Kong. Measurements were made only on sunny days with clear sky condition. The reasons for taking *in situ* measurement during this period are two-fold. Firstly, the climate during this period is dry and cool. There were more sunny days for taking measurements. Secondly, aerial photos and satellite images are usually obtained during this period of time in Hong Kong so that hyperspectral data can be compared

with the data obtained from aerial photos and satellite images.

In situ spectral measurements were made between 10 am to 3 pm of local time because sun angle would not change considerably during this period of time. Dark and white references were measured every five to ten minutes as necessary to minimize the effect of possible change in illumination. Thirty-six samples were taken for each surface type. For tree canopies, measurements were taken from shaded and sunlit portions of the canopies in order to analyze the effect of different light conditions.

3.5. Methods of data analysis

3.5.1. Preprocessing of data

Data which were shorter than 400 nm and longer than 900 nm were eliminated to avoid noisy bands. There were totally 689 bands within the 400 nm to 900 nm region. The original spectra were smoothed with a 20-channel Fast Fourier Transform algorithm using the Origin 5.0 package (MicroCal Software, Inc., 1999).

Before 20-channel Fast Fourier Transform algorithm was adopted, several smoothing algorithms had been used and compared. Centered moving average with 5-channel to 20-channel and Fast Fourier Transform with 5-channel to 10-channel have been tested. The smoothed spectral reflectance produced by these algorithms were similar to each other and the classification results using these smoothed original spectra revealed no significant difference between one another. However, significant differences appeared after the derivatives procedure. The derivatives generated from the spectral reflectance which were smoothed by 20-channel Fast Fourier Transform

had clear and dominate features and were free of noise from 500 to 750 nm, but the derivatives generated from the spectra which were smoothed by other algorithms were extremely noisy for the whole spectral range and no significant features could be identified from the resultant derivatives spectra. Centered moving average and 5-channel to 10-channel Fast Fourier Transform could not reduce noises effectively from the very noisy raw spectral bands. Derivatives procedures induced more noises to the spectra as the spectrometer had very narrow band-width and fine spectral resolution.

The smoothed spectra also contained 689 bands. The smoothed original spectra were then merged and averaged for every five consecutive bands. As a result, the reduced data set contained 138 bands. First and second derivatives were then taken from the reduced reflectance data using the Origin 5.0 package. The number of bands remained the same after the derivative procedures. Thus, three data sets were produced and used for data analysis. They were the reduced original spectra (OS), the first derivatives of the reduced spectra (1D) and the second derivatives of the reduced spectra (2D).

Due to the property of neural network, values in each band of smoothed and derivative spectra were linearly adjusted to the range of [0,1] before they were used in training and testing the neural network. However, linear adjustment was not done to any data which were trained and tested by linear discriminant analysis. This arrangement should have no effect on the comparison of the performance of the two classification algorithms because linear discriminant analysis is based on the statistical structure of the data which will not be affected by linear adjustment.

3.5.2. Compilation of hyperspectral database

A hyperspectral database was compiled and stored in excel files after the spectral data were processed by the methods explained in the previous section. The data stored in the database can be retrieved, processed, displayed and outputted in various forms and formats according to the interest of the users.

The structure of the database was shown systematically in Figure 3.2. The database was divided into two parts, laboratory database and *in situ* database. The laboratory database was composed of twelve excel files. Each season had three separate files which contained the original spectra, the first derivatives of the spectra and the second derivatives of the spectra for the measured tree species respectively. The derivatives of the spectra were included in the database for their frequent uses in data analysis. The *in situ* database contained only one file in which the original spectral reflectance of the ten surface covers were stored.

3.5.3. Tree species recognition

Tree species recognition was done by two algorithms, linear discriminant analysis and artificial neural networks.

Data were divided into two parts: the training set and the testing set. The training set was inputted to train the classifiers and the testing set was used to test the accuracy of classification. For each tree species, six spectral data were selected as the training set in which two samples were randomly selected respectively from the three levels of leaf density. The rest 30 samples were the testing set. Thus, the training set represents 16.67% of the whole data set.

Figure 3.2. The structure of hyperspectral database

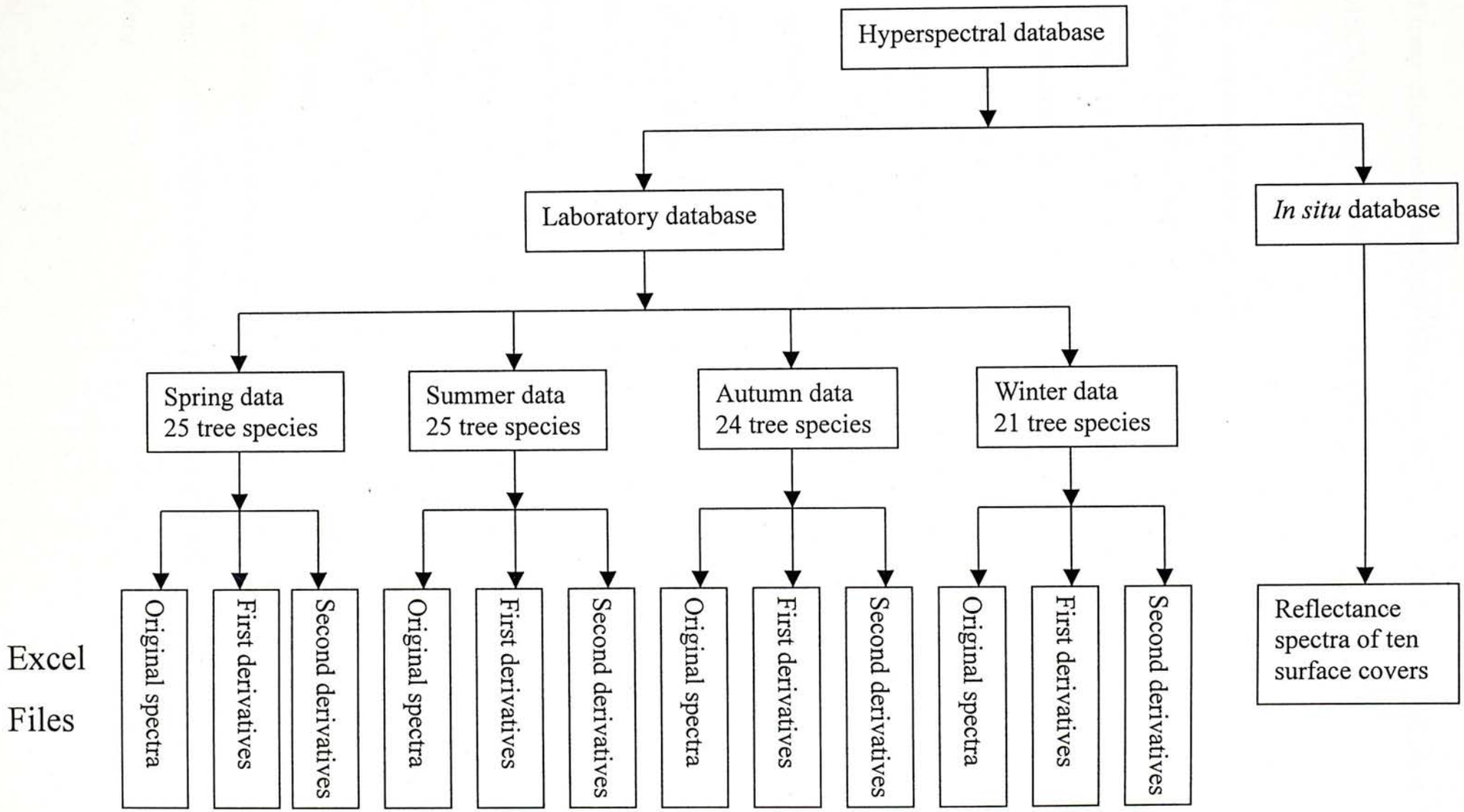

3.5.3.1. Linear discriminant analysis

Linear discriminant analysis (DA) was done for tree species recognition using the DISCRIM procedure in the SAS package (SAS Institute, 1990).

3.5.3.2. Artificial neural network

A feed-forward neural network (NN) algorithm with back-propagation training mechanism was used for tree species recognition to compare with DA. A neural network program developed by Pao (1989) and modified by Gong *et al.* (1997) was adopted and used in this research. In order to build an efficient NN structure, the learning rate (η), momentum coefficient (α), the number of hidden layers and the number of hidden nodes should be optimized. According to Gong *et al.* (1997)'s investigation, NN structure with η=0.2, α=0.7 and one hidden layer with 50 nodes was applied in this study. Several other NN topologies had also been tested using the spring original spectral data set before the above NN structure was adopted. One hidden layer with 50, 80 and 100 hidden nodes and several topologies using two hidden layers with 20 to 80 hidden nodes were tested. Similar classification results were obtained. NN structure of one hidden layers with 50 hidden nodes was adopted due to faster training process.

The training convergence criterion was set such that the testing accuracy was highest within 20000 iterations. Usually, the network was trained to reach its highest accuracy within 20000 iterations and the testing accuracy declined beyond its maxima.

3.5.3.3. Accuracy assessment

For each classification, a confusion matrix was generated. Two methods of accuracy assessment were adopted. The first method was the overall accuracy which was computed by dividing the total number of correctly classified samples (sum of the major diagonal cells of the confusion matrix) by the total number of test samples used. However, this accuracy index does not take into account the off diagonal cells of the confusion matrix. In other words, the errors of commission and the errors of omission are not accounted for. Thus, the second method, Kappa coefficient of agreement (K) developed by Cohen (1960), was introduced for accuracy assessment. The estimate of Kappa is the proportion of agreement (diagonal cells of the confusion matrix) after chance agreement (product of row and column marginals) is removed from consideration (Rosenfield and Fitzpatrick-Lins, 1986). Perfect agreement is represented by a Kappa value of one while zero for chance agreement.

3.5.3.4. Comparison of different data processing strategies and classifiers

A test of significance between two independent Kappa coefficients (Cohen, 1960) was used for assessing the difference between different methods of classification. The standard normal deviate (Z) is calculated as

$$Z = \frac{K_1 - K_2}{\sqrt{V(K_1) + V(K_2)}}$$

where $V(K_1)$ and $V(K_2)$ are the approximate large sample variance of K_1 and K_2 respectively. If the absolute value of Z exceeds 1.96, then the difference between the two Kappa coefficients is significant at the 95 percent probability level.

Z was calculated between any two methods of classification within every data set of the same season. The results were then justified to determine which method of

classification was better for tree species identification.

3.5.3.5. Comparison of data among different seasons

Since the data sets of different seasons contained different number of tree species, it is difficult for comparison. Thus, the spring, summer and autumn data were reduced to 21 tree species as the winter ones. Linear discriminant analysis was then adopted to classify the 21 tree species for data of each season using the original spectra. Significant testing of Kappa was also done among different seasons.

3.5.3.6. Comparison of laboratory and *in situ* data

In situ spectral measurements were done for five tree species, namely *Acacia confusa*, *Castanopsis fissa*, *Dimocarpus longan*, *Ficus microcarpa* and *Taxodium distichum*. As the illumination condition, background effect and leaf orientation in the field were totally different from those in the laboratory, *in situ* spectral reflectance data were expected to be different from the laboratory data. In order to investigate how the two differed from each other, an analysis of means for comparing the means of two independent samples with unequal variances was performed (Norcliffe, 1982). A t value was calculated for each wavelength using the *in situ* and laboratory data of each tree species. The t value was calculated as

$$t = \frac{\overline{X}_1 - \overline{X}_2}{s_{\overline{X}_1 - \overline{X}_2}}$$

where $\overline{X}_1$ and $\overline{X}_2$ were the mean of data set one and data set two respectively and $s_{\overline{X}_1 - \overline{X}_2}$ was the standard deviation of the sampling distribution of the means which was estimated from

$$s_{\bar{X}_1-\bar{X}_2} = \sqrt{\frac{s_1^2}{N_1} + \frac{s_2^2}{N_2}}$$

where s_1^2 and s_2^2 were the variance of the data sets one and data sets two respectively and N_1 and N_2 were the sample sum of the data set one and data set two. In this case, the difference between the two data sets was significant at the 0.05 significance level if the absolute value of t exceeded 2.

3.5.4. Data compression

With the tremendous volume of spectral bands obtained, a certain degree of data redundancy was expected. Principal components analysis (PCA) which is a common tool to transform multidimensional data and extract useful vectors for data compression was thus used for data compression. PCA was performed to investigate how the spectral bands would be rotated and what information could be available from PCA.

Separate PCAs were performed using the smoothed *in situ* spectral reflectance of the ten surface covers and the smoothed spectral reflectance of the 25 tree species for each season respectively. The PC loadings were then investigated. For the PCs generated by the 25 tree species, linear discriminant analysis was performed using the first eight PC scores for each season in order to investigate the differentiating power of the PCs. Another seasonal comparison was also performed with 21 tree species using stepwise discriminant analysis.

3.5.5. Band selection

Other than data compression, band selection can be done to reduce data

redundancy. Band selection is essential for data analysis in order to save computational time and facilities as well as to improve analysis results. Two algorithms were adopted for band selection. A preliminary band selection procedure was first done using stepwise discriminant analysis for the spectral data of the 25 tree species. Linear discriminant analysis was then performed to classify the tree species using the selected bands. Significant testing of Kappa was done for comparing the difference in accuracy between two classifications using all bands and selected bands.

After the preliminary analysis, a hierarchical clustering procedure was carried out using the original spectral data in autumn. The 400 – 900 nm spectral region was grouped into clusters. The boundary and the spectral bands of the clusters were then investigated in detail. In order to identify which spectral regions contain more information for tree species recognition, several spectral band sets were selected from the centers of the clusters and used to classify the tree species of four seasons respectively. Again, significant testing of Kappa was then done to determine which spectral band sets produced a better classification accuracy.

3.6. Summary

In this study, the Chinese University of Hong Kong campus was selected as a primary study site to measure hyperspectral data. A high spectral resolution spectrometer was available for data collection which was divided into two parts, laboratory measurement and *in situ* measurement. Twenty-five tree species were selected for laboratory measurement to test the separability of hyperspectral data of different tree species. For *in situ* measurement, spectral reflectance of ten surface

covers including several tree species, grass, fern, water and concrete were taken. A hyperspectral database was then set up. The spectral reflectance and their derivatives were eventually analyzed for tree species recognition, data compression and band selection. The twenty-five tree species were classified using two classifiers, linear discriminant analysis and neural network. For data compression, principal components analysis was used whilst band selection was performed using stepwise discriminant analysis and hierarchical clustering.

CHAPTER FOUR

RESULTS AND DISCUSSIONS OF TREE SPECIES RECOGNITION

4.1. Introduction

This chapter presents the results and discussions of tree species recognition. First, the characteristics of the hyperspectral data collected in this study are described. They include the smoothed spectral reflectance curves, the first derivatives and the second derivatives of the 25 tree species as well as the spectral reflectances of the ten surface covers measured in the field. Then, the results of tree species recognition are presented followed by discussions on comparison of different classifiers, comparison of different data processing strategies, comparison of different seasonal data and comparison of laboratory and *in situ* data.

4.2. Characteristics of hyperspectral data

Hyperspectral data measurements were taken in the laboratory for 25 tree species in the four seasons as well as in the field for ten surface covers.

Figures 4.1 to 4.4 illustrated the smoothed spectral reflectance curves of the 25 tree species in spring, summer, autumn and winter respectively. In each season, the 25 tree species were separated into four groups, and their corresponding reflectance curves were presented in four graphs. In general, low reflectance was found in the spectral range from 400 to 690 nm where lied the visible bands and a peak appeared centering at around 550 nm presenting the green peak. From 690 to 750 nm, the reflectance rose markedly from very low to very high values. This rise was the red edge. The high reflectance leveled off from 750 to 900 nm which was the near-

Figure 4.1a Spectral reflectance curve of the first seven tree species in spring

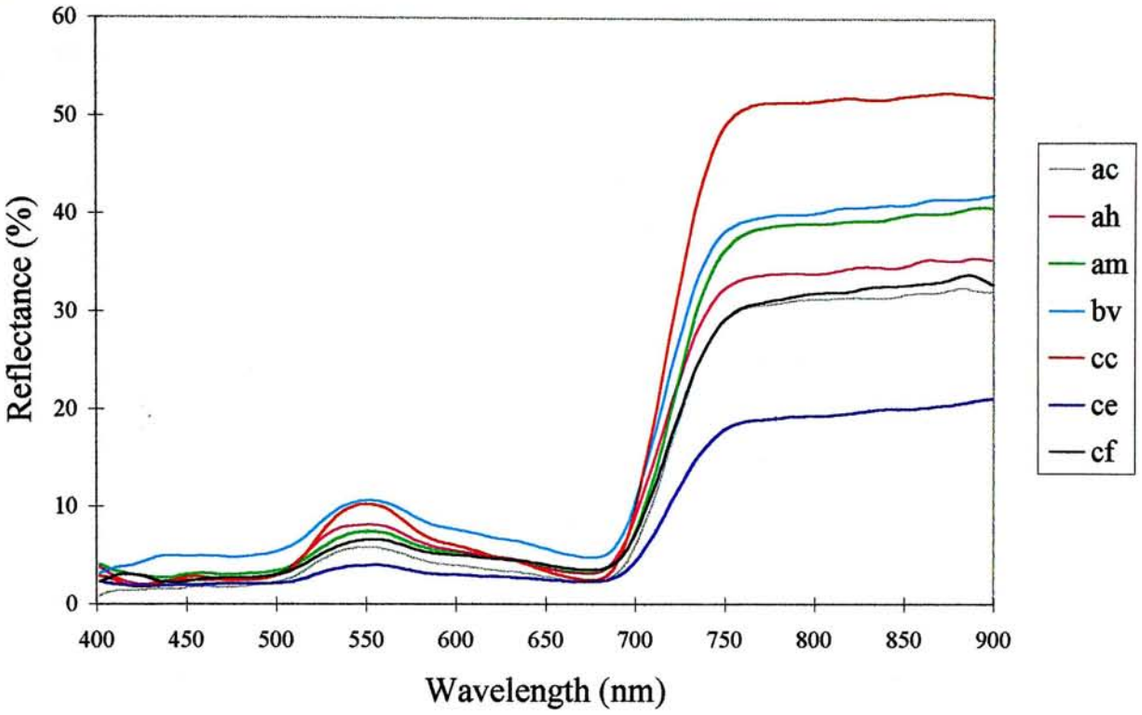

Figure 4.1b Spectral reflectance curve of the second six tree species in spring

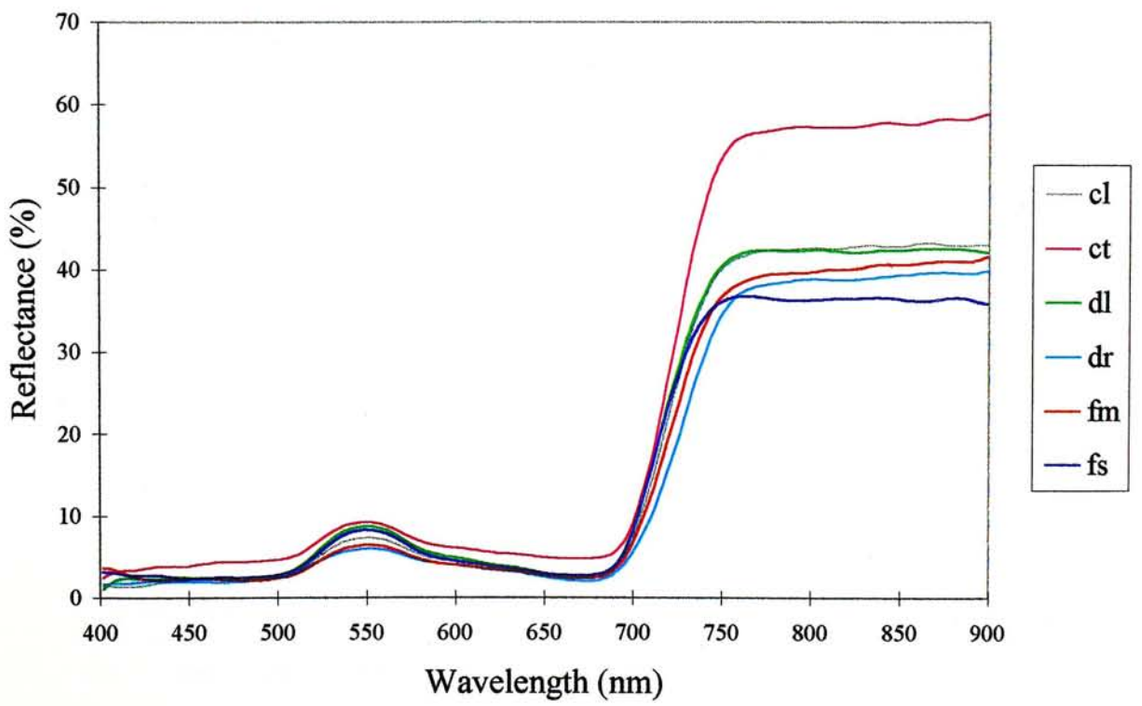

Figure 4.1c Spectral reflectance curve of the third six tree species in spring

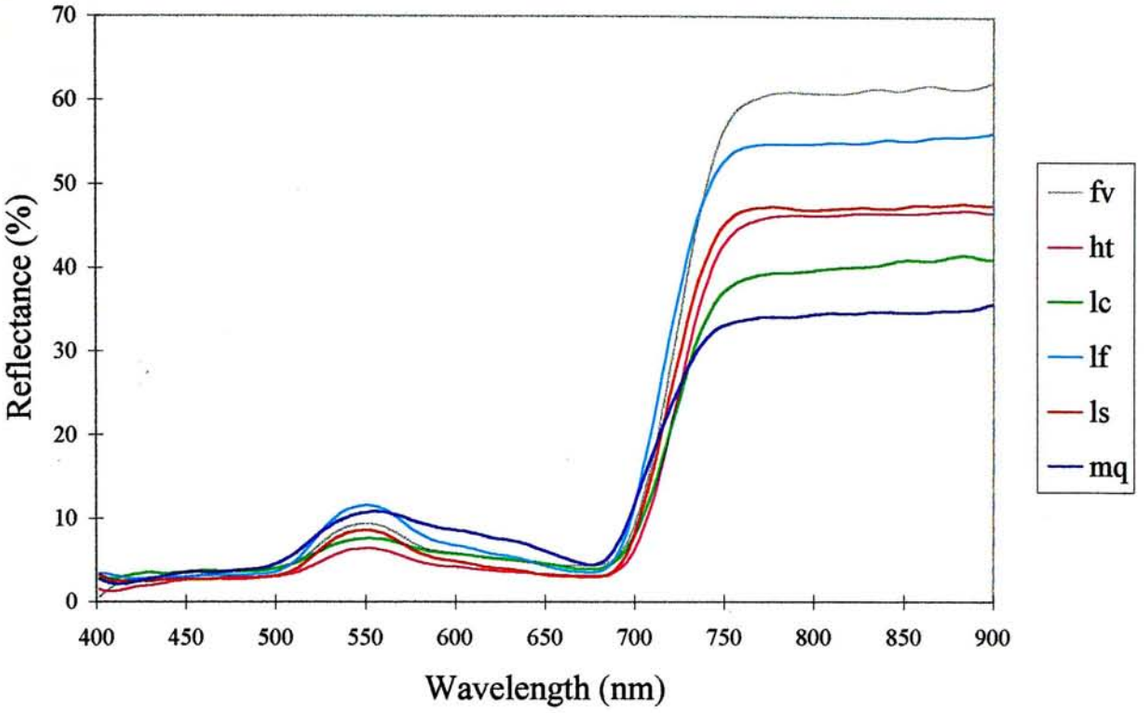

Figure 4.1d Spectral reflectance curve of the fourth six tree species in spring

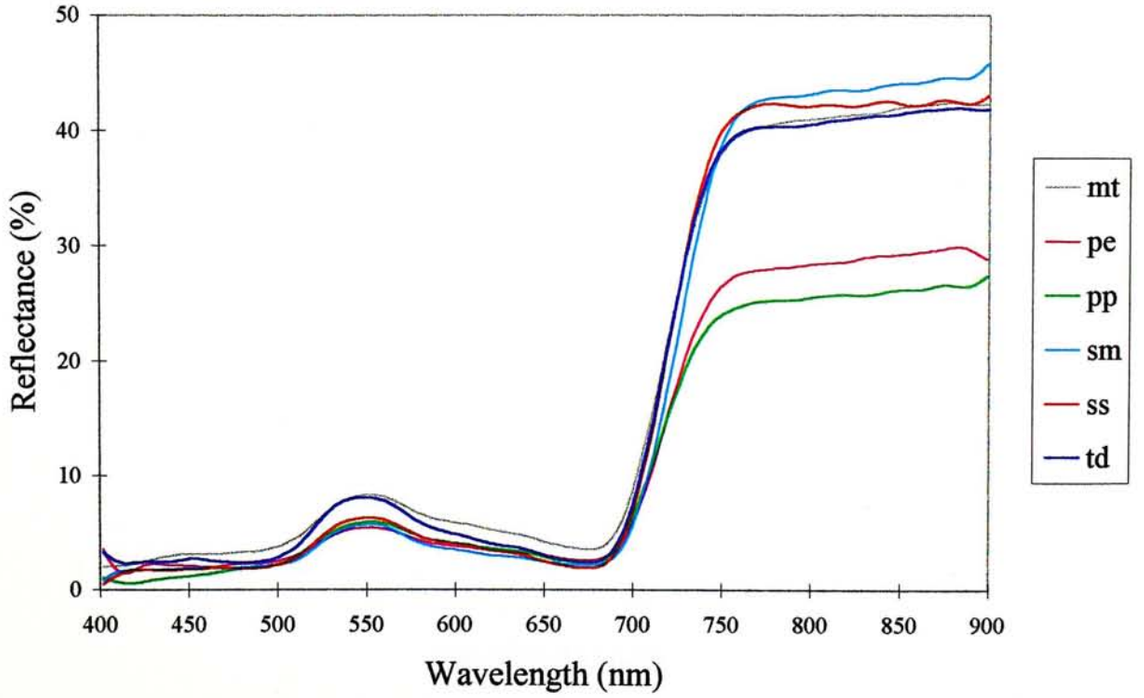

Figure 4.2a Spectral reflectance curve of the first seven tree species in summer

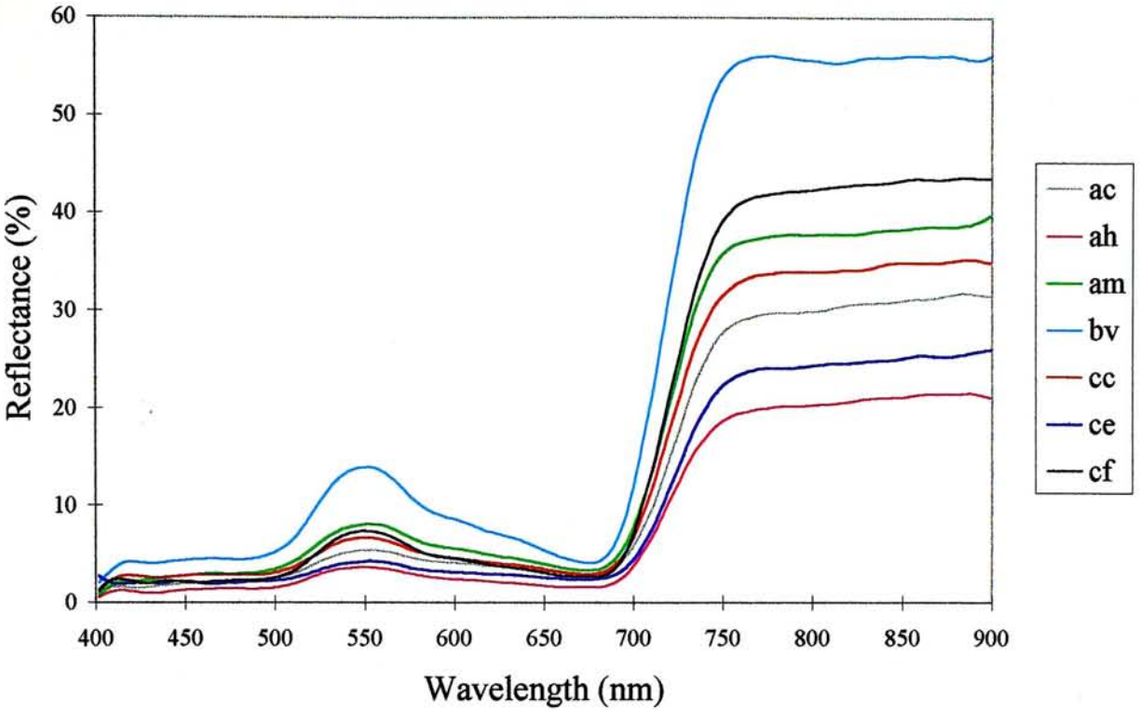

Figure 4.2b Spectral reflectance curve of the second six tree species in summer

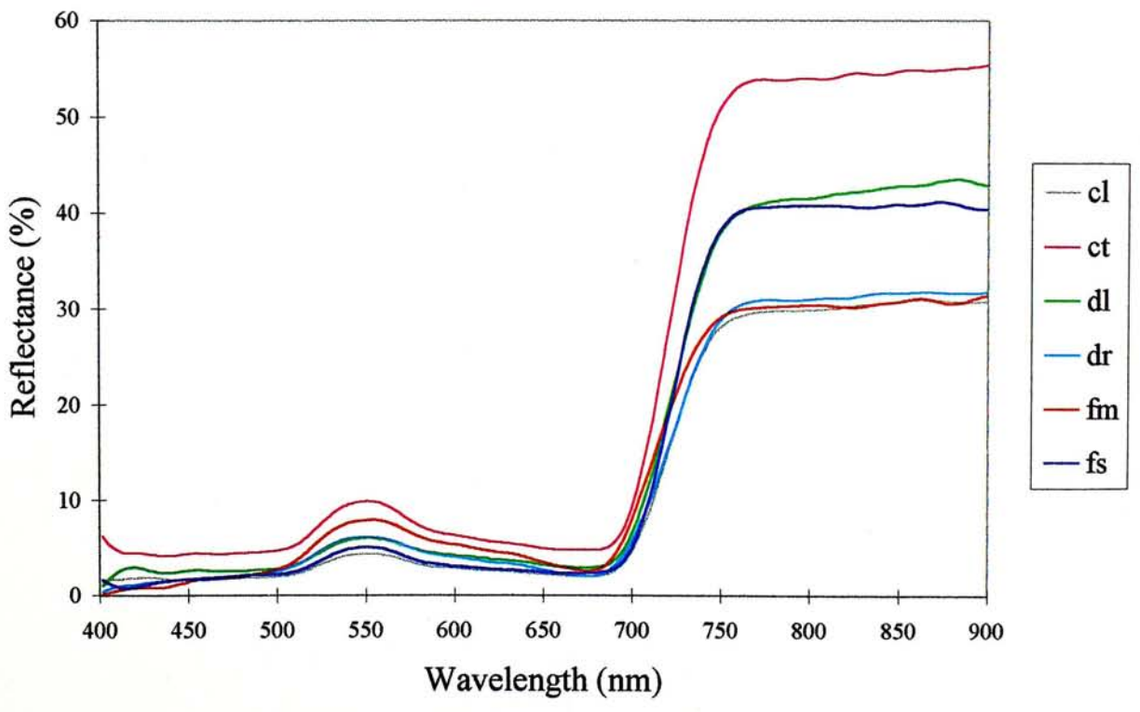

Figure 4.2c Spectral reflectance curve of the third six tree species in summer

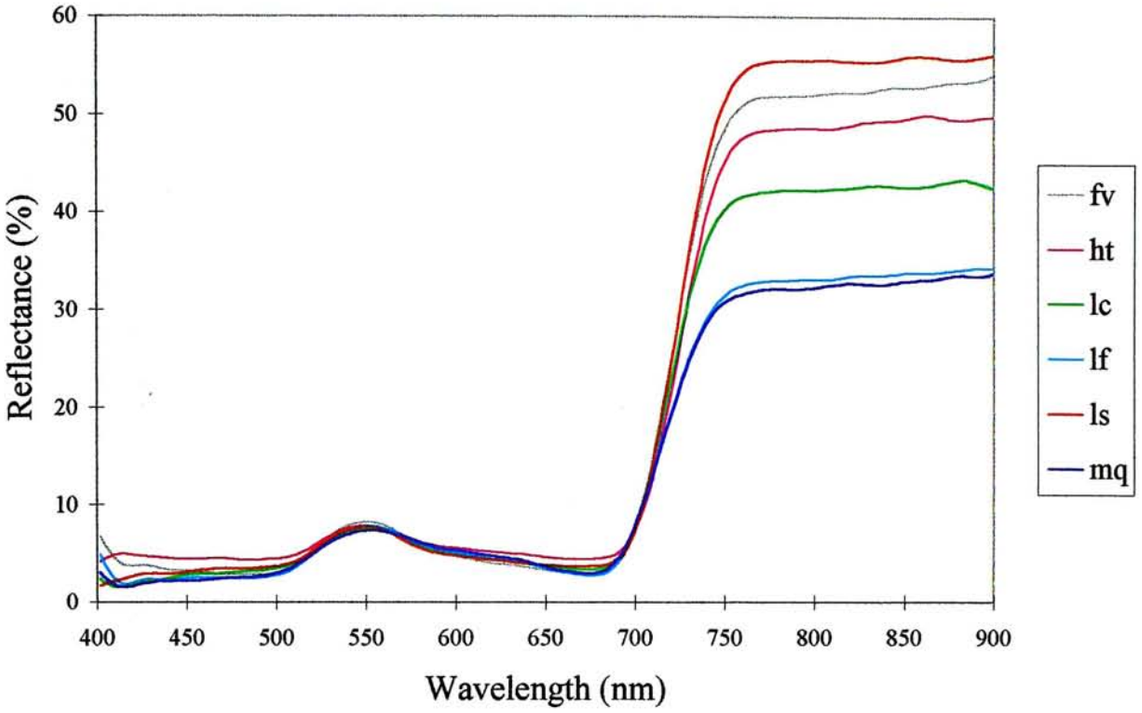

Figure 4.2d Spectral reflectance curve of the fourth six tree species in summer

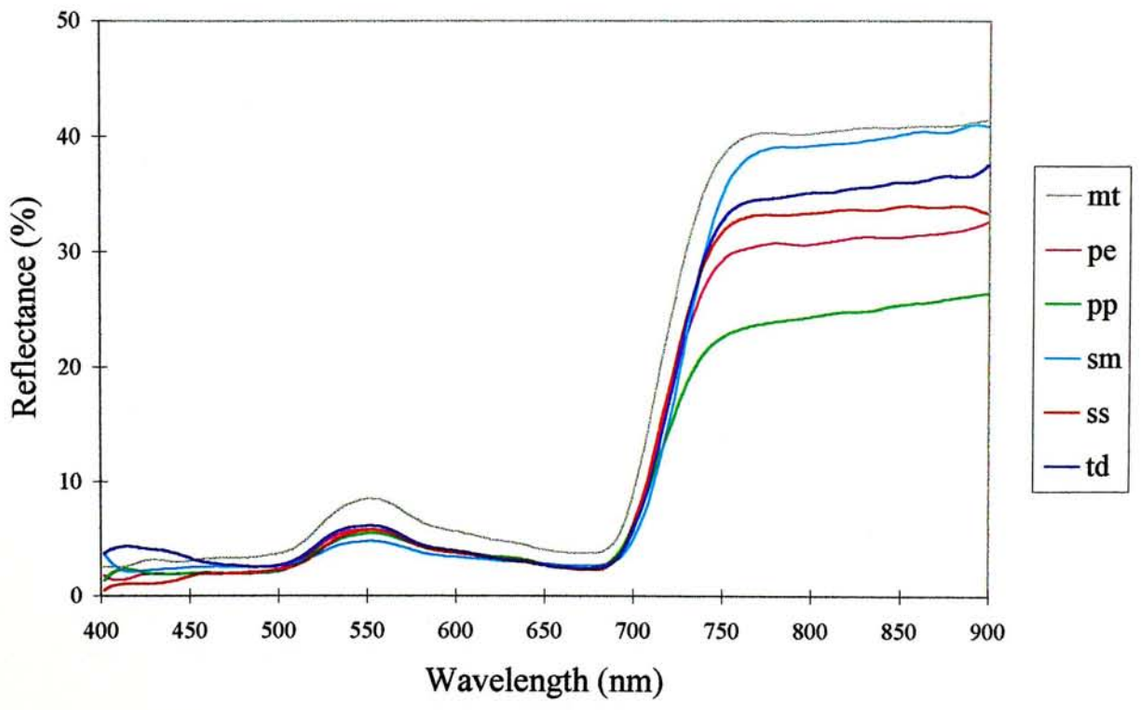

Figure 4.3a Spectral reflectance curve of the first six tree species in autumn

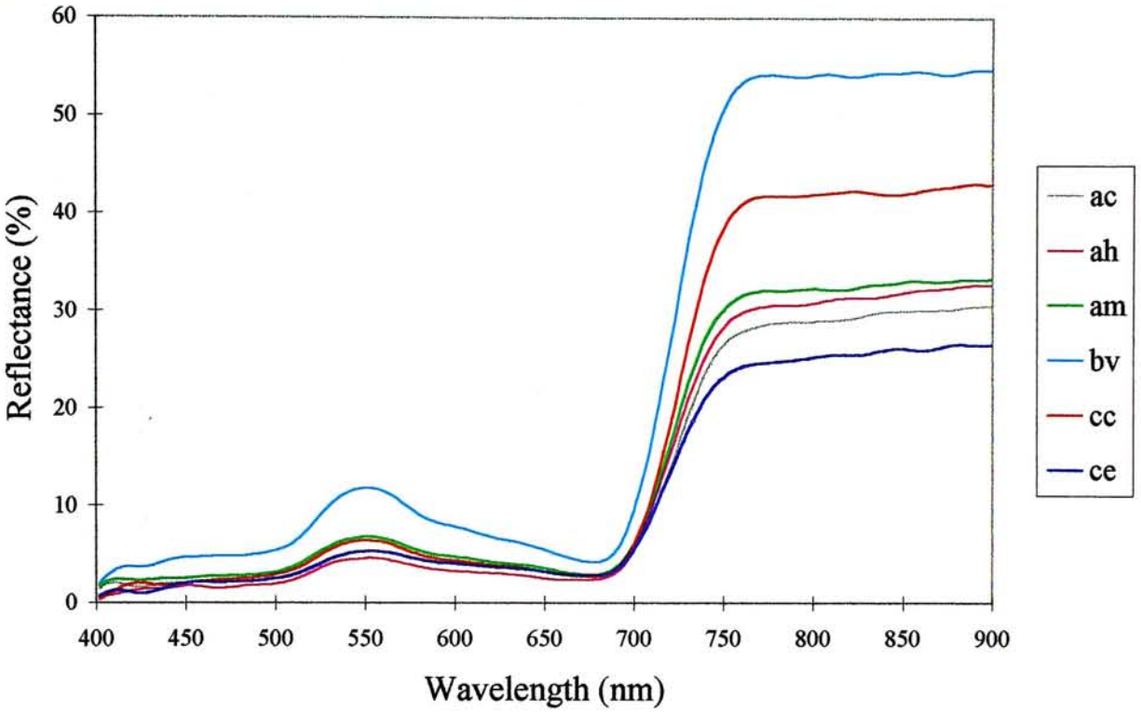

Figure 4.3b Spectral reflectance curve of the second six tree species in autumn

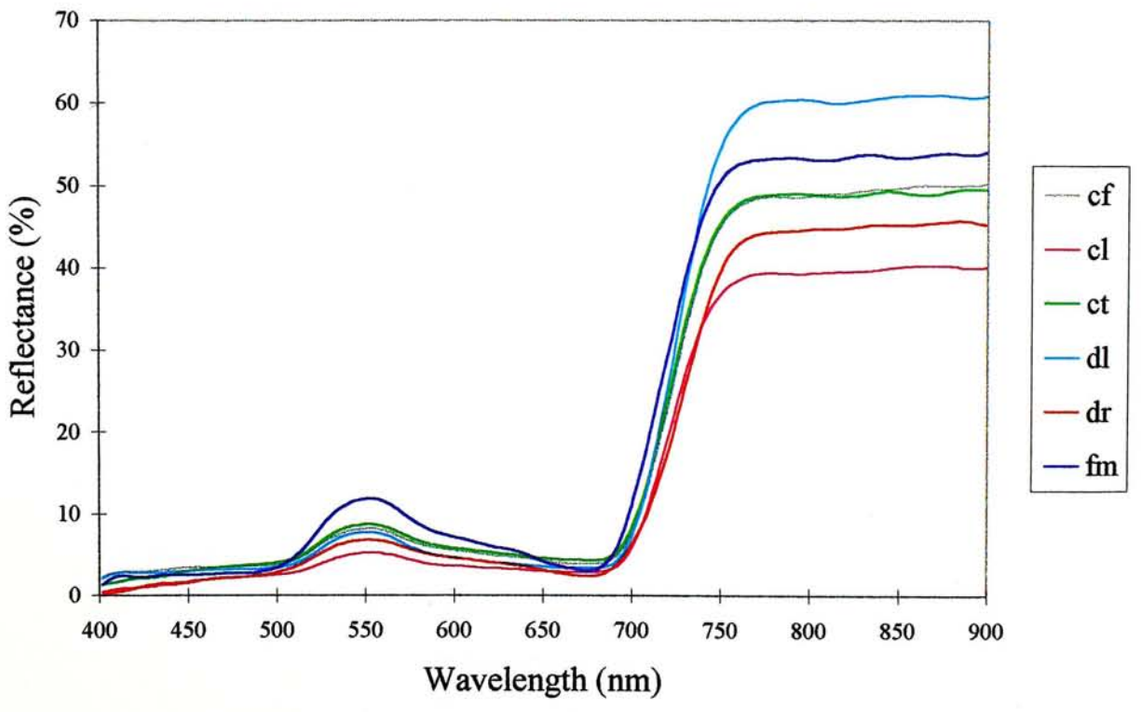

Figure 4.3c Spectral reflectance curve of the third six tree species in autumn

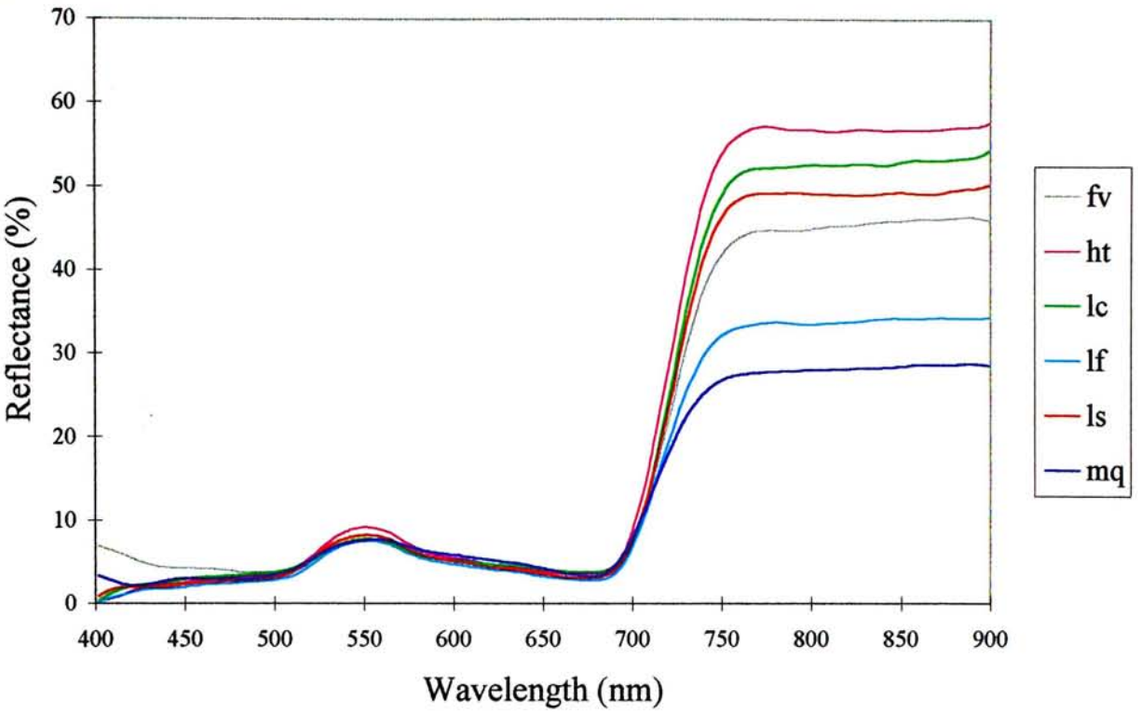

Figure 4.3d Spectral reflectance curve of the fourth six tree species in autumn

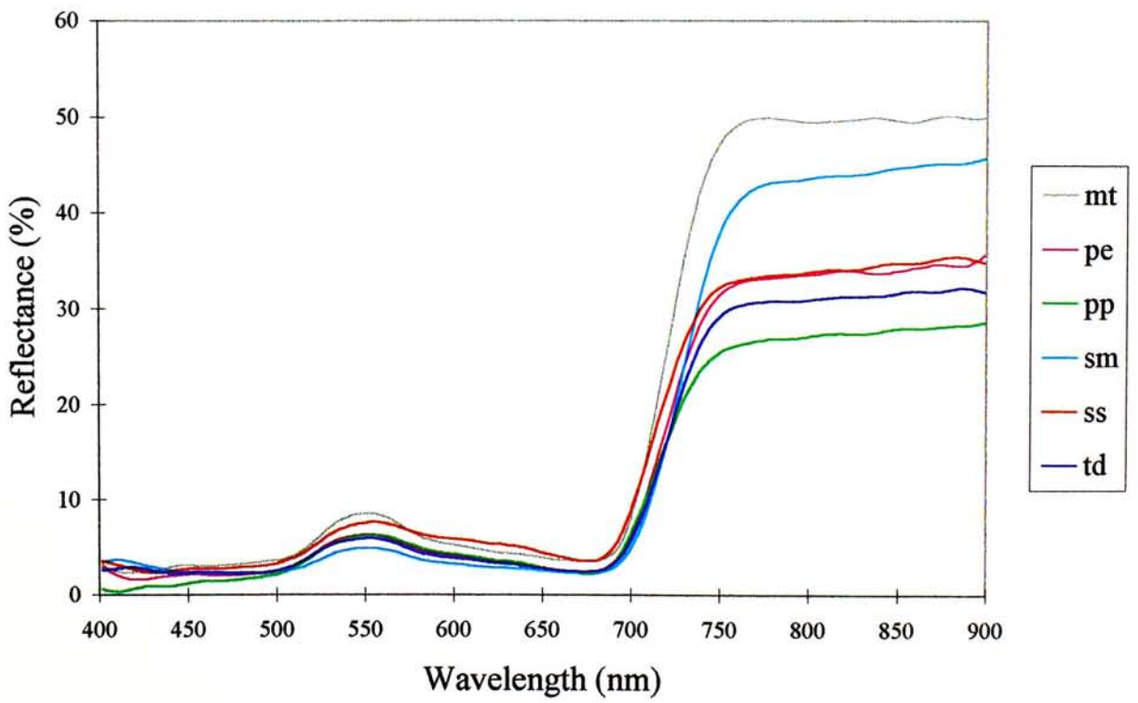

Figure 4.4a Spectral reflectance curve of the first six tree species in winter

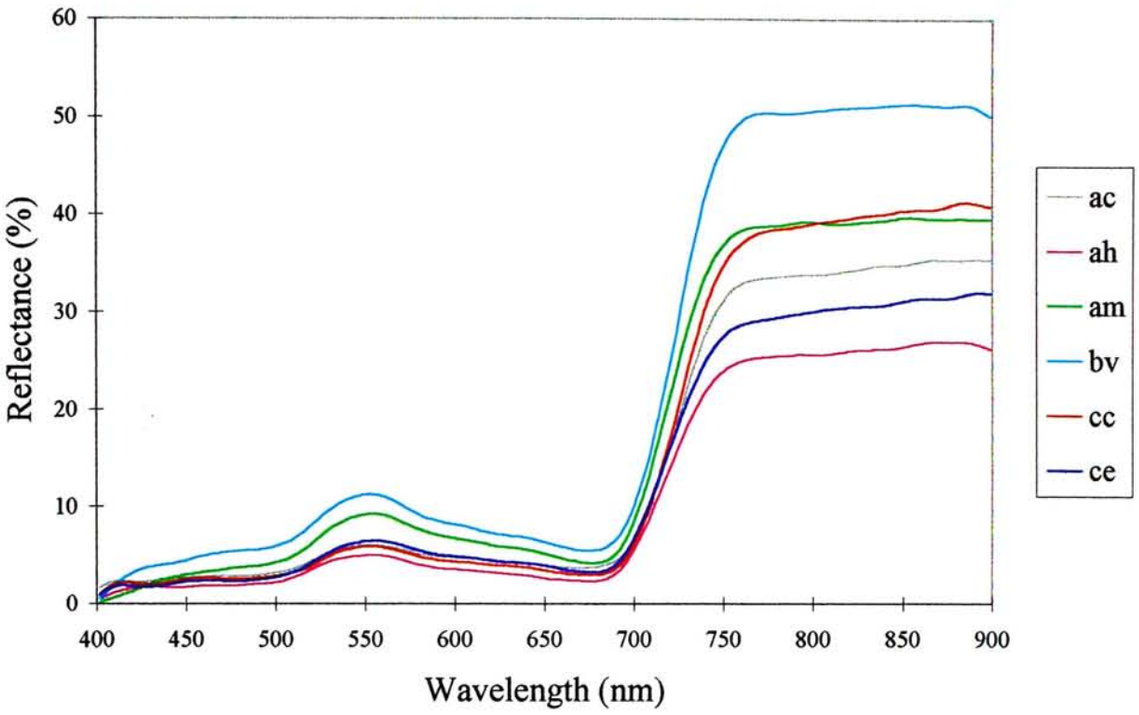

Figure 4.4b Spectral reflectance curve of the second five tree species in winter

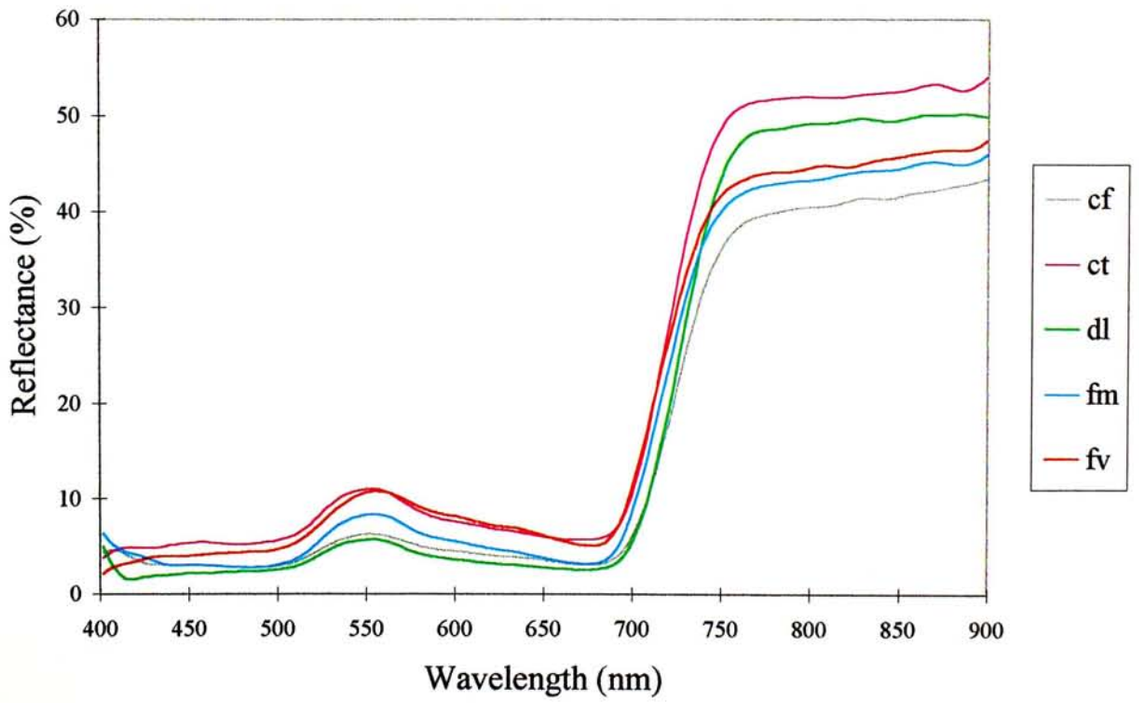

Figure 4.4c Spectral reflectance curve of the third five tree species in winter

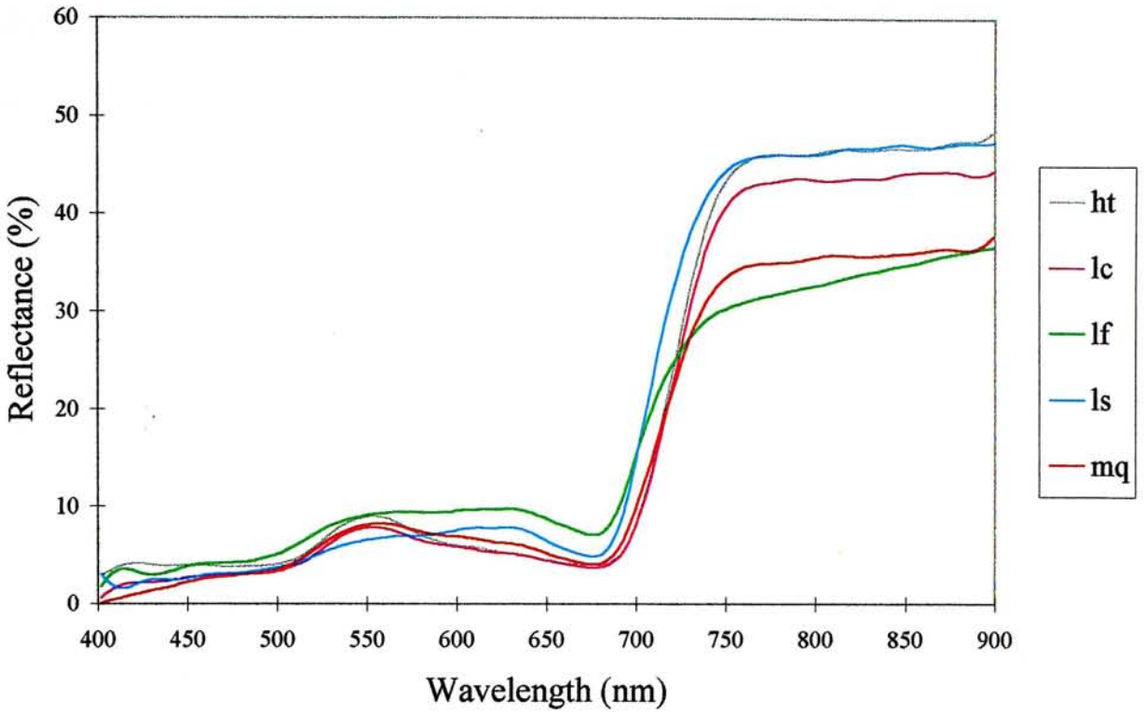

Figure 4.4d Spectral reflectance curve of the fourth five tree species in winter

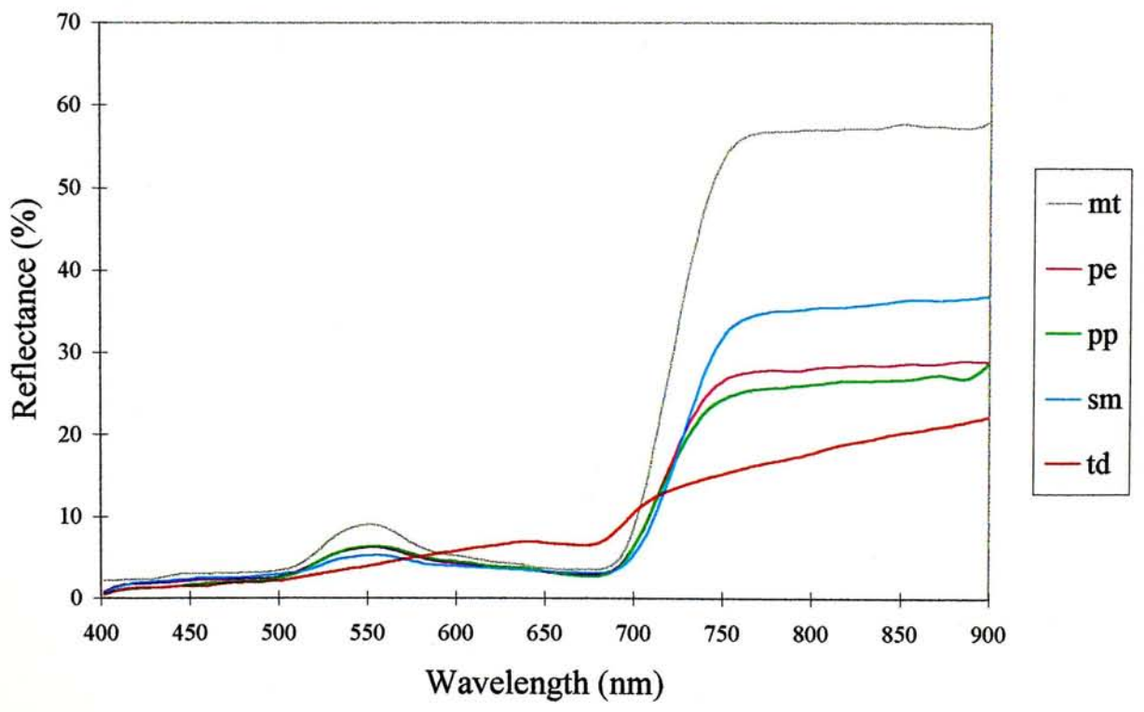

infrared bands. While all trees demonstrated a similar pattern of reflectance, a great variation was found among them. Trees with large broad leaves tended to have a comparatively high reflectance in the near-infrared bands, for example, *Bauhinia variegata*. On the other hand, trees with small leaves like *Acacia confusa* or trees with needle-leaves such as *Pinus elliottii* were low in the near-infrared bands.

Figures 4.5 to 4.8 showed the first derivatives of the 25 tree species in the four seasons. The first derivatives had some dominate peaks in the spectral bands from 500 to 770 nm whilst the bands with wavelengths shorter than 550 nm and longer than 770 nm remained approximately around zero value with some noises. A positive peak and a negative peak were found at around 525 nm and 570 nm respectively whilst zero value was found in between the two peaks at 550 nm. These features demonstrated clearly the characteristics of the green peak which had a maxima at 550 nm and a positive slope before the maxima and vice versa. Some negative irregularities with two small negative peaks were found between the green peak and the red edge that indicated the some variations of the downward slope occurred in this region. A very high peak occurred at around 725 nm illustrated the marked rise of the red edge. Different tree species tended to have the peaks centered at slightly different wavelengths. This might help to improve recognizing tree species.

Figure 4.5a First derivatives of the first seven tree species in spring

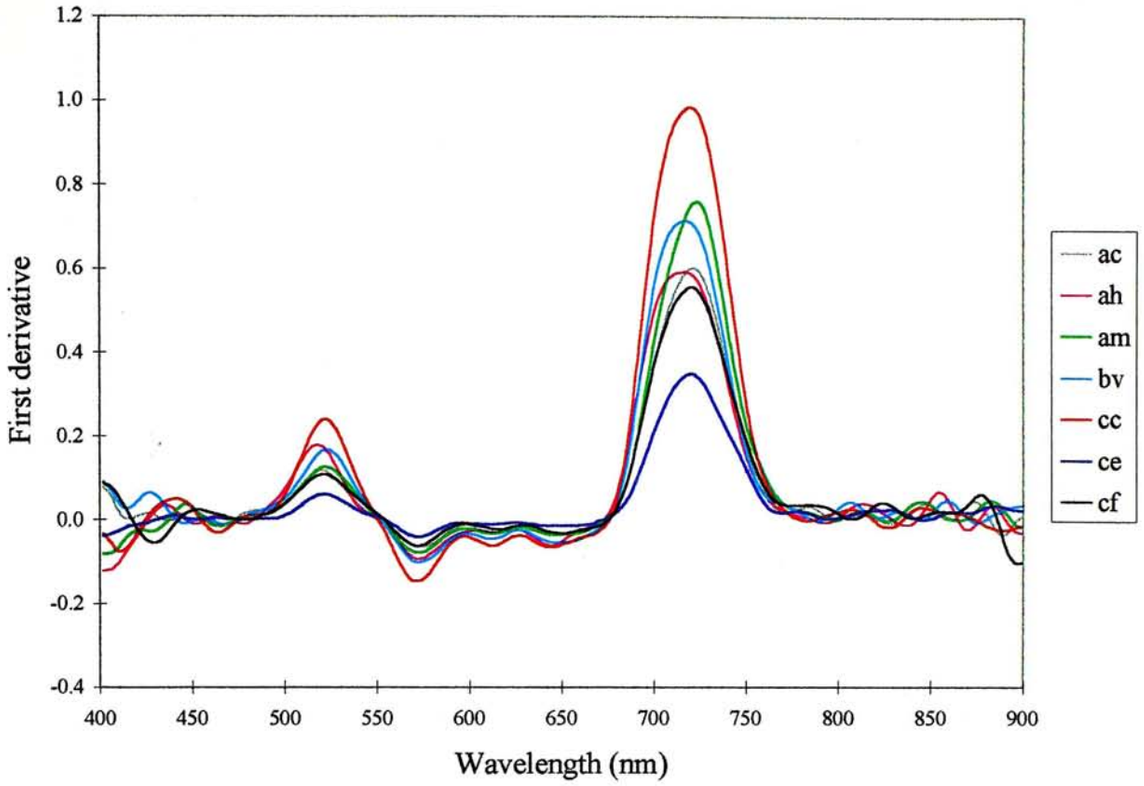

Figure 4.5b First derivatives of the second six tree species in spring

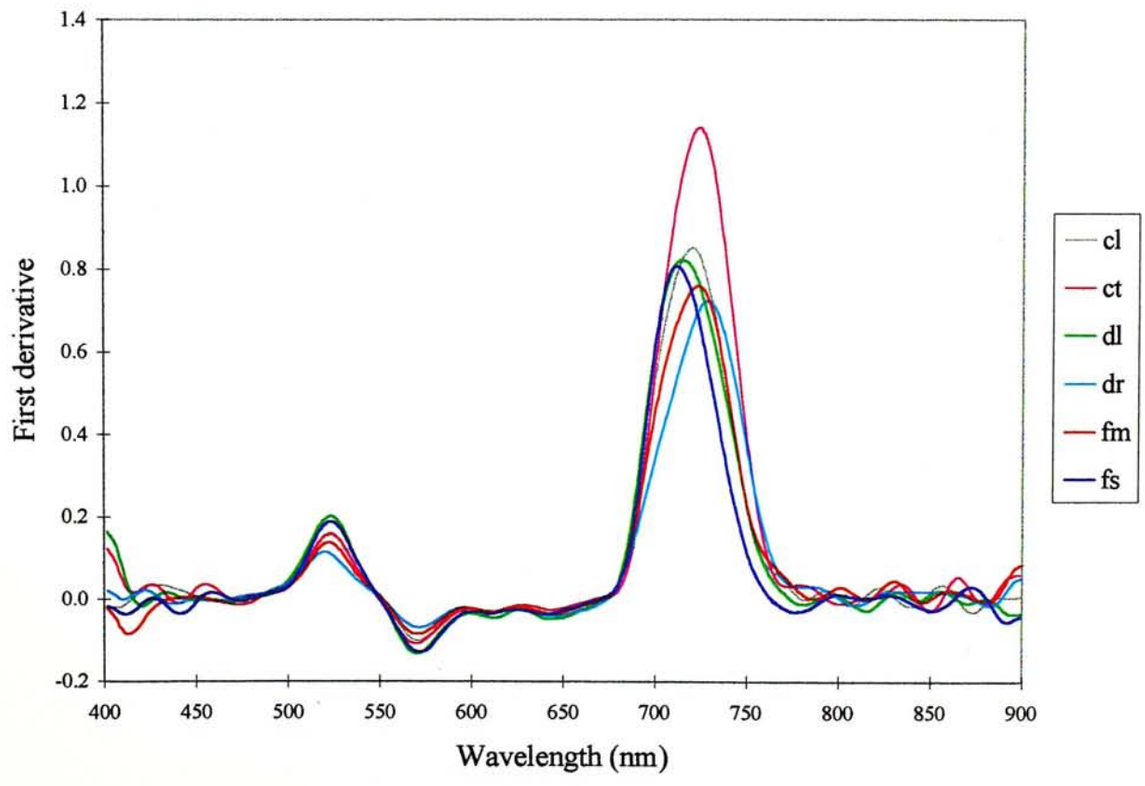

Figure 4.5c First derivatives of the third six tree species in spring

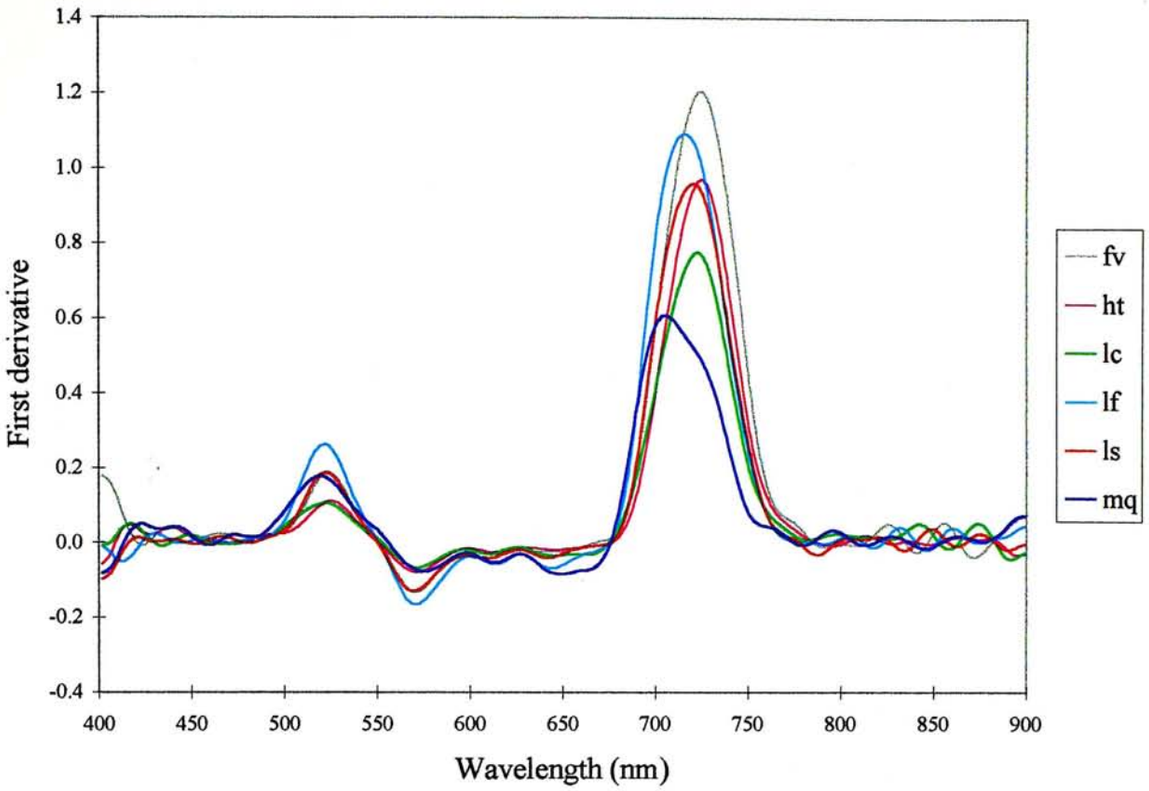

Figure 4.5d First derivatives of the fourth six tree species in spring

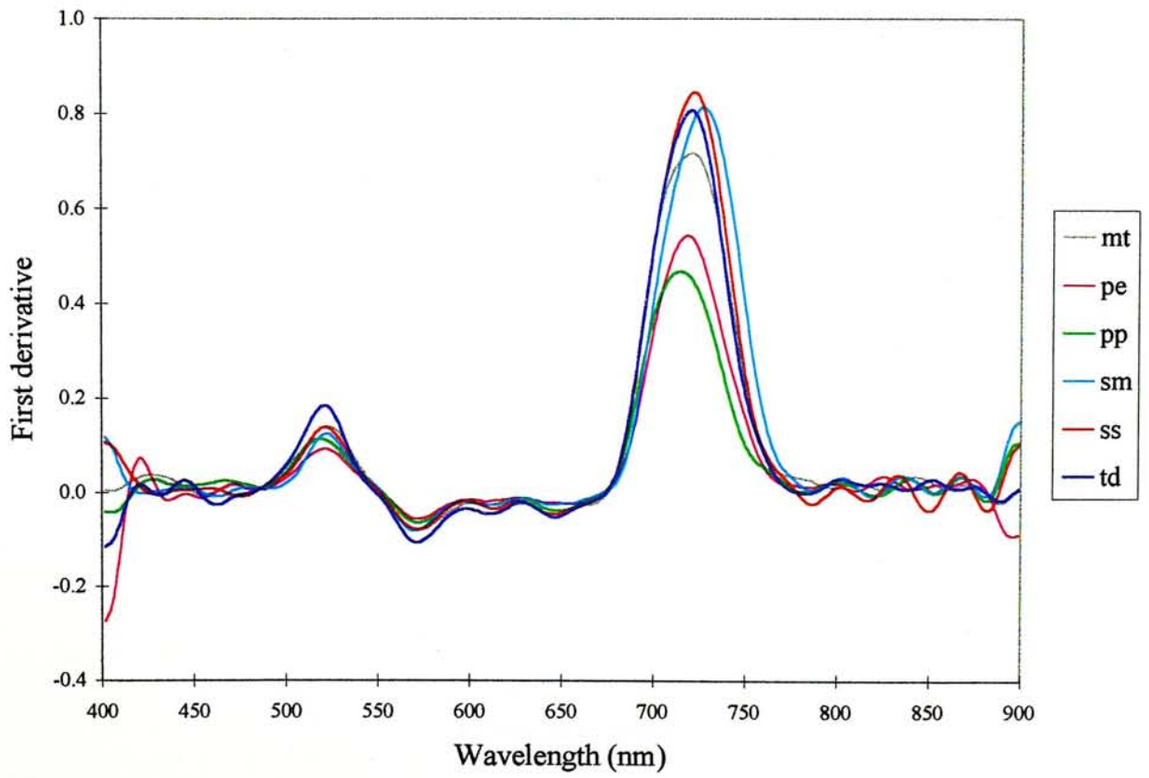

Figure 4.6a First derivatives of the first seven tree species in summer

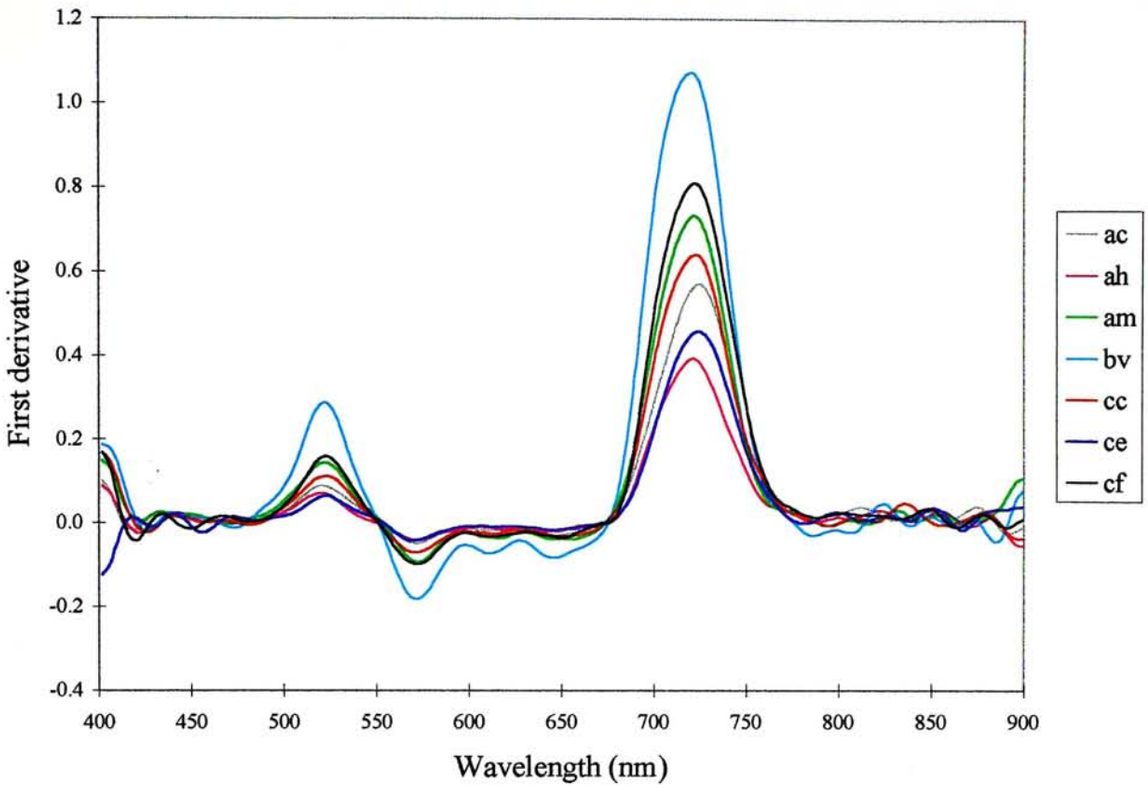

Figure 4.6b First derivatives of the second six tree species in summer

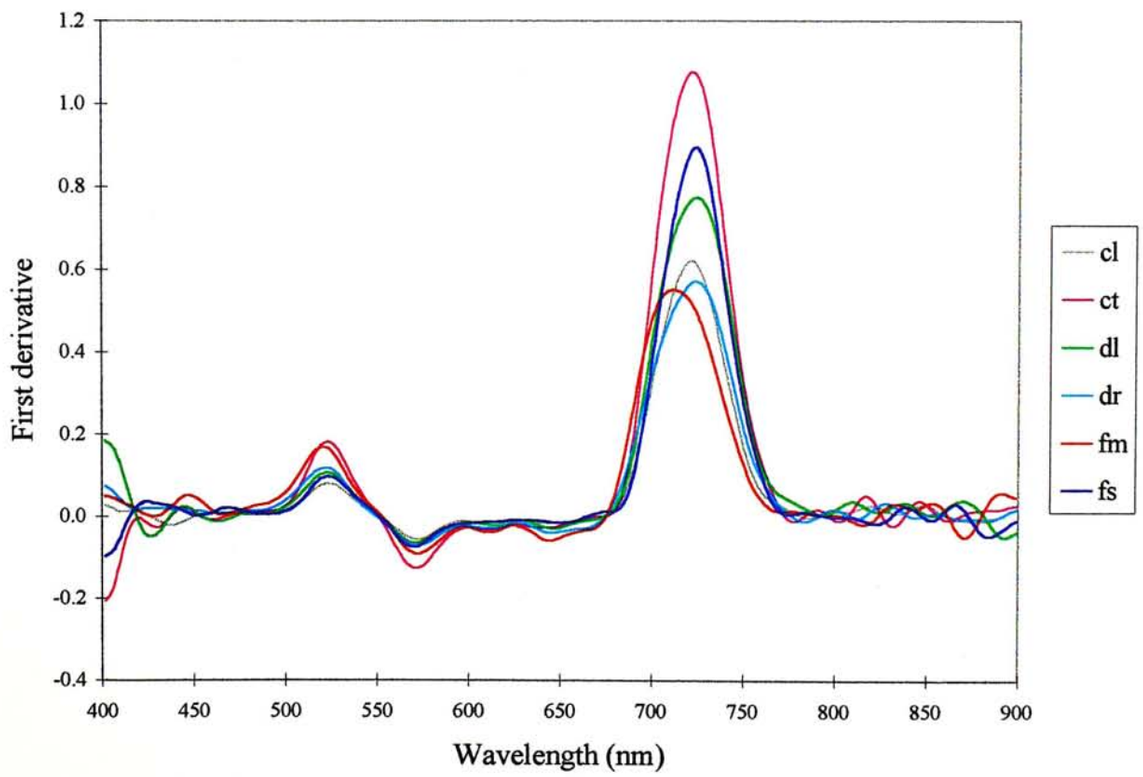

Figure 4.6c First derivatives of the third six tree species in summer

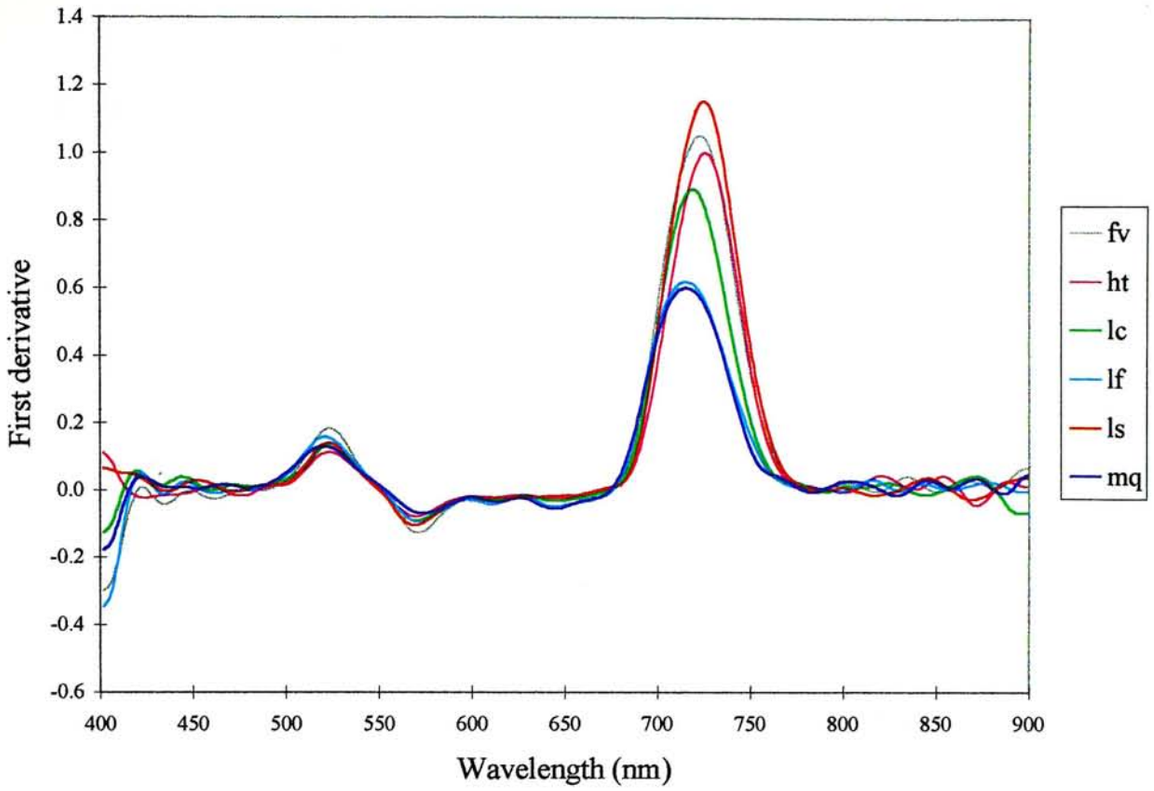

Figure 4.6d First derivatives of the fourth six tree species in summer

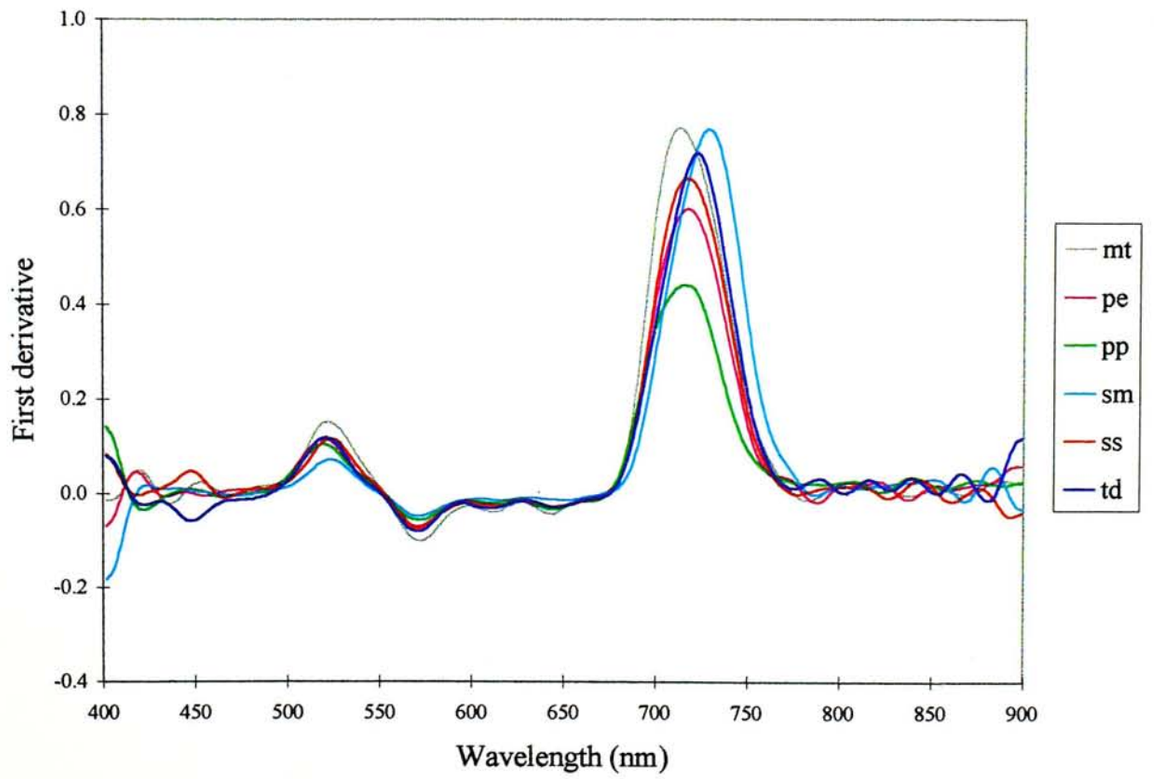

Figure 4.7a First derivatives of the first six tree species in autumn

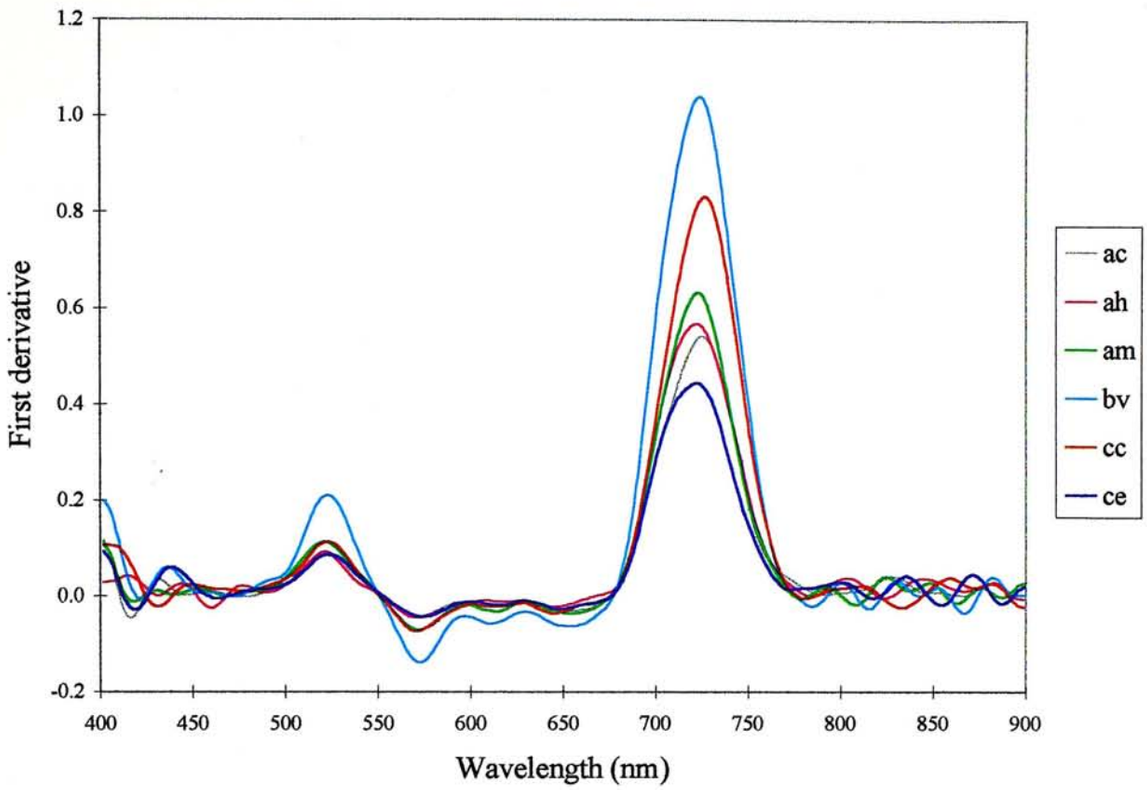

Figure 4.7b First derivatives of the second six tree species in autumn

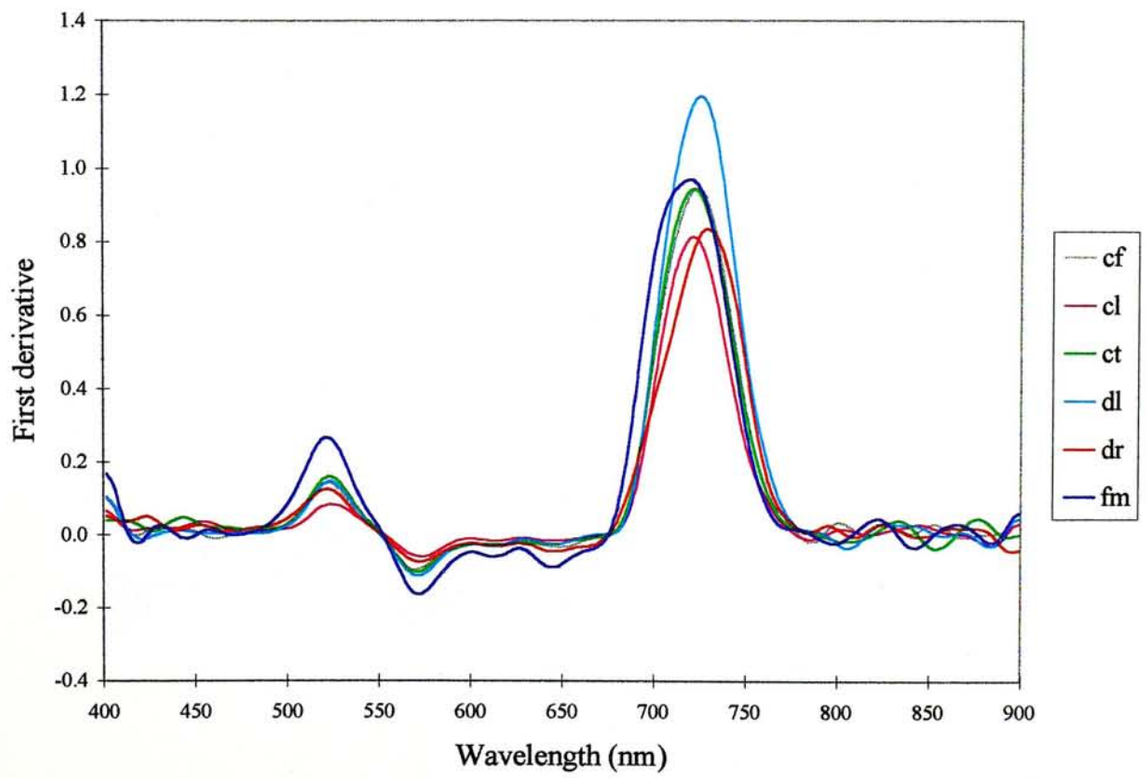

Figure 4.7c First derivatives of the third six tree species in autumn

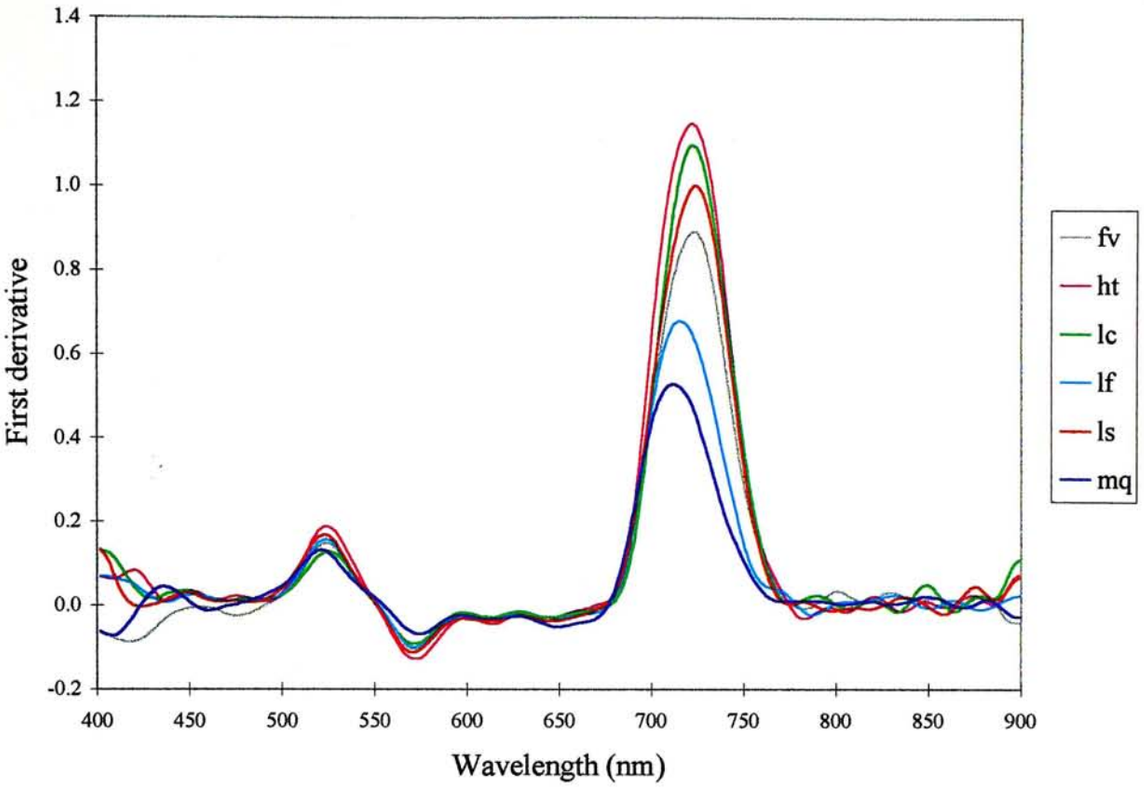

Figure 4.7d First derivatives of the fourth six tree species in autumn

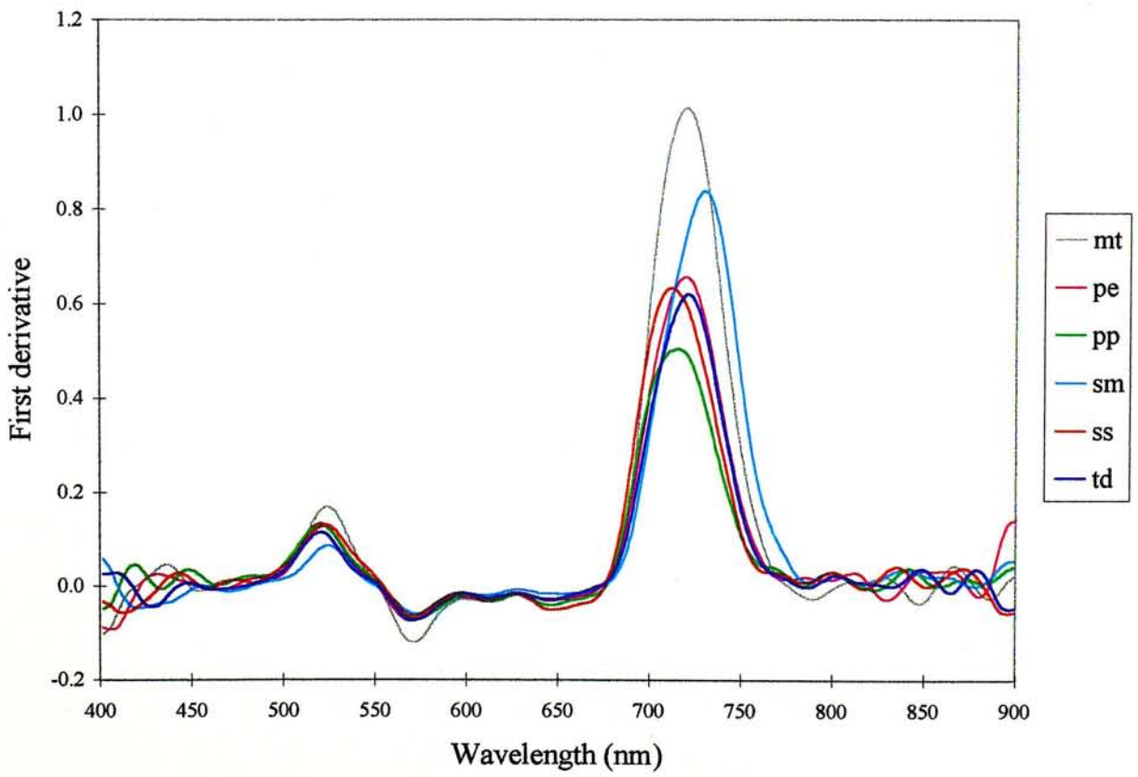

Figure 4.8a First derivatives of the first six tree species in winter

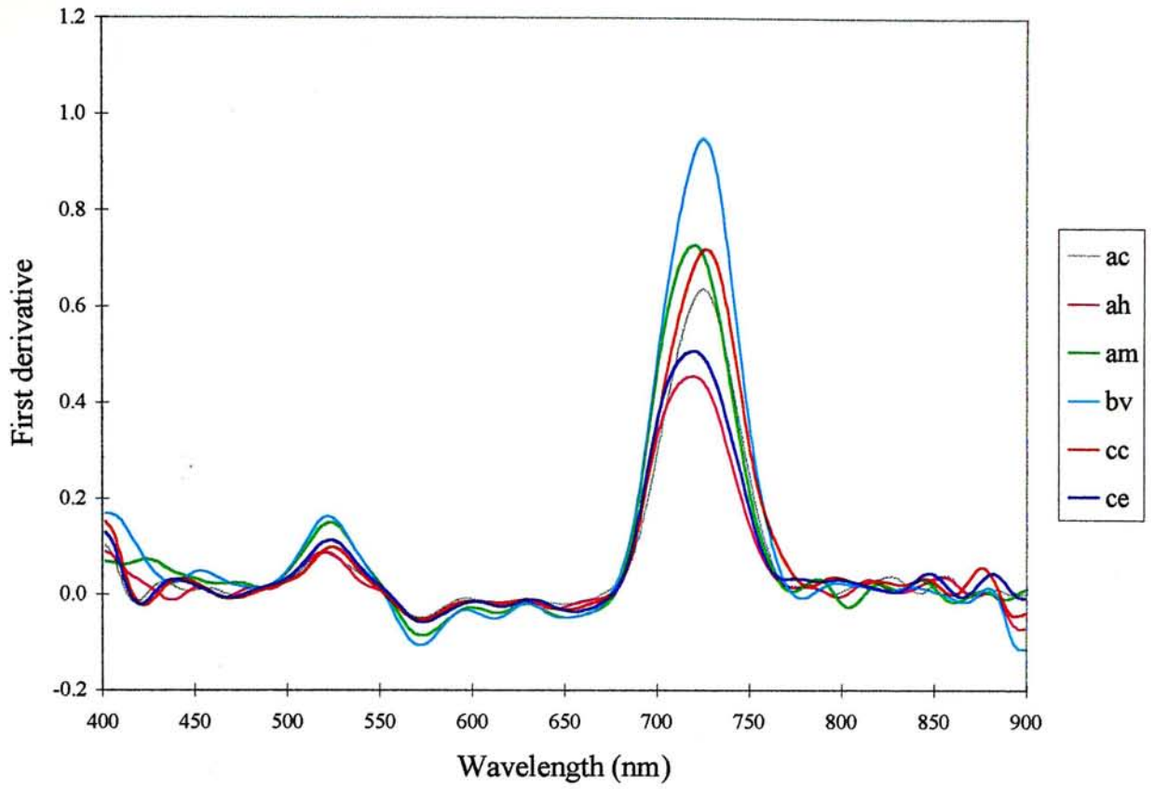

Figure 4.8b First derivatives of the second five tree species in winter

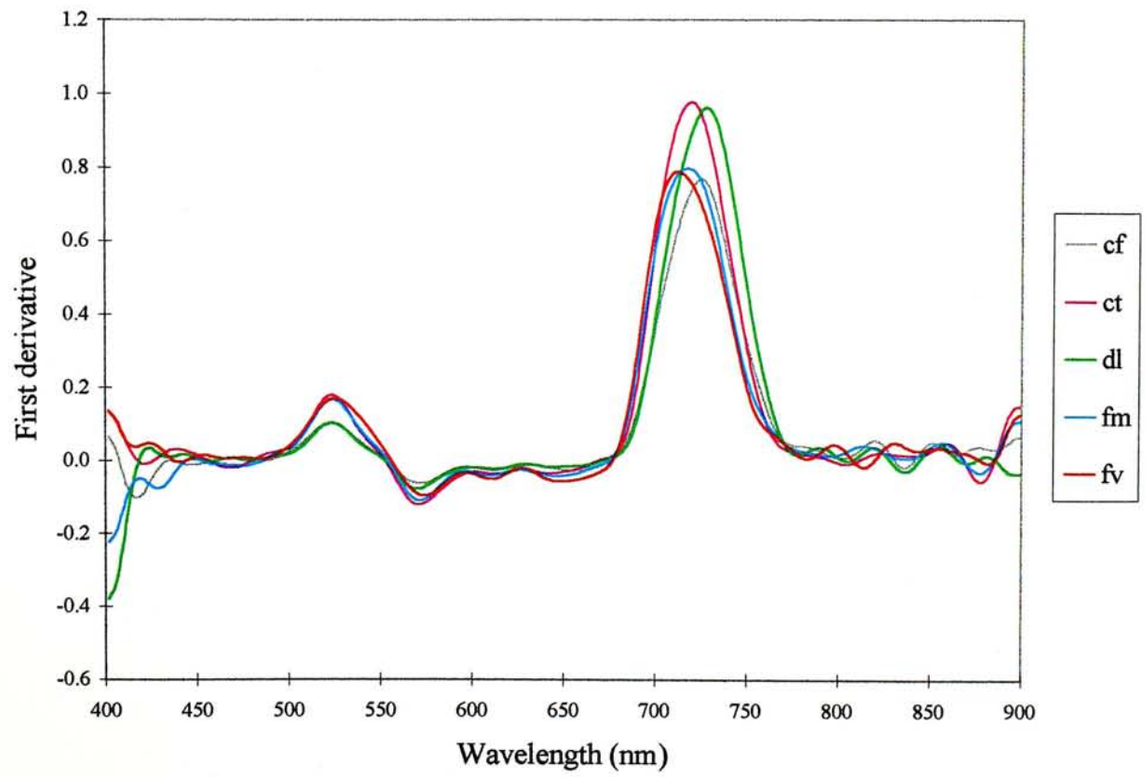

Figure 4.8c First derivatives of the third five tree species in winter

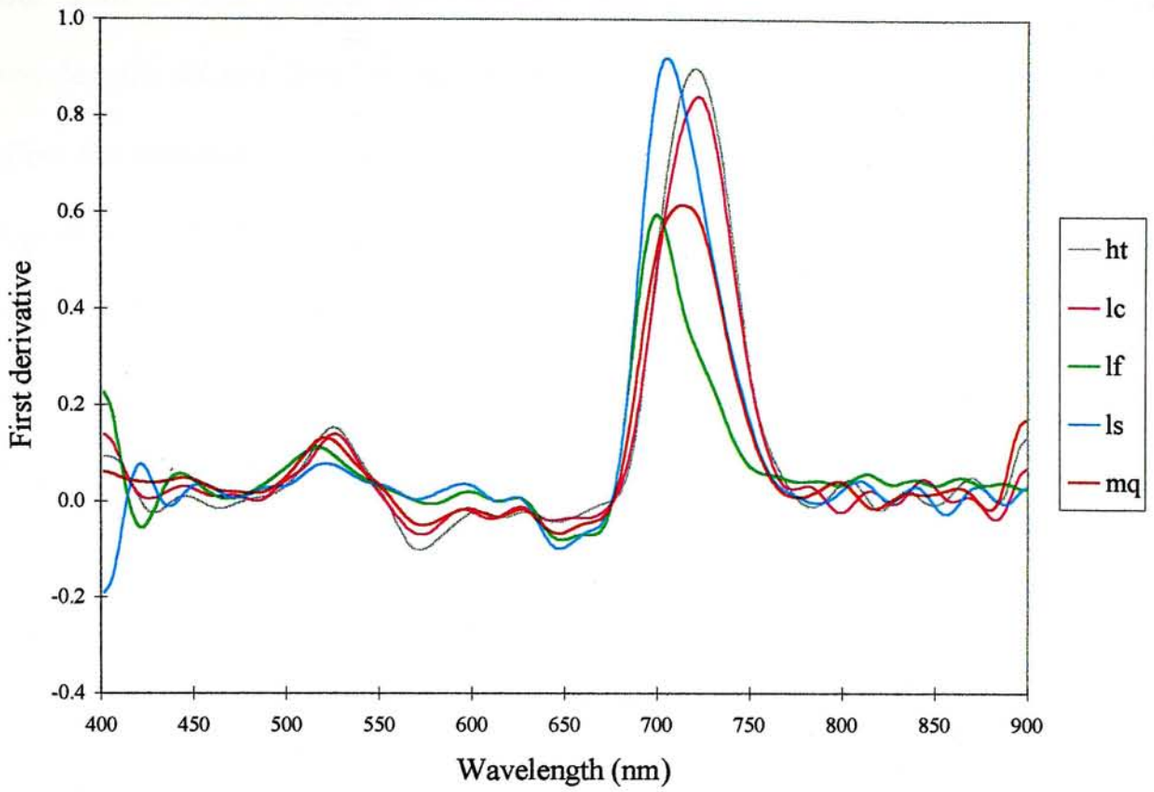

Figure 4.8d First derivatives of the fourth five tree species in winter

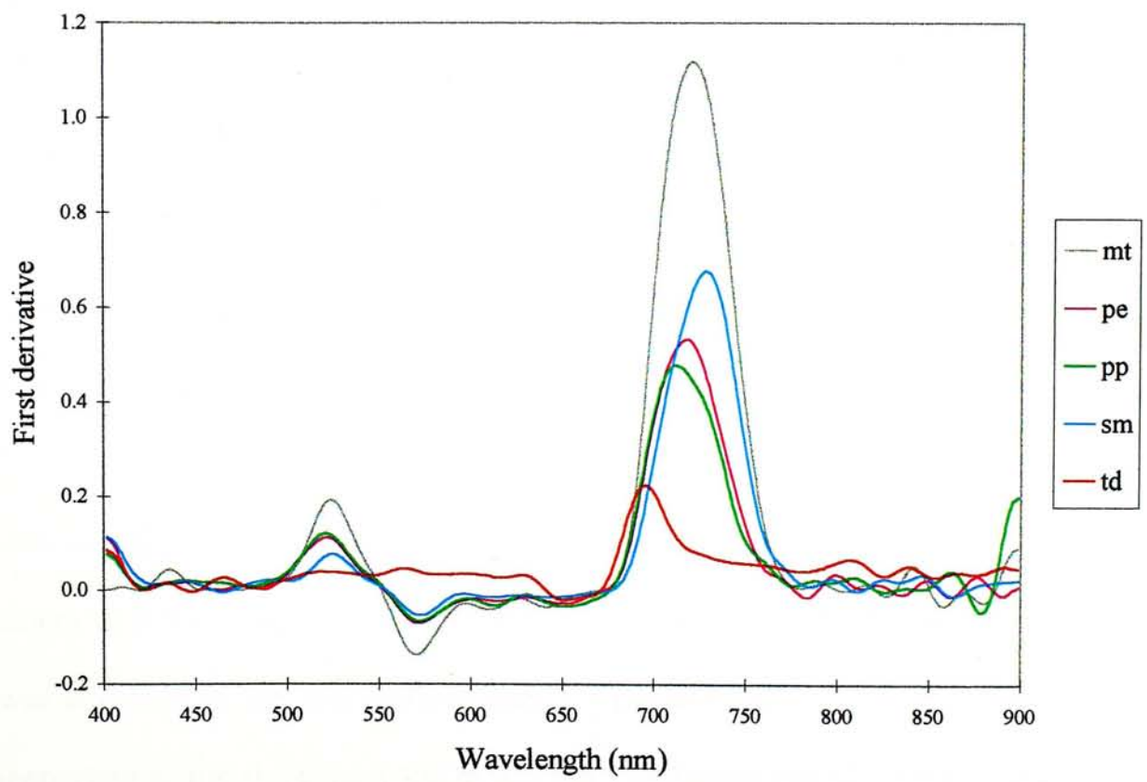

Figures 4.9 to 4.12 showed the second derivatives of the 25 tree species in the four seasons. The second derivatives tended to have rather noisy bands in the wavelengths shorter than 550 nm and longer than 770 nm. These noisy bands might affect the recognition of tree species and lead to unsatisfactory classification results. A positive peak at 510 nm and a negative peak at 530 nm demonstrated the positive peak at 525 nm found in the first derivatives. Similarly, a negative peak at 560 nm and a positive peak at 580 nm explained the negative peak at 570 nm in the first derivatives. The two small negative peaks found in the first derivatives between the green peak and the red edge were magnified in the second derivatives with some obvious small positive and negative peaks in this region. The peak found in the first derivatives at 725 nm created a dominant positive peak at 700 nm and a dominant negative peak at 750 nm in the second derivatives.

Figure 4.13 showed the spectral reflectance of the ten surface covers measured in the field. They were concrete, pond water, grass lawn, grass slope, fern (*Dicranopteris linearis*) and five tree species including *Acacia confusa*, *Castanopsis fissa*, *Dimocarpus longan*, *Ficus microcarpa* and *Taxodium distichum*. The five tree species, grass lawn and fern had similar reflectance pattern as those measured in the laboratory. Meanwhile, the spectral reflectance of fern appeared to be the greenest. It had the highest green peak comparing with those of tree species and grass lawn. Since grass in the site where reflectance of grass slope was measured did not grow well and quite a lot of bare soil was exposed which was a common situation for grass slopes in Hong Kong, the reflectance of grass slope showed no clear green peak but was still high in the near-infrared bands. Concrete had reflectance with constantly increasing gentle slope from 400 to 900 nm. Pond water had low reflectance in the

Figure 4.9a Second derivatives of the first seven tree species in spring

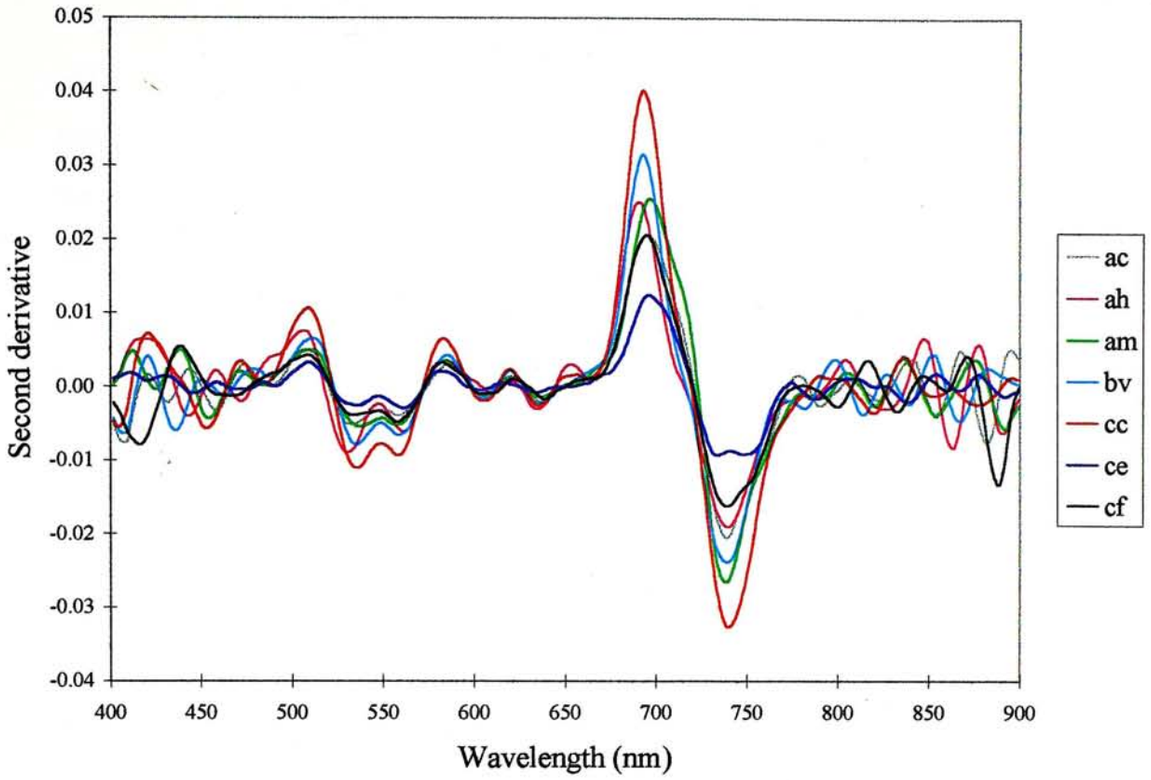

Figure 4.9b Second derivatives of the second six tree species in spring

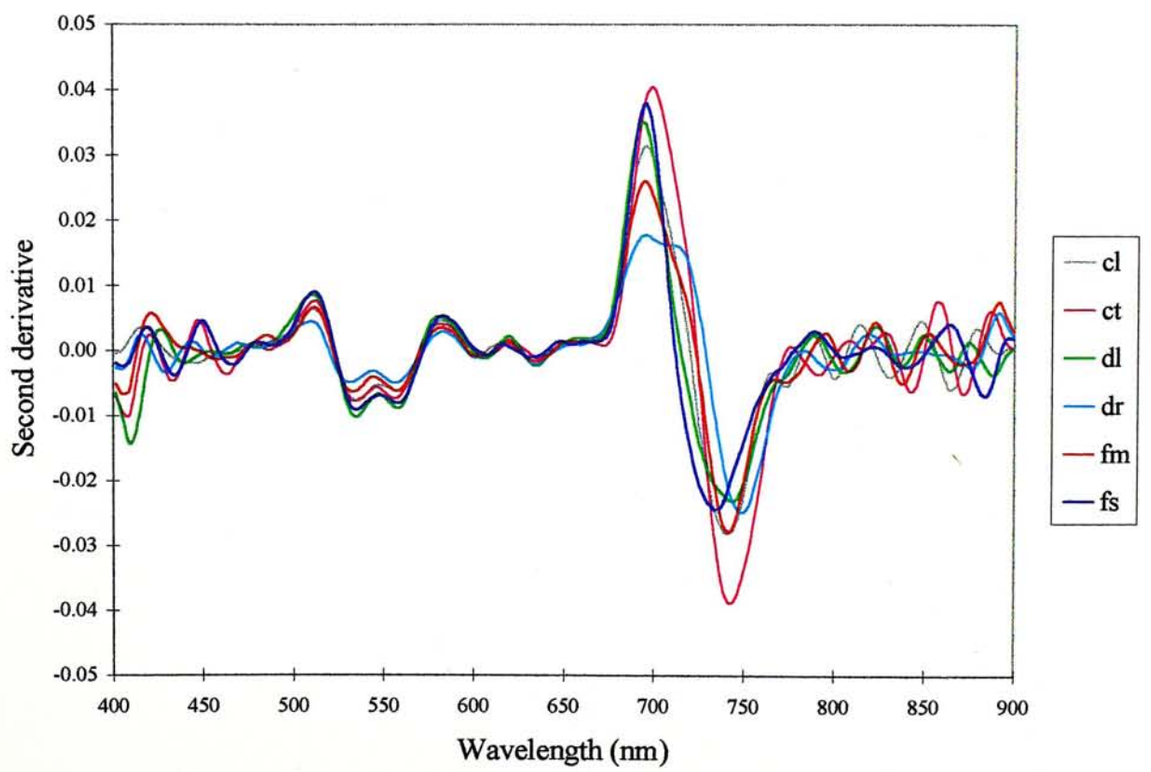

Figure 4.9c Second derivatives of the third six tree species in spring

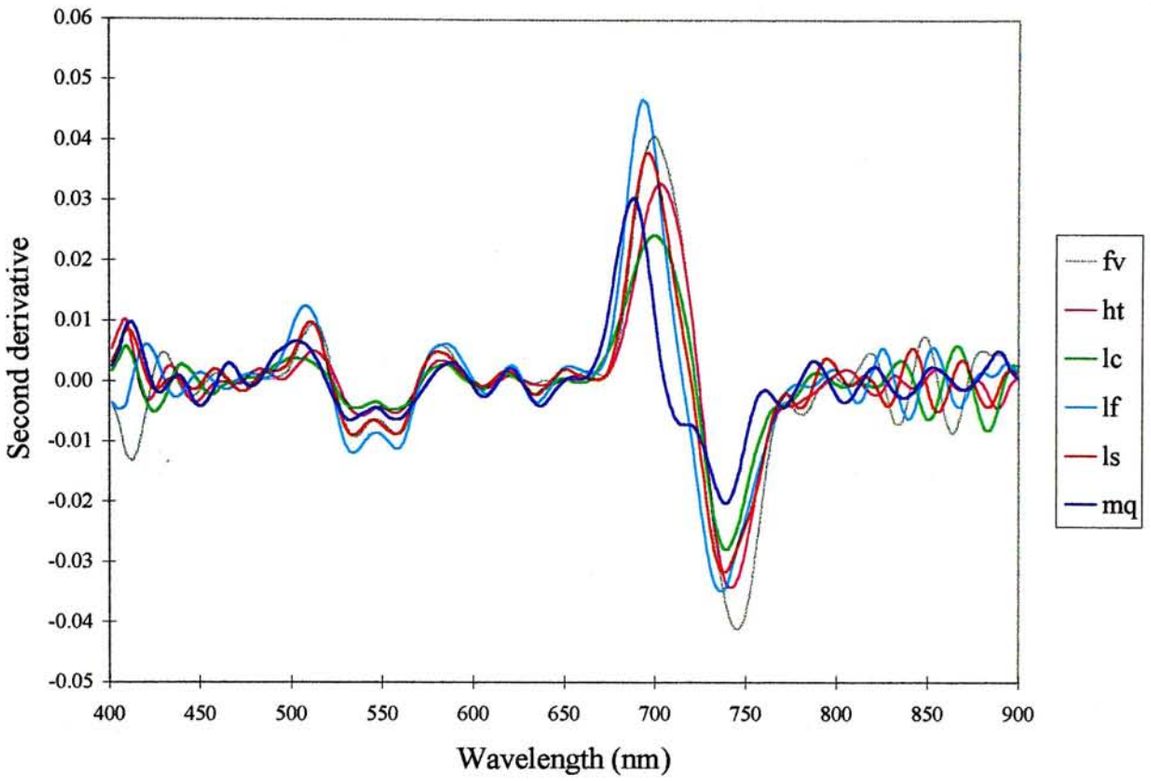

Figure 4.9d Second derivatives of the fourth six tree species in spring

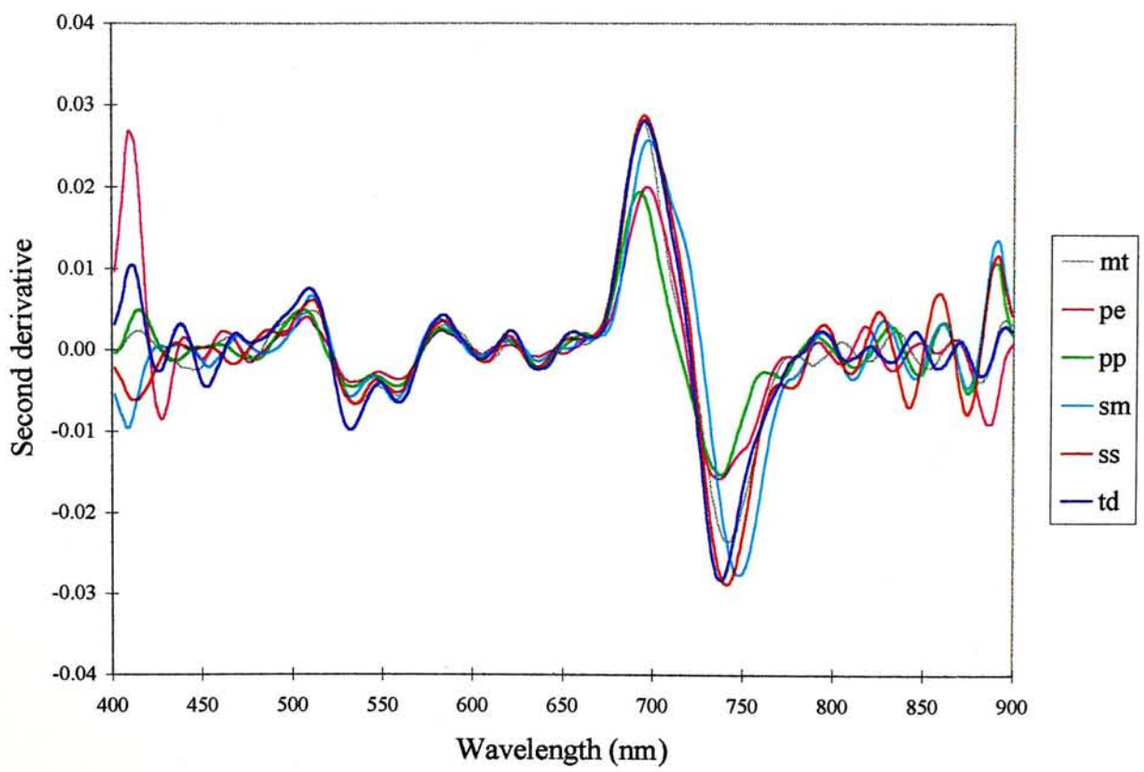

Figure 4.10a Second derivatives of the first seven tree species in summer

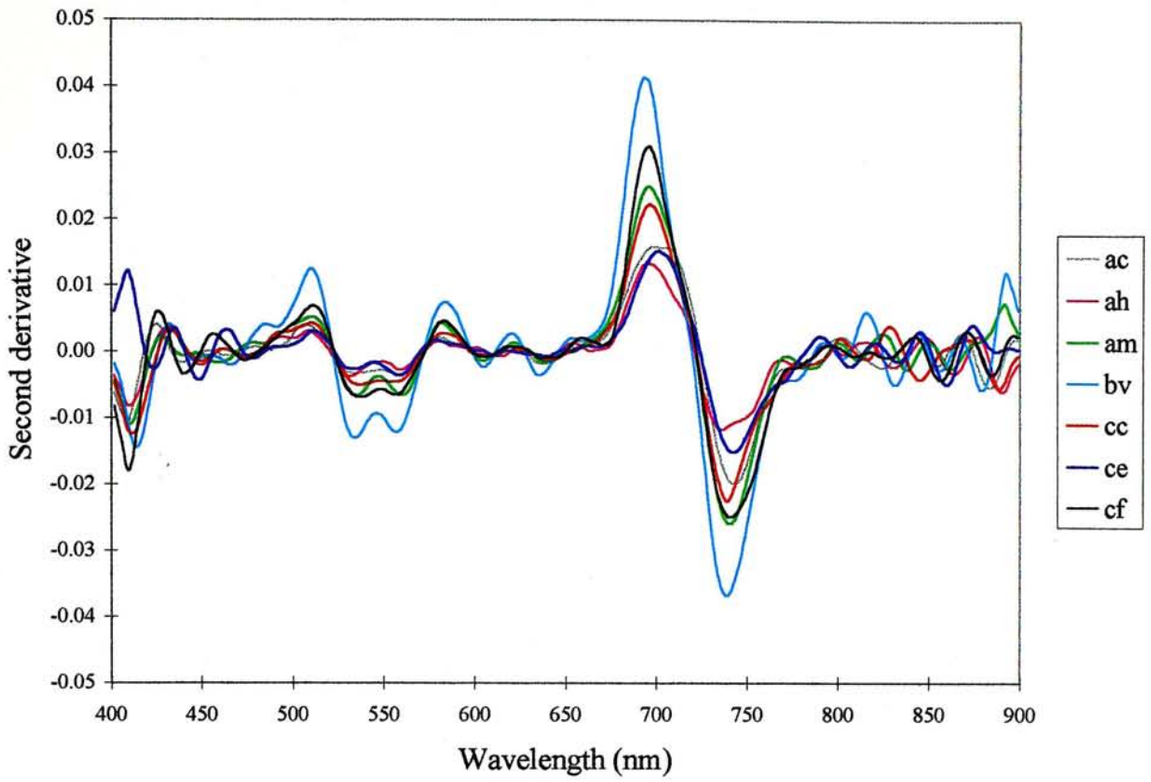

Figure 4.10b Second derivatives of the second six tree species in summer

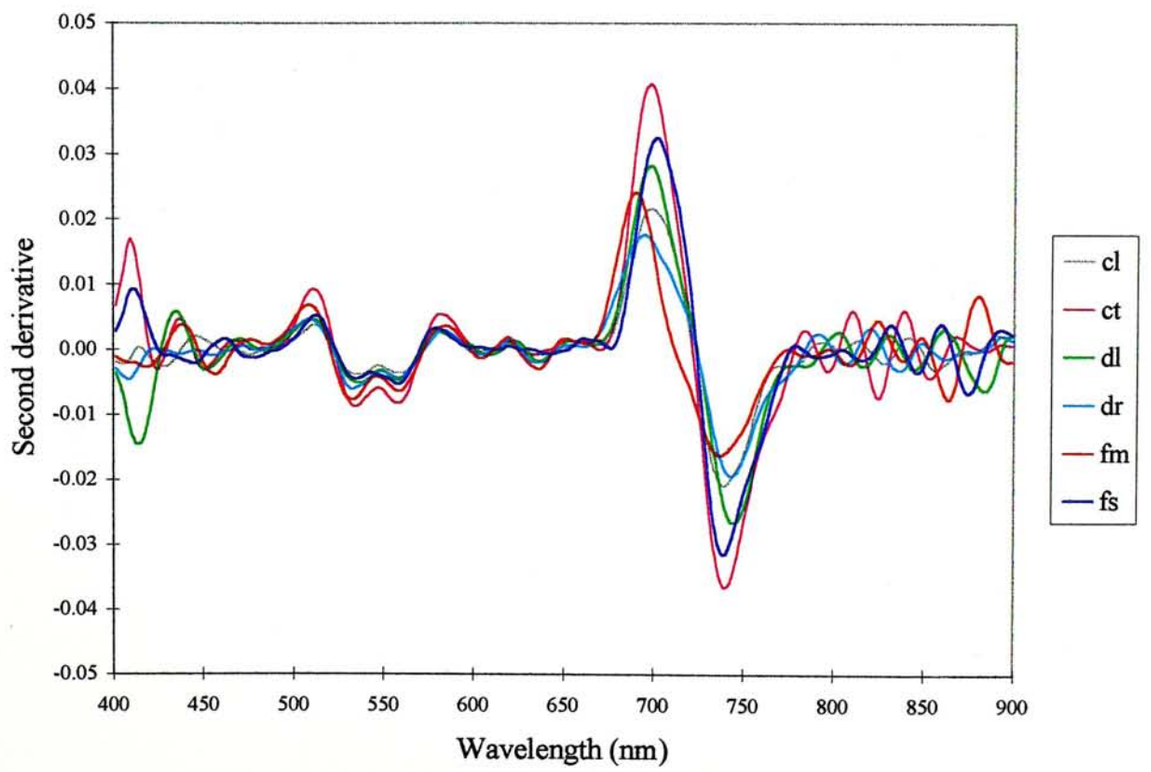

Figure 4.10c Second derivatives of the third six tree species in summer

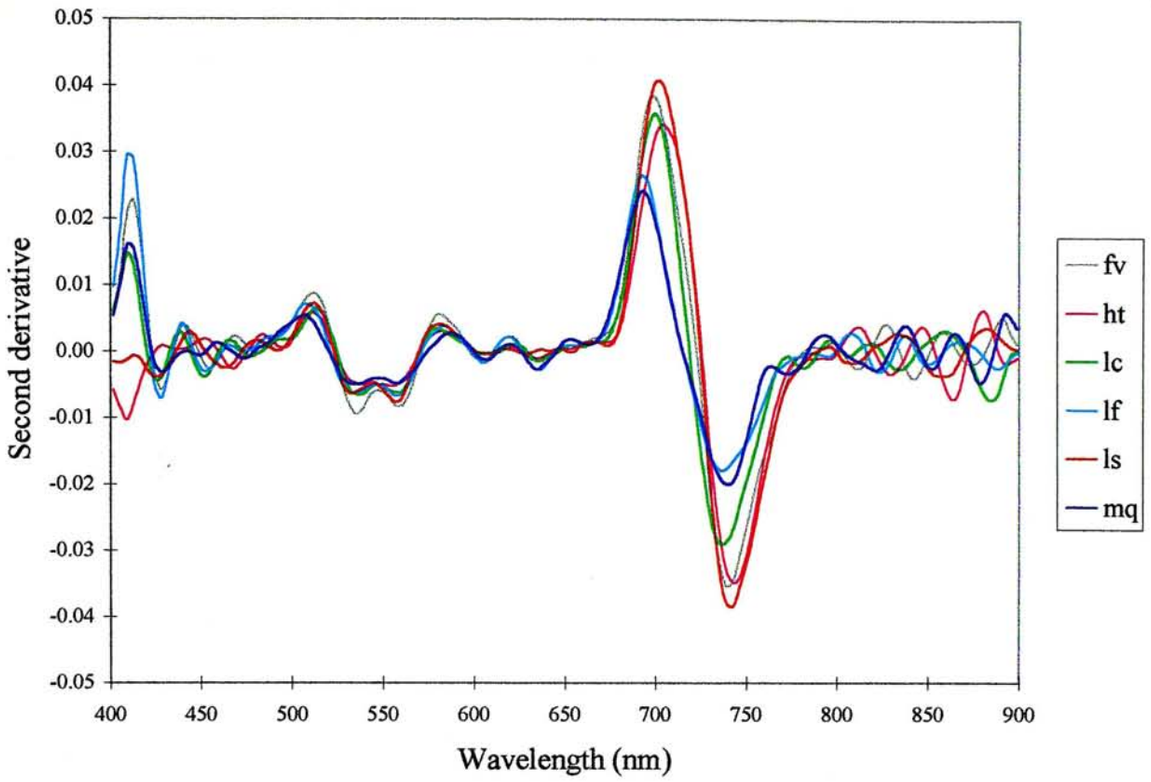

Figure 4.10d Second derivatives of the fourth six tree species in summer

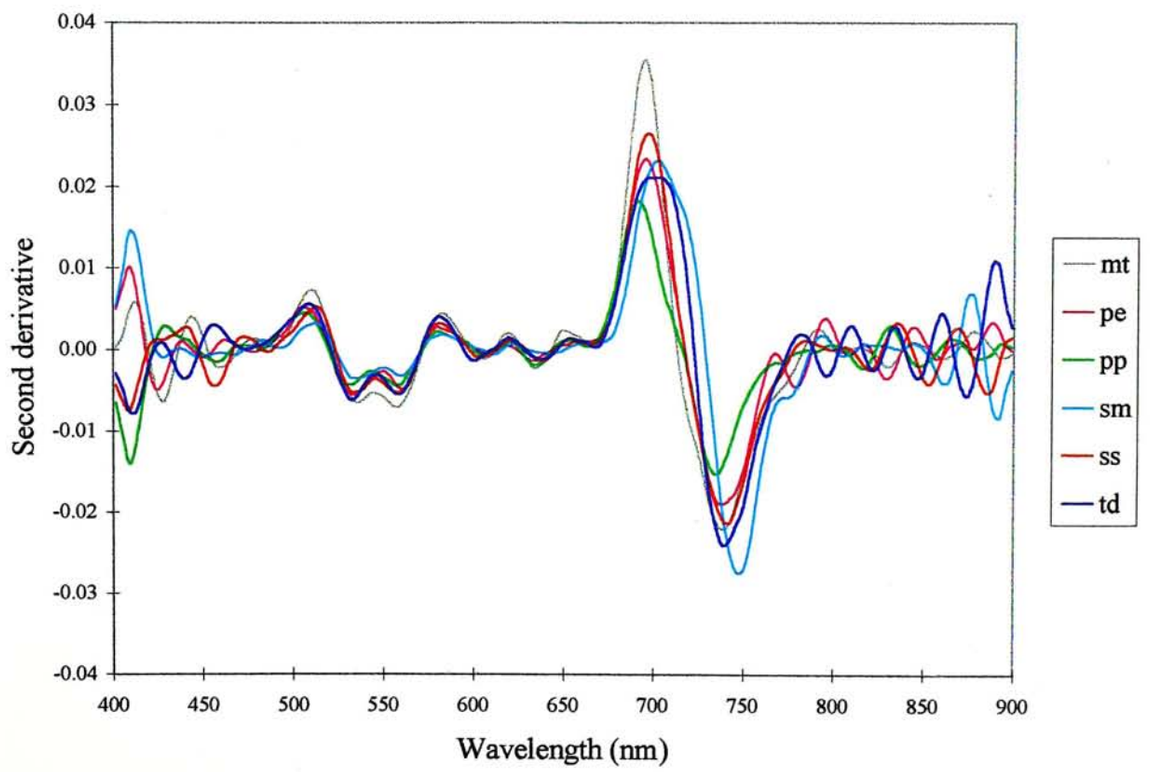

Figure 4.11a Second derivatives of the first six tree species in autumn

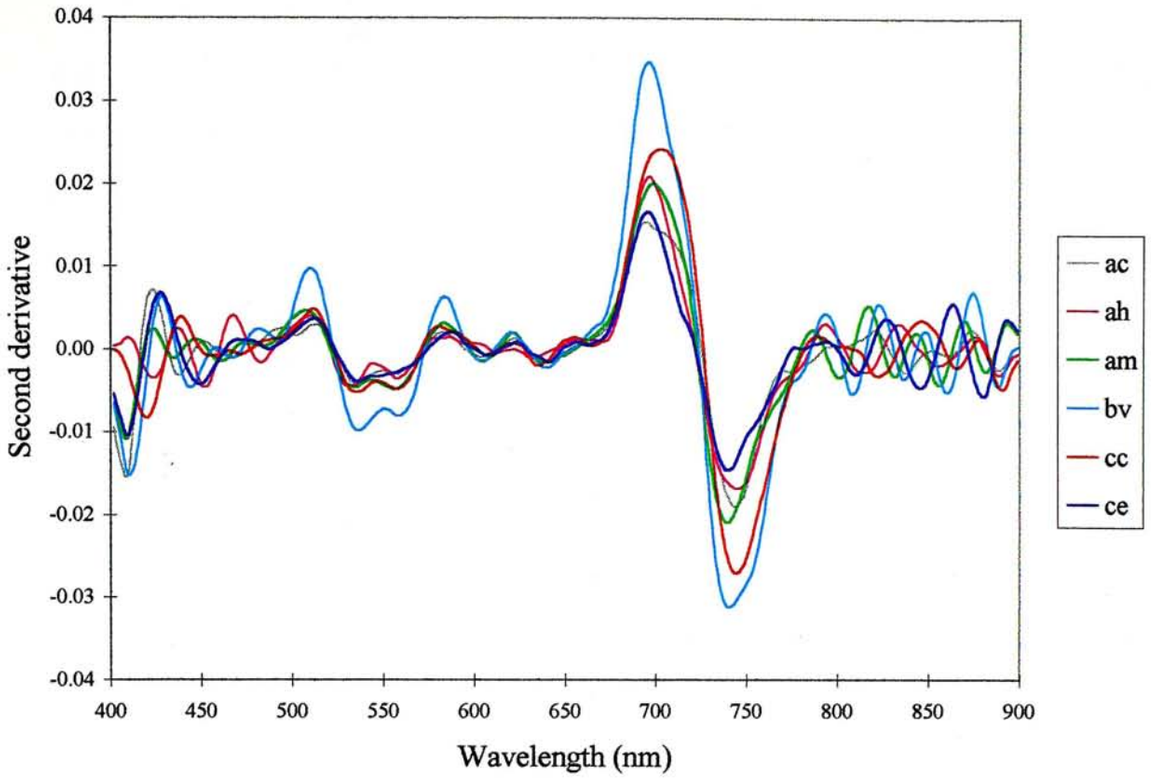

Figure 4.11b Second derivatives of the second six tree species in autumn

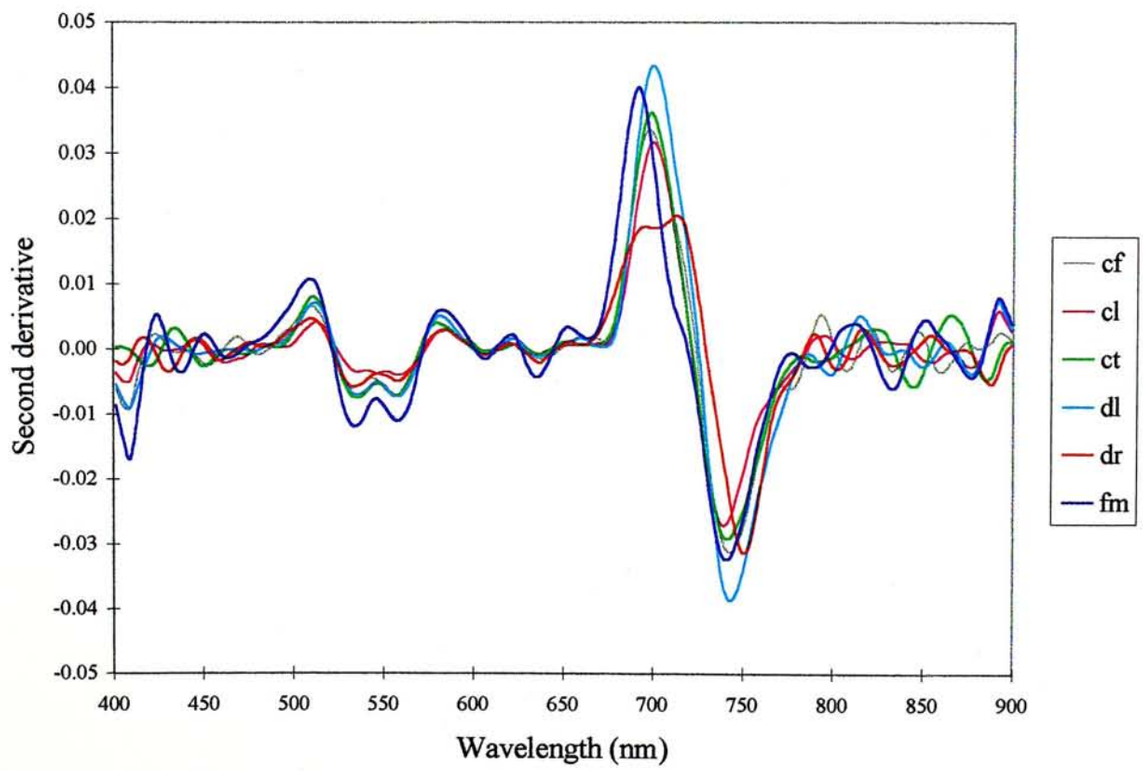

Figure 4.11c Second derivatives of the third six tree species in autumn

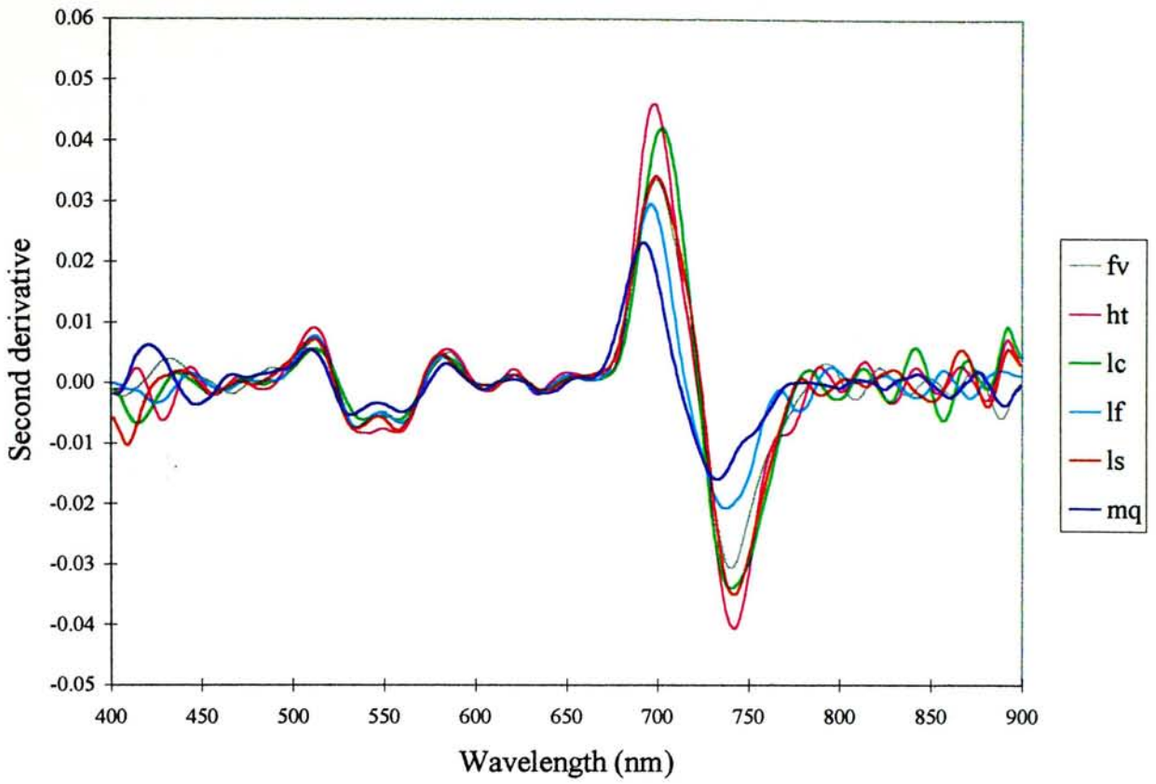

Figure 4.11d Second derivatives of the fourth six tree species in autumn

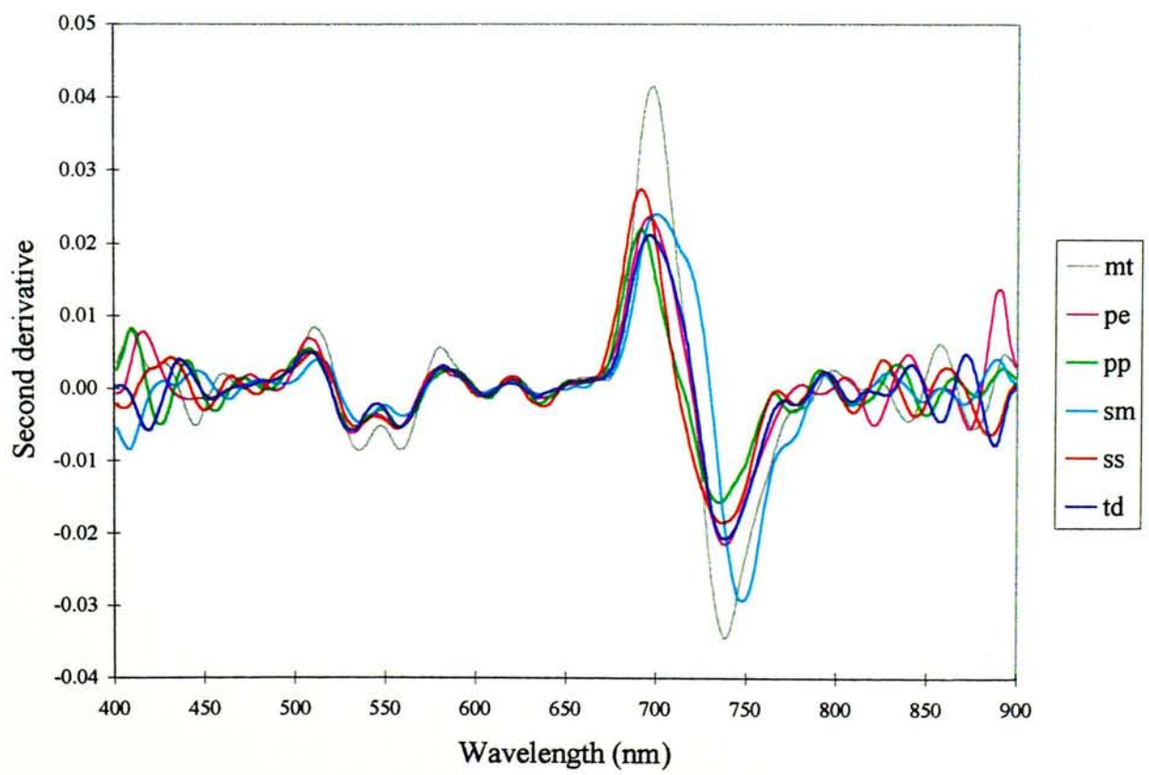

Figure 4.12a Second derivatives of the first six tree species in winter

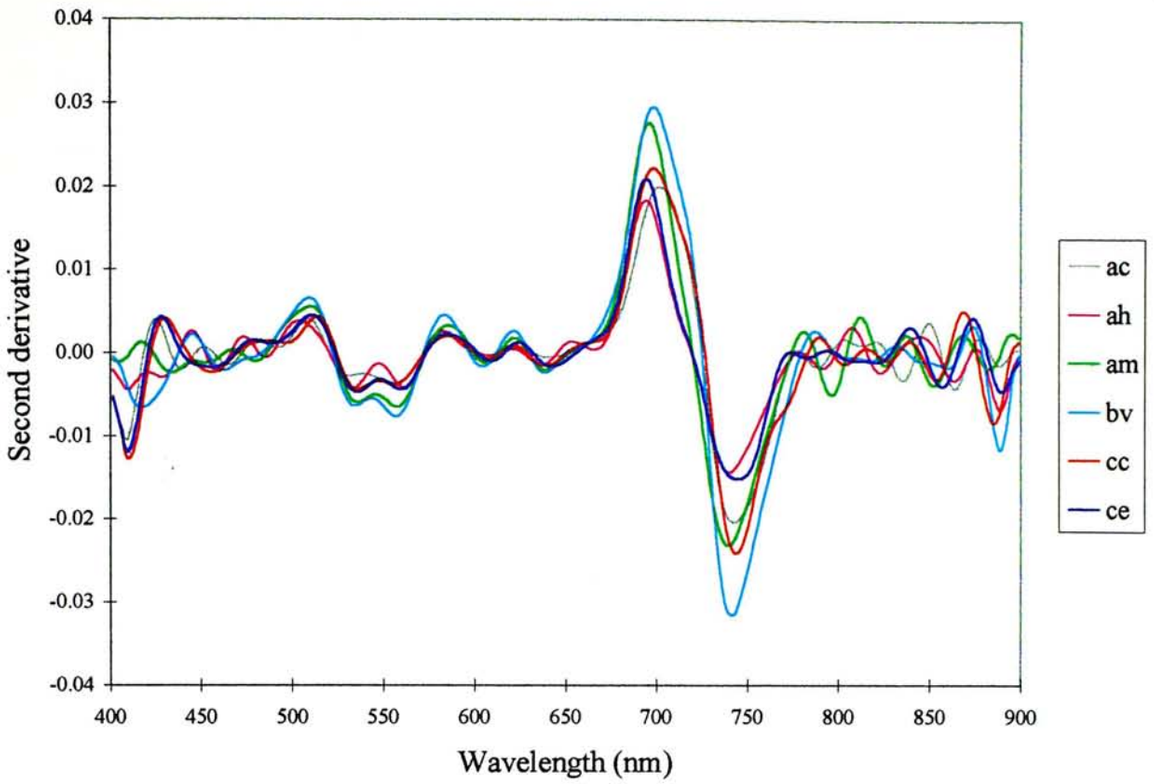

Figure 4.12b Second derivatives of the second five tree species in winter

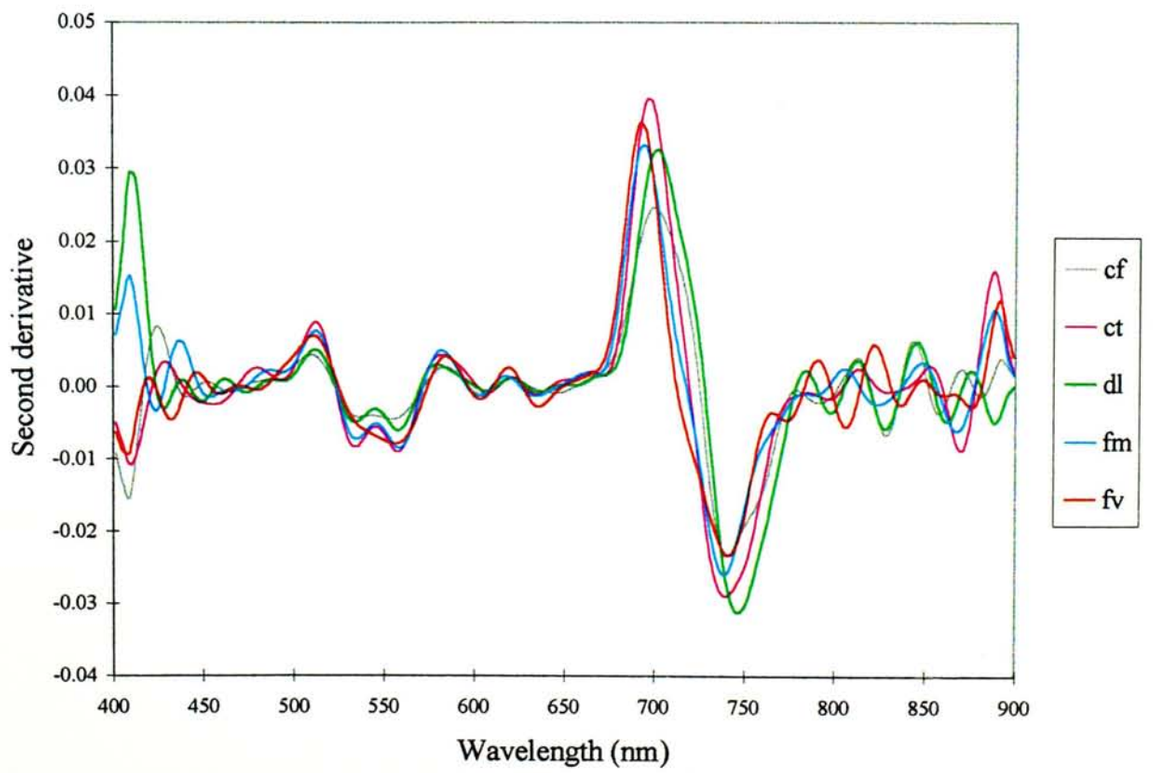

Figure 4.12c Second derivatives of the third five tree species in winter

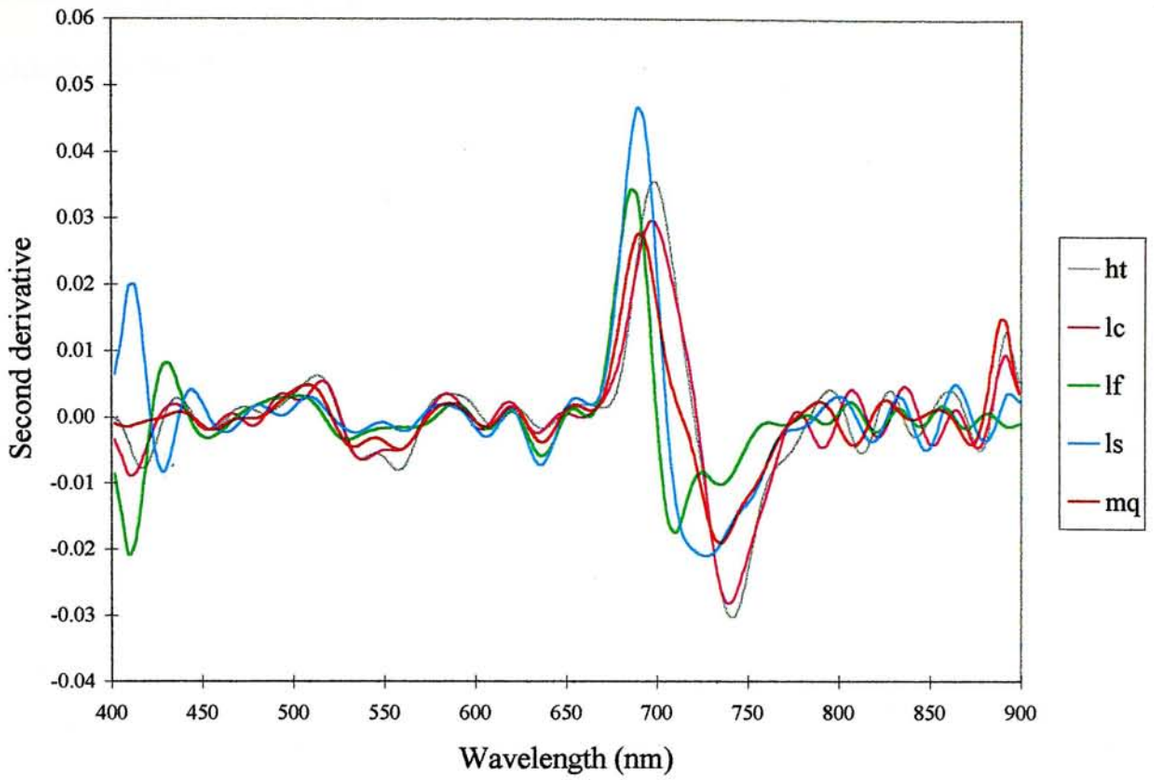

Figure 4.12d Second derivatives of the fourth five tree species in winter

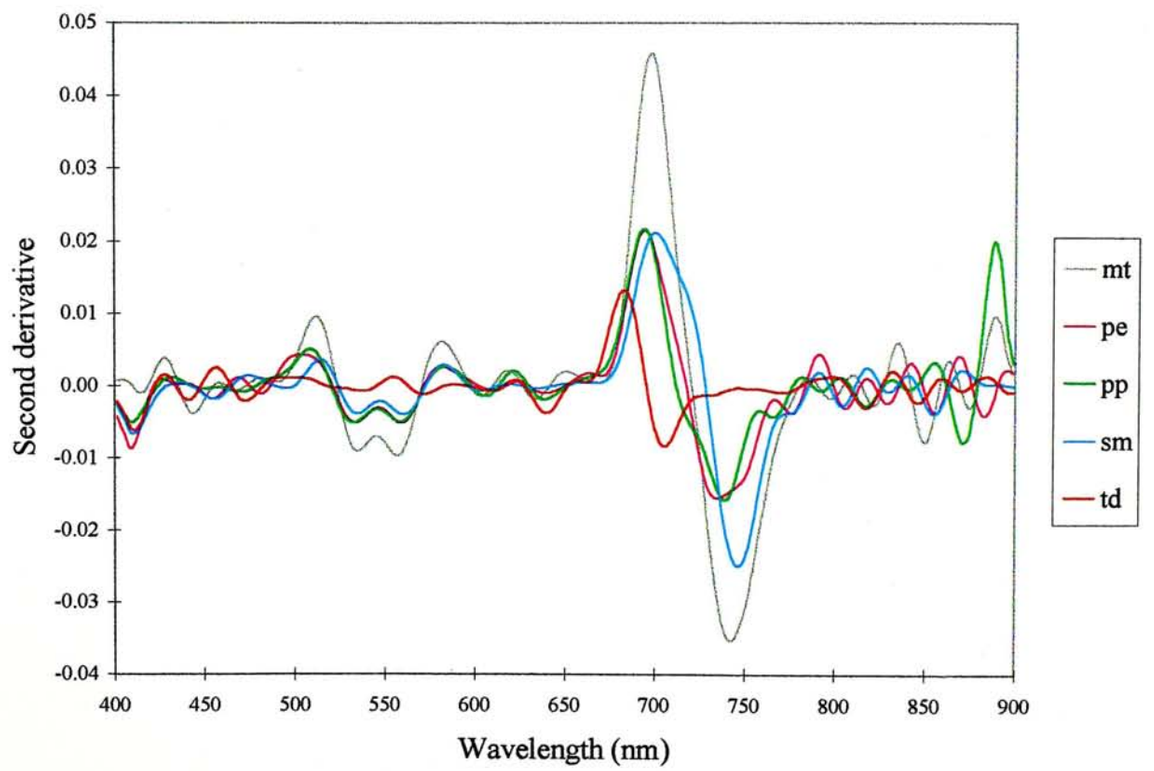

near-infrared bands which was a typical feature for the reflectance of water body. Relatively higher reflectance was found in the visible bands with a dominant peak centered at 560 nm.

Figure 4.13. Reflectance spectral curves of the *in situ* surface covers

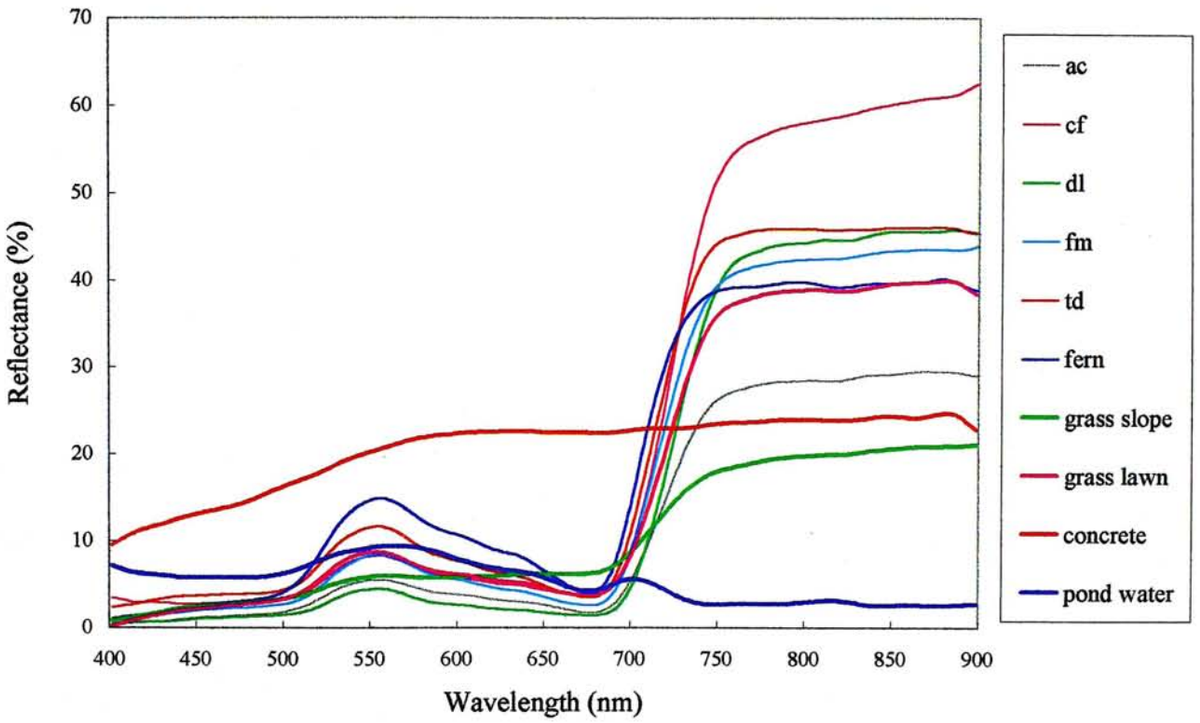

Appendix 1 showed the plots of spectral reflectance of the 25 tree species in different seasons for each density level. Each curve was the average of 12 spectra measured in different seasons for each density level. Different seasonal patterns could be traced visually from the plots. Some deciduous tree species, for example, *Liquidambar formosana*, *Lagerstroemia speciosa* and *Taxodium distichum*, had obvious annual cycle. In spring, new green leaves started to grow again. New-growth leaves tended to be in lighter and brighter green color so that spectral reflectance were the highest in spring. In winter, leaves changed from green to red and yellow in the beginning of winter and finally fell. A reduction in green and near-infrared reflectance and a gain in yellow and red reflectance were found. This pattern was obviously noticed in the spectral curves of *Taxodium distichum.* The green peak and the near-infrared bands were the highest in spring while these bands were lower in summer and autumn. In winter, the green peak disappeared. The reflectance increased gradually from 400 nm to 600 nm. A small peak was found centered at around 640 nm presenting the red bands and the reflectance dropped into a small trough centered at 680 nm. From 680 nm onwards, a relatively steep rise occurred until 720 nm presenting the red edge. In the near-infrared region from 720 nm to 900 nm, the reflectance increased with a gentle slope instead of leveled off.

Other deciduous tree species, for example, *Ficus variegata* lost their leaves in late winter so that spectral measurement could be done before their leaves disappeared. Their leaves turned dull and dry in winter while new-grown leaves in spring were bright and light green. Thus, the spectral reflectance especially for the green peak and the near-infrared bands were higher in spring and summer but lower in autumn and winter. There was no consistent pattern for evergreen trees. Some

evergreen tree species, for example, *Acacia mangium* and *Cinnamomum camphora*, had higher spectral reflectance in spring and summer and lower reflectance in autumn and winter. Especially for *Cinnamomum camphora*, the green peak and the near-infrared regions in spring were dominantly higher than those in other seasons. However, some evergreen species got a reversed pattern such as *Ficus microcarpa* and *Lophostemon conferta*. The green peak and the near-infrared regions of *Ficus microcarpa* were especially higher in autumn than those in other seasons.

4.3. Tree species recognition

The 25 tree species were classified by two recognition algorithms, linear discriminant analysis (DA) and artificial neural networks (NN). Table 4.1 showed the classification results of the four seasonal data sets by these two algorithms. The confusion matrices for each classification using linear discriminant analysis and neural networks were listed in Appendix 2 and Appendix 3 respectively. The overall accuracies for linear discriminant analysis ranged from 9.07% to 80.69% and those for neural networks were from 40.40% to 76.67%. Except the very poor results obtained by linear discriminant analysis using derivatives data, the classification results were satisfactory particularly for the original spectral reflectance data which yielded over 70% overall accuracy. It confirmed the discriminating power of hyperspectral data to recognize different tree species.

Table 4.1. Classification results of tree species recognition using all 138 bands

Original Spectra

	DA		*NN*		
	OA (%)	*Kappa (×100)*	*OA (%)*	*Kappa (×100)*	$Z_{DA,\,NN}{}^{a}$
Spring	74.27	73.19	72.27	71.11	0.8751
Summer	68.93	67.64	72.40	71.25	-1.4762
Autumn	80.69	79.86	76.67	75.65	1.8931
Winter	70.16	68.67	74.29	73.00	-1.6378
Average accuracy	73.51	72.34	73.91	72.75	

First Derivatives

	DA		*NN*		
	OA (%)	*Kappa (×100)*	*OA (%)*	*Kappa (×100)*	$Z_{DA,\,NN}{}^{a}$
Spring	20.67	17.36	60.40	58.75	-17.2458
Summer	9.07	5.28	62.13	60.56	-25.9166
Autumn	17.36	13.77	63.19	61.59	-20.0825
Winter	14.44	10.17	61.59	59.67	-19.9130
Average accuracy	15.39	11.65	61.83	60.14	

Second Derivatives

	DA		*NN*		
	OA (%)	*Kappa (×100)*	*OA (%)*	*Kappa (×100)*	$Z_{DA,\,NN}{}^{a}$
Spring	9.73	5.97	40.40	37.92	-14.9923
Summer	10.40	6.67	49.87	47.78	-18.6676
Autumn	13.61	9.86	50.14	47.97	-16.2671
Winter	25.87	22.17	50.48	48.00	-9.3461
Average accuracy	14.90	11.17	47.72	45.42	

$^{a}Z_{DA,NN} = \dfrac{K_{DA} - K_{NN}}{\sqrt{V(K_{DA}) + V(K_{NN})}}$ where K_{DA} and K_{NN} are the Kappas calculated from the classification results using linear discriminant analysis and neural networks respectively.

When the confusion matrices were compared with one another, no consistency was found among the patterns of classification and misclassification. Table 4.2 showed a summary of the classification results of each tree species for the four seasons using original spectra. The average accuracy of each tree species was calculated and compared. The average accuracy of *Bauhinia variegata* was 91.25% which was the highest among all tree species. *Bauhinia variegata* had large leaves and possessed the highest reflectance in green and near-infrared spectral regions in

the four seasons which made it more distinctive from other species. *Araucaria heterophylla, Delonix regia, Liquidambar formosana, Melaleuca quanqueenervia, Sapium sebiferum* and *Taxodium distichum* also obtained good classification results with the average accuracy of 80% to 84%. On the contrary, *Ficus microcarpa* got the lowest average accuracy among all with only 60.00% whilst *Castanopsis fissa, Dimocarpus longan* and *Lophostemon conferta* had average accuracy of 61% to 65%. Unlike *Bauhinia variegata*, these trees did not have any particularly distinctive characteristics in terms of leaf size and spectral reflectance which made them more easily differentiated from each other. The confusion matrices also did not reveal a consistent confusion pattern (Appendix 2 and 3).

Table 4.2 Classification results of each tree species using original spectra for the four seasons

	Spring		Summer		Autumn		Winter		Overall accuracy of each tree species (%)
	DA	NN	DA	NN	DA	NN	DA	NN	
ac	66.67	33.33	83.33	100.00	76.67	93.33	43.33	56.67	69.17
ah	100.00	86.67	83.33	96.67	90.00	83.33	80.00	40.00	82.50
am	66.67	66.67	40.00	40.00	96.67	96.67	50.00	83.33	67.50
bv	93.33	100.00	100.00	93.33	96.67	86.67	83.33	76.67	91.25
cc	70.00	83.33	43.33	60.00	90.00	93.33	56.67	56.67	69.17
ce	70.00	96.67	53.33	100.00	80.00	83.33	63.33	86.67	79.17
cf	70.00	50.00	76.67	56.67	73.33	50.00	56.67	56.67	61.25
cl	53.33	83.33	50.00	56.67	93.33	96.67	-	-	72.22
ct	93.33	73.33	70.00	70.00	83.33	93.33	90.00	33.33	75.83
dl	53.33	30.00	66.67	53.33	86.67	70.00	66.67	90.00	64.58
dr	90.00	70.00	93.33	70.00	80.00	100.00	-	-	83.89
fm	60.00	23.33	43.33	23.33	96.67	96.67	56.67	80.00	60.00
fs	60.00	90.00	63.33	90.00	-	-	-	-	75.83
fv	86.67	73.33	83.33	90.00	76.67	13.33	66.67	96.67	73.33
ht	86.67	93.33	66.67	83.33	86.67	56.67	66.67	66.67	75.84
lc	56.67	76.67	73.33	33.33	96.67	50.00	63.33	56.67	63.33
lf	90.00	66.67	86.67	86.67	100.00	63.33	86.67	76.67	82.09
ls	60.00	40.00	73.33	43.33	70.00	56.67	93.33	96.67	66.67
mq	93.33	100.00	53.33	70.00	76.67	96.67	83.33	90.00	82.92
mt	63.33	33.33	60.00	73.33	70.00	76.67	83.33	76.67	67.08
pe	70.00	83.33	83.33	86.67	46.67	50.00	83.33	73.33	72.08
pp	63.33	90.00	63.33	90.00	70.00	93.33	66.67	76.67	76.67
sm	56.67	96.67	76.67	70.00	80.00	86.67	33.33	90.00	73.75
ss	100.00	83.33	53.33	86.67	70.00	93.33	-	-	81.11
td	83.33	83.33	83.33	86.67	50.00	60.00	100.00	100.00	80.83
Average overall accuracy of each algorithm (%)	74.27	72.27	68.93	72.40	80.69	76.67	70.16	74.29	

4.3.1. Comparison of different classifiers

Table 4.1 showed the classification results of the two classifiers and also the results of significant testing of Kappa between the two classifiers. For the classifications using original spectra, discriminant analysis obtained better results for spring and autumn with overall accuracy of 74.27% and 80.69% respectively while neural network algorithm was better for summer and winter with overall accuracy of 72.40% and 74.29% respectively. However, the differences were not statistically significant as all absolute values of Z were less than the critical value of 1.96 at 0.05 significance level. In addition, the average overall accuracy of four seasons for discriminant analysis and neural network is 73.51% and 73.91% respectively which also suggested no significant differences for the two classifiers.

For the classifications using first and second derivatives, the differences between neural networks and discriminant analysis were greatly significant. Neural networks generated average overall accuracy of 61.83 and 47.72% by using first and second derivatives respectively. However, the average overall accuracy generated by discriminant analysis were extremely poor with 15.39% and 14.90% by using first and second derivatives respectively. Neural networks outperformed discriminant analysis by using either first or second derivatives. It has been shown earlier that within the first derivatives data, many spectral bands had data value close to zero whilst the second derivatives data possessed a lot of noisy bands. The presence of these bands might have detrimental effect on the classification results in using linear discriminant analysis which relied on the ratio of between-group variance versus within-group variance as zero data values and noisy bands might decrease these ratio. This effect was less critical in neural networks which was more adaptive to the data

themselves.

4.3.1.1. Efficiency of the classifiers

For the efficiency of the classifiers, discriminant analysis worked better than neural networks in two aspects. Firstly, the training process required to produce a neural network was extremely time and computational intensive although the trained classifier worked very fast. It spent more than one day on a Sun SPARCstation 10 for the training process. On the contrary, discriminant analysis was less time and computation consuming. Only a few seconds were used for the training and testing process on the same system used by the neural networks. Secondly, neural networks needed to specify obscure parameters such as learning rate, momentum rate, hidden layer size and training convergence criterion which made neural network less convenient and more difficult to use.

4.3.1.2. Discussions

After discussing the performance of the two classifiers in terms of their classification accuracy and efficiency, several implications can be drawn. The new technique, neural networks did outperform the traditional linear discriminant analysis in classification accuracy for the derivatives data. But the results were indifferent if the original spectra were used. The advantages of neural network to deal with distribution-free, nonlinear, multi-source and ancillary data make it a trend for classification technique in the future. However, neural network algorithms are still not mature enough for classification of hyperspectral data. The large number of input nodes and output nodes necessitates lengthy training time and a number of parameters such as learning rate and momentum rate need to be specified. These two

factors can solely hinder users from choosing neural networks for classification. For efficiency, it is obvious that linear discriminant analysis excels.

The backpropagation feed-forward neural network used in this study was among the slowest neural networks developed so far. Apart from backpropagation feed-forward neural network, another neural network, Kohonen's learning vector quantization (LVQ) has been used and tested (Neural Network Research Center, 1998). The time for training and testing process is only a few seconds which is much shorter than that used by backpropagation feed-forward neural network. However, the results were not satisfactory. Classification accuracy of around 20% was obtained for classifying an original spectra data set. More studies should be made to develop convenient and fast neural networks for hyperspectral data analysis.

4.3.2. Comparison of different data processing strategies

Using the original spectra produced better results than using either the first or the second derivatives. It is particularly obvious when discriminant analysis is used. Table 4.3 showed the significant testing of Kappa comparing different data processing strategies. Overall accuracy generated from discriminant analysis ranged from 70.16% to 80.69% for the four seasons using the original spectra. But it reduces to only 9.07% to 25.87% when using the first and second derivatives. The significant testing of Kappa also demonstrated very high degree of significance between the original spectra and the derivatives spectra.

Table 4.3. Significant testing of Kappas for comparing different data processing strategies (absolute value > 1.96 indicates significant difference at 0.05 significance level)

Spring Data

	Original spectra		*First derivatives*		*Second derivatives*	
	DA	*NN*	*DA*	*NN*	*DA*	*NN*
Original spectra	-	-	14.7477	4.9165	33.6111	13.3402
First derivatives	-14.7477	-4.9165	-	-	6.0276	8.0294
Second derivatives	-33.6111	-13.3402	-6.0276	-8.0294	-	-

Summer Data

	Original spectra		*First derivatives*		*Second derivatives*	
	DA	*NN*	*DA*	*NN*	*DA*	*NN*
Original spectra	-	-	30.2852	4.2692	29.2339	9.2341
First derivatives	-30.2852	-4.2692	-	-	-0.8947	4.8338
Second derivatives	-29.2339	-9.2341	0.8947	-4.8338	-	-

Autumn Data

	Original spectra		*First derivatives*		*Second derivatives*	
	DA	*NN*	*DA*	*NN*	*DA*	*NN*
Original spectra	-	-	31.1192	5.6466	34.6128	10.9074
First derivatives	-31.1192	-5.6466	-	-	1.9814	5.0549
Second derivatives	-34.6128	-10.9074	-1.9814	-5.0549	-	-

Winter Data

	Original spectra		*First derivatives*		*Second derivatives*	
	DA	*NN*	*DA*	*NN*	*DA*	*NN*
Original spectra	-	-	24.4815	4.8805	17.6258	9.0270
First derivatives	-24.4815	-4.8805	-	-	-5.1881	4.2138
Second derivatives	-17.6258	-9.0270	5.1881	-4.2138	-	-

For neural networks, overall accuracy ranging from 72.27% to 76.67% were produced using original spectra. Using first and second derivatives generated lower overall accuracy of 60.40% to 63.19% and 40.40% to 50.48% respectively. The tests of significance, again, invoked that using original spectra was significantly better than using derivatives data. The poor results obtained by derivatives data contradict the results done by previous researchers. For example, Gong *et al.* (1997) obtained higher overall accuracy in classifying six tree species with spectral derivatives than reflectance spectra using neural networks. Their spectral measurements were made in the field which background soil effect posed an important factor on the reflectance

spectral data. Derivatives procedure could partly remove the effects of low frequency background soil spectra in target spectra, therefore, leading to an increase in recognition accuracy. However, spectral measurements in this study were taken in a controlled environment where a black cloth was used as a background to minimize the background effect. Thus, derivatives procedure did not help to improve recognition accuracy in this study. On the contrary, it enhanced noise during the procedure and led to decreased recognition accuracy.

The difference between first and second derivatives spectra was not obvious using discriminant analysis. Spring and autumn data produced higher overall accuracy using first derivatives but summer and winter data had opposite results. However, neural networks yielded significantly better results when using first derivatives than using second derivatives. Using first derivatives produced an average overall accuracy of 61.83% which was 14.11% higher than that of using second derivatives. The very noisy bands in second derivatives with wavelengths shorter than 550 nm and wavelengths longer than 770 nm might reduce the classification accuracy in second derivatives.

4.3.3. Comparison of data among different seasons

Vegetation changes during the course of a year, especially for deciduous trees which lose their leaves during winter. The changes of leaf colors from green to red and yellow during autumn and winter can markedly affect their spectral reflectances. Besides, many trees have distinct seasonal peaks of growth, flowering and fruiting activities that can also affect spectral reflectance. Among the 25 tree species that were investigated, some of the tree species did change color during winter and their

spectral reflectances were significantly different from those measured in other seasons.

Based on the discriminant analysis results using the original spectra of 21 tree species for each season, a comparison among different seasons was performed. The classification results of the four seasons were shown in Table 4.4 while the results of significant testing of Kappas comparing classifications of different seasons were listed in Table 4.5. The confusion matrices were shown in Appendix 4. Autumn data was able to generate the most accurate results with overall accuracy of 72.86%. Spring and winter data produced slightly lower accuracy of 71.90% and 70.16% respectively, but the different is statistically insignificant. Summer data generated the lowest classification accuracy of 65.71%.

Table 4.4. Classification results of linear discriminant analysis using 21 tree species with the original spectra for seasonal comparison

	OA (%)	*K (×100)*
Spring	71.90	70.50
Summer	65.71	64.00
Autumn	72.86	71.50
Winter	70.16	68.67

Table 4.5. Significant testing of Kappas for comparing classification results using linear discriminant analysis for seasonal comparison (absolute value >1.96 indicates significant difference at 0.05 significance level)

	Spring	*Summer*	*Autumn*	*Winter*
Spring	-	2.2649	-0.3602	0.6512
Summer	-2.2649	-	-2.6257	-1.6122
Autumn	0.3602	2.6257	-	1.0113
Winter	-0.6512	1.6122	-1.0113	-

4.3.4. Comparison of laboratory and *in situ* data

Five tree species were selected for *in situ* spectral measurements, namely *Acacia confusa*, *Castanopsis fissa*, *Dimocarpus longan*, *Ficus microcarpa* and *Taxodium distichum*. Figure 4.14 showed individual plots of laboratory and *in situ* average spectral reflectance of the five tree species. The *in situ* data tended to have higher reflectance. This might be due to the different illumination conditions. Besides, the laboratory data were averaged by the 36 samples for each species. Two third of the 36 samples were measured with low and medium level of leaf density which might lower the average reflectance. No particular conclusion could be drawn visually from the plots. All five tree species had higher near-infrared bands for *in situ* data than for laboratory data. The green peaks of *Castanopsis fissa* were similar for both *in situ* and laboratory data. *Acacia confusa* and *Taxodium distichum* had higher green peaks for *in situ* data than for laboratory data while *Dimocarpus longan* had lower green peaks for *in situ* data. The green peak of *Ficus microcarpa* shifted slightly to a longer wavelength in the *in situ* data than in the laboratory data.

An analysis of means was performed to compare the laboratory and *in situ* spectral reflectance data statistically for the five tree species. Figure 4.15 showed the t value calculated for each wavelength. If the absolute value of t exceeds 2, the difference is significant at the 0.05 significance level. Most t values obtained were greater than 2. The results showed that the laboratory and *in situ* data were significantly different. This might be due to the different illumination conditions between the laboratory and the field as well as the different background conditions in the locations of *in situ* measurement.

Figure 4.14a *In situ* and laboratory reflectance spectra of *Acacia confusa*

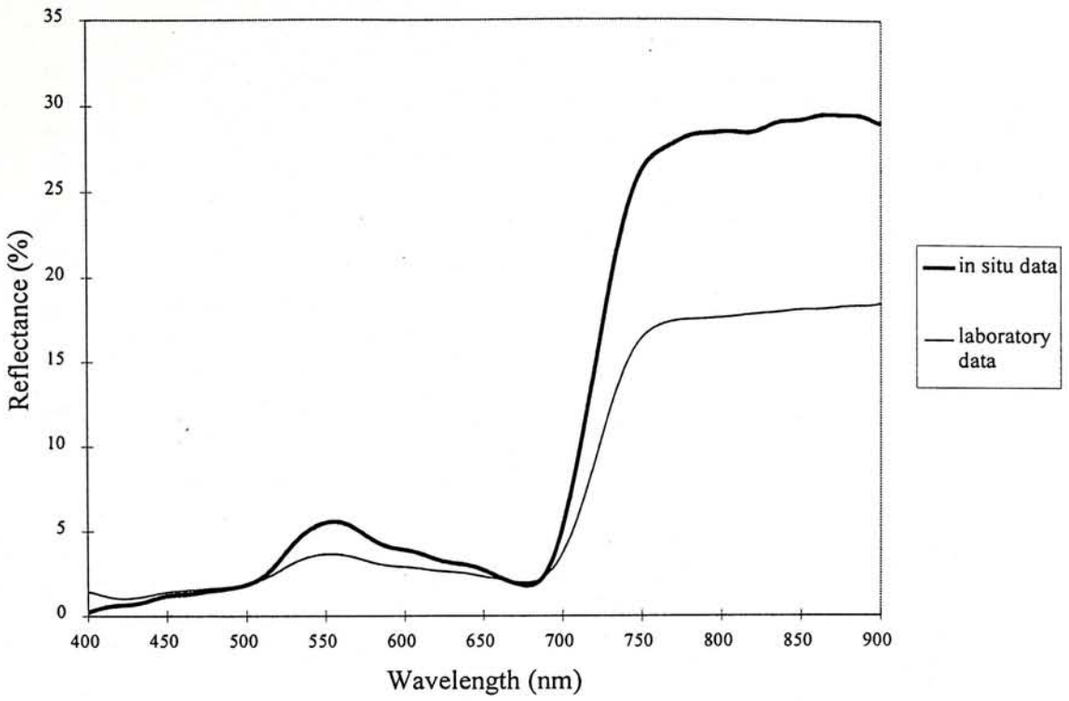

Figure 4.14b *In situ* and laboratory reflectance spectra of *Castanopsis fissa*

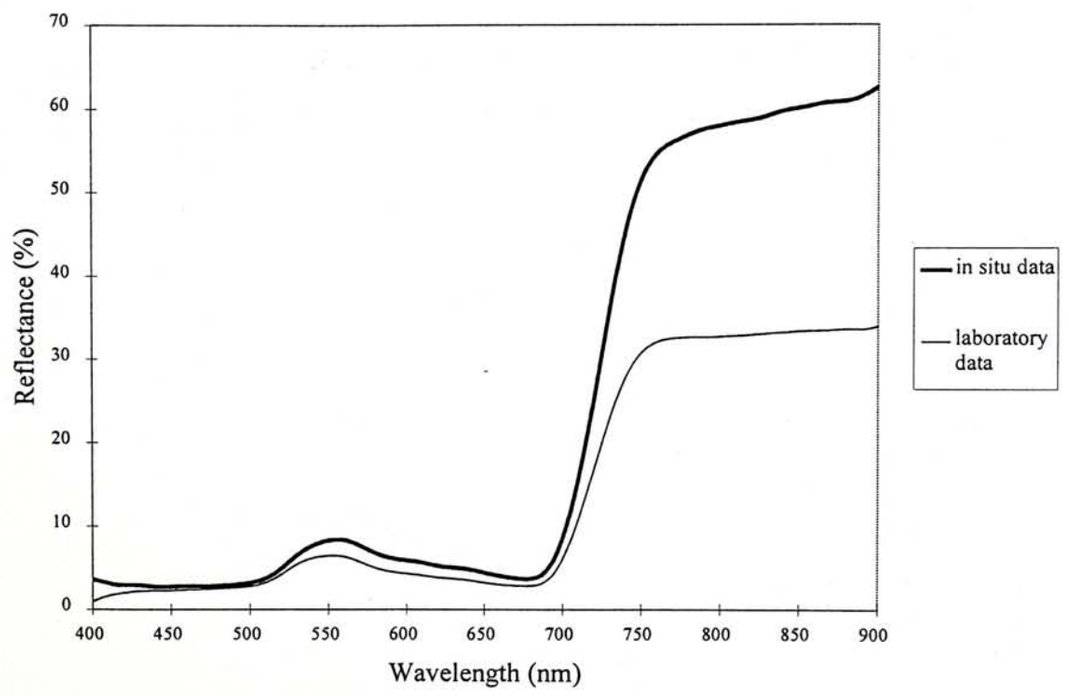

Figure 4.14c *In situ* and laboratory reflectance spectra of *Dimocarpus longan*

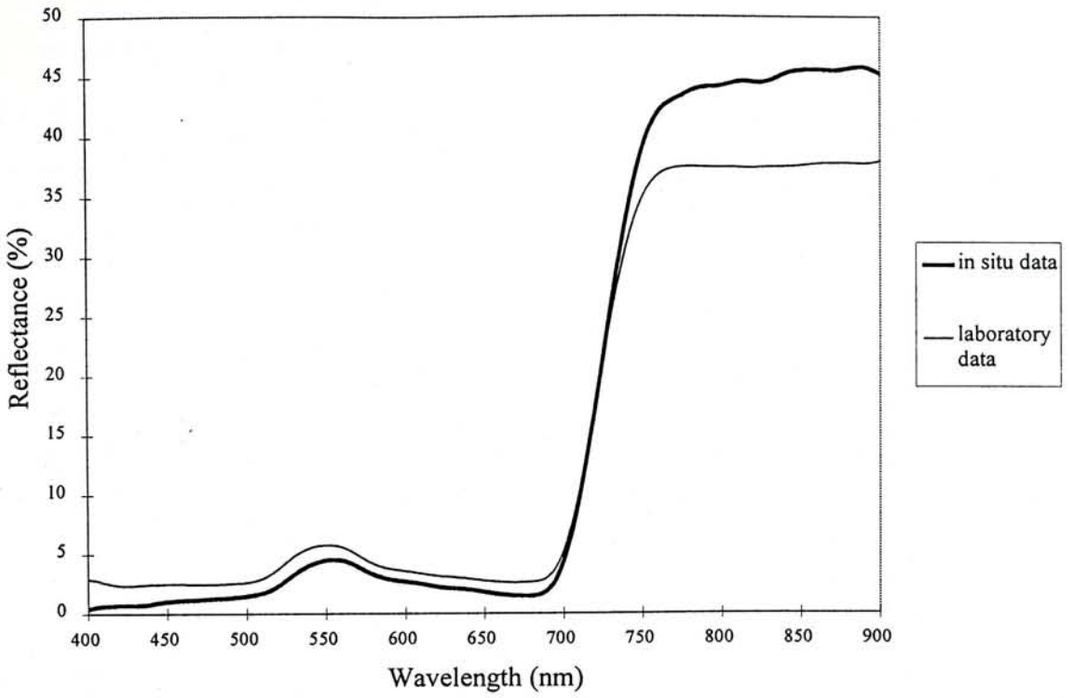

Figure 4.14d *In situ* and laboratory reflectance spectra of *Ficus microcarpa*

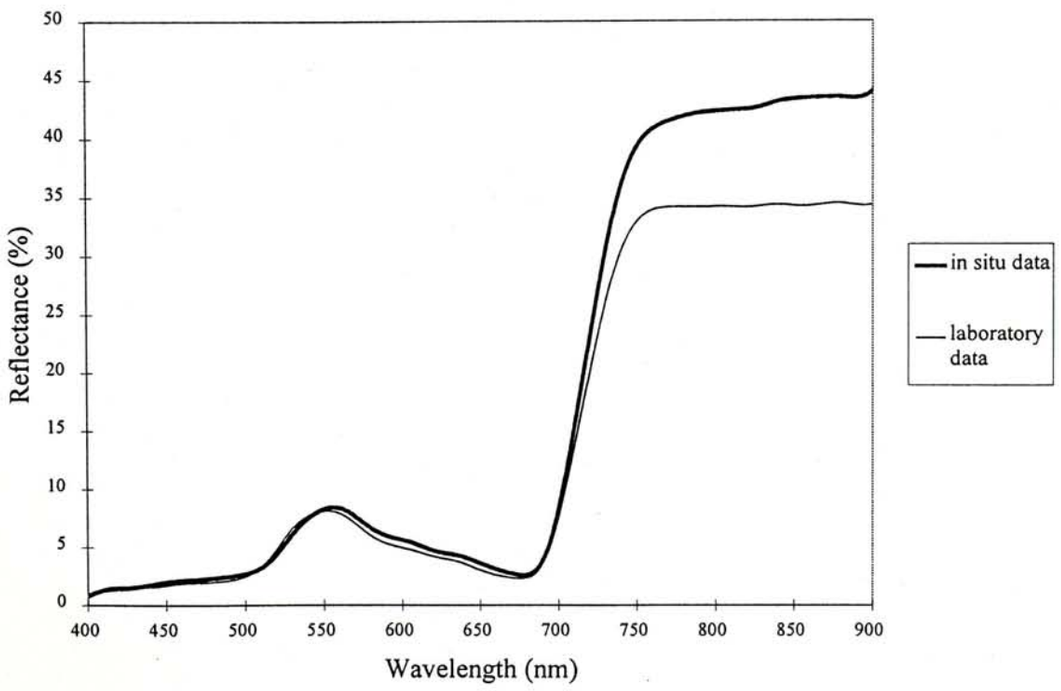

Figure 4.14e *In situ* and laboratory reflectance spectra of *Taxodium distichum*

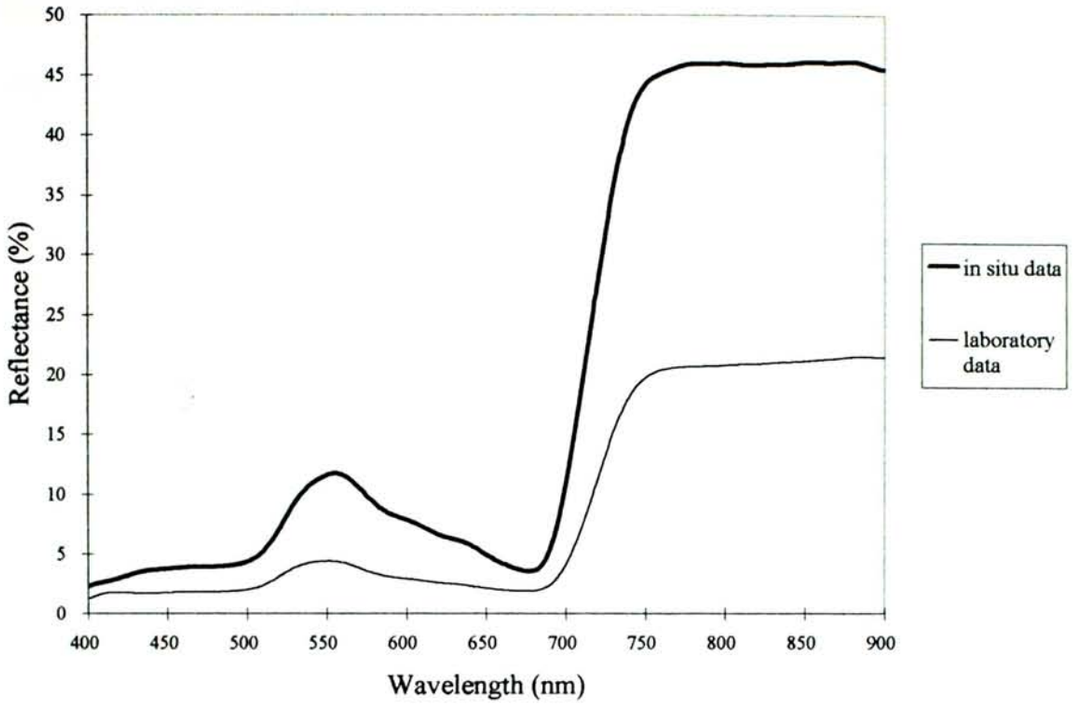

Figure 4.15 The *t* value for comparison between *in situ* and laboratory data

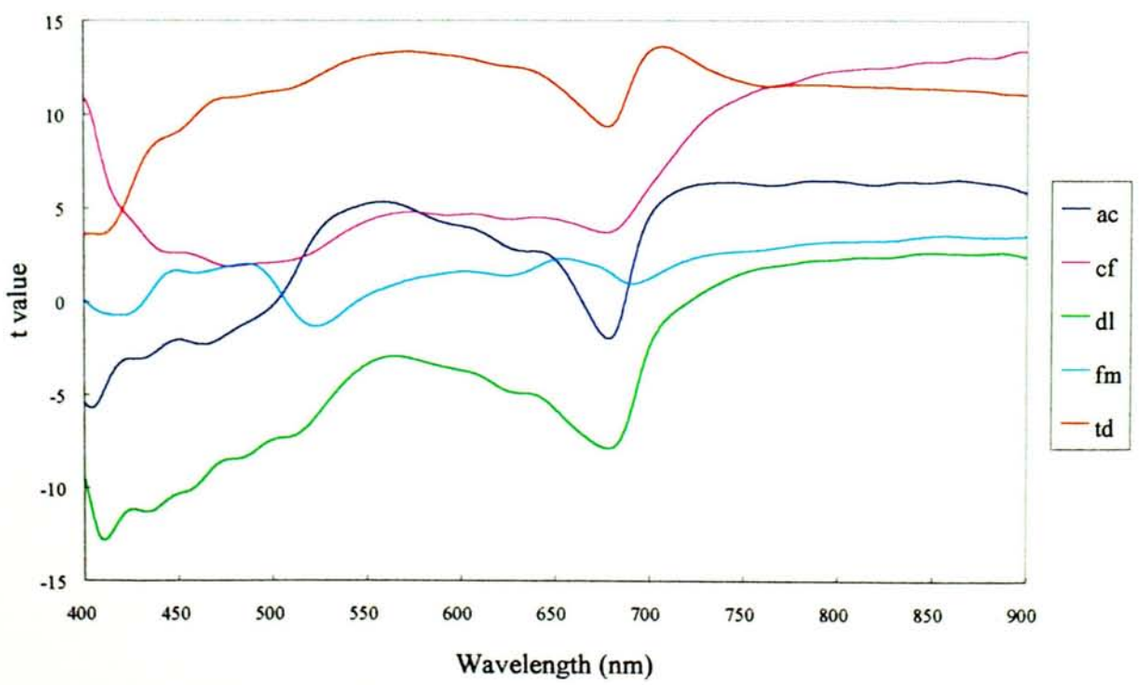

4.4. Summary

The results of tree species recognition were satisfactory with over 70% overall accuracy using original spectral reflectance data. In general, neural networks outperformed linear discriminant analysis. Using original spectral reflectance generated significantly better classification results than using either first derivatives spectra or second derivatives spectra. Meanwhile, classification results using first derivatives were better than those using second derivatives. For seasonal comparison, autumn data yielded the best classification result while summer data produced the lowest accuracy. It is found that seasonal effect did pose a great concern for tree species recognition. Finally, the laboratory and *in situ* data were found to be statistically different that might be due to the different illumination conditions and background effect.

CHAPTER FIVE

RESULTS AND DISCUSSIONS OF DATA COMPRESSION AND BAND SELECTION

5.1. Introduction

This chapter presents the results and discussions of data compression and band selection. Principal components analysis is performed for data compression using the *in situ* spectral reflectance of the ten surface covers and the laboratory data of the tree species. Band selection is done by stepwise discriminant analysis and hierarchical clustering procedure using the laboratory data of the tree species.

5.2. Data compression

Data compression was done by principal components analysis (PCA). Two separate PCAs were done using *in situ* data and laboratory data respectively.

5.2.1. PCA using *in situ* spectral data

For *in situ* data, PCA was performed using the smoothed spectral reflectance of the ten surface covers. Figure 5.1 showed the first five PC loadings. Table 5.1 showed the eigenvalues and the percentage variance explaining the first four PCs. The reflectance data were rotated such that the majority of the spectral information was contained in the first four PCs which totally expressed 99.78% of the total variability in the spectral data.

Table 5.1. Eigenvalues and percentage variance of the first four PCs for *in situ* data

	Eigenvalue	% of variance	Cumulative % of variance
PC1	411.166	59.676	59.676
PC2	242.337	35.172	94.848
PC3	20.120	2.920	97.768
PC4	12.379	1.797	99.565

Figure 5.1. The first five PC loadings of *in situ* data

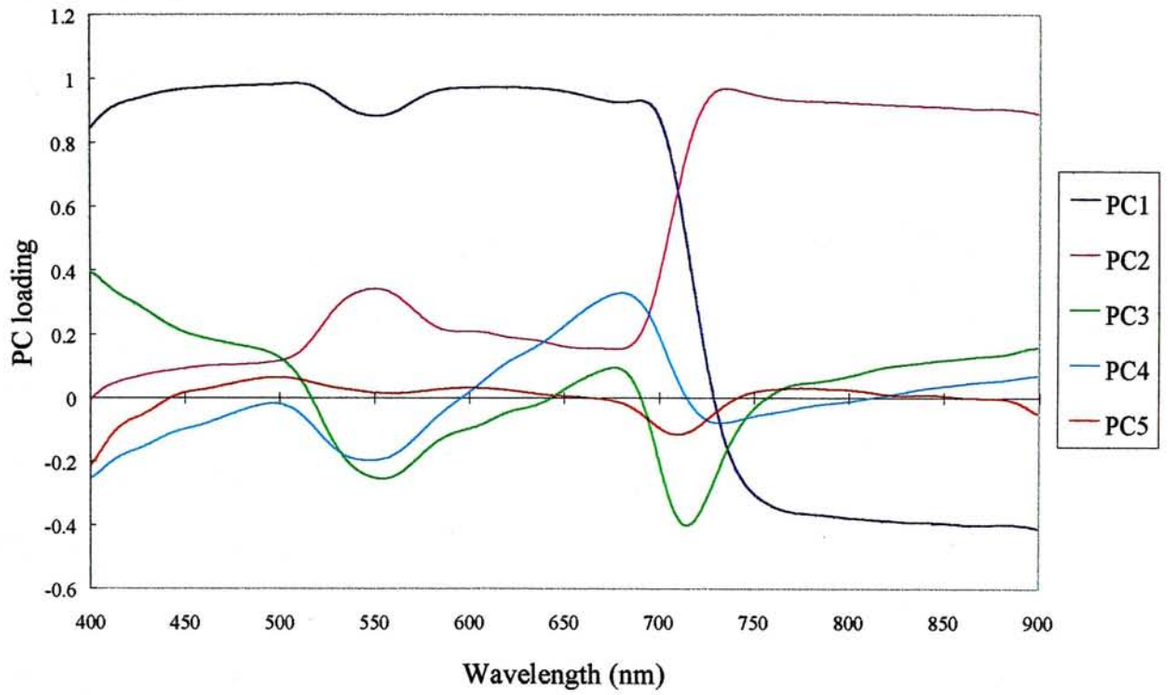

5.2.1.1. Characteristics of PC loadings

The first principal component (PC1) represented 59.68 % of the total variance in the spectral data and had heavy positive loadings from 400 nm to around 700 nm which was visible spectral range while a very small trough was found near the green peak centered at 550 nm. It dropped sharply from positive to negative value around the red edge between 700 nm and 750 nm and leveled off. Significant contrast between the visible and the near-infrared bands was formed in PC1 which was analogous to the greenness measures obtained from PCA or tasseled cap transformation using broadband satellite multispectral data (Crist and Cicone, 1984).

PC2 loaded positively for all bands and expressed 35.17% of the total variance of the data. It could be considered as similar to the brightness measures derived from broadband data. Its pattern was very similar to the spectral reflectance of trees in which a green peak was found at round 550 nm and a sharp rise occurred at the red edge with a very high near-infrared plateau.

Most broadband multispectral data normally yielded two-dimensional information in terms of brightness and greenness from visible and near-infrared bands. PC3s and PC4s produced from hyperspectral data, however, possessed useful information. PC3 derived from *in situ* spectral data explained 2.92% of the total variance. PC3 had positive loadings from 400 nm to 520 nm in the blue bands and dropped to a negative trough centered at the green band of 550 nm. It rose to positive value from 640 nm to 690 nm with a little peak at 675 nm in the red bands and dropped again to a deeper trough centered at around 720 nm along the red edge. It rose again to positive from 750 nm onwards. It could be interpreted as a contrast

between the strong absorption blue and red bands versus the strong reflectance green bands and the steep rise of the red edge.

PC4 explained 1.80% of the total variance. PC4 had negative loadings from 400 nm to around 600 nm in which a trough was found at 550 nm in the green bands similar to that found in PC3. It rose to positive values from 600 nm to 720 nm in which a higher peak was found at also 675 nm in the red bands as compared to that in PC3. It dropped to negative again from 720 nm to 820 nm and rose slightly to positive afterwards. It could be interpreted as a contrast between the green bands and the red bands.

5.2.1.2. Scatter plots of PC scores

Figure 5.2 showed the scatter plots of PC1 versus PC2, PC1 versus PC3 and PC1 versus PC4. In the three plots, pond water, concrete and grass slope in which quite a lot of bare soil was exposed tended to scatter into separate clusters from the vegetated covers of grass, fern and trees. The vegetated covers appeared to group together. Meanwhile, different vegetation was clearly separated from each other. For example, fern came out as a distinct cluster as shown in Figure 5.2b. It showed that different surface cover types including different tree species had distinct inherent spectral characteristics that can be discriminated by PCA.

Figure 5.2a Scatter plot of PC score 1 versus PC score 2 for *in situ* data

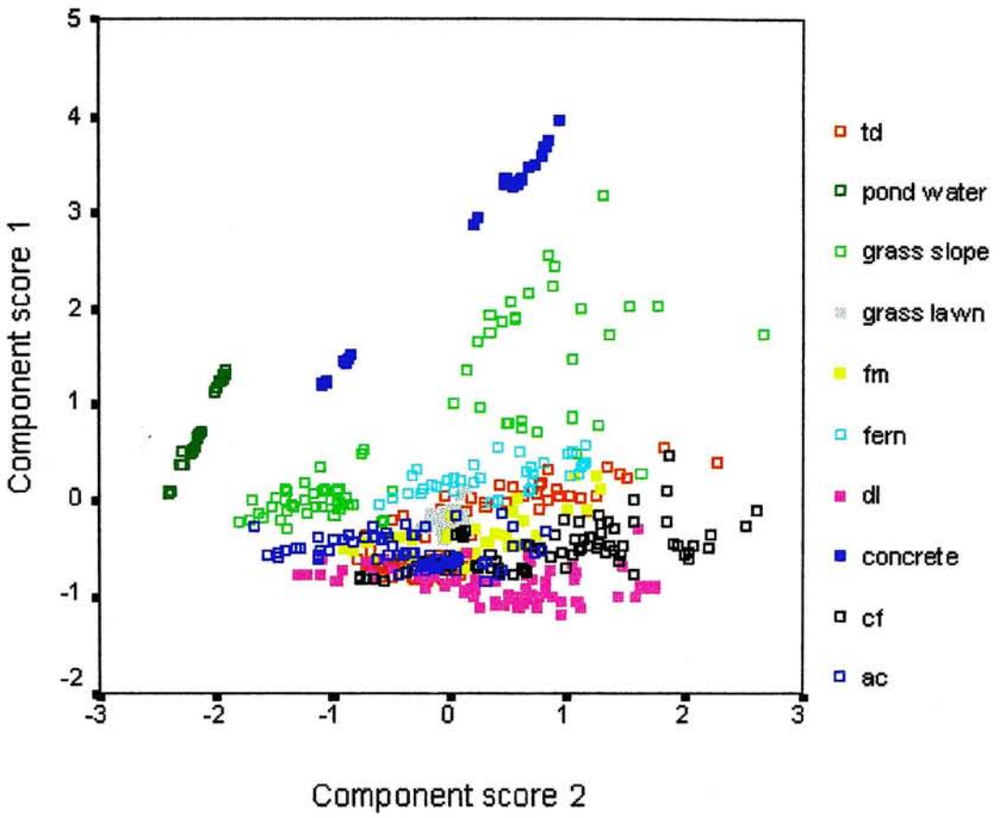

Figure 5.2b Scatter plot of PC score 1 versus PC score 3 for *in situ* data

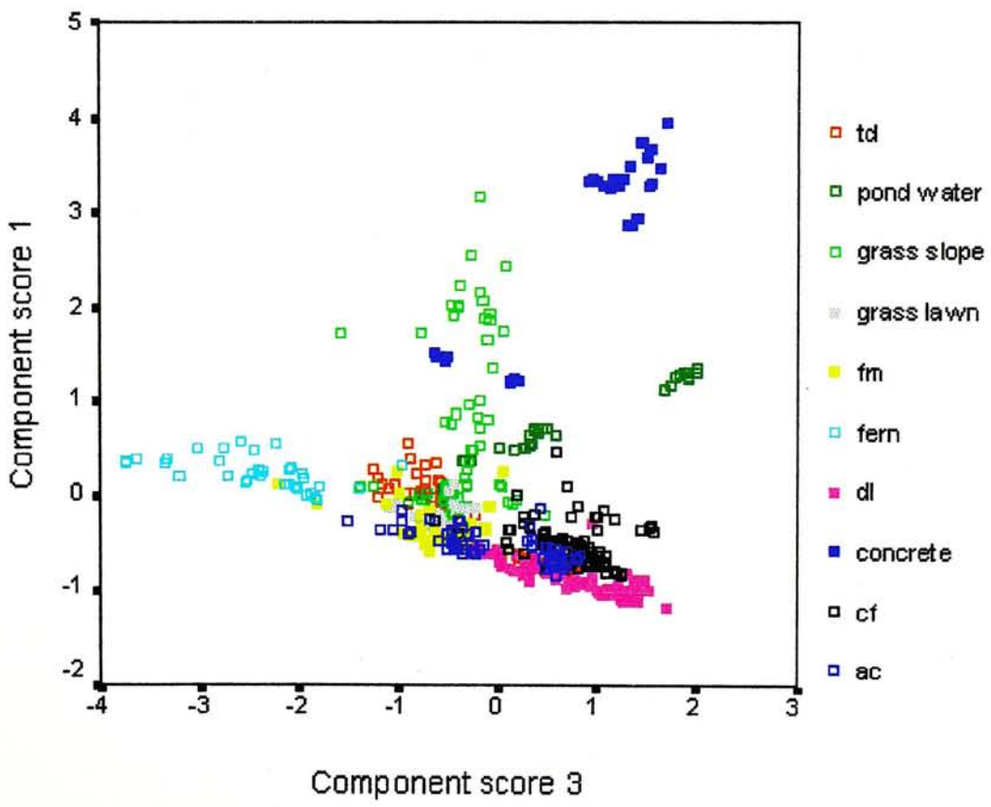

Figure 5.2c Scatter plot of PC score 1 versus PC score 4 for *in situ* data

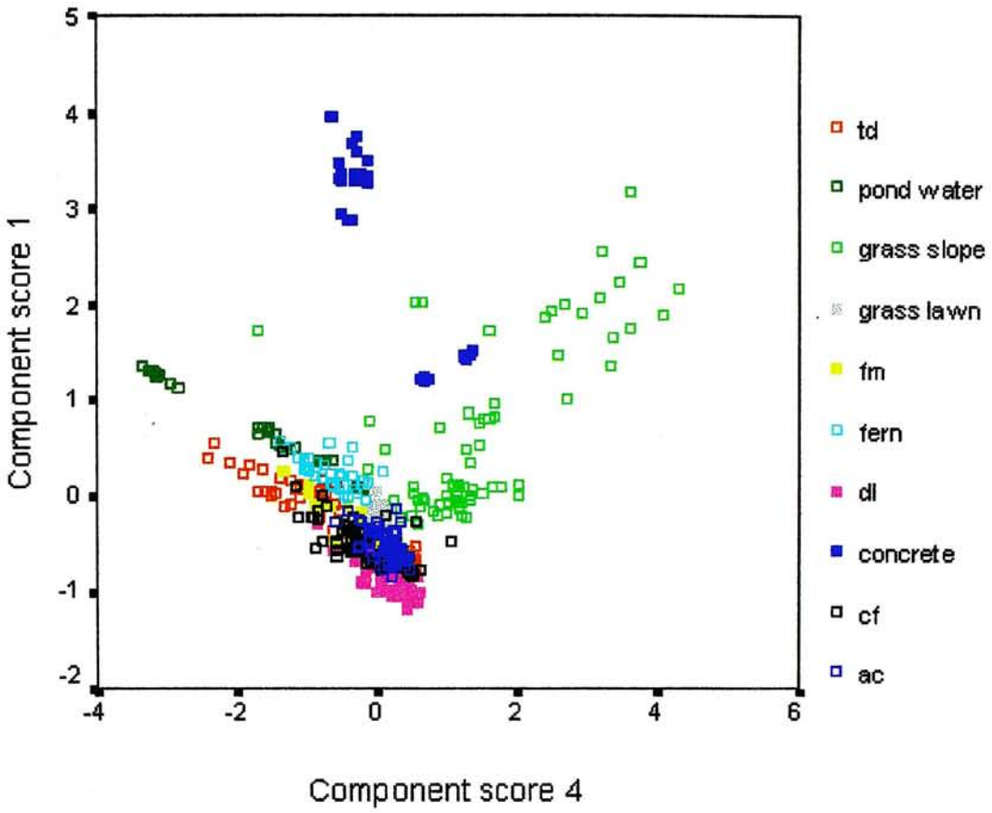

5.2.2. PCA using laboratory spectral data

For laboratory data, separate PCA was performed for each season using the smoothed reflectance spectra of the tree species. Figure 5.3 showed the first five PC loadings for the four seasons. Table 5.2 showed the eigenvalues and the percentage variance of the first four PCs for the four seasons. The first four PCs totally expressed more than 97.5% of the total variability in the spectral data of the four seasons.

Table 5.2. Eigenvalues and percentage variance of the first four PCs for laboratory data

Spring data

	Eigenvalue	% of variance	Cumulative % of variance
PC1	109.421	79.290	79.290
PC2	18.507	13.411	92.701
PC3	5.976	4.331	97.032
PC4	2.301	1.667	98.699

Summer data

	Eigenvalue	% of variance	Cumulative % of variance
PC1	120.349	87.209	87.209
PC2	8.923	6.466	93.675
PC3	5.669	4.108	97.783
PC4	1.382	1.001	98.785

Autumn data

	Eigenvalue	% of variance	Cumulative % of variance
PC1	115.384	83.611	83.611
PC2	11.733	8.502	92.114
PC3	7.227	5.237	97.351
PC4	1.644	1.191	98.542

Winter data

	Eigenvalue	% of variance	Cumulative % of variance
PC1	104.107	75.440	75.440
PC2	19.488	14.122	89.562
PC3	7.762	5.625	95.186
PC4	3.309	2.398	97.584

Figure 5.3a The first five PC loadings of spring data

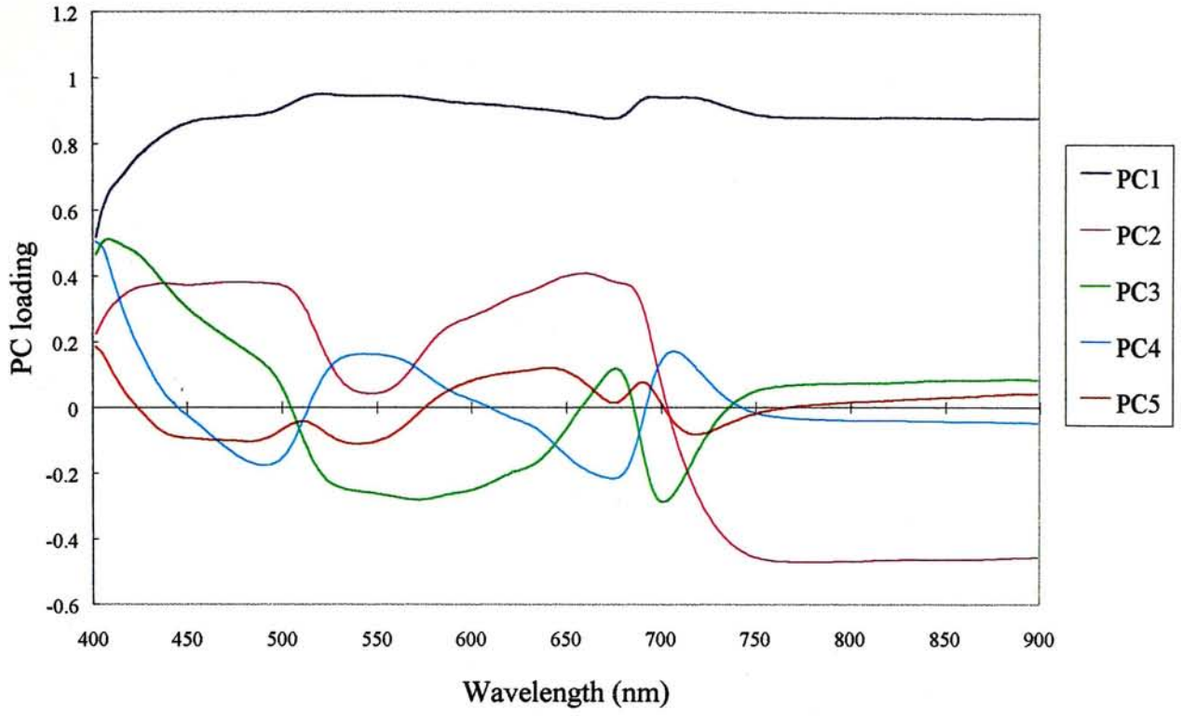

Figure 5.3b The first five PC loadings of summer data

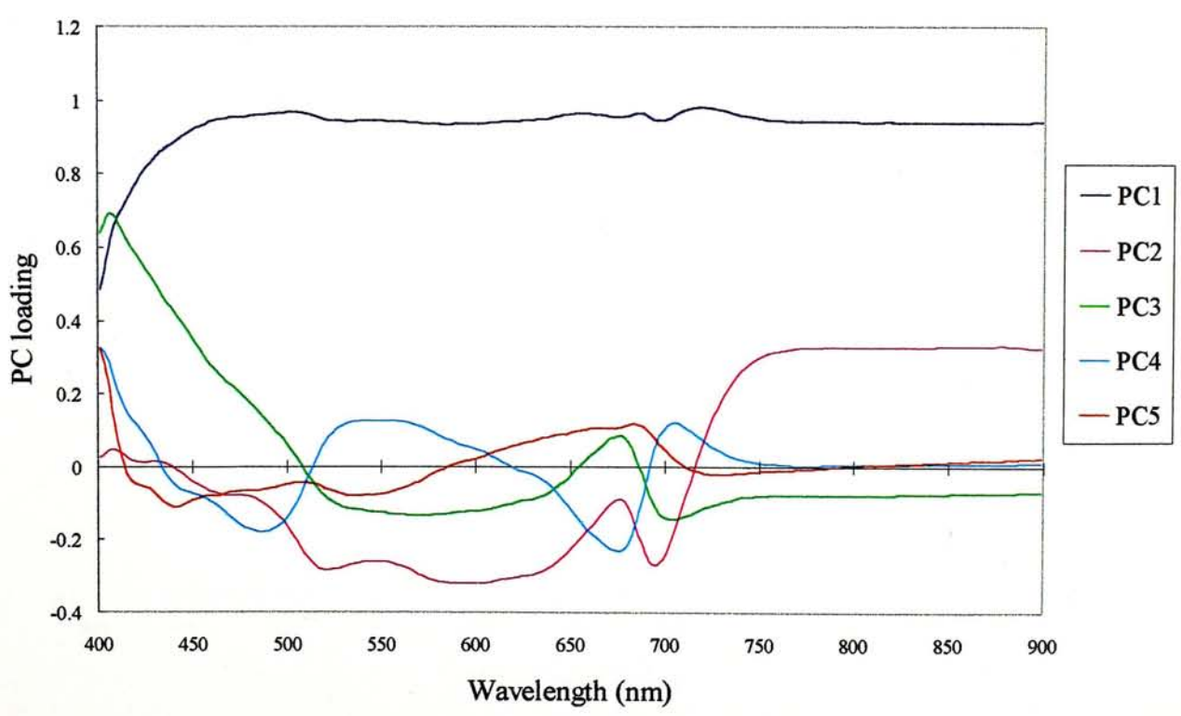

Figure 5.3c The first five PC loadings of autumn data

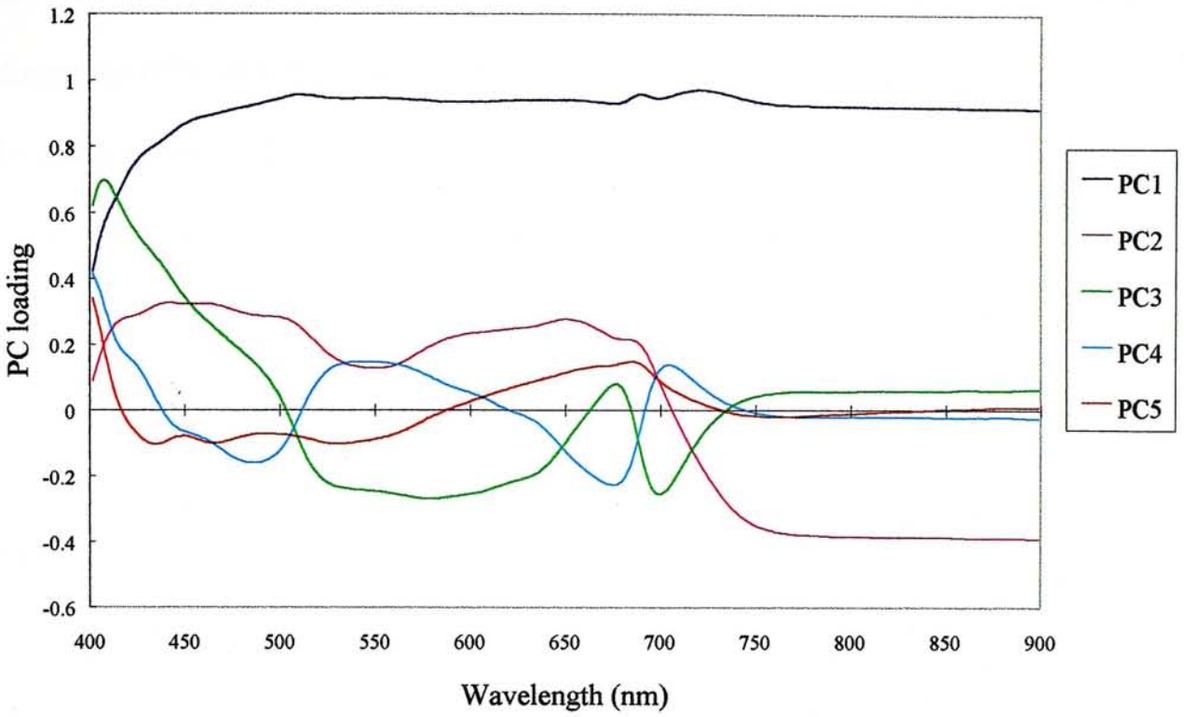

Figure 5.3d The first five PC loadings of winter data

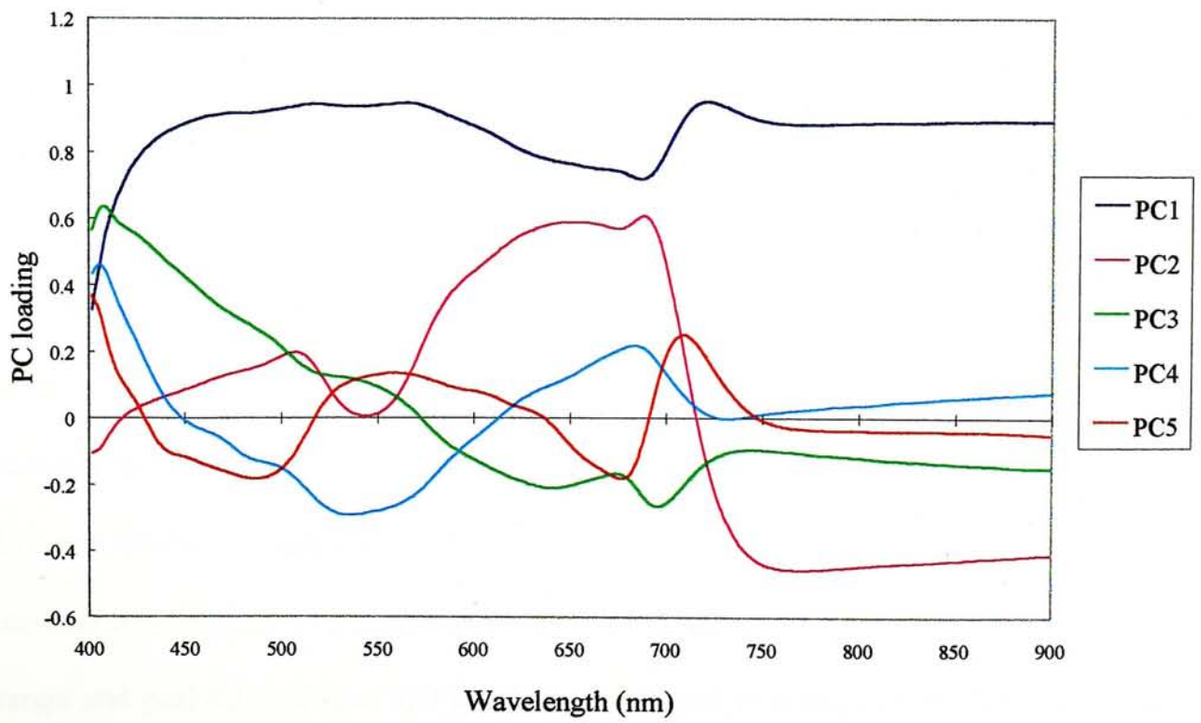

5.2.2.1. Characteristics of PC loadings

Results of the four seasons were quite consistent. PC1s were loaded positively and heavily from the 450 to 900 nm spectral range which did not reveal any contrast among specific spectral bands. They represented more than 75% of the variance in the spectral data and were approximately the average brightness from all bands. This was quite similar to brightness vector derived from broadband multispectral data.

PC2s were consistent for spring, summer and winter in which positive loadings were found in the visible bands from 400 nm to around 700 nm while the loadings dropped to negative values along the red edge from 690 nm to 750 nm and leveled off in the near-infrared bands from 750 nm to 900 nm. For the positive loadings along the visible bands, troughs were found at around 550 nm in which the green peak was located. PC2s formed significant contrast between the visible and near-infrared bands. A similar but opposite pattern was found in summer in particular in longer wavelengths beyond the red edge. However, the loadings in the visible band region were not totally negative values. The peak at 550 nm raised to positive values from 510 nm to 620 nm. PC2s can be considered as greenness measures similar to those obtained using broadband spectral data.

Similar to the situation using *in situ* data, PC3s and PC4s generated by laboratory data also possessed useful information. PC3s were consistent for spring, summer and autumn. Positive loadings were found in the blue bands from 400 nm to 510 nm. Loadings dropped to negative values in the green bands from 510 nm to 660 nm and rose slightly to positive again just before the red edge in the 660 to 680 nm range and peaked at around 670 nm. It then dropped to a negative trough at 700 nm

and leveled off. PC3s had a similar pattern as the PC3 derived from *in situ* data. PC3 of winter data were different from PC3s of the other seasons. It had positive loadings from 400 nm to 570 nm which were the blue and green bands and negative loadings from 570 nm to 900 nm. PC3s for spring, summer and autumn could be interpreted as a contrast between the blue and red bands versus the green and yellow bands plus the red edge.

PC4s for spring, summer and autumn and PC5 for winter were consistent and the pattern of the loadings was in a reversed trend from 560 nm to 900 nm as compared to PC3s for spring, summer and autumn. From 400 nm to 560 nm, positive loadings were found before 440 nm while loadings dropped to negative from 440 nm to 560 nm. Thus, a contrast between the shorter blue bands and the longer blue bands existed. In both PC3 and PC4, the red edge formed a very distinct phenomenon which was previously overlooked. It might contain useful information that deserve further investigation.

5.2.2.2. Scatter plots of PC scores

Scatter plots of PC1 versus PC2, PC2 versus PC3 and PC2 versus PC4 were shown in Figure 5.4. These plots showed that different tree species were slightly scattered into different groups. However, tree species in the plot of PC1 versus PC2 were grouped more disperse than the other two plots. In the plot of PC1 versus PC2, *Bauhinia variegata*, *Delonix regia* and *Schima superba* were separated from other tree species while more tree species were dispersed and mixed with other tree species, for example, *Aleurites moluccana*, *Liquidambar formosana and Lagerstroemia speciosa*.

Figure 5.4a Scatter plot of PC score 1 versus PC score 2 for laboratory data

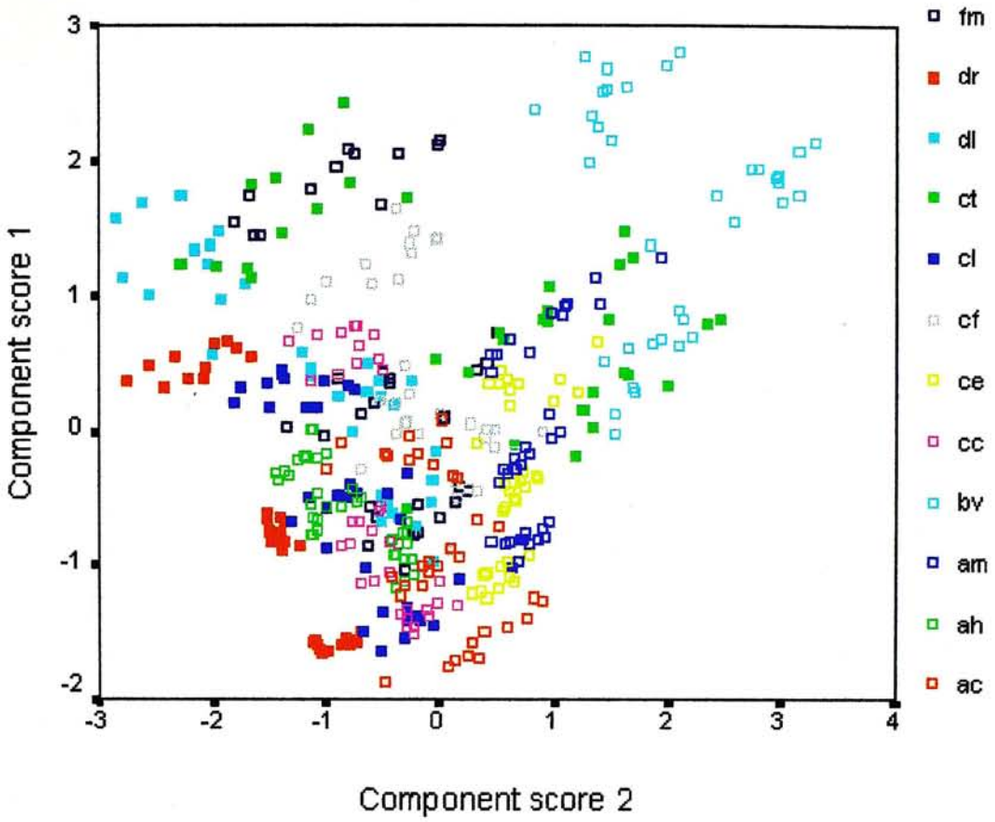

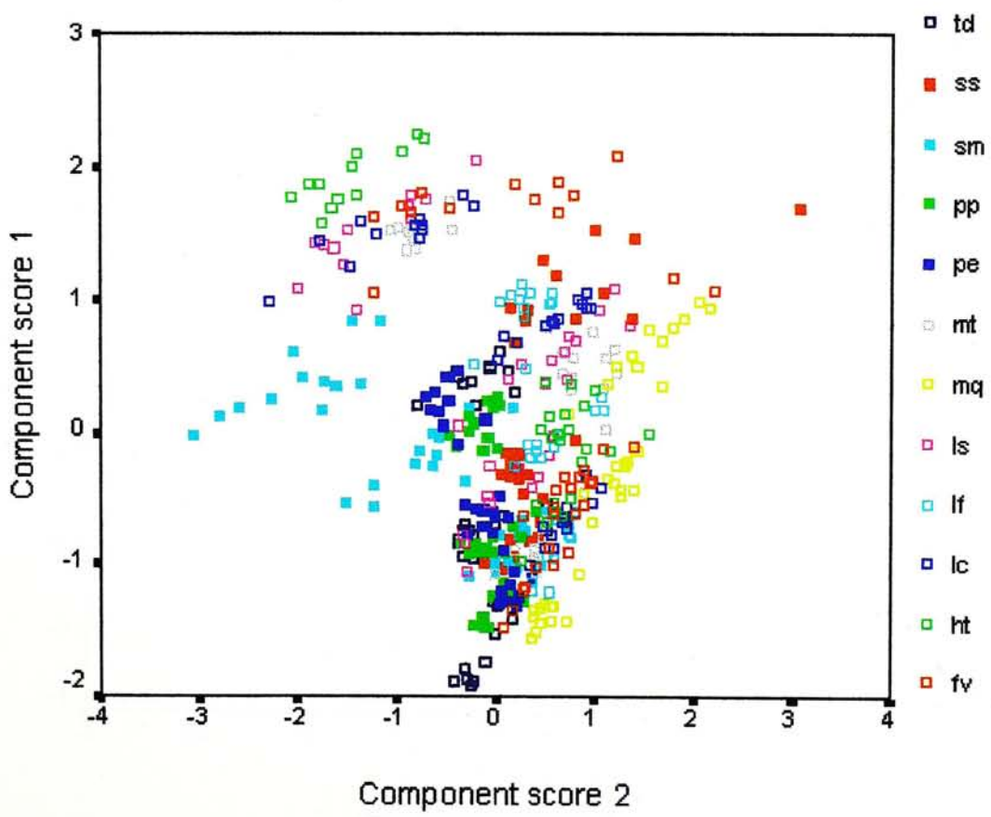

Figure 5.4b Scatter plot of PC score 2 versus PC score 3 for laboratory data

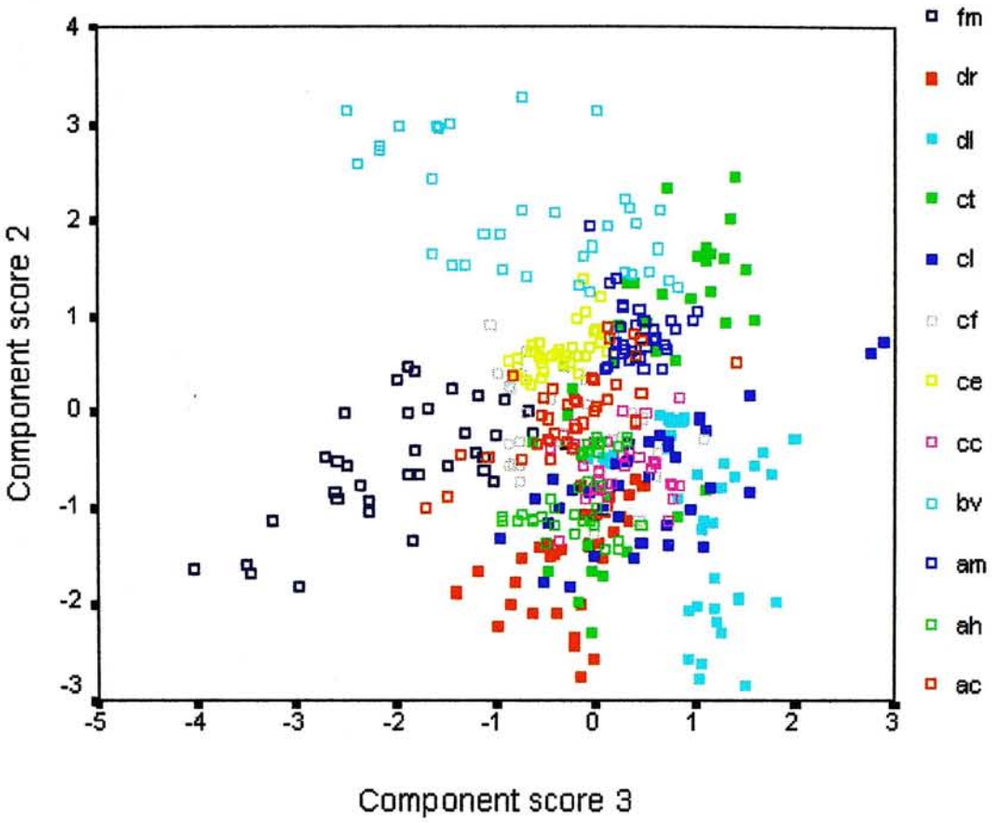

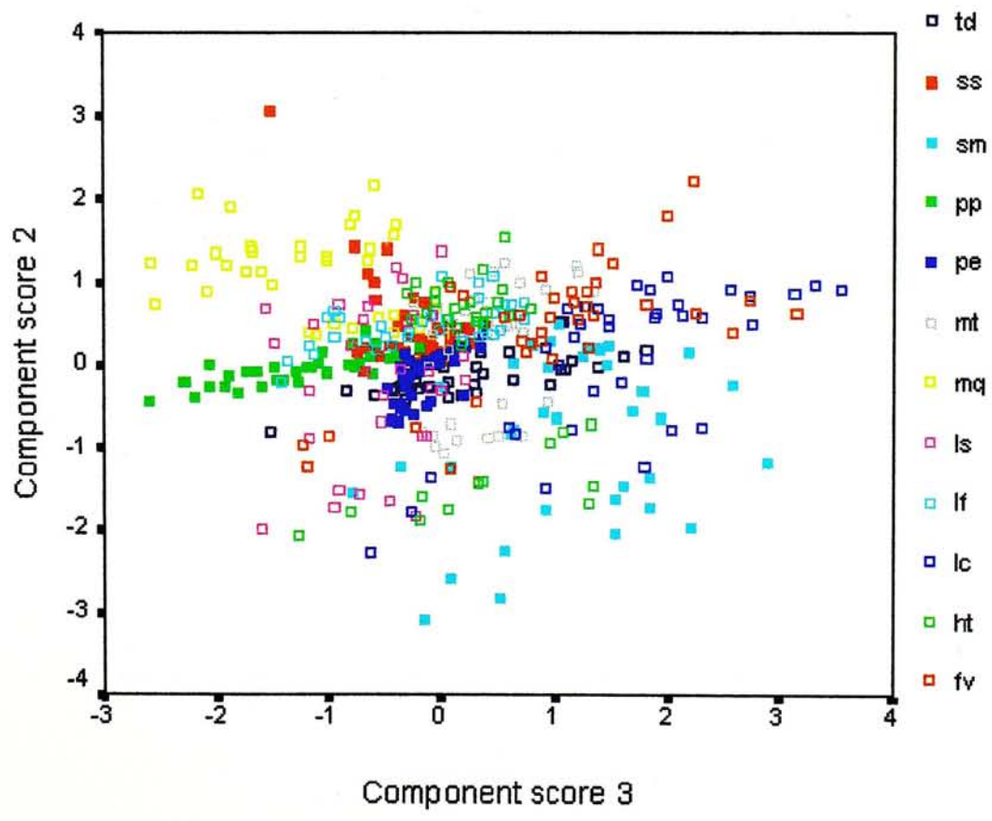

Figure 5.4c Scatter plot of PC score 2 versus PC score 4 for laboratory data

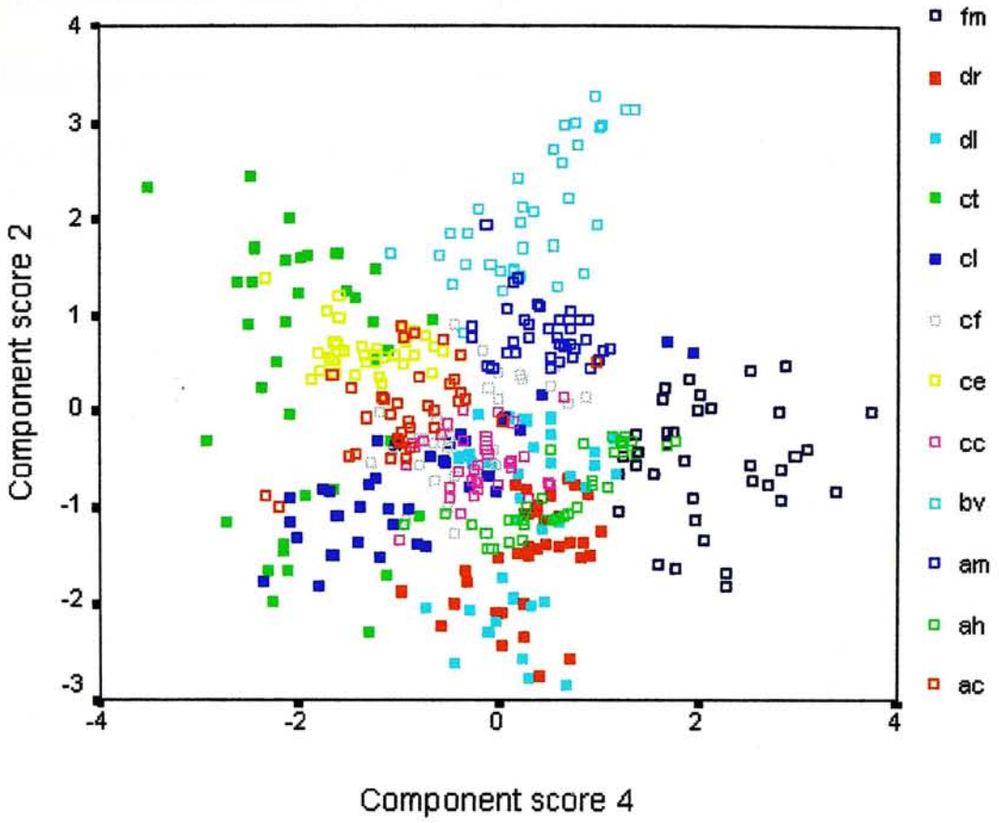

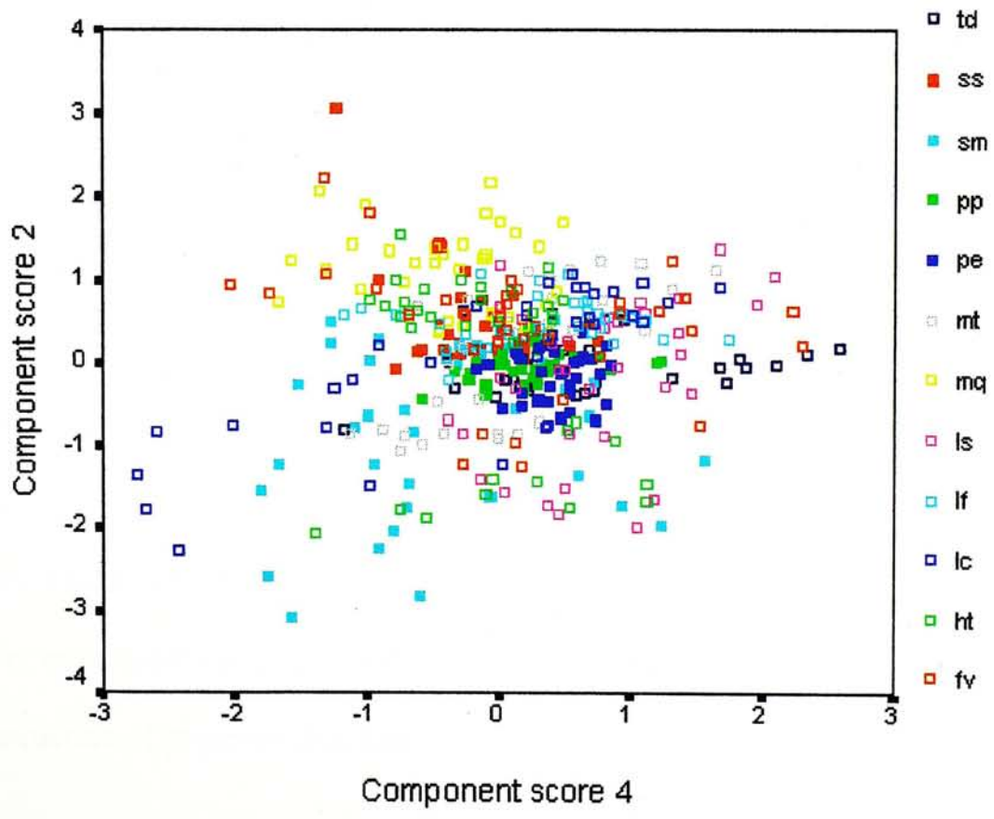

In the plot of PC2 versus PC3 and PC2 versus PC4, more tree species appeared to group together among themselves, for example, *Ficus microcarpa*, *Melaleuca quanqueenervia* and *Thuja orientalis* in the former and *Aleurites moluccana*, *Bauhinia variegata* and *Ficus microcarpa* in the latter. It revealed that the minor PCs, PC3 and PC4, did contain useful information in differentiating different tree species.

5.2.2.3. Results of tree species recognition using PC scores

In order to further investigate the differentiating power of these PCs, linear discriminant analysis was performed to identify tree species using the first eight PCs which explained more than 99.7% of the variance of the spectral data. The confusion matrices of the classification results were shown in Appendix 5. Overall accuracy of around 74% were yielded for spring, autumn and winter and 68.67% was found for summer. The results were similar to those obtained by linear discriminant analysis and neural network using all of the 138 bands. This showed that the PCs possessed similar differentiating power to the original spectral bands.

5.2.3. Implications

For hyperspectral data, similar results were found for PC1 and PC2 compared with two-dimensional information obtained by broadband multispectral data in terms of brightness and greenness from visible and near-infrared bands. However, PC3 and PC4 generated by hyperspectral data possess extra information that is not provided by broadband multispectral data and give insight to the understanding of the inherent structure of hyperspectral data.

In this study, the PCA using *in situ* spectral data can be considered as a preliminary study of extracting information for hyperspectral images with various surface covers whilst the PCA using laboratory data of tree species represents PCA to extract information for vegetation studies.

5.3. Band selection

Two separate band selection schemes were used in this study. In order to determine whether band selection helped to improve classification results, a preliminary band selection procedure was done by stepwise discriminant analysis. Then a hierarchical clustering procedure was performed for the original spectral data. Spectral bands were selected from the centers of the clusters formed during the clustering procedure to determine which spectral regions were useful for tree species recognition.

5.3.1. Preliminary band selection using stepwise discriminant analysis

Preliminary band selection was done using stepwise discriminant analysis. The bands that were selected and entered into the analysis were adjusted by the F probability of entry and removal or F value of entry and removal. In this study, two independent stepwise discriminant analyses were done. The first one used a criterion that bands entered if the significance level of F value was smaller than 0.05 and removed if the significance level of F was greater than 0.1. A different criterion was used in the second analysis with F value greater than 3.84 for band entry and F value less than 2.71 for band removal. The latter criterion was the default setting used in the SPSS package while the former criterion allowed more bands to be selected.

5.3.1.1. Selection of spectral bands

Figure 5.5 showed the bands selected by these two criteria. Nine to 37 bands and seven to thirteen bands were selected using the first and second criterion respectively. Using the first criterion, more bands were selected but no particular pattern could be found. In general, fewer bands were selected in the infrared region from 770 to 900 nm that a consistent information was formed in this spectral range. However, with the second criterion, fewer bands were selected and the bands tended to cluster into two groups. The first group ranged approximately from 500 to 570 nm that was centered in spectral region of the green peak. The second one was from 650 to 750 nm around the red edge. It revealed that important spectral bands were mainly found within the spectral range of the green peak and along the red edge. It was interesting that one isolated band was found in the infrared region for the original spectra of summer, autumn and winter data but no bands were selected from this spectral region for the derivatives data. It suggested that the infrared plateau of the spectral reflectance gave some information for identifying tree species, but no significant information was found for the derivatives data which were approximately zero or quite noisy in this spectral region.

5.3.1.2. Classification results of the selected bands

In order to determine how band selection affected the classification results, linear discriminant analysis was performed using all the spectral bands (Case 1), the bands selected by the first criterion (Case2) and the bands selected by the second criterion (Case 3). Table 5.3 listed the classification results and Table 5.4 showed the significant testing of Kappas. The confusion matrices were shown in Appendix 6 and Appendix 7 for Case 2 and Case 3 respectively.

Figure 5.5a The bands selected by stepwise discriminant analysis using the first criterion (Case 2)

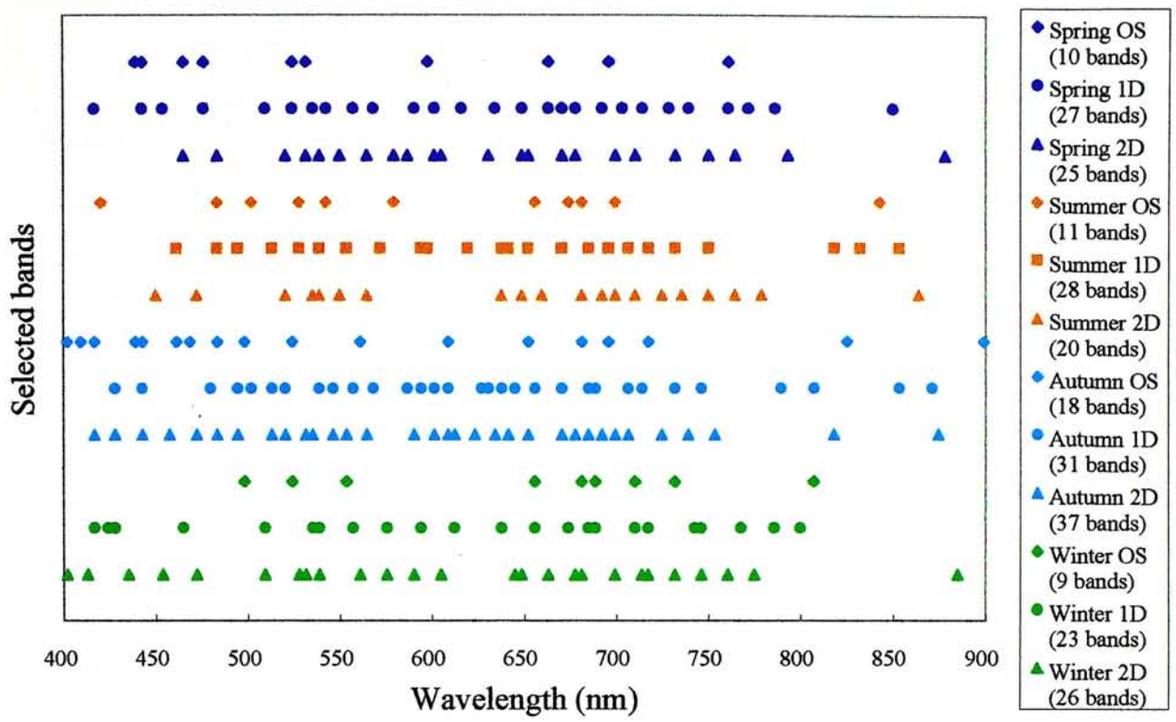

Figure 5.5b The bands selected by stepwise discriminant analysis using the second criterion (Case 3)

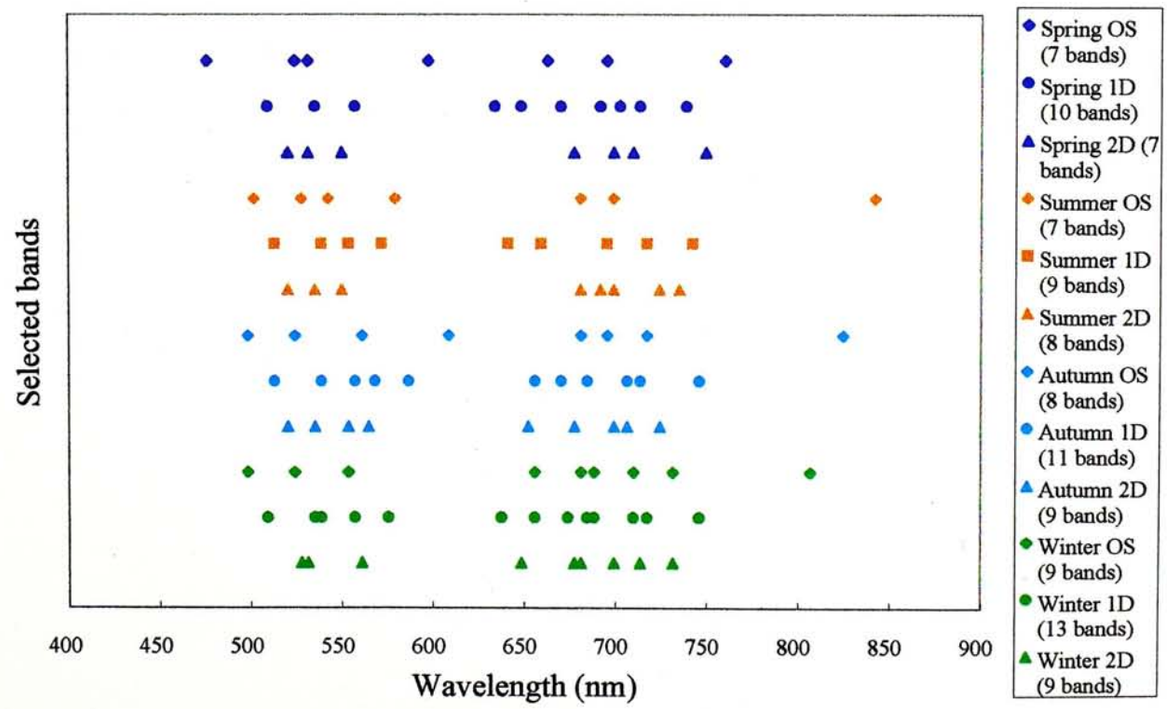

Table 5.3. Classification results using stepwise linear discriminant analysis for band selection

Original spectra

	Case 1			*Case 2*			*Case 3*		
	No. of bands	*OA (%)*	*K (×100)*	*No. of bands*	*OA (%)*	*K (×100)*	*No. of bands*	*OA (%)*	*K (×100)*
Spring	138	74.27	73.19	10	79.73	78.89	7	77.60	76.67
Summer	138	68.93	67.64	11	81.20	80.42	7	81.73	80.97
Autumn	138	80.69	79.86	18	90.28	89.86	8	87.78	87.25
Winter	138	70.16	68.67	9	91.27	90.83	9	91.27	90.83
Average accuracy		73.51	72.34		85.62	85.00		84.58	83.93

First Derivatives

	Case 1			*Case 2*			*Case 3*		
	No. of bands	*OA (%)*	*K (×100)*	*No. of bands*	*OA (%)*	*K (×100)*	*No. of bands*	*OA (%)*	*K (×100)*
Spring	138	20.67	17.36	27	81.47	80.69	10	79.07	78.19
Summer	138	9.07	5.28	28	82.40	81.67	9	79.73	78.89
Autumn	138	17.36	13.77	31	86.67	86.09	11	85.55	84.93
Winter	138	14.44	10.17	23	88.10	87.50	13	86.03	85.33
Average accuracy		15.39	11.65		84.66	83.99		82.60	81.84

Second Derivatives

	Case 1			*Case 2*			*Case 3*		
	No. of bands	*OA (%)*	*K (×100)*	*No. of bands*	*OA (%)*	*K (×100)*	*No. of bands*	*OA (%)*	*K (×100)*
Spring	138	9.73	5.97	25	70.13	68.89	7	64.13	62.64
Summer	138	10.40	6.67	20	72.00	70.83	8	73.87	72.78
Autumn	138	13.61	9.86	37	75.56	74.49	9	71.11	69.86
Winter	138	25.87	22.17	26	84.44	83.67	9	75.08	73.83
Average accuracy		14.90	11.17		75.53	74.47		71.05	69.78

Table 5.4. Significant testing of Kappas for comparing classification results of stepwise linear discriminant analysis (absolute value >1.96 indicates significant difference at 0.05 significance level)

Original Spectra

	Z between Case 1 and Case 2	*Z between Case 1 and Case 3*	*Z between Case 2 and Case 3*
Spring	-2.5221	-1.5126	1.0090
Summer	-5.5503	-5.8191	-0.2657
Autumn	-5.2129	-3.7096	1.5188
Winter	-9.8640	-9.8640	0

First Derivatives

	Z between Case 1 and Case 2	*Z between Case 1 and Case 3*	*Z between Case 2 and Case 3*
Spring	-29.8225	-28.0008	1.1695
Summer	-42.3729	-39.4597	1.3198
Autumn	-36.5732	-35.4470	0.6094
Winter	-39.2600	-36.8978	1.0930

Second Derivatives

	Z between Case 1 and Case 2	*Z between Case 1 and Case 3*	*Z between Case 2 and Case 3*
Spring	-30.4475	-26.5366	2.4802
Summer	-31.4225	-32.8509	-0.8145
Autumn	-30.3694	-27.2727	1.9109
Winter	-25.9885	-20.1571	4.1665

Note:
Case 1 represents classification using all 138 bands
Case 2 represents classification using bands selected by the first criterion with 9-37 selected bands
Case 3 represents classification using bands selected by the second criterion with 7-13 selected bands

Better recognition accuracy was obtained using the selected bands than using all bands available. It was particularly obvious for the derivatives data. For original spectra, overall accuracy of 68.93% to 74.27% were obtained in Case 1. Better results with overall accuracy of 79.73% to 91.27% and 77.60% to 91.27% were produced in Case 2 and Case 3 respectively. Table 4.8 showed that Case 2 and Case 3 which used selected bands produced significantly better recognition accuracy than using all bands. The average overall accuracy for Case 2 (85.62%) was slightly higher than that for Case 3 (84.58%), but the difference was statistically insignificant.

For the first derivatives, the classification accuracy of using selected bands were significantly much better than using all bands. Only accuracy of 9.07% to 20.67% were obtained in Case 1, but much higher accuracy of 81.47% to 88.10% and 79.09% to 86.03% were produced in Case 2 and Case 3 respectively. Results of Case 2 with an overall accuracy of 84.66% were better than that of Case 3 which had an overall accuracy of 82.60%. Again, their difference was statistically insignificant.

Similar to the first derivatives case, second derivatives produced significantly much better classification results when using selected bands than using all bands. Case 1 produced overall accuracy of 9.73% to 25.87% only, but Case 2 and Case 3 generated much higher overall accuracy of 70.13% to 84.44% and 64.13% to 75.08% respectively. Again, results of Case 2 with an overall accuracy of 75.53% were better than that of Case 3 which had an overall accuracy of 71.05%. The difference was quite significant for spring and winter.

5.3.1.3. Seasonal comparison using stepwise linear discriminant analysis

As the classification results of the derivatives data using linear discriminant analysis with 138 bands were poor and the previous seasonal comparison showed no significant difference among the four seasons, another comparison among different seasons was performed. The seasonal comparison used stepwise linear discriminant analysis in which the spectral bands were selected by the second criterion with 21 tree species for each season. The classification results of the four seasons were shown in Table 5.5 while the results of significant testing of Kappas comparing classifications of different seasons were listed in Table 5.6. The confusion matrices were shown in Appendix 8.

Again, using the original spectra produced better results than those using the first and second derivatives. Winter data was able to generate the most accurate results with overall accuracy of 91.27% using the original spectra. The fact that some of the tree species changed in leaf color during winter might help to improve the classification results. Autumn data yielded a slightly lower accuracy of 87.62% than the winter ones but statistically the differences were only marginal. The results of summer and spring, however, were significantly lower than those in autumn and winter. In general, autumn and winter data outperformed those in spring and summer.

The results were consistent with previous studies in which seasonal variability was shown to affect tree species classification accuracy significantly (Eder, 1989 and Schriever and Congalton, 1995). Eder (1989) showed that autumnal senescence helped to increase accuracy in hardwood forest type delineation when applied to aerial photography. However, Schriever and Congalton (1995) showed that spring

data produced better results than autumn data for the identification of hardwood species. The fact that bud break of some species was sooner than others in spring helped to improve classification results in spring. Although the previous two studies contradict with one another, the most important implication is that seasonal variability can significantly affect the results of tree species recognition. Whether the data should be collected in a particular season or month for best classification results depends on different leaf phenology of different forest types in particular areas.

Table 5.5. Classification results of stepwise linear discriminant analysis using 21 tree species for seasonal comparison

	Original Spectra		*First Derivatives*		*Second Derivatives*	
	OA (%)	*K (×100)*	*OA (%)*	*K (×100)*	*OA (%)*	*K (×100)*
Spring	83.97	83.17	83.81	83.00	64.29	62.50
Summer	81.43	80.50	83.17	82.33	77.78	76.67
Autumn	87.62	87.00	84.60	83.83	71.43	70.00
Winter	91.27	90.83	86.03	85.33	75.08	73.83

Table 5.6. Significant testing of Kappas for comparing classification results of stepwise linear discriminant analysis for seasonal comparison (absolute value >1.96 indicates significant difference at 0.05 significance level)

Original Spectra

	Spring	*Summer*	*Autumn*	*Winter*
Spring	-	1.1938	-1.8594	-3.9643
Summer	-1.1938	-	-3.0506	-5.1474
Autumn	1.8594	3.0506	-	-2.1134
Winter	3.9643	5.1474	2.1134	-

First Derivatives

	Spring	*Summer*	*Autumn*	*Winter*
Spring	-	0.3037	-0.3864	-1.1036
Summer	-0.3037	-	-0.6897	-1.4064
Autumn	0.3864	0.6897	-	-0.7167
Winter	-1.1036	1.4064	0.7167	-

Second Derivatives

	Spring	*Summer*	*Autumn*	*Winter*
Spring	-	-5.3469	-2.7278	-4.2033
Summer	5.3469	-	2.5990	1.1298
Autumn	2.7278	-2.5990	-	-1.4668
Winter	4.2033	-1.1298	-1.4668	-

5.3.1.4. Implications

Some implications could be drawn from this preliminary band selection analysis using stepwise discriminant analysis. Firstly, band selection did help to improve classification accuracy. It suggested further studies for comparing different band selection methods. Secondly, redundancy in spectral bands occurred remarkably in hyperspectral data. In Case 3, using only seven to thirteen bands could produce better results than using all 138 bands. Only little improvements in accuracy were found when more spectral bands (9 to 37 bands) were used in Case 2. Thirdly, the selected bands mainly lied in the spectral regions of the green peak and the red edge. This indicated that spectral bands in these regions had stronger discriminating power than other regions such as the blue and red regions.

5.3.2. Band selection using hierarchical clustering technique

5.3.2.1. Hierarchical clustering procedure

A hierarchical clustering procedure was done using the original spectral data of autumn. Figure 5.6 showed the clusters generated throughout the first twenty-two iterations during the clustering procedure. In the first iteration, the 400 – 900 nm spectral region was divided into two clusters such that one belonged to the visible bands (400 – 720 nm) and the other lied on the infrared region (720 – 900 nm). This indicates that these two spectral regions had different inherent spectral properties. This was consistent with our well-accepted understanding of the spectral bands.

Figure 5.6 Result of the first 22 hierarchical clustering iterations

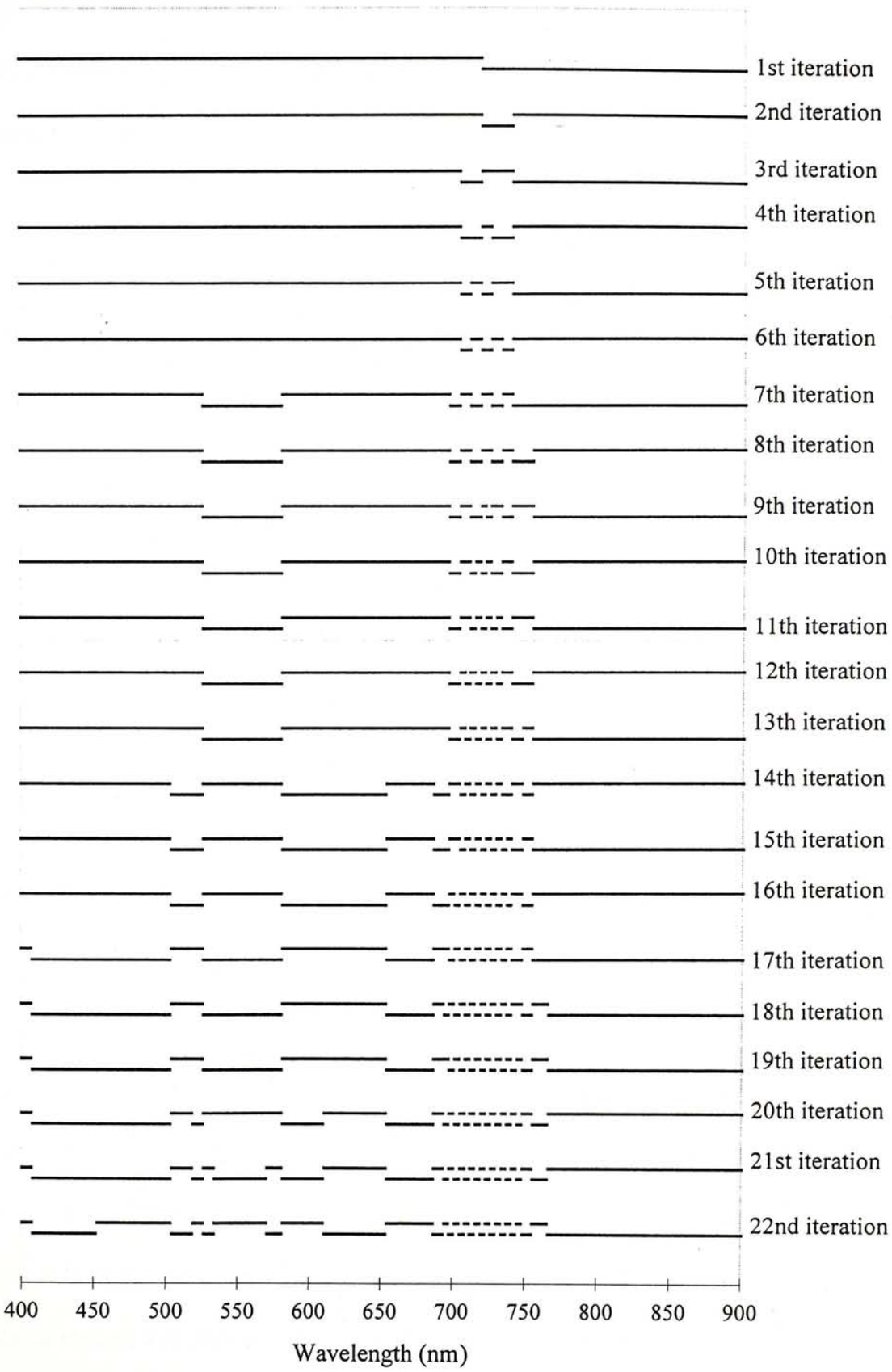

From the second to the sixth iterations, small clusters were generated in the spectral range from 705 nm to 740 nm along the red edge. Spectral bands in the region of the red edge tended to be differentiated from the visible and near-infrared bands. It shows that the red edge may contain different information other than that obtained from the visible and infrared regions.

From the seventh to the thirteenth iterations, one more cluster was generated in the visible region which was the green bands from 525 nm to 580 nm whilst more clusters came out in the region of the red edge from 697 nm to 755 nm. The results were as expected since spectral information did contain in the green peak. Except the clusters found in the red edge, the three clusters in the visible region and the single cluster in the infrared bands can be considered as the blue, green, red and near-infrared bands present in traditional broadband multispectral sensors. Certainly, these four broad bands contain useful information. However, they are not informative enough to recognize tree species. The spectral bands in the red edge which have been neglected in traditional multispectral sensors seem to contain extra information for tree species recognition.

From the fourteenth to the nineteenth iterations, two more clusters were generated in the visible region so that a total of five clusters appeared in the visible region. The first cluster lied from 400 nm to 504 nm which was the blue bands. It is noted that a small cluster from 400 nm to 407 nm was generated from the seventeenth iteration onwards. This cluster may be formed due to relatively noisy bands existed in this region so that it was ignored and combined into the first cluster. The second one was in the spectral range of the edge appeared before the green peak

from 504 nm to 526 nm and the third one was the green peak which lied from 526 nm to 582 nm. The fourth one was another edge after the green peak from 582 nm to 654 nm while the last cluster was the red bands from 654 nm to 686 nm. Again, more clusters were generated in the red edge from 686 nm to 766 nm. The infrared bands remained a single cluster. From the five clusters generated in the visible region, the two edges before and after the green peak may contain information other than that obtained from the traditional blue, green and red broad bands. More experiments should be implemented to explore how the spectral bands in the edges including the two edges before and after the green peak as well as the red edge help to recognize tree species.

From the twentieth to the twenty-second iterations, more clusters were formed in the visible region as most clusters in the red edge cannot be divided any further. The newly generated clusters appeared mainly in the spectral region of the two edges before and after the green peak except the two clusters which divided the blue bands into two groups from 400 nm to 452 nm and from 452 nm to 504 nm respectively. This suggests that more information may exist in the two edges before and after the green peak than the traditional blue, green and red bands.

5.3.2.2. Selection of spectral band sets

Seven sets of spectral band were selected to test the discriminating power of different spectral regions. Table 5.7 showed the seven selected spectral band sets systematically. The bands were selected at the center of the clusters formed in different stages of the previous hierarchical clustering procedure.

Table 5.7. Spectral band sets selected from hierarchical clustering to test the discriminating power of different spectral regions

Spectral band sets	*Description*	*Selected bands*
4 bands	Represents the four traditional blue, green, red (RGB) and near-infrared (NIR) broad bands.	450.28 nm (blue) 550.00 nm (green) 670.37 nm (red) 835.39 nm (infrared)
3 edges	Includes the two edges before and after the green peak and one red edge.	516.89 nm (edge before green peak) 619.51 nm (edge after green peak) 728.14 nm (red edge)
7 bands	Includes the RGB and NIR bands and 3 edges.	450.28 nm (blue) 516.89 nm (edge before green peak) 550.00 nm (green peak) 619.51 nm (edge after green peak) 670.37 nm (red) 728.14 nm (red edge) 835.39 nm (infrared)
5 red edges	Includes five red edges to determine the discriminating power of the red edge only.	695.69 nm (red edge) 710.13 nm (red edge) 728.14 nm (red edge) 742.52 nm (red edge) 760.46 nm (red edge)
7 edges	Includes the two edges before and after the green peak and five red edges to determine the discriminating power of the edges.	516.89 nm (edge before green peak) 619.51 nm (edge after green peak) 695.69 nm (red edge) 710.13 nm (red edge) 728.14 nm (red edge) 742.52 nm (red edge) 760.46 nm (red edge)
11 bands	Includes the RGB and NIR bands and the seven edges.	450.28 nm (blue) 516.89 nm (edge before green peak) 550.00 nm (green peak) 619.51 nm (edge after green peak) 670.37 nm (red) 695.69 nm (red edge) 710.13 nm (red edge) 728.14 nm (red edge) 742.52 nm (red edge) 760.46 nm (red edge) 835.39 nm (infrared)
13 bands	Includes bands from "11 bands" set with the blue region and the edge after green peak region divided into two bands.	427.29 nm (blue) 476.24 nm (blue) 516.89 nm (edge before green peak) 550.00 nm (green) 597.62 nm (edge after green peak) 630.43 nm (edge after green peak) 670.37 nm (red) 695.69 nm (red edge) 710.13 nm (red edge) 728.14 nm (red edge) 742.52 nm (red edge) 760.46 nm (red edge) 835.39 nm (infrared)

The first band set (4 bands) included four spectral bands which represented the traditional multispectral broad bands including blue, green, red (RGB) and near-infrared (NIR) bands. As the traditional broad bands did not consider the edges including the edges before and after the green peak and the red edge, the second band set (3 edges) tried to determine the potential of using these edges for tree species recognition. Thus, the second band sets included three bands taking from the spectral regions of the edges before and after the green peak and the red edge. In the previous two band sets, the bands were selected from the center of clusters formed throughout the fourteenth to the nineteenth iteration of the clustering procedure. The third band set (7 bands) included seven bands which contained in the previous two band sets i.e. the four traditional multispectral broad bands, RGB and NIR, and the three edges.

As most of the clusters generated from the clustering procedure lied in the red edge region, five spectral bands were selected from this region solely to determine the discriminating power of the red edge in the fourth band set (5 red edges). Then, the fifth band set (7 edges) included the five red edges and the two edges before and after the green peak to further investigate the discriminating power of the edges. The sixth band set (11 bands) included eleven bands containing RGB and NIR bands in the first band set and the seven edges in the fifth band set.

Finally, the seventh band set (13 bands) included thirteen bands which were selected from the center of the clusters from throughout the twentieth and the twenty-second iterations of the clustering procedure. The blue region and the edge after the green peak region were divided into two bands in the seventh band set while other bands remained the same.

The bands in the "13 bands" band set were compared with the wavelengths that were correlated with biochemical or biophysical information found by other researchers (Table 5.8). The selected bands found by Curran (1989) and Martin *et al.* (1998) were mainly the near-infrared and mid-infrared bands while those found by Thenkabail *et al.* (1999) and the thirteen bands found in this study mainly lied in the visible and the near-infrared bands. Although the bands found by these researchers and in this study were not consistent with one another, some wavelengths or spectral regions were commonly selected.

The two blue bands found in this study, 429 nm and 476 nm, were close to the two found by Curran (1989), 430 nm and 460 nm while Thenkabail *et al.* found one blue band at 495 nm. It is interesting that no green bands were selected by Curran (1989) and Martin *et al.* (1998) when three green bands were included by Thenkabail *et al.* (1999) and in this study. The three green bands found in these two studies were quite consistent. Both studies selected 550 nm which is the green peak. The other two green bands represented the two edges after and before the green peak respectively in both studies. Three red bands were found by Thenkabail *et al.* (1999) and in this study while two were selected by Curran (1989) and one by Martin *et al.* (1998). The spectral bands, 640 nm selected by Curran (1989), 627 nm selected by Martin *et al.* (1998) and 630 nm found in this study were consistent. They represented the yellow edge after the green peak. Moreover, the spectral bands, 660 nm found by Curran (1989), 668 nm found by Thenkabail *et al.* (1999) and 670 nm found in this study were consistent such that they represented the red trough. Both in this study and by Thenkabail *et al.* (1999) used the 696-nm band. The commonly selected bands in the visible region reveals that some particular wavelengths are

Table 5.8. Comparison of the spectral bands that are correlated with biochemical or biophysical information found by different researchers and the 13 bands selected from hierarchical clustering procedures in this study

	Curran, 1989	*Martin et al., 1998*	*Thenkabail et al., 1999*	*This study*
Number of bands	42	9	12	13
Spectral range	400 – 2400 nm	400 – 2500 nm	350 – 1050 nm	400 – 900 nm
Blue bands	430	–	495	429
(400 – 500 nm)	460			476
Green bands	–	–	525	517
(500 – 600 nm)			550	550
			568	598
Red bands	640	627	668	630
(600 – 700 nm)	660		682	670
			696	696
Near-infrared bands	910	750	720	710
(700 – 1300 nm)	930	783	845	728
	970	822	920	743
	990		982	760
	1020		1025	835
	1040			
	1120			
	1200			
Mid-infrared bands	1400	1641	–	–
(1300 – 2500 nm)	1420	1660		
	1450	2140		
	1490	2280		
	1510	2290		
	1530			
	1540			
	1580			
	1690			
	1780			
	1820			
	1900			
	1940			
	1960			
	1980			
	2000			
	2060			
	2080			
	2100			
	2130			
	2180			
	2240			
	2250			
	2270			
	2280			
	2300			
	2310			
	2320			
	2340			
	2350			

useful and important for vegetation studies. An optimal combination of narrow bands exists in the visible spectral region.

In the near-infrared region, the selected bands were less consistent. Curran (1989) included no bands in the red edge. Martin *et al.* (1998) and Thenkabail *et al.* (1999) selected one band in the red edge from 700 nm to 760 nm while four red edges were selected in this study. For the near-infrared plateau from 760 nm to 940 nm, Curran (1989), Martin *et al.* (1998) and Thenkabail *et al.* (1999) selected two bands while one band was included in this study.

5.3.2.3. Classification results of the selected band sets

Linear discriminant analysis was used again to classify tree species using original spectra of the selected band sets for four seasons in order to determine which spectral regions were important in tree species recognition. Table 5.9 showed the classification results and Table 5.10 showed the significant testing of Kappas among the classification results. The confusion matrices were shown in Appendix 9.

Table 5.9. Classification results of the selected band sets generated from hierarchical clustering procedures

		Spring	*Summer*	*Autumn*	*Winter*	*Average overall accuracy (%)*
4 bands	OA (%)	48.27	39.20	50.00	46.98	46.11
	K ($^{\times}$100)	46.11	36.67	47.83	44.33	43.74
3 edges	OA (%)	42.40	47.73	39.44	49.05	44.66
	K ($^{\times}$100)	40.00	45.56	36.81	46.50	42.22
7 bands	OA (%)	76.00	76.27	79.86	76.51	77.16
	K ($^{\times}$100)	75.00	75.28	78.99	75.33	76.15
5 red edges	OA (%)	54.53	55.20	54.17	58.57	55.62
	K ($^{\times}$100)	52.64	53.33	52.17	56.50	53.66
7 edges	OA (%)	72.13	73.60	69.31	76.83	72.97
	K ($^{\times}$100)	70.97	72.50	67.97	75.67	71.78
11 bands	OA (%)	86.80	87.33	88.89	86.03	87.26
	K ($^{\times}$100)	86.25	86.81	88.41	85.33	86.70
13 bands	OA (%)	87.47	88.40	91.94	89.37	89.30
	K ($^{\times}$100)	86.94	87.92	91.59	88.83	88.82

Table 5.10. Significant testing of Kappas for comparing classification results with different selected band sets generated from hierarchical clustering procedures (value > 1.96 indicates significant difference at 0.05 significance level)

Spring

	4 bands	*3 edges*	*7 bands*	*5 red edges*	*7 edges*	*11 bands*	*13 bands*
4 bands	-	2.2967	-11.5927	-2.4413	-9.7664	-17.5348	-17.9759
3 edges	-2.2967	-	-14.1364	-4.7533	-12.2428	-20.3604	-20.8282
7 bands	11.5927	14.1364	-	8.3684	1.7128	-5.4316	-5.8213
5 red edges	2.4413	4.7533	-8.3684	-	-7.2076	-14.6971	-15.1168
7 edges	9.7664	12.2428	-1.7128	7.2076	-	-7.1545	-7.5462
11 bands	17.5348	20.3604	5.4316	14.6971	7.1545	-	-0.3858
13 bands	17.9759	20.8282	5.8213	15.1168	7.5462	0.3858	-

Summer

	4 bands	*3 edges*	*7 bands*	*5 red edges*	*7 edges*	*11 bands*	*13 bands*
4 bands	-	-3.3742	-15.7761	-6.3311	-14.4259	-22.4678	-23.2475
3 edges	3.3742	-	-11.9657	-2.9169	-10.6926	-18.1593	-18.8691
7 bands	15.7761	11.9657	-	8.8417	1.1954	-5.6183	-6.2495
5 red edges	6.3311	2.9169	-8.8417	-	-7.6121	-14.7497	-15.4200
7 edges	14.4259	10.6926	-1.1954	7.6121	-	-6.8277	-7.4607
11 bands	22.4678	18.1593	5.6183	14.7497	6.8277	-	-0.6331
13 bands	23.2475	18.8691	6.2495	15.4200	7.4607	0.6331	-

Autumn

	4 bands	*3 edges*	*7 bands*	*5 red edges*	*7 edges*	*11 bands*	*13 bands*
4 bands	-	4.0683	-12.5341	-1.5897	-7.6414	-17.7104	-19.8129
3 edges	-4.0683	-	-16.9648	-5.6897	-11.9844	-22.9364	-25.2963
7 bands	12.5341	16.9648	-	10.8203	4.6503	-4.7641	-6.7014
5 red edges	1.5897	5.6897	-10.8203	-	-6.0095	-15.8735	-17.9183
7 edges	7.6414	11.9844	-4.6503	6.0095	-	-9.4460	-11.3789
11 bands	17.7104	22.9364	4.7641	15.8735	9.4460	-	-1.9736
13 bands	19.8129	25.2963	6.7014	17.9183	11.3789	1.9736	-

Winter

	4 bands	*3 edges*	*7 bands*	*5 red edges*	*7 edges*	*11 bands*	*13 bands*
4 bands	-	-0.7350	-11.3423	-4.1585	-11.4874	-16.1688	-18.1822
3 edges	0.7350	-	-10.5284	-3.4120	-10.6715	-15.2788	-17.2538
7 bands	11.3423	10.5284	-	6.9373	-0.1334	-4.3685	-6.1619
5 red edges	4.1585	3.4120	-6.9373	-	-7.0746	-11.4602	-13.3227
7 edges	11.4874	10.6715	0.1334	7.0746	-	-4.2350	-6.0286
11 bands	16.1688	15.2788	4.3685	11.4602	4.2350	-	-1.8050
13 bands	18.1822	17.2538	6.1619	13.3227	6.0286	1.8050	-

The "4 bands" and "3 edges" band set obtained the lowest classification accuracy with average overall accuracy of 46.11% and 44.66 % respectively. Although the average overall accuracy for "4 bands" was higher than "3 edges", "4 bands" obtained higher overall accuracy for spring and autumn while "3 edges" had higher overall accuracy for summer and winter. Thus, it was difficult to conclude which band set got higher discriminating power for tree species recognition. However, the results confirmed that the spectral region of the edges which had been ignored in traditional multispectral broadband sensors contained considerably useful information as the traditional RGB and NIR spectral bands.

The "7 bands" band set comprised of the bands in the previous two band sets. The average overall accuracy was 77.16% which was significantly better than that in the previous band sets. This indicates that the spectral bands in the edges do help to differentiate different tree species instead of using the traditional RGB and NIR bands only. Besides, "7 bands" also generated better classification results than using all 138 bands. This, again, shows that redundancy exists in hyperspectral spectra and band selection can not only save computational time and resources, but also improve tree species recognition.

The "5 red edges" band set contained five spectral bands located only in the red edge in order to investigate the discriminating power of the red edge. The average overall accuracy was 53.66% which was significantly higher than those obtained using "4 bands" and "3 edges". The results clearly show that spectral bands in the red edge contain quite a lot of information for tree species recognition. The "7 edges" band set added the two bands located in the region of the edges before and after the

green peak to the "5 red edges" band set. The average overall accuracy was 72.97% which is only slightly lower than those using all 138 bands. It further convinces the potential of including the edges for tree species recognition.

The "11 bands" and "13 bands" band set performed the best with average overall accuracy of 87.26% and 89.30% respectively. Significant improvements of 9.03% to 12.86% in overall accuracy for four seasons were found when "11 bands" were used instead of "7 bands". It means that including four more spectral bands in the red edge region helps to improve classification accuracy for more than 9%. Besides, the "13 bands" band set had higher overall accuracy than the "11 bands" band set for each season although significant testing showed insignificant differences between the two. This indicates that classification accuracy can be improved further when more bands are appropriately selected for tree species recognition. Furthermore, the results were also superior to those produced using selected bands obtained by stepwise discriminant analysis.

5.4. Summary

Data compression was done by principal components analysis using *in situ* data and laboratory data separately. For both PCAs, more information was yielded from hyperspectral data as compared to the two dimensional PCs representing greenness and brightness measures obtained from PCA or tasseled cap transformation using broadband multispectral data. PC3 and PC4 possessed useful information in interpretation and understanding of the inherent structure of hyperspectral reflectances in different surface types.

Band selection was performed using stepwise discriminant analysis and hierarchical clustering procedures. Both band selection procedures improved significantly the classification accuracies of tree species recognition. The bands that were selected by stepwise discriminant analysis mainly lied in the spectral regions around the green peak and the red edge. Hierarchical clustering suggested that the spectral bands along the edges including two edges before and after the green peak as well as the red edge contain useful information for tree species recognition.

CHAPTER SIX

SUMMARY AND CONCLUSION

6.1. Introduction

This chapter is the summary and conclusion of this study. A brief summary on the results and discussions of tree species recognition, data compression and band selection is presented. The limitation of this study is then stated followed by recommendations for further studies. Finally, a conclusion on this study is given.

6.2. Summary

In this study, hyperspectral data were collected in the Chinese University of Hong Kong campus. Laboratory data of 25 tree species were taken to test the separability of hyperspectral data of different tree species. *In situ* spectral reflectance of ten surface covers including several tree species, grass, fern, water and concrete were measured to set up a hyperspectral database.

6.2.1. Tree species recognition

Tree species recognition was done by two classification algorithms, linear discriminant analysis and artificial neural networks, using 138 bands from 400 nm to 900 nm. The classification results were satisfactory for the original spectral reflectance data which yielded over 70% overall accuracy using both classifiers. It confirms the differentiating power of hyperspectral data for tree species recognition.

When the classification results generated from linear discriminant analysis were compared with those from neural networks, no significant differences existed

between the two using original spectra. Both classifiers yielded overall average accuracy of around 73%. However, linear discriminant analysis generated very poor results with under 26% overall accuracy using both the first and the second derivatives data. Neural network generated better results for the derivatives data from overall accuracy of 40.40% to 63.19%. For the efficiency of the classifiers, linear discriminant analysis worked faster and more convenient than neural networks.

For comparison of different data processing strategies, using the original spectra produced better classification results than using either the first or the second derivatives of the spectra. Meanwhile, using the first derivatives spectra generated better results than using the second derivatives spectra.

For the seasonal comparison of 21 tree species using linear discriminant analysis, autumn data obtained the most accurate results while summer data produced the lowest accuracy. However, the differences were statistically insignificant.

6.2.2. Data compression

Data compression was done by principal components analysis using *in situ* data and laboratory data separately. For both PCAs, more information was yielded from hyperspectral data as compared to the two dimensional PCs representing greenness and brightness measures obtained from PCA or tasseled cap transformation using broadband multispectral data such as Landsat MSS or SPOT. PC3 and PC4 possessed useful information in interpretation and understanding of the inherent structure of hyperspectral reflectances in different surface types.

6.2.3. Band selection

Band selection was performed using stepwise discriminant analysis and hierarchical clustering procedures. It was found that both band selection procedures improved significantly the classification accuracies of tree species recognition. An overall accuracy of over 87% was attained using 8 – 18 bands selected by stepwise discriminant analysis for the original spectra of autumn and winter data. The 13 bands selected from hierarchical clustering procedures were able to obtain an overall accuracy of over 89% using the original spectra of autumn and winter data.

Seasonal comparison done by stepwise linear discriminant analysis showed that autumn and winter data outperformed those in spring and summer. Winter data was able to produce the most accurate results with overall accuracy of 91.27% using the original spectra. It was shown that seasonal variability affected tree species recognition significantly.

The bands that were selected by stepwise discriminant analysis mainly lied in the spectral regions around the green peak and the red edge. Hierarchical clustering suggested that the spectral bands along the edges including two edges before and after the green peak as well as the red edge which were neglected in traditional broadband multispectral sensors tended to contain useful information for tree species recognition.

6.3. Limitations of this study

Several limitations exist in this study. First, hyperspectral data of tree species were measured in a controlled environment with leaf and branch samples lied on a surface instead of collected above tree canopies in the field. Although leaves and branches contain essential biochemical, biophysical and physiological information of trees, the spectral characteristics of a forest canopy as recorded in airborne or spaceborne remotely sensed data cannot be completely and precisely accounted for by the spectra of their leaf and branch components. The canopy shape, LAI and the orientation of leaves and branches cannot be simulated by the three density levels of leaf and branch samples in this experiment. The difference between laboratory data and *in situ* data is well demonstrated by the t-test between the two.

Second, the hyperspectral database being set up is far from comprehensive due to time limitation. The *in situ* data were intended to be collected in autumn. At the same time, autumn data of tree species were measured. As a result, only ten *in situ* surface cover types were measured. Many dominant surface cover features have not been included in the database such as sands, soils, rocks, coastal water, mangroves and different types of grass, fern, shrub and trees, etc.

Third, foliar biochemical data are not included in this study. The spectral bands in the edges including two edges before and after the green peak as well as the red edge are proved to be useful for tree species recognition only empirically by band selection procedures. However, the reasons why these bands were selected and how they help to recognize tree species are unknown. Combining foliar biochemical data to hyperspectral data may give us hints for interpretation of the selected spectral

bands.

Fourth, the number of data samples for tree species recognition should be increased. Thirty-six samples were totally taken for each tree species in each season with only six of them used as training samples. Theoretically, the number of training samples should exceed ten times the number of variables i.e. the number of spectral bands (Jensen, 1994). However, 689 bands are present from 400 nm to 900 nm in hyperspectral data for this study. It means that it requires 6890 training samples which is quite an impossible number.

Finally, hyperspectral imagery is not available in this study. Currently, no airborne hyperspectral sensors are available in Hong Kong. If hyperspectral images are available, tree species recognition using the laboratory data can be verified with the image data in larger area and including more tree species types. Moreover, principal components analysis can be performed to generate principal components images which are more easily interpretable than using the principal components loadings and the scatterplots of the principal components scores.

6.4. Recommendations for further studies

After discussing the limitations of this study, some recommendations for further studies are listed in this section. First, a more comprehensive hyperspectral database with *in situ* data and airborne or spaceborne hyperspectral imagery is recommended. The hyperspectral data that were collected in this study are far from comprehensive as a hyperspectral database for the subtropical environment. Tropical and subtropical forests are mixed with hundreds to thousands tree species that cannot be found in

other areas. More samples for tree species and other surface covers in tropical and subtropical environment should be included in the future hyperspectral database.

Moreover, hyperspectral database should focus on *in situ* measurements of tree canopies instead of laboratory measurements of leaf and branch components. However, tropical and subtropical climate with high annual rainfall and relatively high subtropical tree stands pose difficulties for *in situ* measurement. A much longer study period is needed to generate a comprehensive database. Thus, large area surveys using airborne or spaceborne hyperspectral imagery are the future trend for obtaining hyperspectral data.

Second, a wider spectral region for tree species recognition is recommended. The spectral region used for data analysis in this study is from 400 to 900 nm which includes the visible and the near-infrared bands. Spectral bands with wavelengths shorter and longer than this region are excluded to avoid too much noise. However, the excluded bands also contain important spectral features which helps to identify tree species, especially wavelengths longer than 900 nm. According to Curran (1989), among 42 absorption features related to particular foliar chemical concentrations, only four bands lie in the 400 to 900 nm region. The other 38 spectral bands fall into the spectral range from 900 to 2400 nm which may contribute to tree species recognition. Thus, more experiments should be carried out to explore the potential of using spectral bands from visible to near and mid-infrared spectral regions for tree species recognition.

Third, biochemical data are suggested to be included for tree species recognition

and band selection. The absorption features of foliar spectra are the results of electron transitions in chlorophyll and of the bending and stretching of the O-H band in water and other chemicals (Curran, 1989). Chlorophyll concentration, water moisture level and concentration of other chemicals vary among different tree species. As a result, these absorption features are crucial factors for tree species recognition. Foliar biochemical data can be correlated with the hyperspectral data collected. Bands that are correlated with the biochemical data can be obtained. Experiments can then be conducted to determine how these bands help to improve tree species recognition.

Martin *et al.* (1998) used AVIRIS imagery to correlate with nitrogen and lignin concentration of foliage. Nine bands that were closely correlated with the two chemicals were selected to classify eleven forest type covers. An overall accuracy of 75% was yielded by a random selection of validation pixels. This showed the potential of using biochemical data for tree species recognition.

On the other hand, foliar biochemical data can help to interpret the bands selected by different band selection procedures. The selected spectral bands are found only empirically with no theoretical explanations on why they are selected. Correlation of the selected bands with different biochemical data may explain why they are useful for tree species recognition.

Fourth, more frequent spectral measurements of tree species, for instance, monthly measurements are recommended to monitor the leaf phenology of different tree species throughout one year. The period of bud break in spring, flowering,

fruiting and autumnal senescence of trees varies from one species to another. These seasonal variability significantly affect the spectral reflectance of the tree species and hence the results of tree species recognition. Thus, a detailed study of the seasonal variability of different tree species is essential.

Finally, more algorithms for band selection are suggested to apply for tree species recognition. Band selection procedures used in this study did help to improve classification results significantly. This reveals the importance of band selection and the redundant nature of hyperpectral data. The optimal number and position of wavebands, useful spectral regions and optimal bandwidth should be identified for different applications. More experiments should be undertaken to explore the various methods of band selection.

6.5. Conclusion

This study successfully classifies 25 subtropical tree species using hyperspectral data with satisfactory classification accuracy. The accomplishment of this preliminary test validates the ability of hyperspectral data for identification of subtropical tree species. In Hong Kong, using original spectra collected in autumn or winter with a stepwise linear discriminant analysis can generate reasonably satisfactory result for tree species recognition. It is also suggested that the spectral bands along the edges including two edges before and after the green peak as well as the red edge which have been neglected in traditional broadband multispectral sensors tended to contain useful information for tree species recognition. More experiments should be conducted to explore the potential of using these spectral bands for vegetation studies in particular tree species recognition.

BIBLIOGRAPHY

Baret, F., 1995, Use of spectral reflectance variation to retrieve canopy biophysical characteristics, in Danson, F. M. and S. E. Plummer (eds), *Advances in Environmental Remote Sensing*, John Wiley & Sons, New York, pp. 33-51.

Blackburn, G. A. and Milton, E. J., 1995, Seasonal variations in the spectral reflectance of deciduous tree canopies, *International Journal of Remote Sensing*, **16**, 709-720.

Blackburn, G. A. and Milton, E. J., 1997, An ecological survey of deciduous woodlands using airborne remote sensing and geographical information systems (GIS), *International Journal of Remote Sensing*, **18**, 1919-1935.

Caetano, M. and Pereira, J., 1996, The effect of the understorey on the estimation of coniferous forest leaf area index (LAI) based on remotely sensed data, in Desachy, J. (ed), *Image and Signal Processing for Remote Sensing III*, SPIE Vol. 2955, pp. 63-71.

Cloutis, E. A., 1996, Review Article: Hyperspectral geological remote sensing: evaluation of analytical techniques, *International Journal of Remote Sensing*, **17**, 2215-2242.

Cohen, J., 1960, A coefficient of agreement of nominal scales, *Educational and Psychological Measurement*, **20**, 37-46.

Crist, E. P. and Cicone, R. C., 1984, Application of the tasseled cap concept to stimulated Thematic Mapper data, *Photogrammetric Engineering and Remote Sensing*, **50**, 343-352.

Curran, J. P., 1989, Remote sensing of foliar chemistry, *Remote Sensing of Environment*, **30**, 271-278.

Curran, J. P., 1994, Imaging spectrometry, *Progress in Physical Geography*, **18**, 247-266.

Danson, F. M., 1995, Developments in the remote sensing of forest canopy structure, in Danson, F. M. and S. E. Plummer (eds), *Advances in Environmental Remote Sensing*, John Wiley & Sons, New York, pp. 53-69.

Demetriades-Shah, T. H., Steven, M. D. and Clark, J. A., 1990, High resolution derivative spectra in remote sensing, *Remote Sensing of Environment*, **33**, 55-64.

Eder, J. J., 1989, Don't shoot unless its autumn, *Journal of Forestry*, **87**, 50-51.

Foody, G. M., 1994, Ordinal-level classification of sub-pixel tropical forest cover, *Photogrammetric Engineering and Remote Sensing*, **60**, 61-65.

Frank, T. D., 1988, Mapping dominant vegetation communities in the Colorado Rocky Mountain Front Range with Landsat Thematic Mapper and digital terrain data, *Photogrammetric Engineering and Remote Sensing*, **54**, 1727-1734.

Franklin, S. E., 1994, Discrimination of subalpine forest species and canopy density using digital CASI, SPOT PLA, and Landsat TM data, *Photogrammetric Engineering and Remote Sensing*, **60**, 1233-1241.

Gong, P., Pu, R. and Yu, B., 1997, Conifer species recognition: and exploratory analysis of *in situ* hyperspectral data, *Remote Sensing of Environment*, **62**, 189-200.

Green, R. O., 1994, *AVIRIS Operational Characteristics*, Jet Propulsion Lab., Pasadena, CA.

Hair, J. F., Jr., Anderson, R. E., Tatham, R. L. and Black, W. C., 1995, *Multivariate Data Analysis with Readings*, Prentice Hall, Upper Saddle River, New Jersey.

Hobbs, R. J., 1991, Remote sensing of spatial and temporal dynamics of vegetation, in Hobbs, R. J. and H. A. Mooney (eds), *Remote Sensing of Biosphere Functioning*, Springer-Verlag, New York, pp. 203-219.

Jensen, J. R., 1994, *Introductory Digital Image Processing: a Remote Sensing Perspective*, Second Edition, Prentice Hall, Upper Saddle River, New Jersey.

Kauth, R. J. and Thomas, G. S., 1976, The tasseled cap---a graphic description of spectral-temporal development of agricultural crops as seen by Landsat, *Proceedings: 2nd International Symposium on Machine Proceedings of Remotely Sensed Data*, Purdue University, West Lafayette, IN, 1976, pp. 41-49.

Kunkel, B., Posselt, W., Schmidt, E., Del Bello, U., Harnisch, B. and Meynart, R., 1997, Hyperspectral imager survey and developments for scientific and operational land processes monitoring applications, in G. Cecchi *et. al.* (eds), *Remote Sensing of Vegetation and Water, and Standardization of Remote Sensing Methods*, SPIE Vol. 3107, pp. 2-14.

Lillesand, T. M. and Kiefer, R. W., 1994, *Remote Sensing and Image Interpretation*, Third Edition, John Wiley & Sons, New York.

Martin, M. E., Newman, S. D., Aber, J. D. and Congalton, R. G., 1998, Determining forest species composition using high spectral resolution remote sensing data, *Remote Sensing of Environment*, **65**, 249-254.

Mehl, W., 1994, Data analysis - Processing requirements and available software tools, in Hill, J. and J. Mgier (eds), *Imaging Spectrometry - a Tool for Environmental Observations*, Kluwer Academic Publishers, Boston, pp. 89-107.

MicroCal Software, Inc., 1999, http://www.microcal.com.

Milton, E. J., Rollin, E. M. and Emery, D. R., 1995, Advances in field spectroscopy, in Danson, F. M. and S. E. Plummer (eds), *Advances in Environmental Remote Sensing*, John Wiley & Sons, New York, pp. 9-31.

Nelson, R. F., Latty, R. S. and Mott, G., 1985, Classifying northern forests using Thematic Mapper Simulator data, *Photogrammetric Engineering & Remote Sensing*, **50**, 607-617.

Neural Networks Research Center, 1998, http://www.cis.hut.fi/nnrc/, Helsinki University of Technology, Finland.

Norcliffe, G. B., 1982, *Inferential Statistics for Geographers*, Hutchinson, London.

Orbital Imaging Co., 1998, http://www.orbimage.com/.

Ocean Optics, Inc., 1999, http://www.oceanoptics.com/ProductSheets/S2000.asp.

Openshaw, S. and Openshaw, C., 1997, *Artificial Intelligence in Geography*, John Wiley & Sons, England.

Palacios-Orueta, A. and Ustin, S. L., 1996, Multivariate statistical classification of soil spectra, *Remote Sensing of Environment*, **57**, 108-118.

Pao, Y., 1989, *Adaptive Pattern Recognition and Neural Networks*, Addison and Wesley, New York.

Paola, J. D., and Schowengerdt R. A., 1995, Review article: A review and analysis of backpropagation neural networks for classification of remotely-sensed multi-spectral imagery, *International Journal of Remote Sensing*, **16**, 3033-3058.

Peterson, D. L., Spanner, M. A., Running, S. W. and Teuber, K. B., 1987, Relationship of Thematic Mapper simulator data to leaf area index of temperate coniferous forest, *Remote Sensing of Environment*, **22**, 323-341.

Petrie, G. M. and Heasler, P. G., 1998, Optimal band selection strategies for hyperspectral data sets, *Proceedings of IGARSS, 1998*, pp. 1582-1584.

Thenkabail, P. S., Smith, R. B. and Pauw, E. D., 1999, Hyperspectral vegetation indices for determining agricultural crop characteristics, http://spectra.ceo.yale.edu/Project/hypaper.html.

Price, J. C., 1994a, How unique are spectral signatures? *Remote Sensing of Environment,* **49**, 181-186.

Price, J. C., 1994b, Band selection procedure for multispectral scanners, *Applied Optics*, **33**, 3281-3288.

Richards, J. A., 1993, *Remote Sensing Digital Image Analysis*, Second Edition,

Springer-Verlag, Berlin, Heidelberg.

Roberts, D. A., Green, R. O. and Adams, J. B., 1997, Temporal and spatial patterns in vegetation and atmospheric properties from AVIRIS, *Remote Sensing of Environment,* **62**, 223-240.

Rosenfield, G. H. and Fitzpatrick-Lins, K., 1986, A coefficient of agreement as a measurement of thematic classification accuracy, *Photogrammetric Engineering and Remote Sensing*, **52**, 223-227.

SAS Institute, Inc., 1990, *SAS/STAT User's Guide*, Version 6, Fourth Edition, Volume 1, Cary, NC.

Shaw, D. T., Malthus, T. J. and Kupiec, J. A., 1998, High-spectral resolution data for monitoring Scots pine (*Pinus sylvestris* L.) regeneration, *International Journal of Remote Sensing*, **19**, 2601-2608.

Schriever, J. R. and Congalton, R. G., 1995, Evaluating seasonal variability as an aid to cover-type mapping from Landsat Thematic Mapper data in the Northeast, *Photogrammetric Engineering and Remote Sensing*, **61**, 321-327.

Shen, S. S., Badhwar, G. D. and Carnes, J. G., 1985, Separability of bereal forest species in the Lake Jennette area, Minnesota, *Photogrammetric Engineering and Remote Sensing*, **51**, 1775-1783.

Skidmore, A. K., 1989, An expert system classifies Eucalypt forest types using Thematic Mapper data and a digital terrain model, *Photogrammetric Engineering and Remote Sensing*, **55**, 1449-1464.

Spanner, M. A., Pierce, L. L., Peterson, D. L. and Running, S. W., 1990, Remote sensing of temperate coniferous forest leaf area index: The influence of canopy closure, understorey vegetation and background reflectance, *International Journal of Remote Sensing*, **11**, 95-111.

Thrower, S. L., 1988, *Hong Kong Trees*, The Urban Council, Hong Kong.

Warner, T. A. and Shank, M. C., 1997, Spatial autocorrelation analysis of hyperspectral imagery for feature selection, *Remote Sensing of Environment,* **60**, 58-70.

Wessman, C. A., Aber, J. D. and Peterson, D. L., 1989, An evaluation of imaging spectrometry for estimating forest canopy chemistry, *International Journal of Remote Sensing*, **10**, 1293-1316.

Wessman, C. A., 1991, Evaluation of Canopy Biochemistry, in Hobbs, R. J. and H. A. Mooney (eds), *Remote Sensing of Biosphere Functioning*, Springer-Verlag, New York, pp. 135-156.

Yoder, B. J. and Pettigrew-Crosby, R. E., 1995, Predicting nitrogen and chlorophyll content and concentrations from reflectance spectra (400-2500 nm) at leaf

and canopy scales, *Remote Sensing of Environment,* **53**, 199-211.

Zagolski, F., Pinel, V., Romier, J., Alcayde, D., Fontanari, J., Gastellu-Etchegorry, J. P., Giordano, G., Marty, G., Mougin, E. and Joffre, R., 1996, Forest canopy chemistry with high resolution remote sensing, *International Journal of Remote Sensing*, **17**, 1107-1128.

Appendix 1.1. Reflectance of *Acacia confusa* in four seasons with low level (top), medium level (middle) and high level (bottom) of leaf density

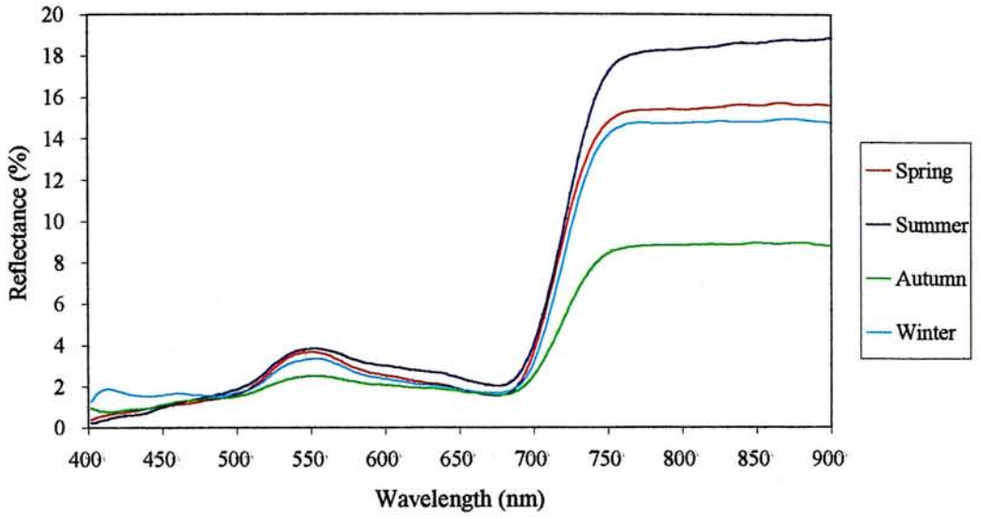

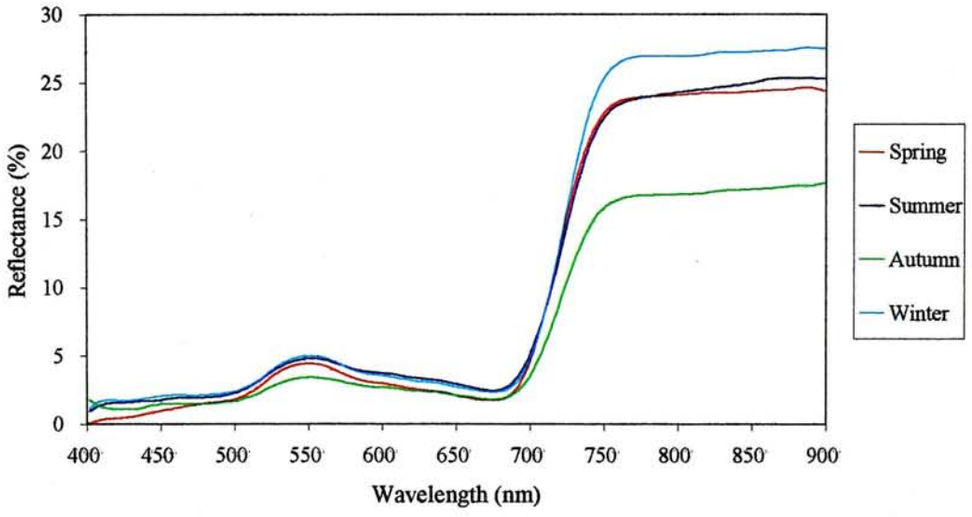

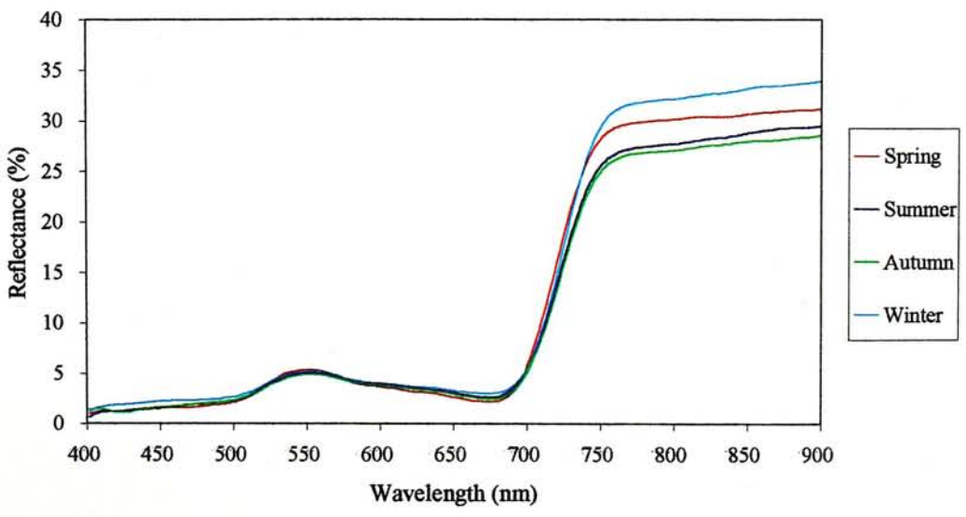

Appendix 1.2. Reflectance of *Araucaria heterophylla* in four seasons with low level (top), medium level (middle) and high level (bottom) of leaf density

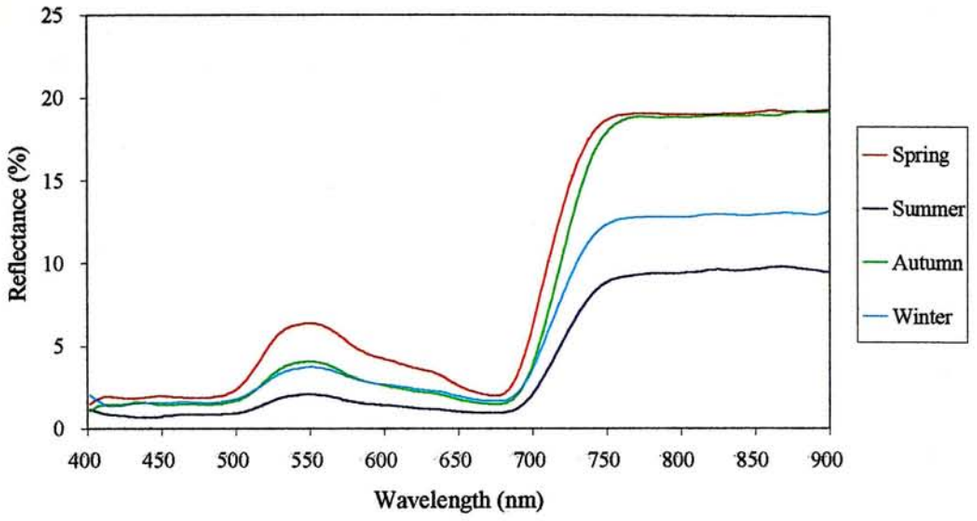

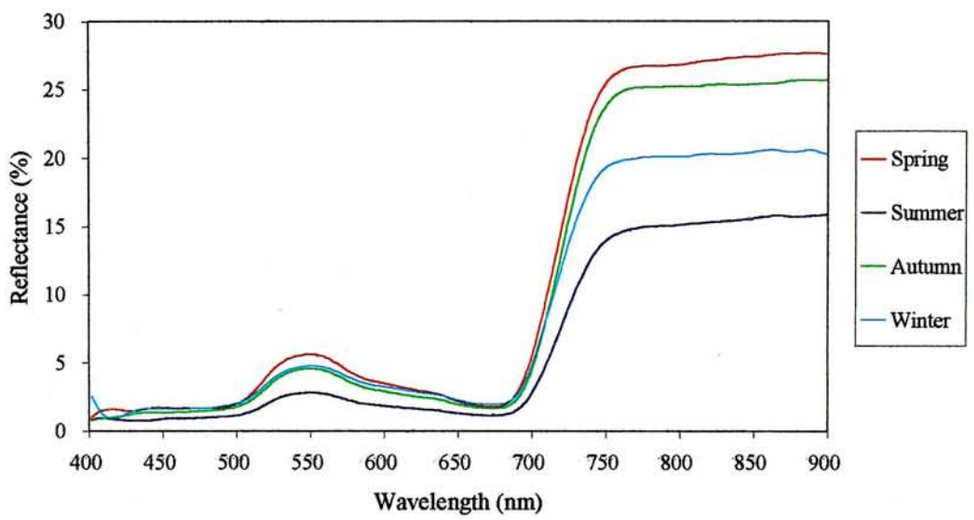

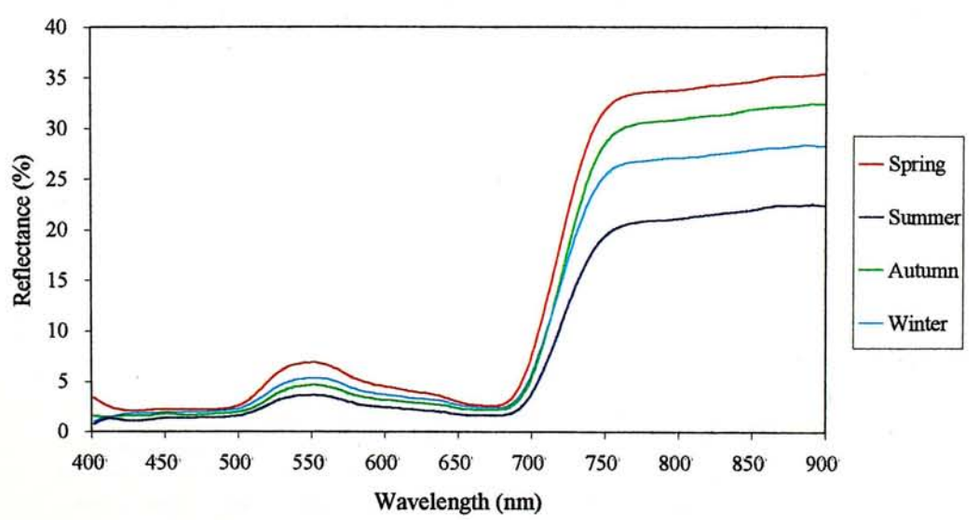

Appendix 1.3. Reflectance of *Acacia mangium* in four seasons with low level (top), medium level (middle) and high level (bottom) of leaf density

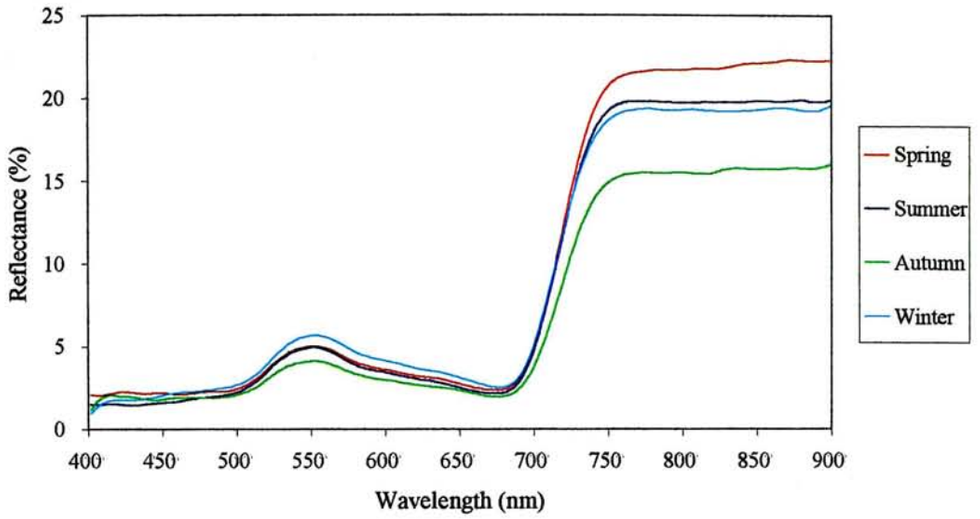

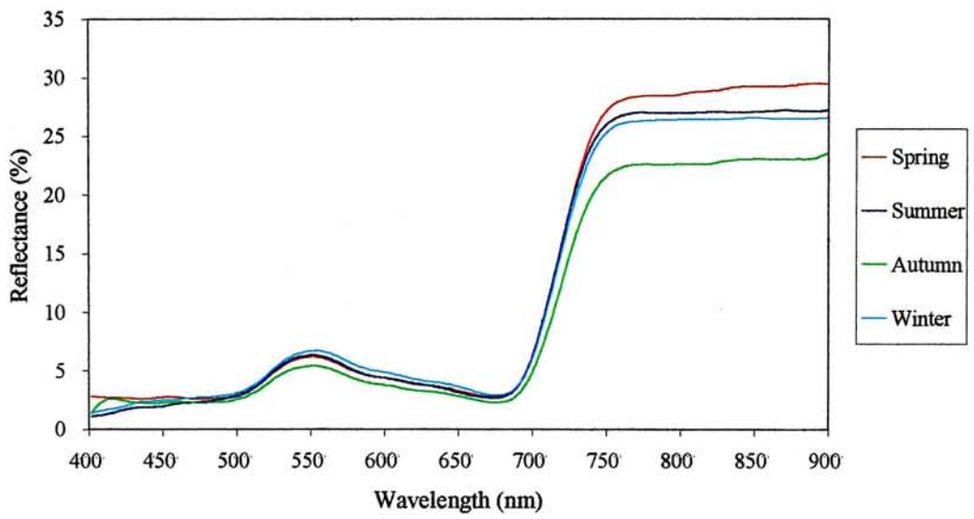

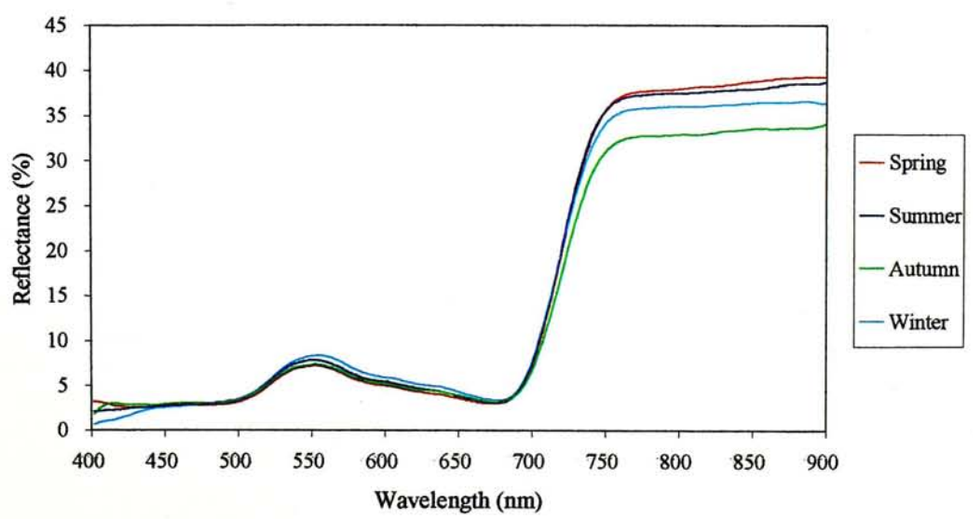

Appendix 1.4. Reflectance of *Bauhinia variegata* in four seasons with low level (top), medium level (middle) and high level (bottom) of leaf density

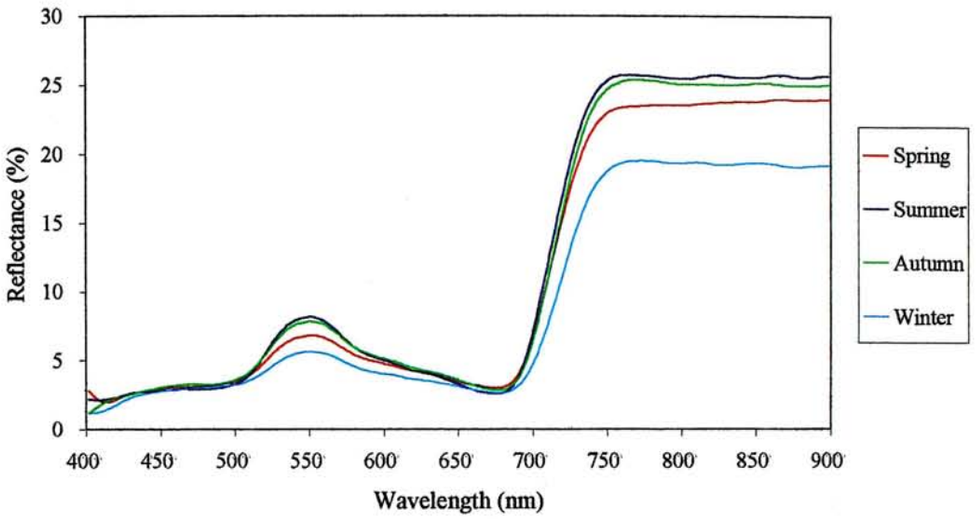

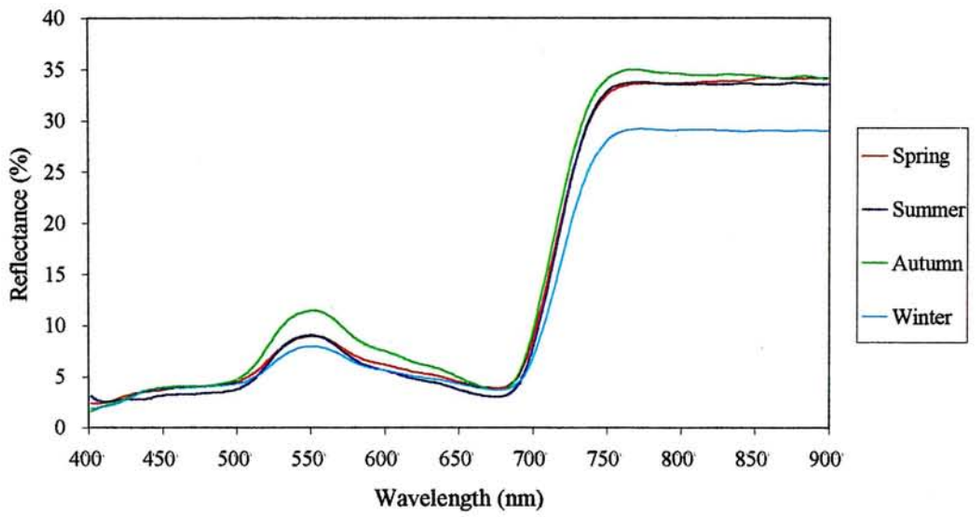

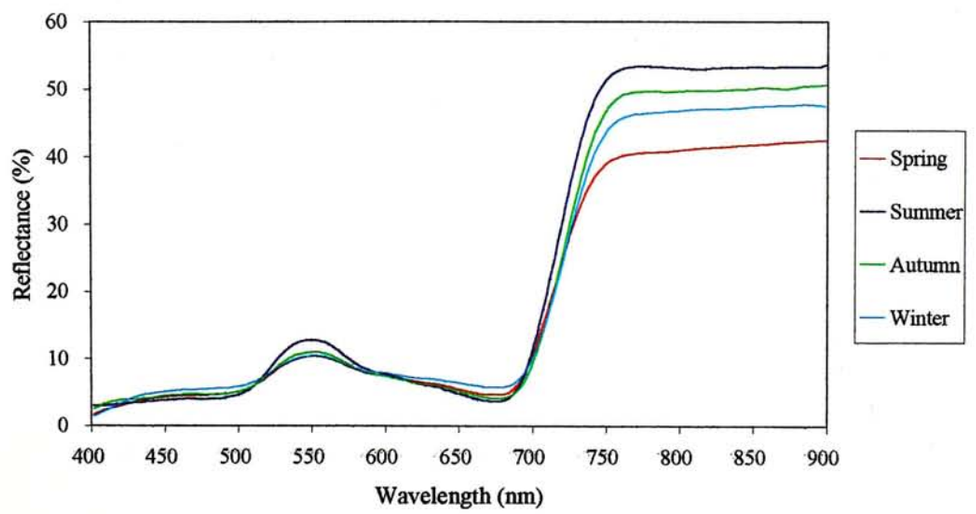

Appendix 1.5. Reflectance of *Cinnamomum camphora* in four seasons with low level (top), medium level (middle) and high level (bottom) of leaf density

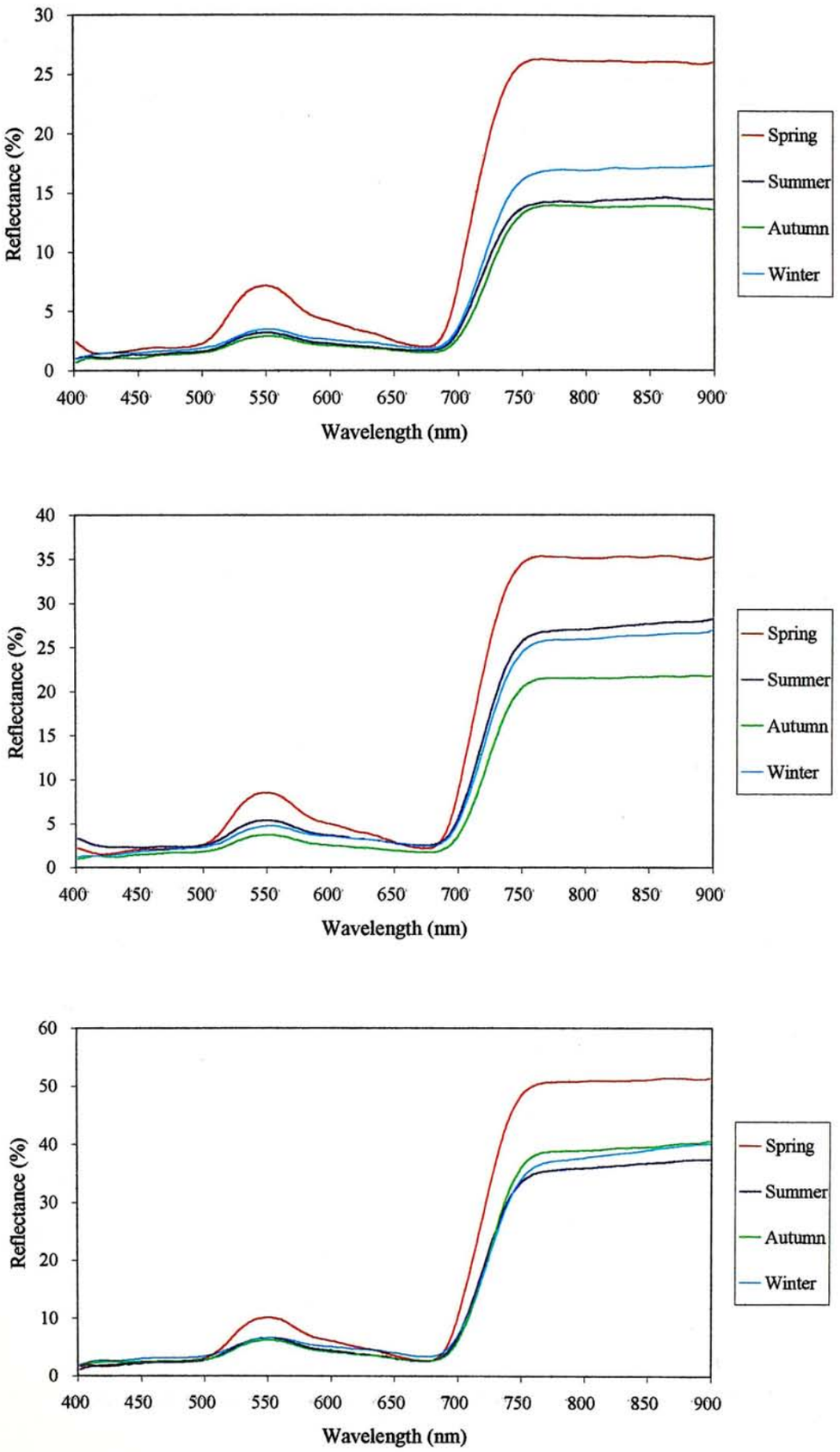

Appendix 1.6. Reflectance of *Casuarina equisetifolia* in four seasons with low level (top), medium level (middle) and high level (bottom) of leaf density

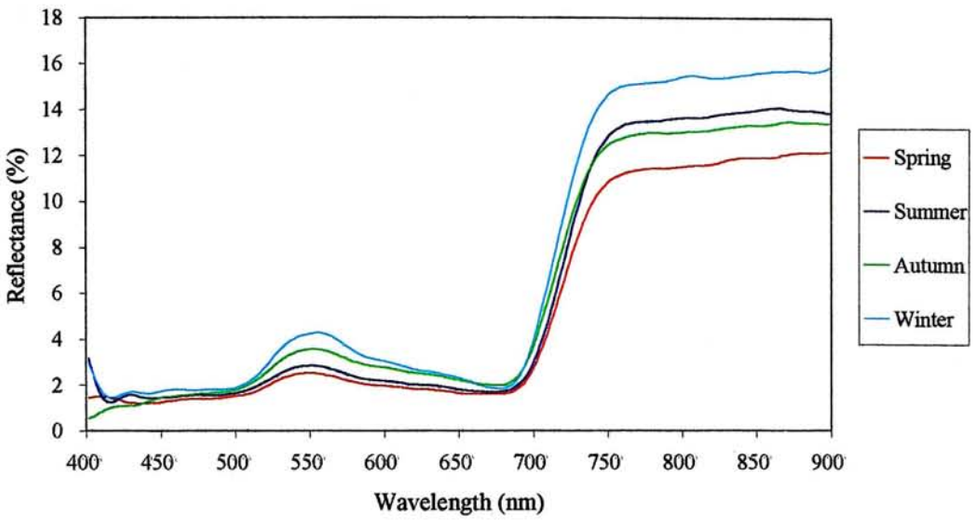

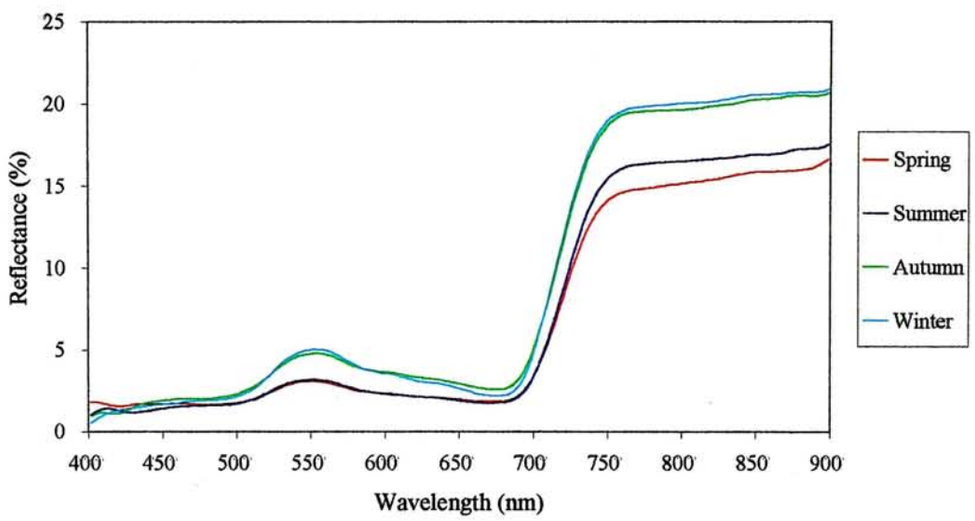

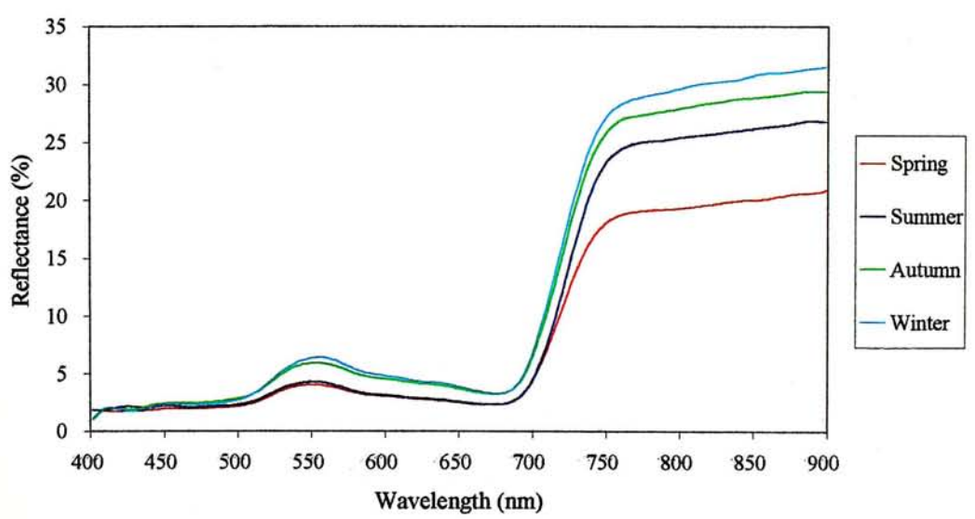

Appendix 1.7. Reflectance of *Castanopsis fissa* in four seasons with low level (top), medium level (middle) and high level (bottom) of leaf density

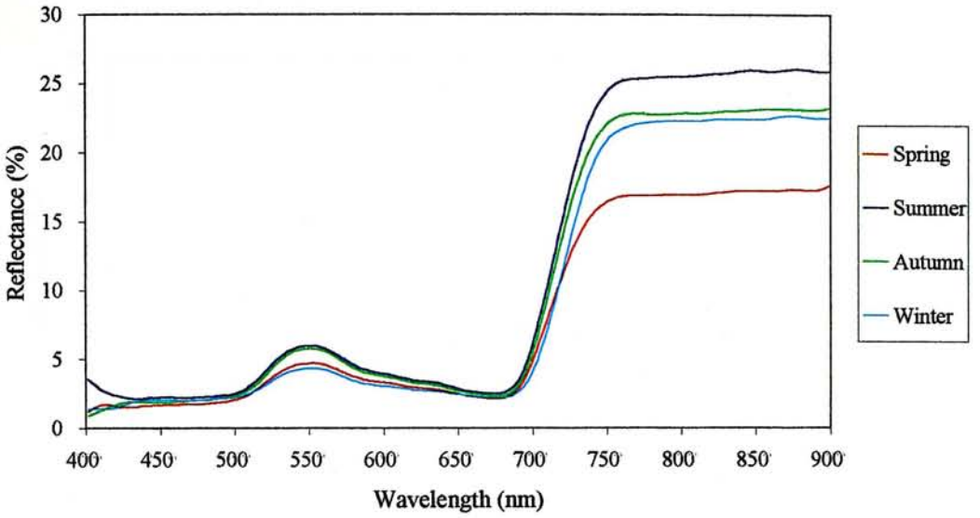

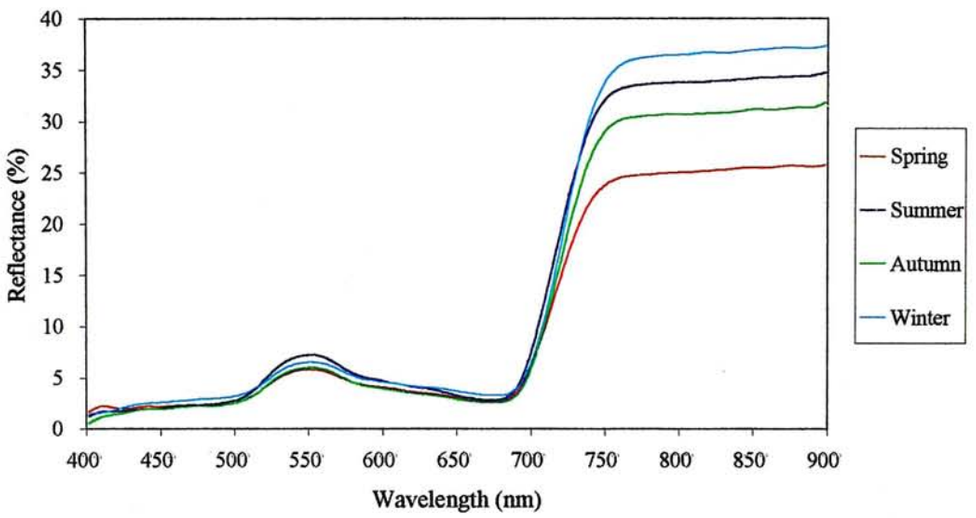

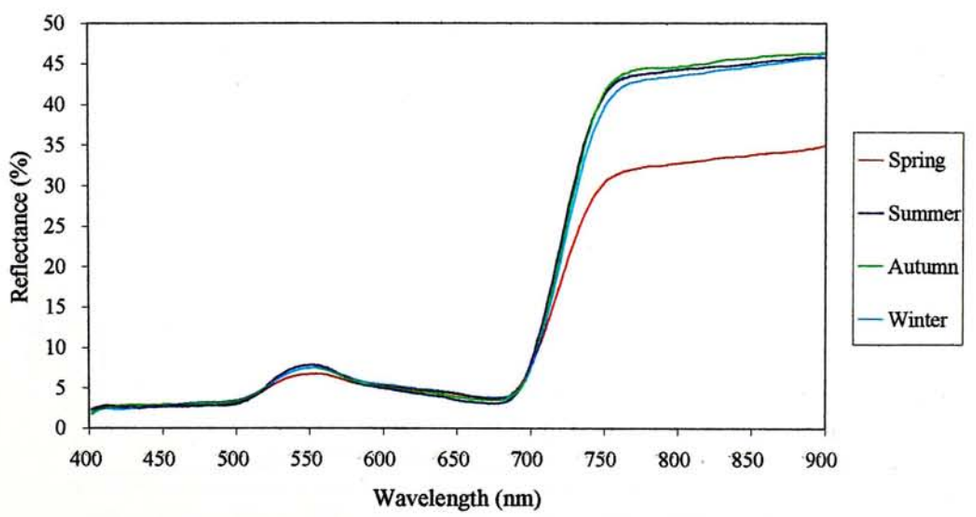

Appendix 1.8. Reflectance of *Cratoxylum ligustrinum* in spring, summer and autumn with low level (top), medium level (middle) and high level (bottom) of leaf density

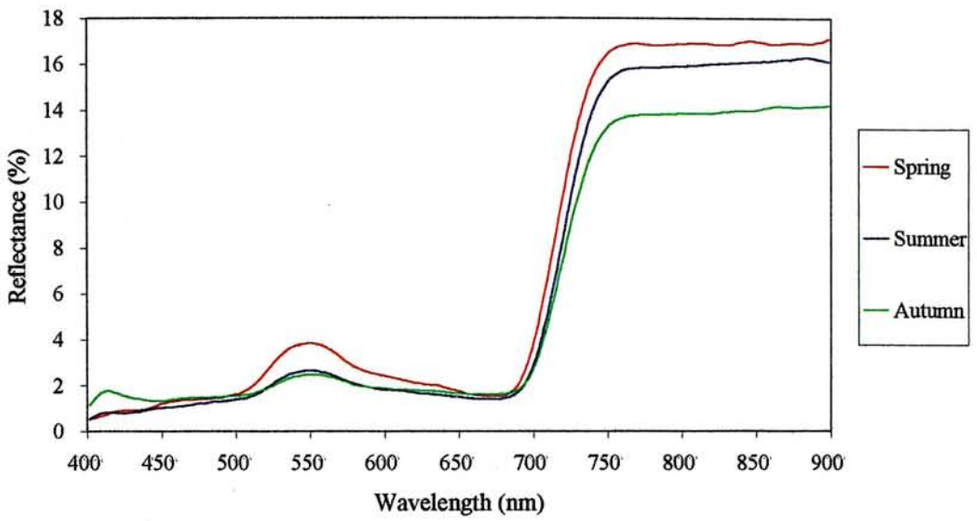

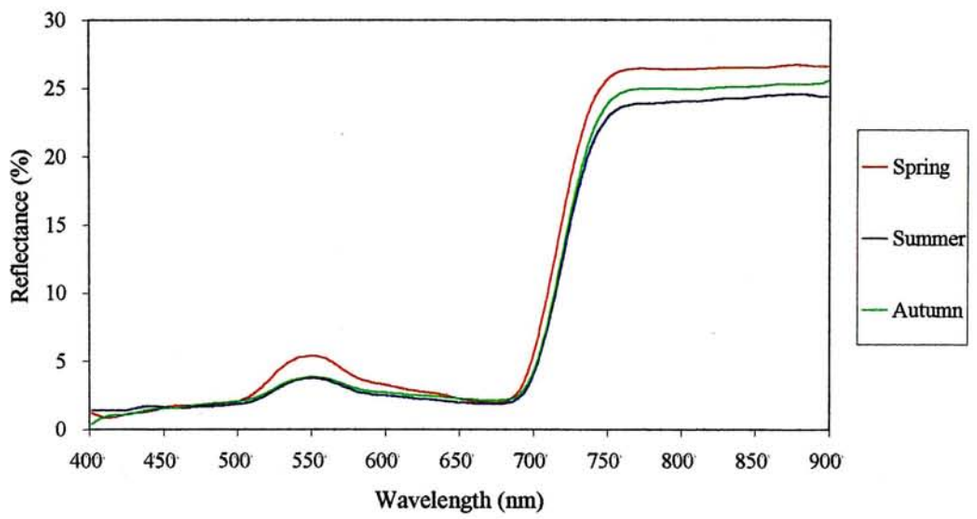

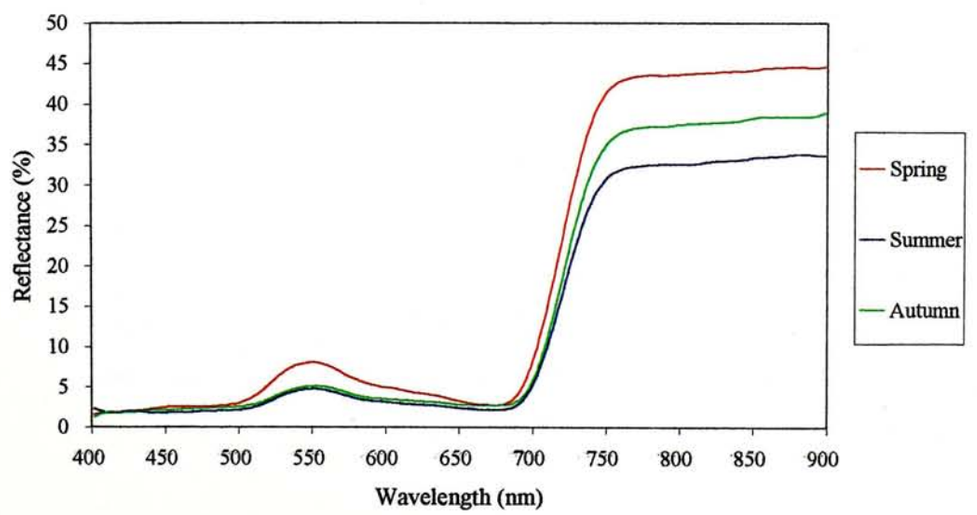

Appendix 1.9. Reflectance of *Aleurites moluccana* in four seasons with low level (top), medium level (middle) and high level (bottom) of leaf density

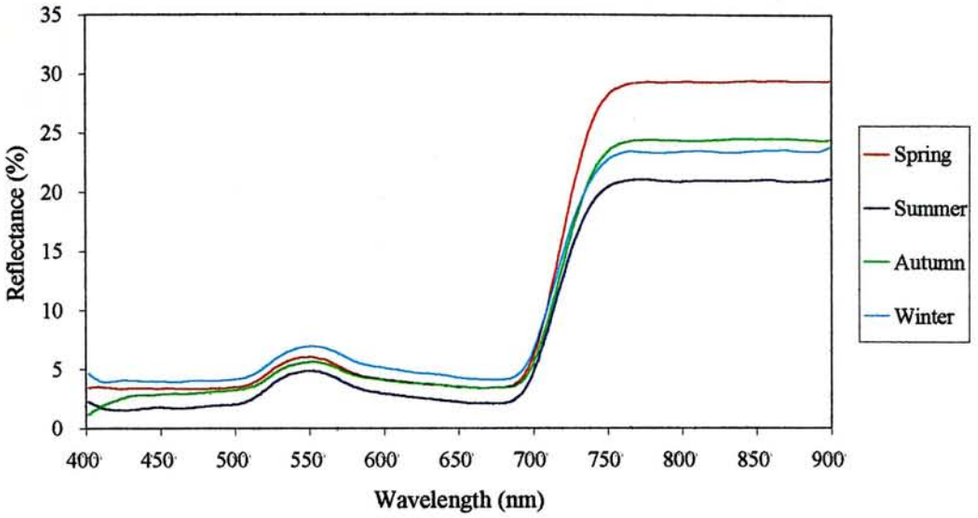

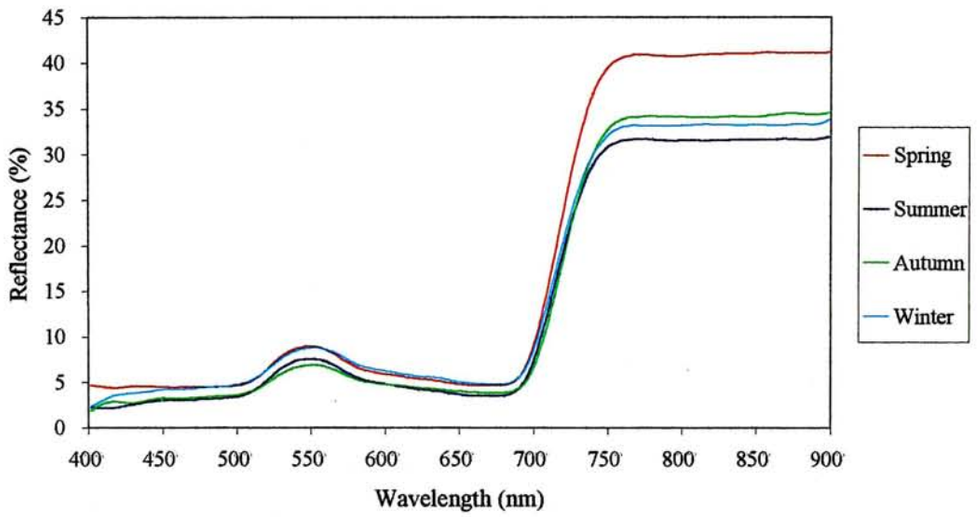

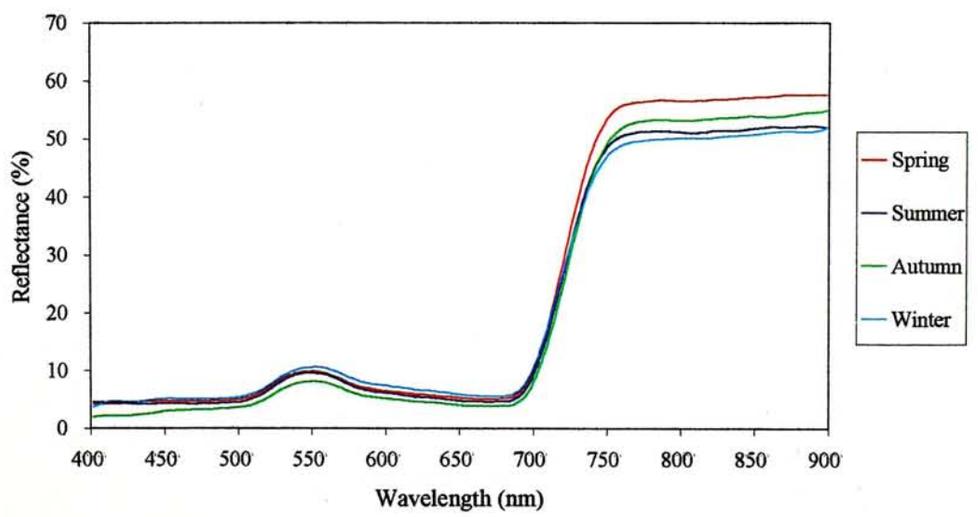

Appendix 1.10. Reflectance of *Dimocarpus longan* in four seasons with low level (top), medium level (middle) and high level (bottom) of leaf density

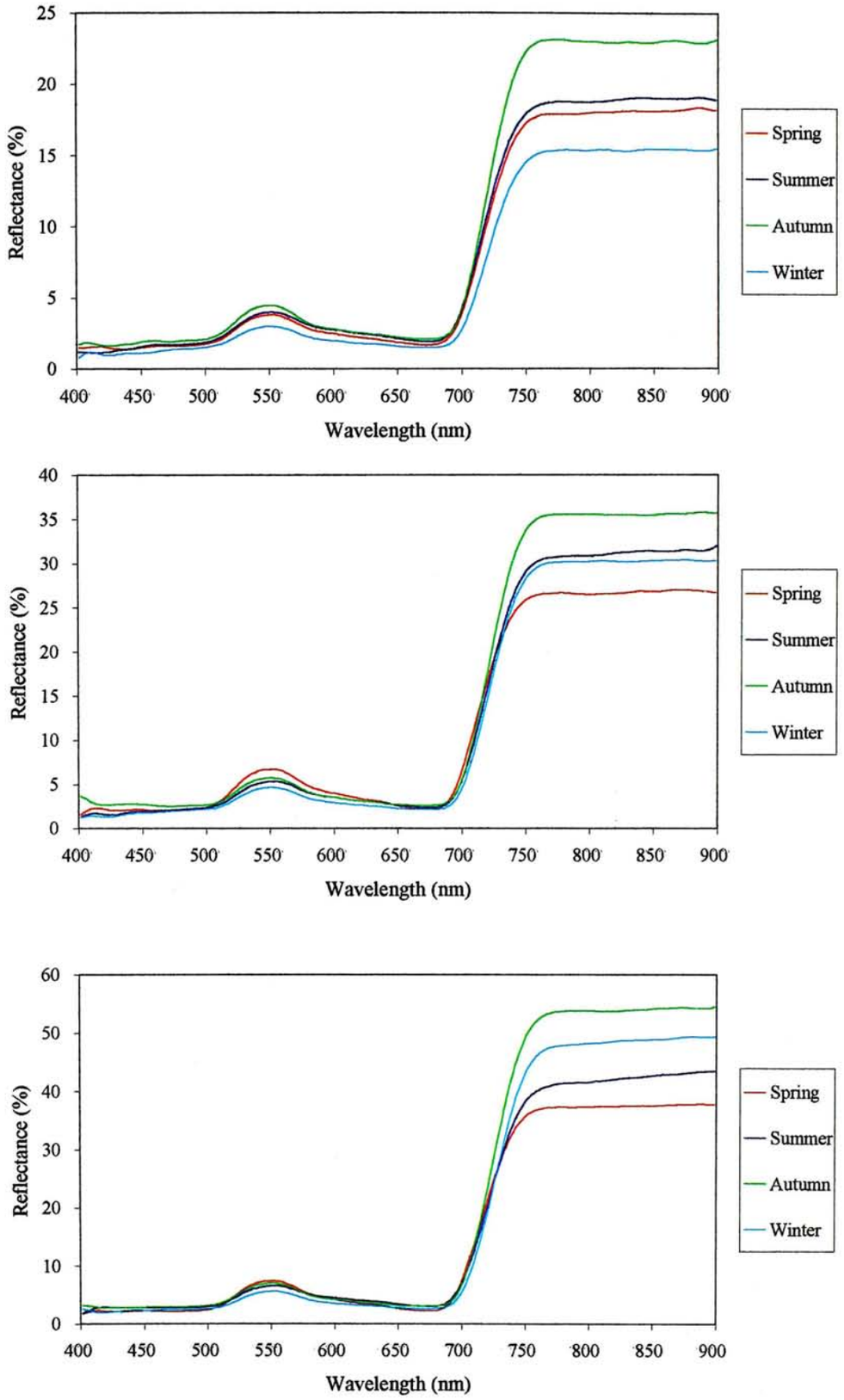

Appendix 1.11. Reflectance of *Delonix regia* in spring, summer and autumn with low level (top), medium level (middle) and high level (bottom) of leaf density

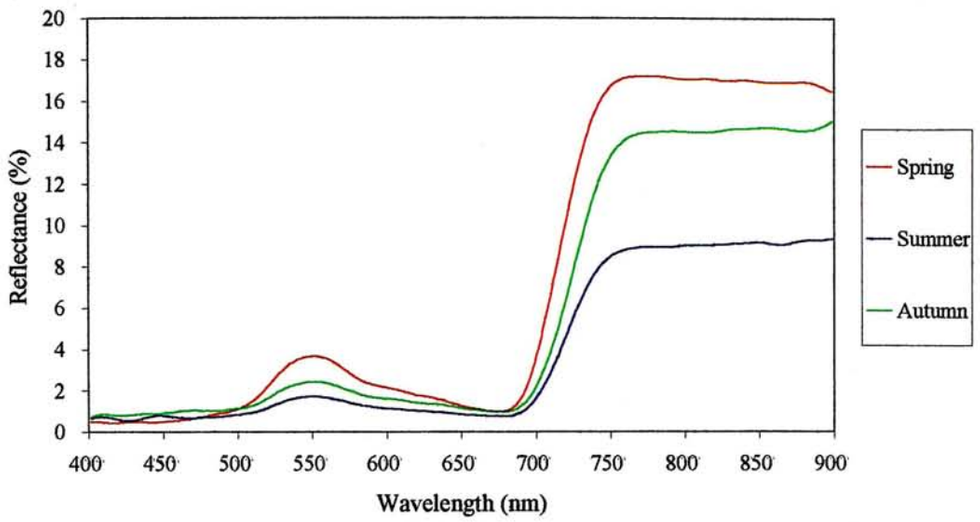

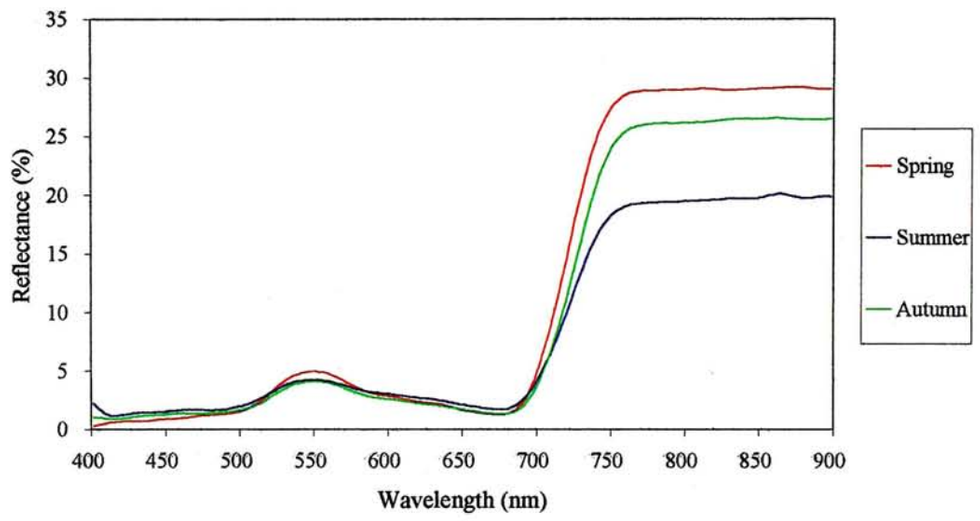

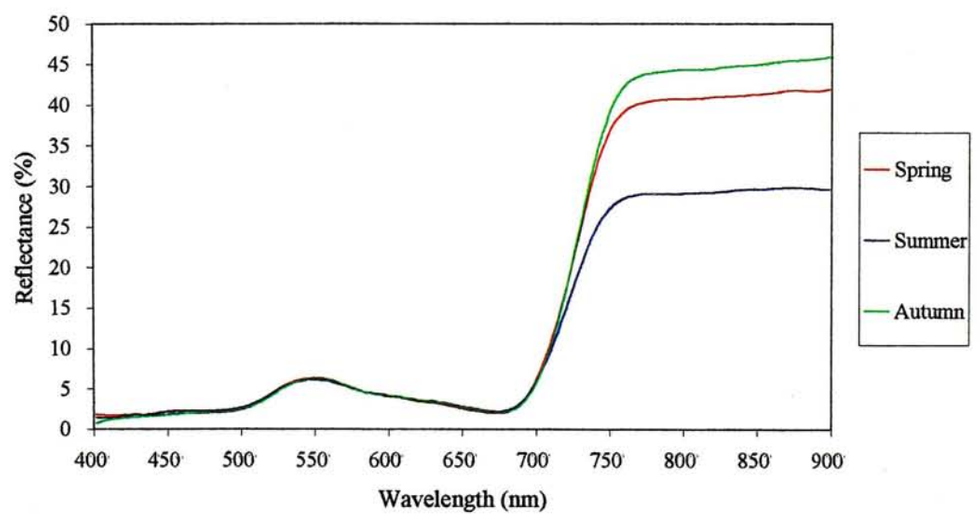

Appendix 1.12. Reflectance of *Ficus microcarpa* in four seasons with low level (top), medium level (middle) and high level (bottom) of leaf density

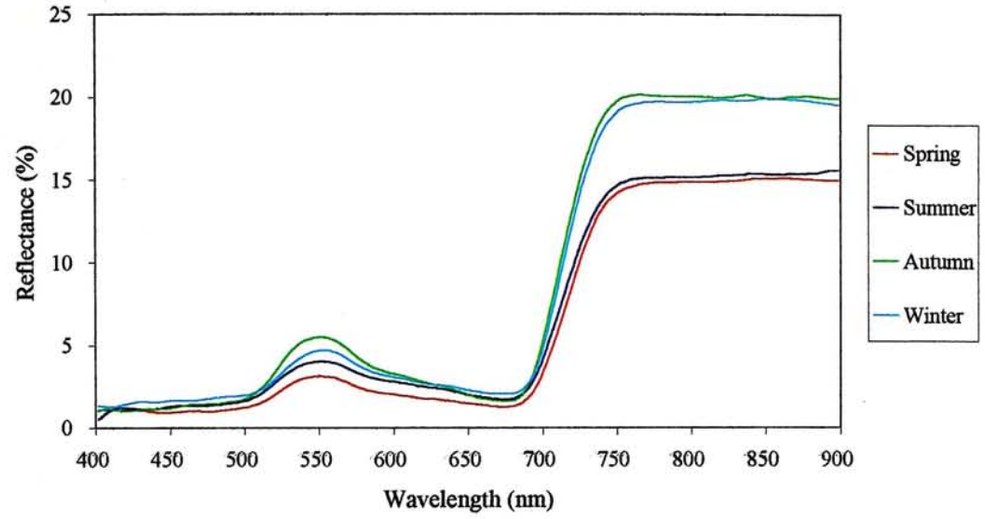

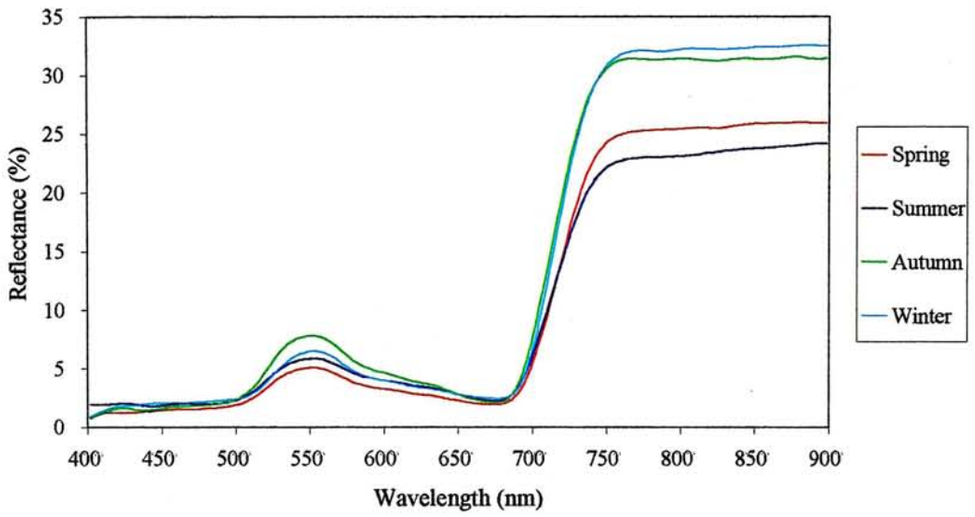

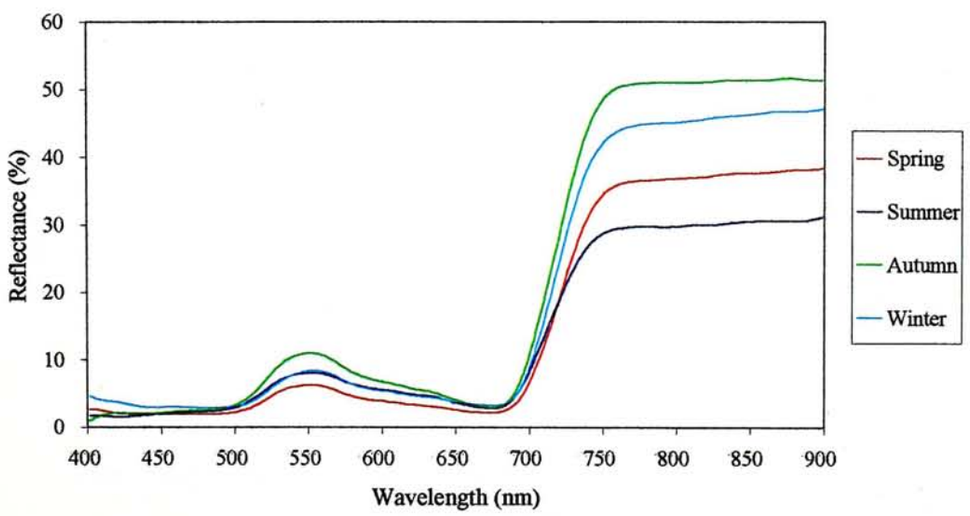

Appendix 1.13. Reflectance of *Firmiana simplex* in spring and summer with low level (top), medium level (middle) and high level (bottom) of leaf density

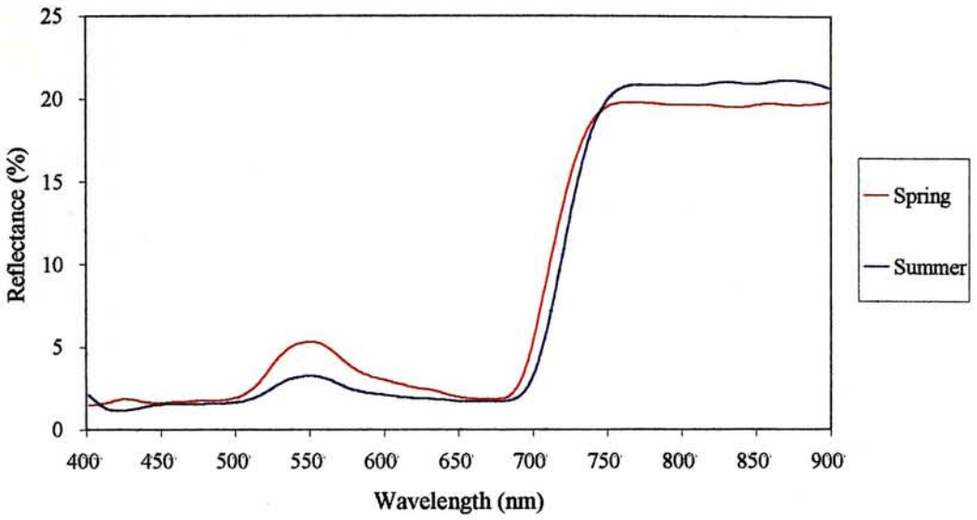

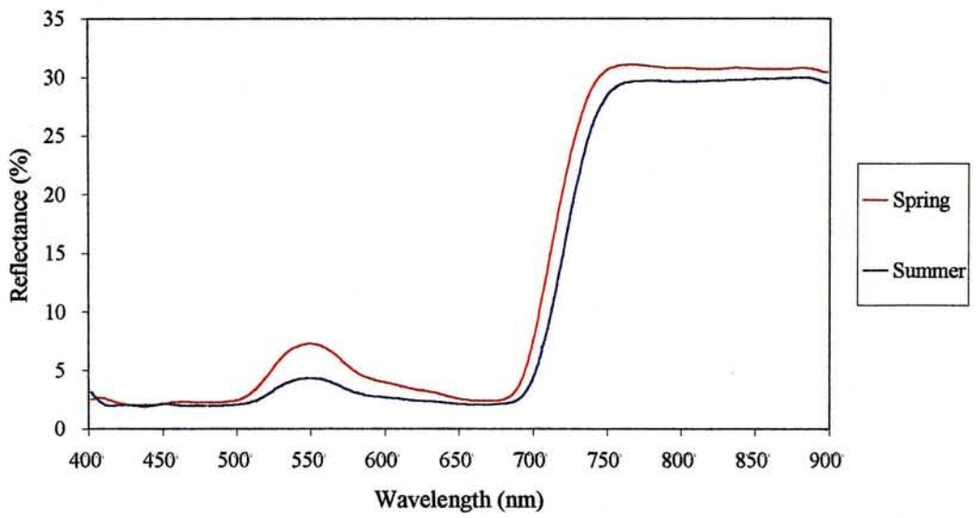

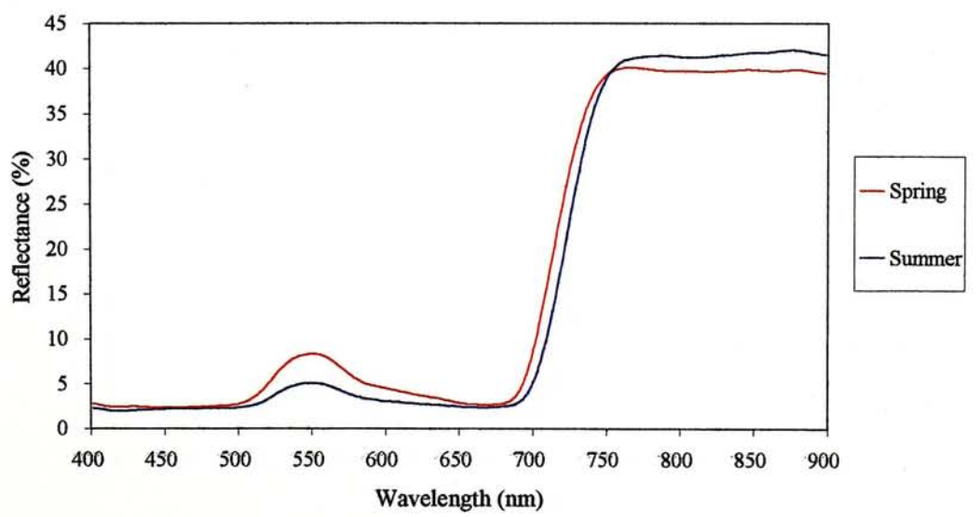

Appendix 1.14. Reflectance of *Ficus variegata* in four seasons with low level (top), medium level (middle) and high level (bottom) of leaf density

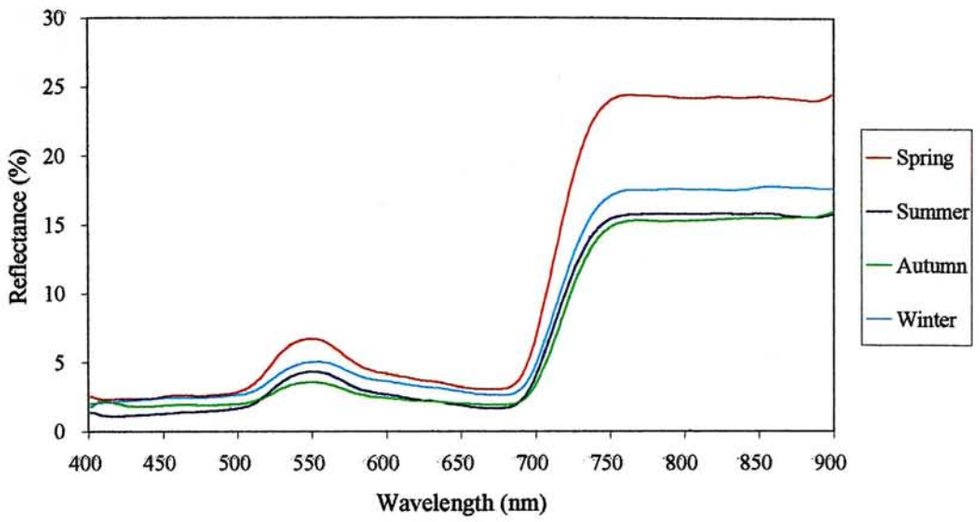

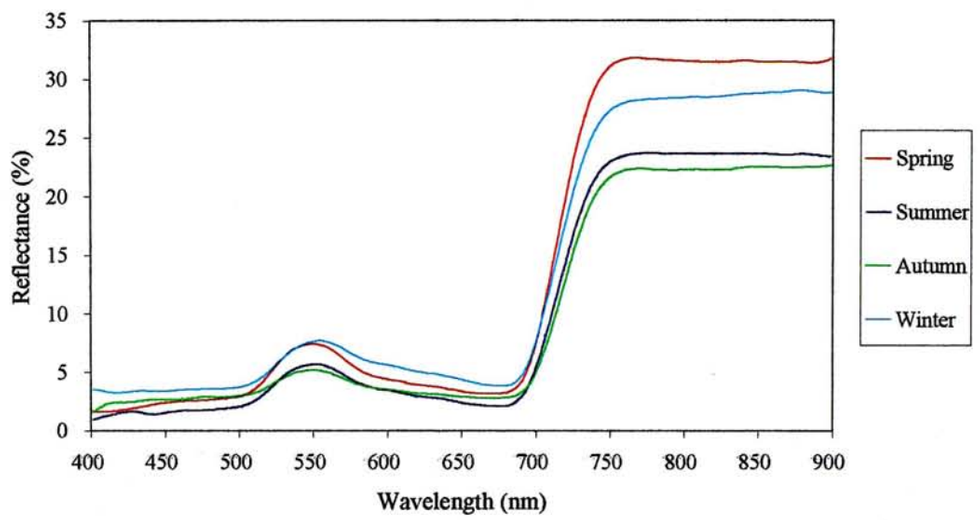

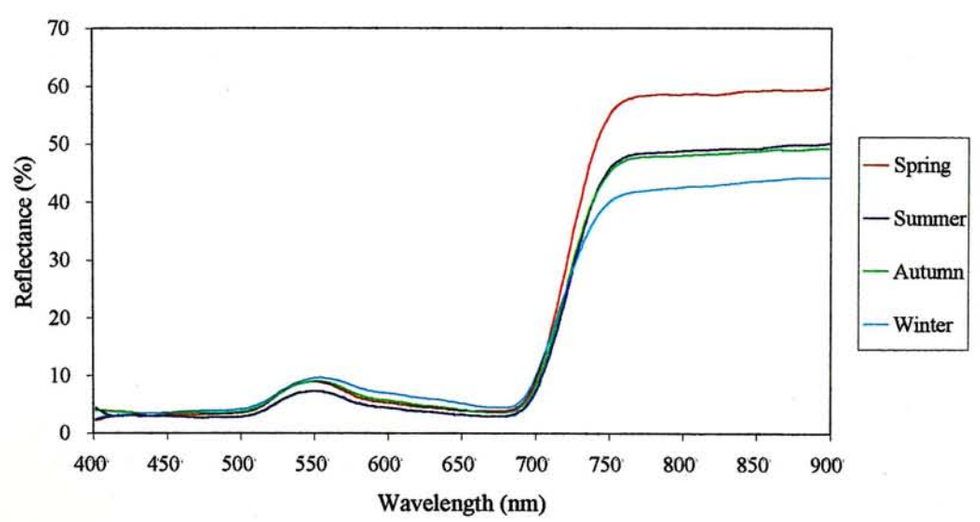

Appendix 1.15. Reflectance of *Hibiscus tiliaceus* in four seasons with low level (top), medium level (middle) and high level (bottom) of leaf density

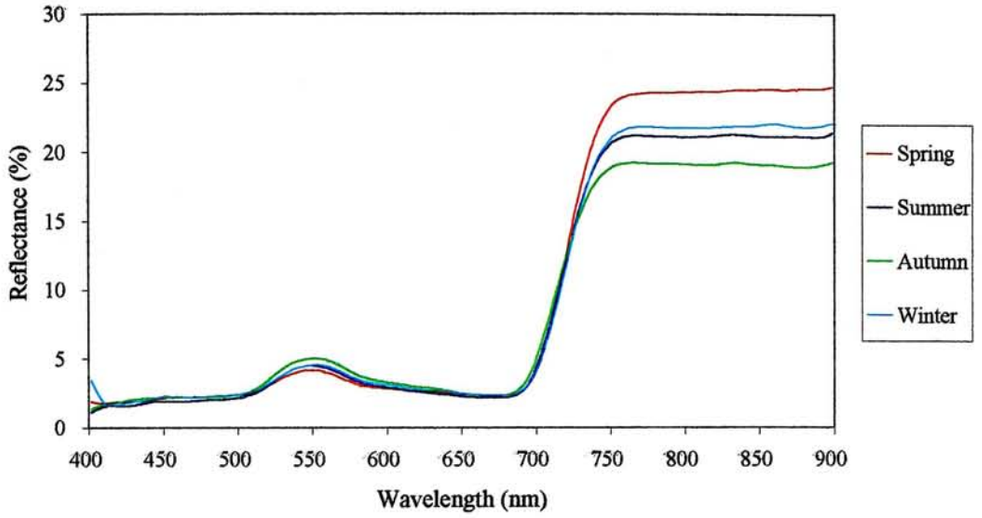

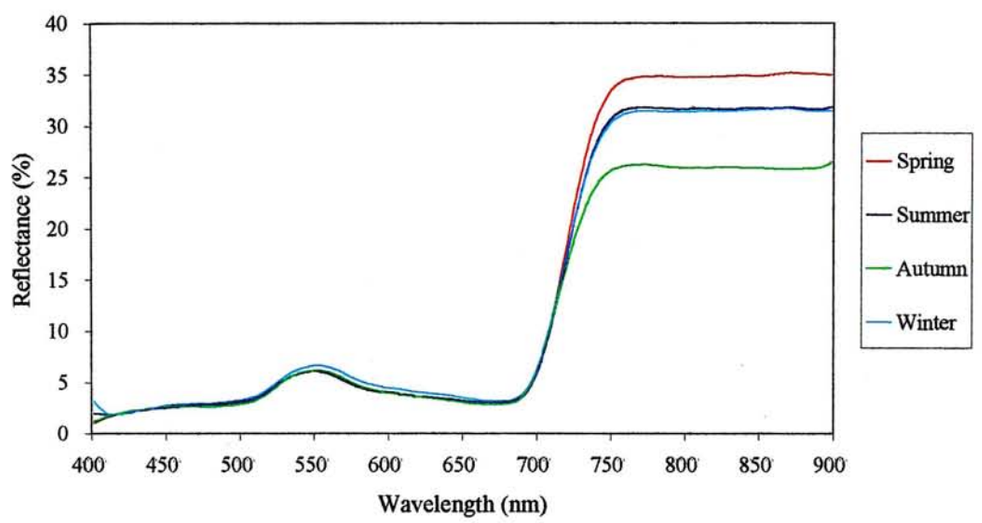

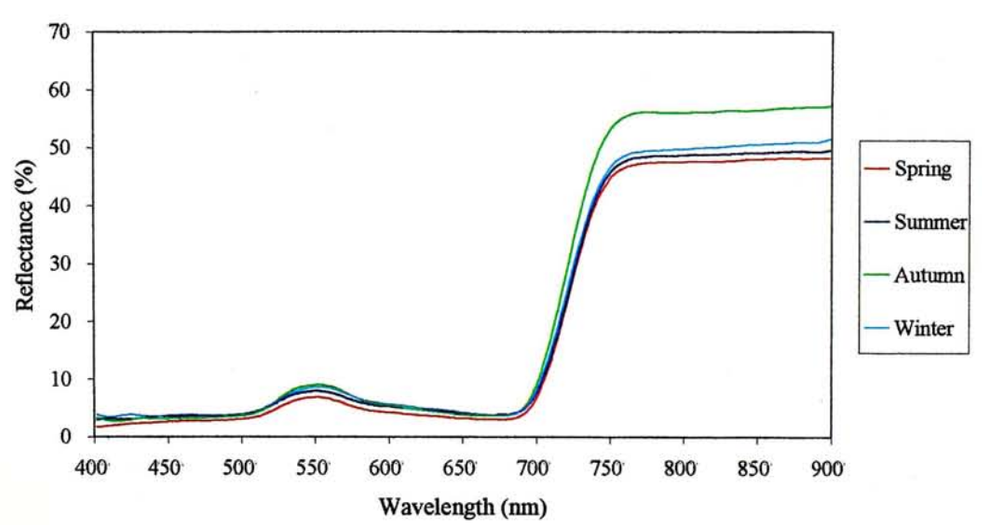

Appendix 1.16. Reflectance of *Lophostemon conferta* in four seasons with low level (top), medium level (middle) and high level (bottom) of leaf density

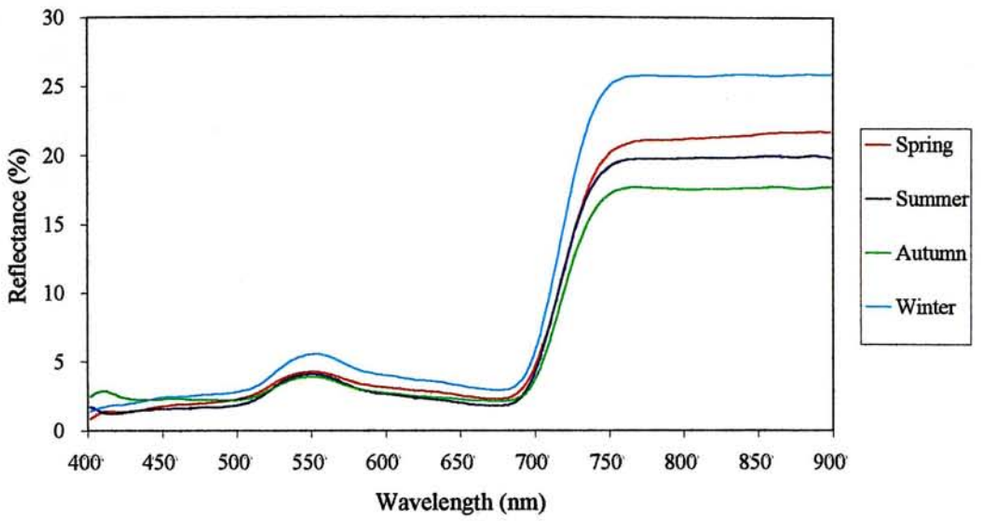

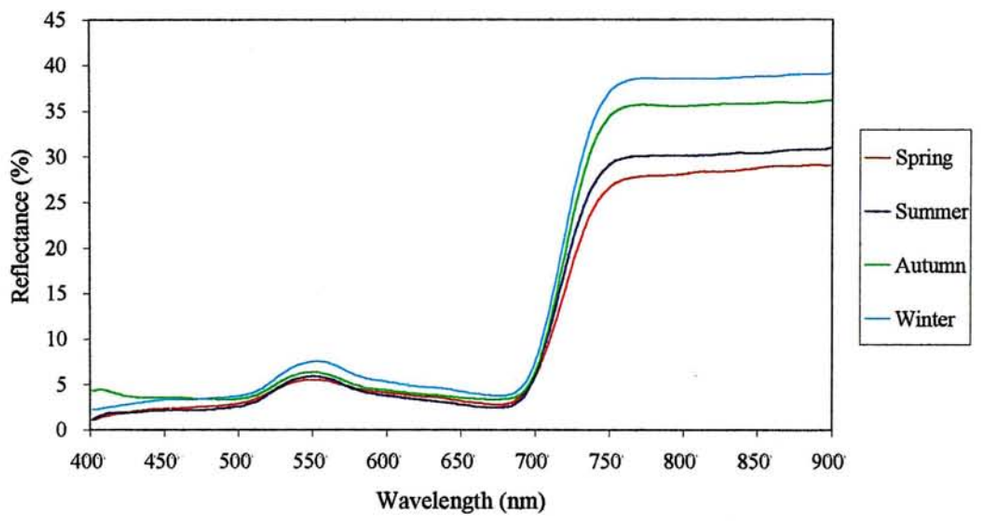

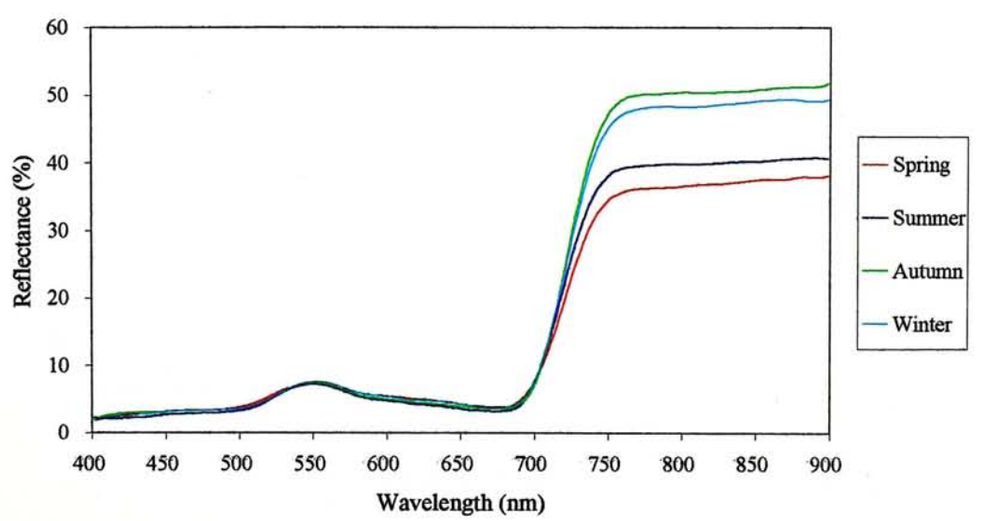

Appendix 1.17. Reflectance of *Liquidambar formosana* in four seasons with low level (top), medium level (middle) and high level (bottom) of leaf density

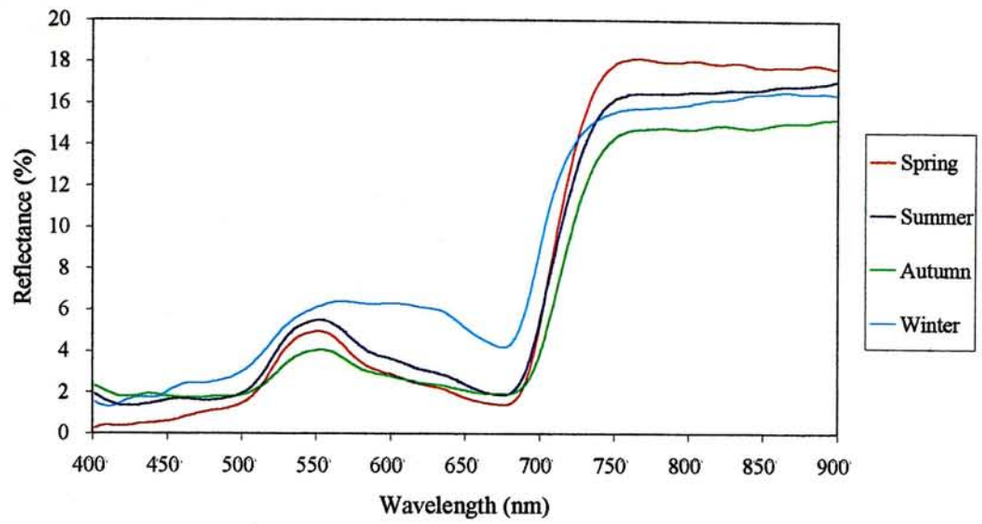

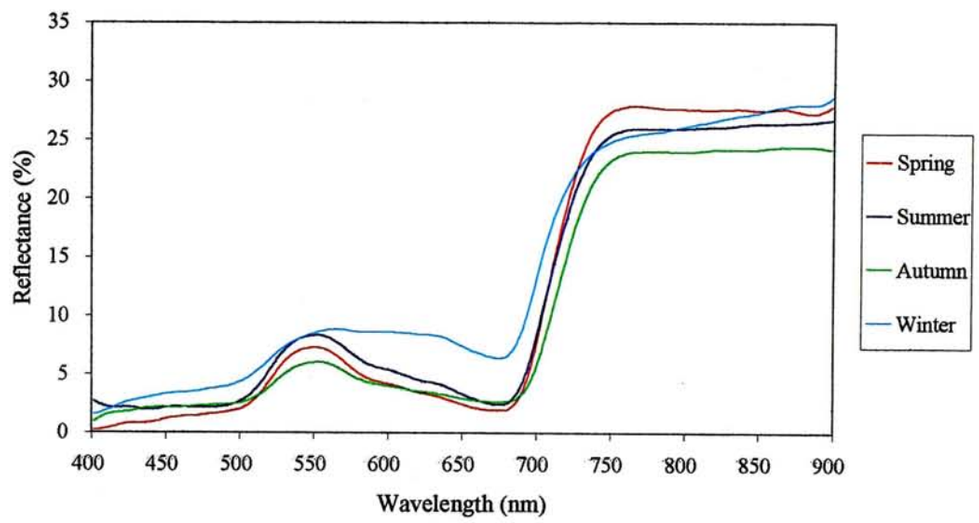

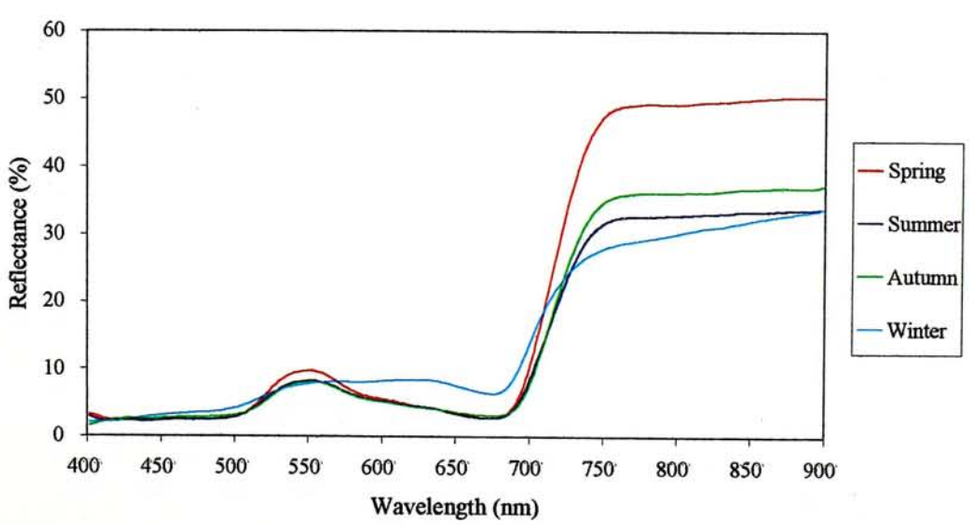

Appendix 1.18. Reflectance of *Lagerstroemia speciosa* in four seasons with low level (top), medium level (middle) and high level (bottom) of leaf density

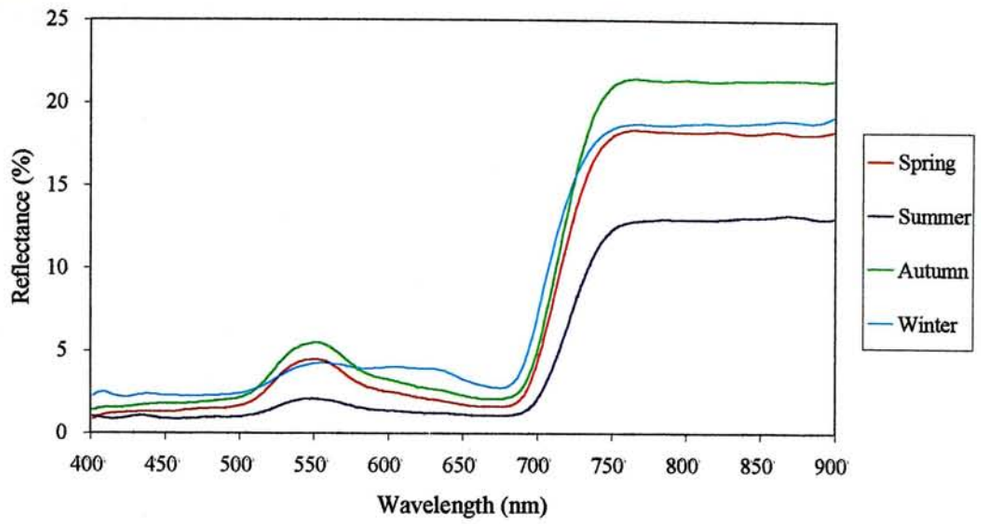

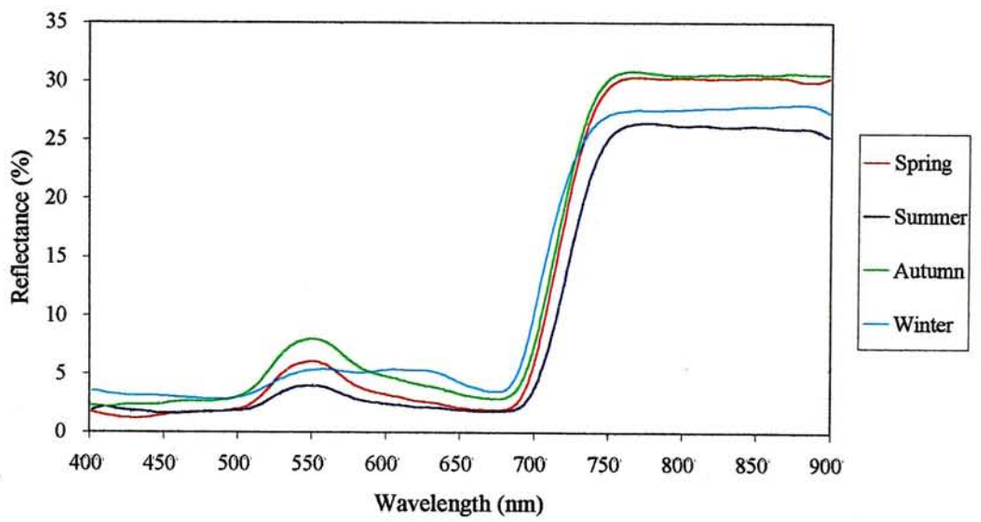

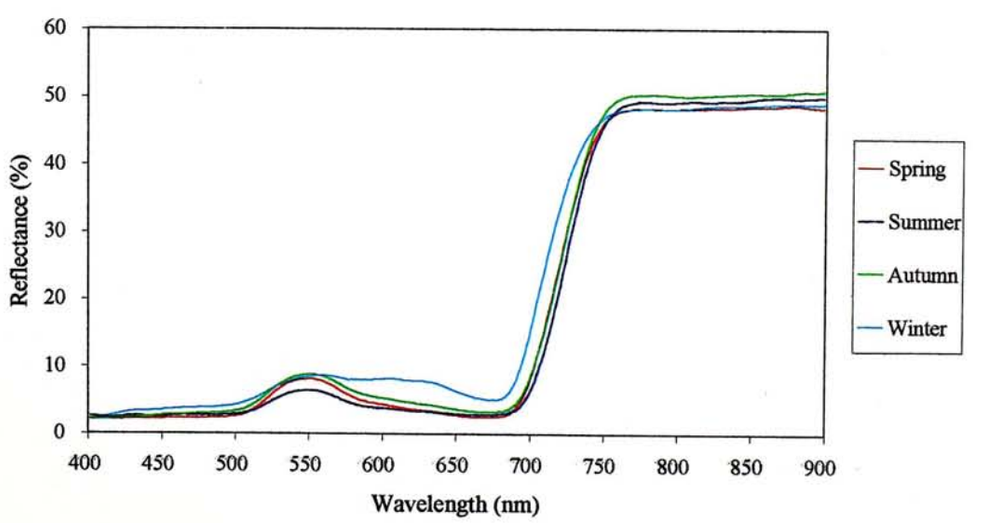

Appendix 1.19. Reflectance of *Melaleuca quanqueenervia* in four seasons with low level (top), medium level (middle) and high level (bottom) of leaf density

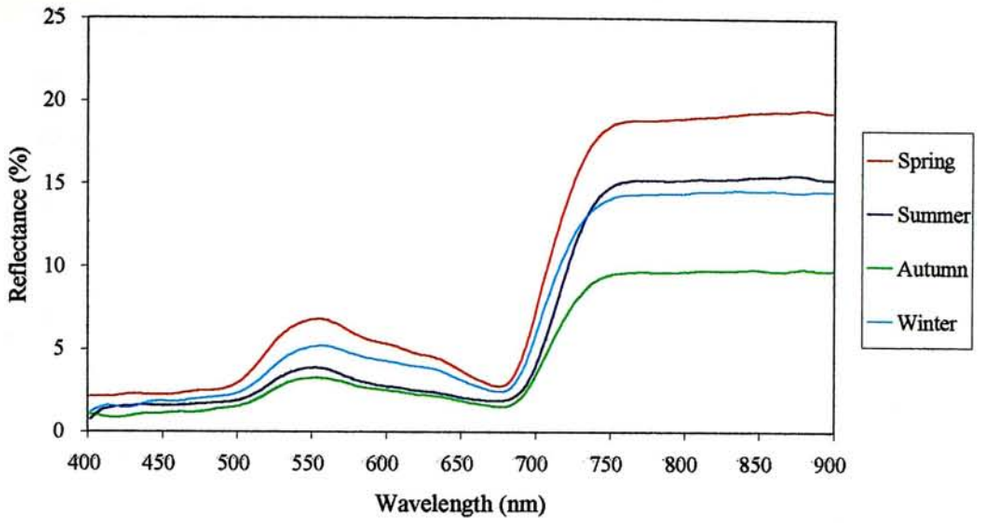

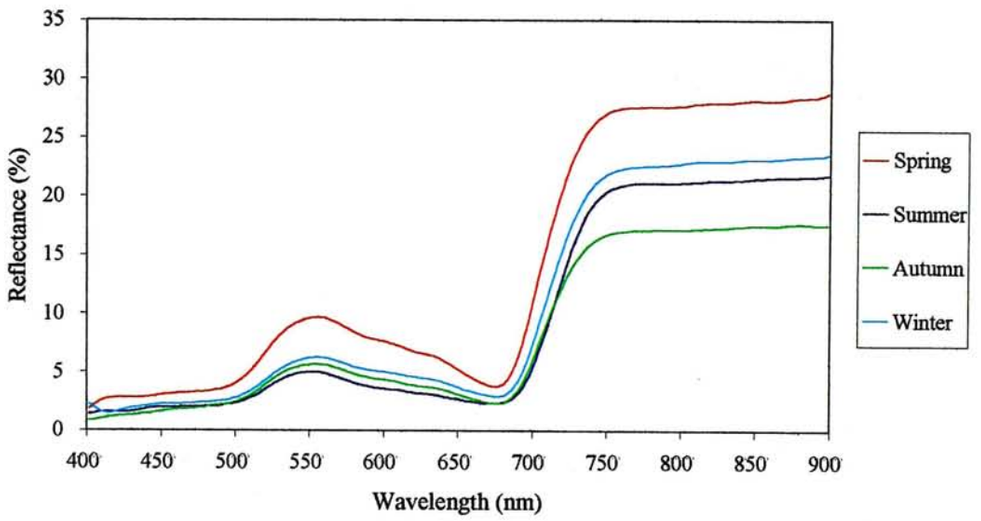

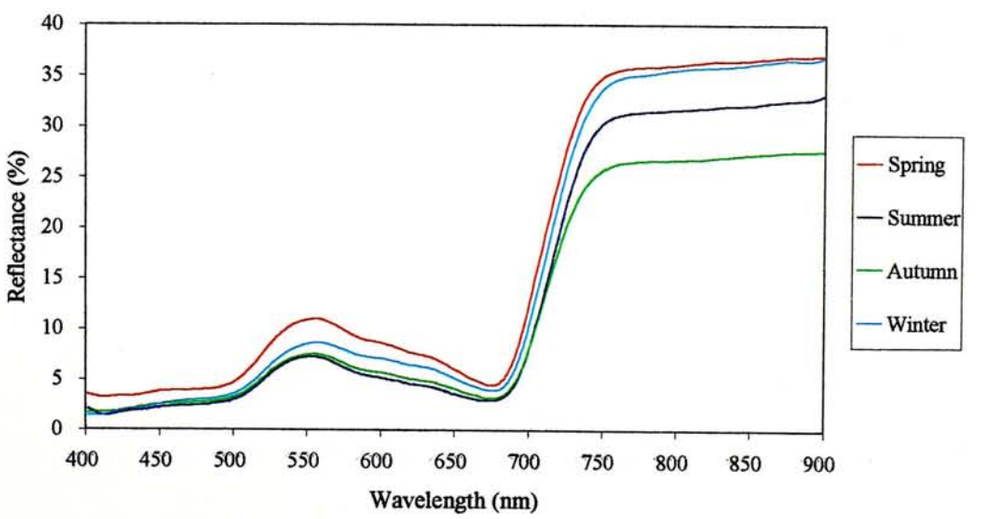

Appendix 1.20. Reflectance of *Macaranga tanarius* in four seasons with low level (top), medium level (middle) and high level (bottom) of leaf density

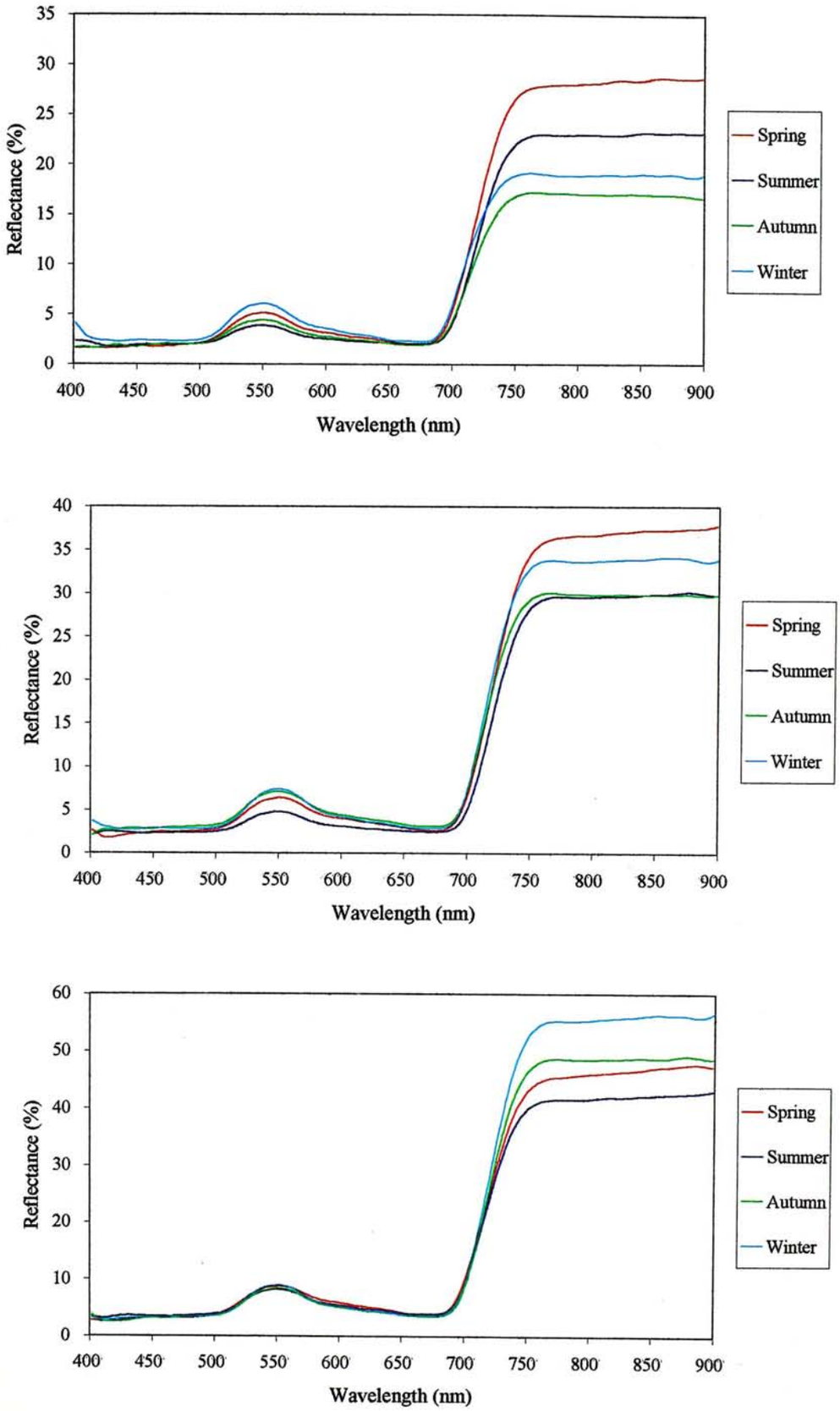

Appendix 1.21. Reflectance of *Pinus elliottii* in four seasons with low level (top), medium level (middle) and high level (bottom) of leaf density

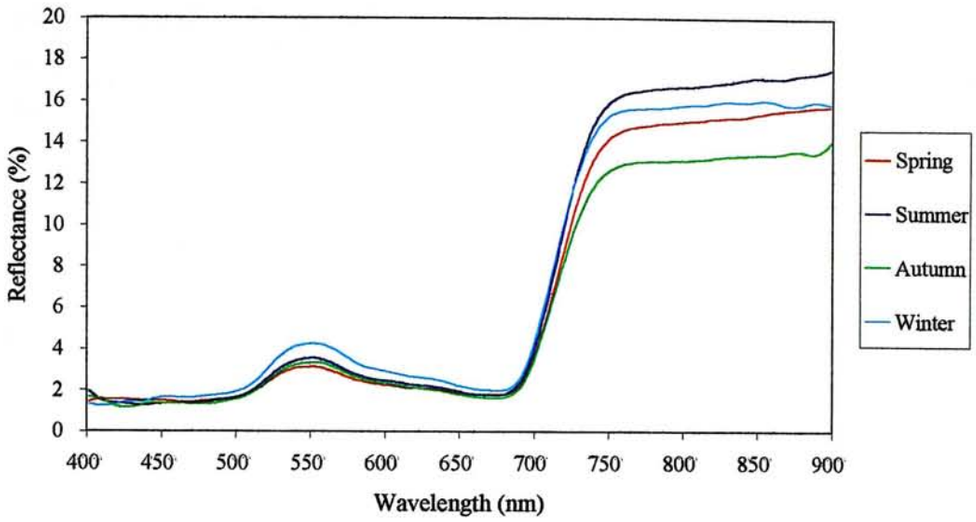

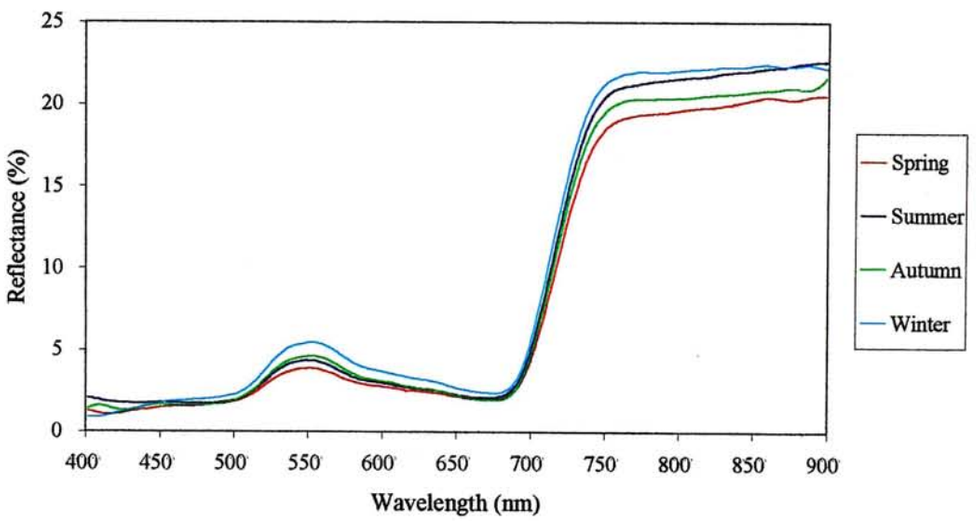

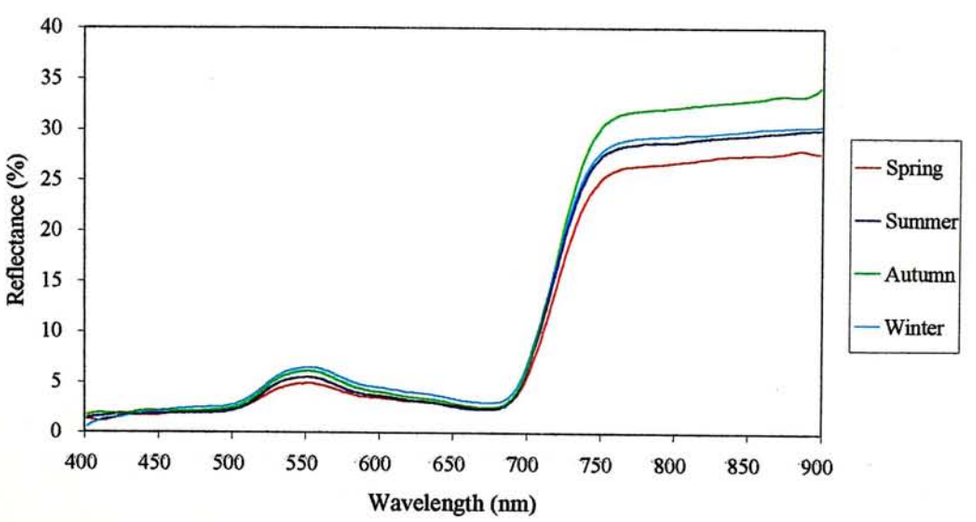

Appendix 1.22. Reflectance of *Thuja orientalis* in four seasons with low level (top), medium level (middle) and high level (bottom) of leaf density

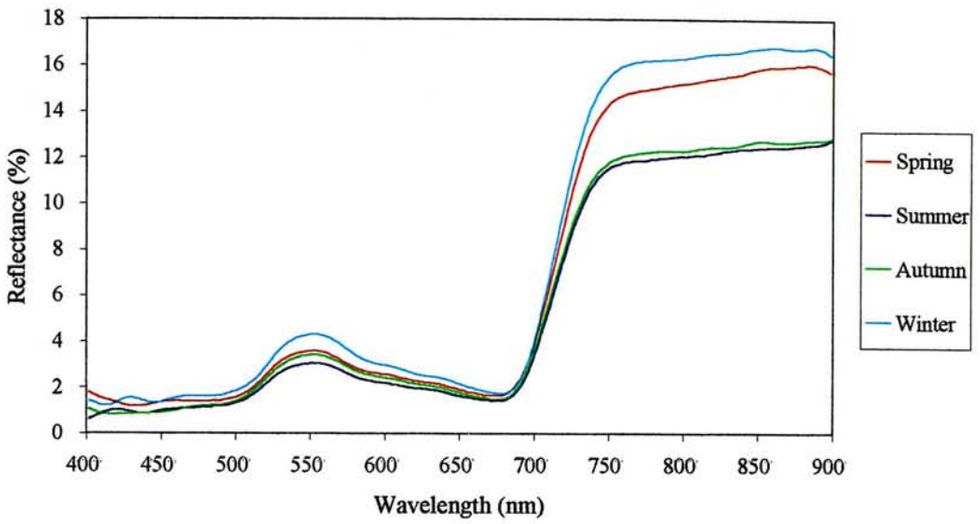

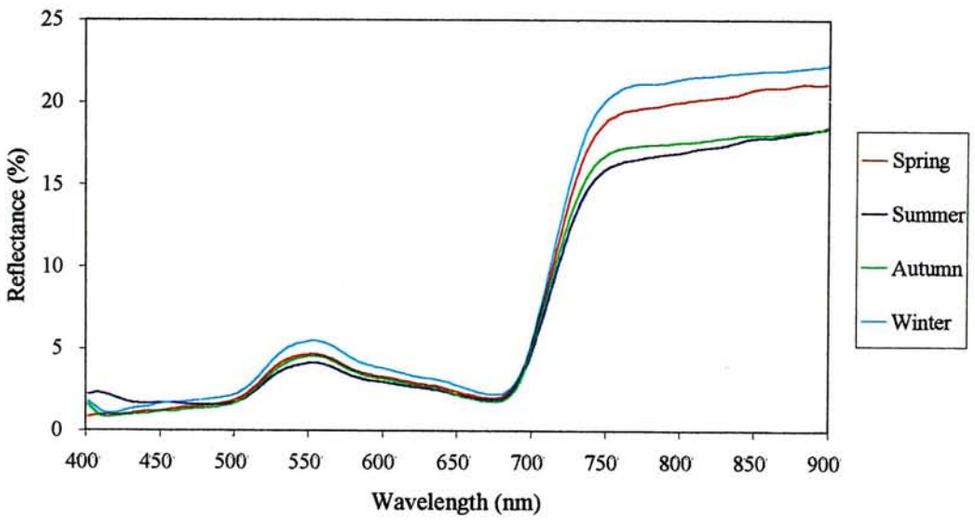

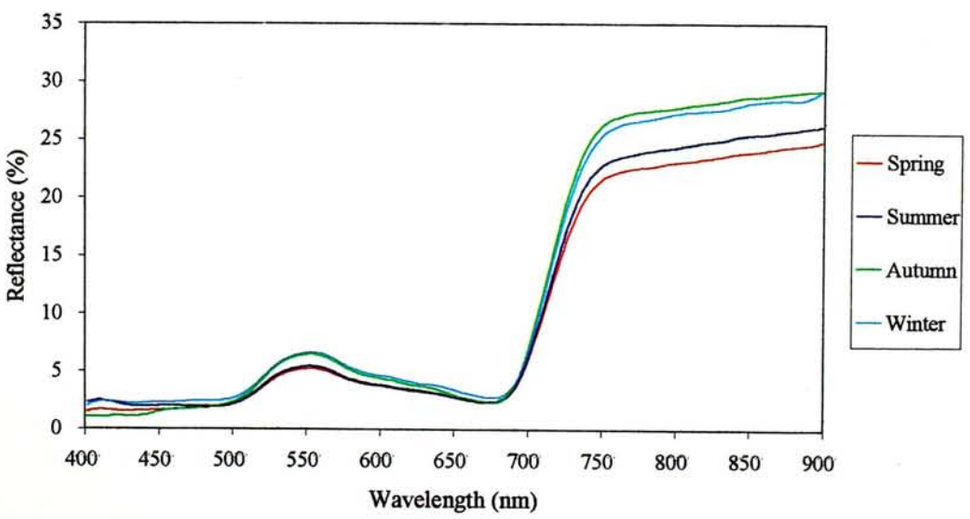

Appendix 1.23. Reflectance of *Schima superba* in four seasons with low level (top), medium level (middle) and high level (bottom) of leaf density

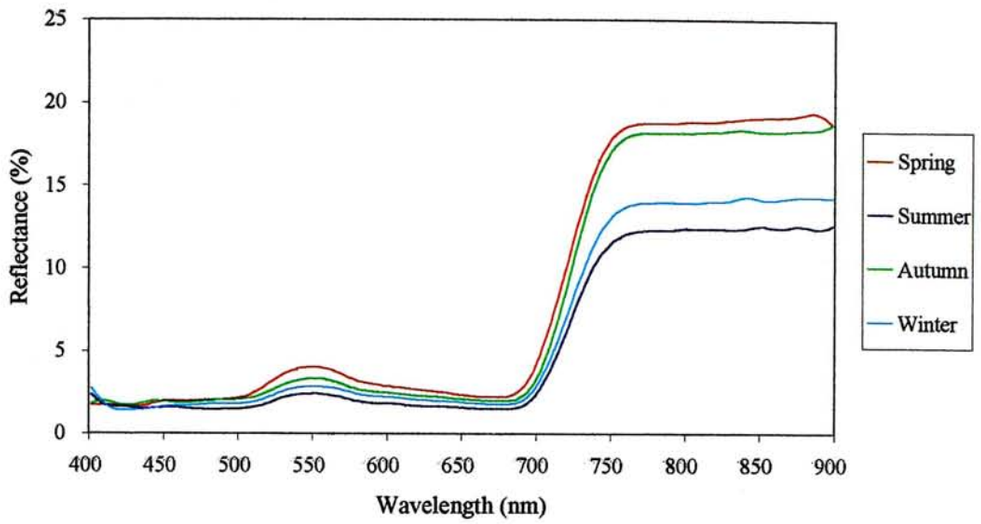

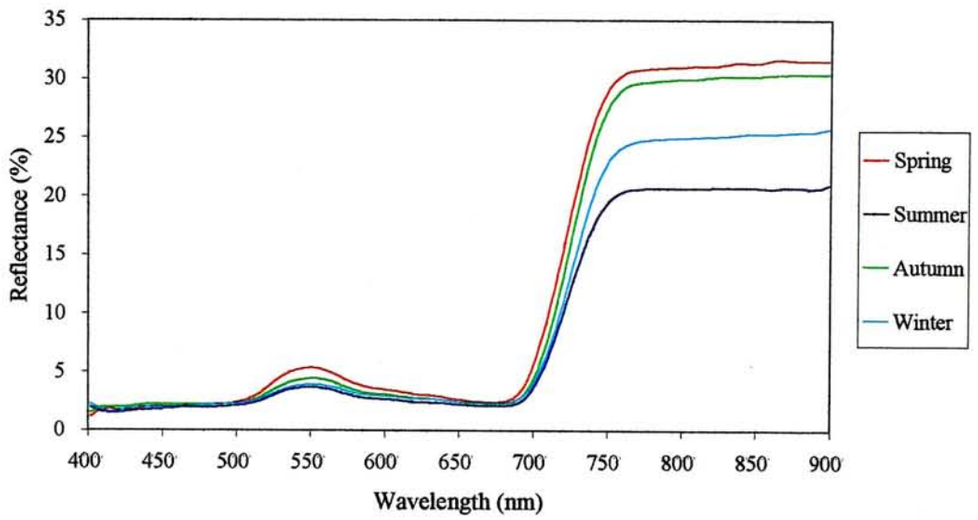

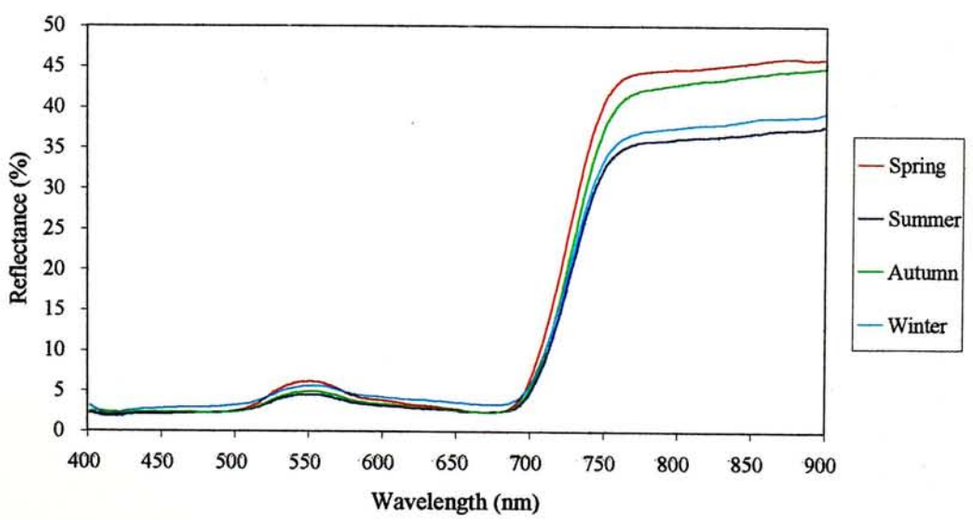

Appendix 1.24. Reflectance of *Sapium sebiferum* in spring, summer and autumn with low level (top), medium level (middle) and high level (bottom) of leaf density

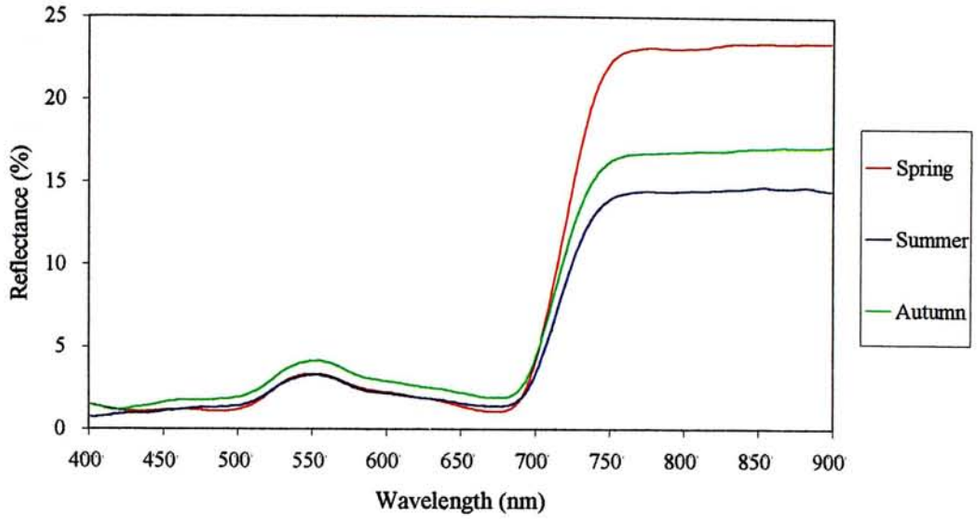

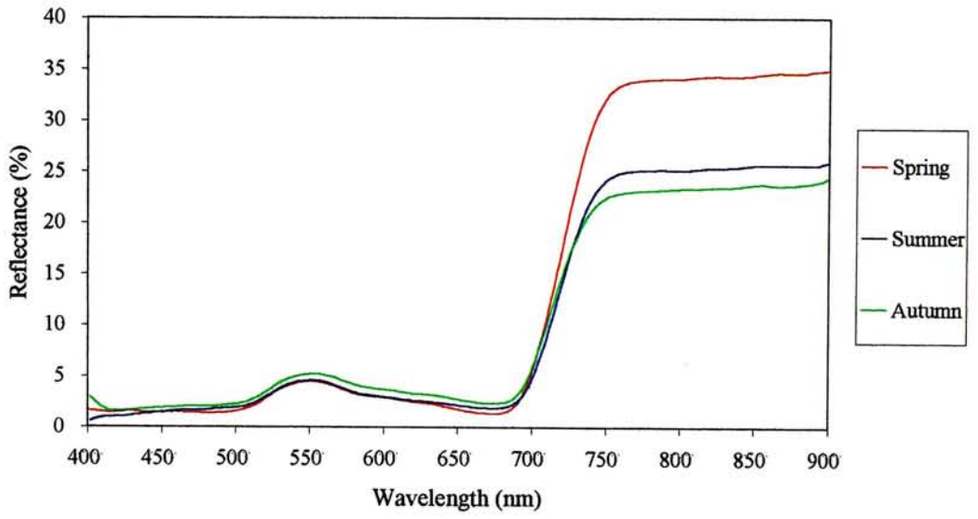

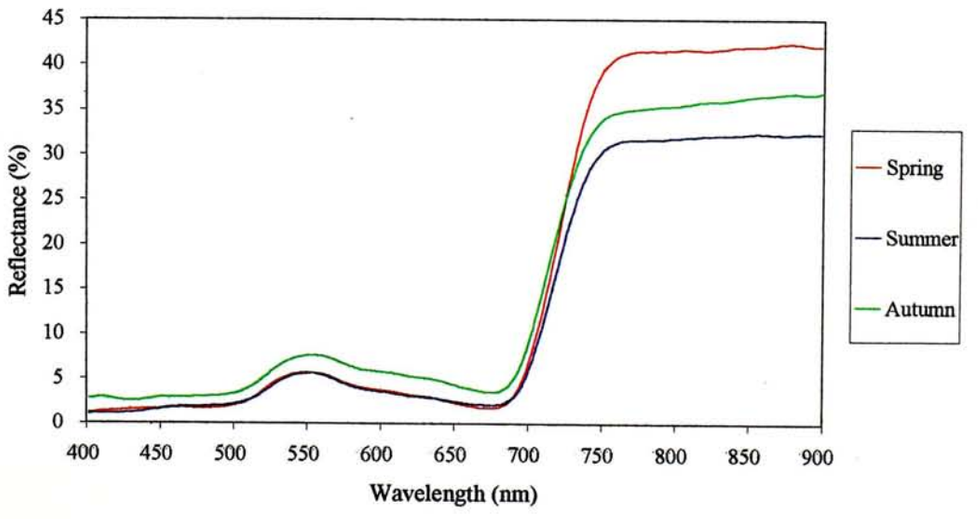

Appendix 1.25. Reflectance of *Taxodium distichum* in four seasons with low level (top), medium level (middle) and high level (bottom) of leaf density

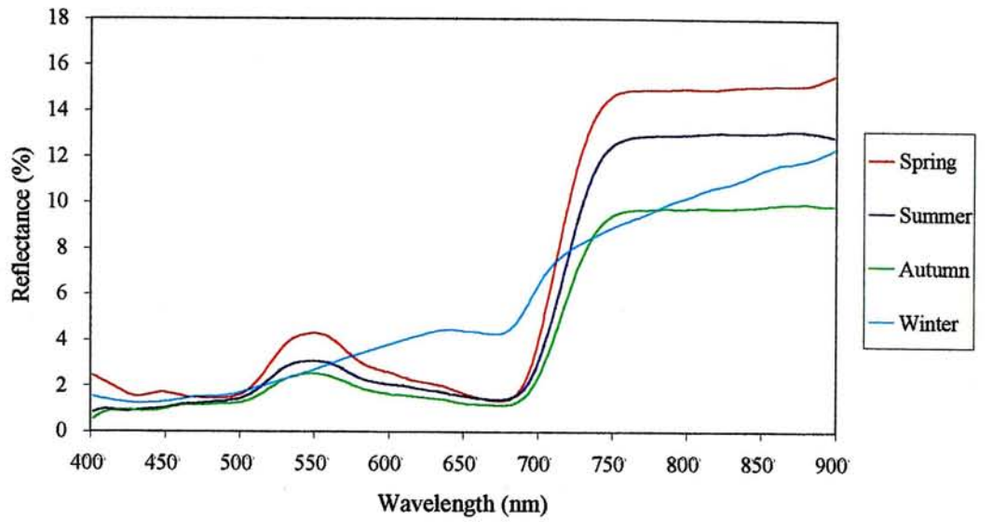

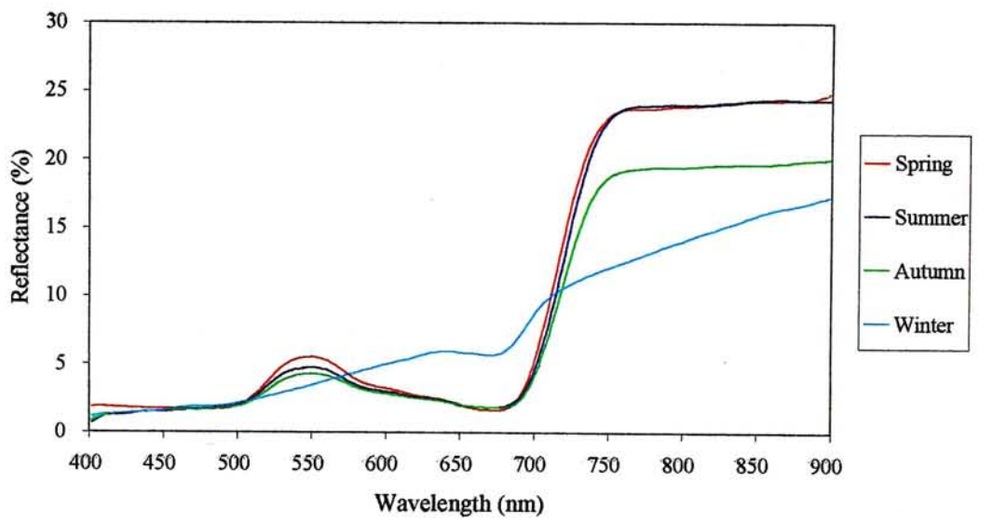

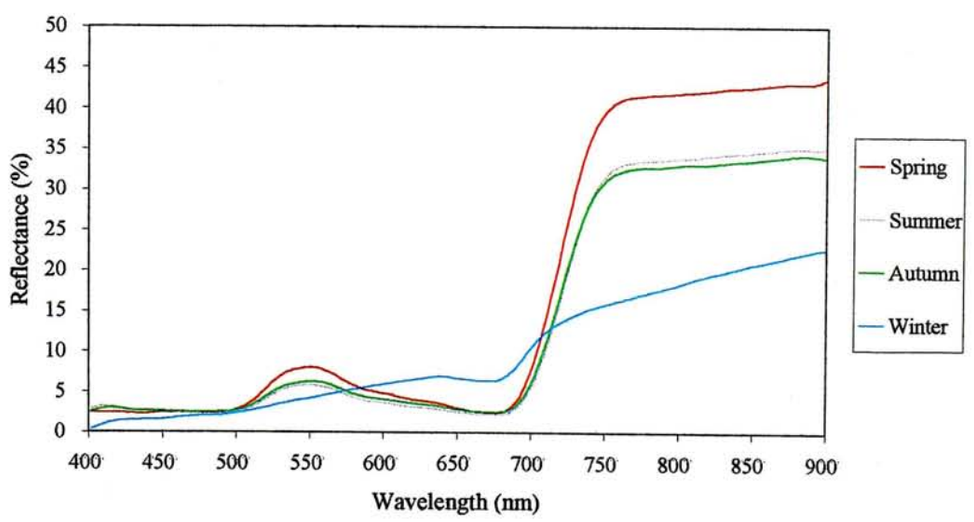

Appendix 2.1. Confusion matrix of tree species recognition using spring original spectra with 138 bands classified by linear discriminant analysis

Predicted class

True class	ac	ah	am	bv	cc	ce	cf	cl	ct	dl	dr	fm	fs	fv	ht	lc	lf	ls	mq	mt	pe	pp	sm	ss	td	Accuracy (%)
ac	20		1			1	1	1				1									4	1				66.67
ah		30																								100.00
am			20			4		1				1				4										66.67
bv	1		1	28																						93.33
cc					21			1					1				6	1								70.00
ce	3		3			21	1					2														70.00
cf						1	21			1		4									2	1				70.00
cl	8							16		2		1								3						53.33
ct	1								28						1											93.33
dl	2						2	1		16							2	4		1			2			53.33
dr	1									1	27	1														90.00
fm	1		1				2			3	1	18						1				3				60.00
fs					1							1	18				4	6								60.00
fv									1					26				1					2			86.67
ht			1					1	1						26					1						86.67
lc	3		3			1									2	17					4					56.67
lf					3												27									90.00
ls	1							1		6			2				1	18				1				60.00
mq			1				1												28							93.33
mt	2							2		4									2	19			1			63.33
pe	3					2						1								1	21	1	1			70.00
pp						4	3	1				2									1	19				63.33
sm	1					2	1				2	2								5			17			56.67
ss																								30		100.00
td	2							1		2															25	83.33
																					Overall accuracy					**74.27**

Appendix 2.2. Confusion matrix of tree species recognition using spring first derivatives spectra with 138 bands classified by linear discriminant analysis

Predicted class

True class	ac	ah	am	bv	cc	ce	cf	cl	ct	dl	dr	fm	fs	fv	ht	lc	lf	ls	mq	mt	pe	pp	sm	ss	td	Accuracy (%)
ac	3	1	1	2		1		4				1				2				7	2	1	1	4		10.00
ah		7		1	1			3		1		4	1	1		1	1		1		2	1	4		1	23.33
am	3	1	3	1				3			1	3	1	1	2	2				4	3		1	1		10.00
bv	6	1	2	8	1	1								1		1		3	1	2					3	26.67
cc		1		6	17		1			2				3												56.67
ce	1	2	2	2		2		2			1	1		1	3	4				2	2		5			6.67
cf	1	4	2			1	1	5					1			7			1		1	1	3	2		3.33
cl	2		2	4		1		5			1	1	1	3		1	1	2		3	1			2		16.67
ct	1	2	3	1		3		1	3	1	2		1		4	1				1	2		2	2		10.00
dl	1	2	3	2		1		1		3	4		4		1		1	1	1	3	1				1	10.00
dr	4		1	3				3	1		1	1		3	1			2		4	3		2	1		3.33
fm	1	1	2	1	3	1	2	4		1		2	1	3		1	1	1		1	2	1	1			6.67
fs		3	2	5	3			1	1				5	2		1		3				1			3	16.67
fv		3			1		4	5				2		5		3	2	1				2	2			16.67
ht	3	1	1	1		1		3	3		1			2	3	2				2	2		1	4		10.00
lc	1	1	1			2		2							2	8				4	3		1	5		26.67
lf	1	2	1	1	5		1	2				1	2	5			3	1	4				1			10.00
ls		2		3	1				2	3		3	2	6		1		3		1	1		1		1	10.00
mq	1	1	1			1	2					1					1		17			1		4		56.67
mt	1	1	2				1	1	2				1	1	1	2			2	3	8	1	1	1	1	10.00
pe		3						4								4			1	1	12		1	4		40.00
pp		6	1	1	1	1	3	1		2		1		1		2	1		1	1	1	5	1			16.67
sm	1	2	1	1			2	3	3	3				1	1	4		2		2	1		2	1		6.67
ss		1														2			1					26		86.67
td		3	1	3	4					1	1	1	2	1			1	2			1		1		8	26.67
																					Overall accuracy					**20.67**

Appendix 2.3. Confusion matrix of tree species recognition using spring second derivatives spectra with 138 bands classified by linear discriminant analysis

Predicted class

True class	ac	ah	am	bv	cc	ce	cf	cl	ct	dl	dr	fm	fs	fv	ht	lc	lf	ls	mq	mt	pe	pp	sm	ss	td	Accuracy (%)
ac	0	2	1	1			1	1			1	1	1	1	2				2	4		8	2	1	1	0.00
ah		1		2		1						1		1	2			3			1	2			16	3.33
am	2		2	2							1	1	1	1	3	1		1	2	3		5			5	6.67
bv	1	1	2	0		1			1	1	1	1	3	3	1	2			2	1	1	7			1	0.00
cc		3		1	5		2			2			2	2			1	2		1		3			6	16.67
ce		2		2		1		2	1	1	3		3		1				2	1		3	2	1	5	3.33
cf		2	1				0	1		2	1		5						4	2		8	3		1	0.00
cl		1	1	1		2	1	1			1	1	1	2	3	2	3			2		5		1	2	3.33
ct	2	2	2				1	2	2	1		1	1		4	1		1	1	3		2		1	3	6.67
dl				2		1	1	1	2	0			3	1	3			1	1			9		1	4	0.00
dr	2	2						1	1		2	1			3	1	1	1		4		9	2			6.67
fm	1	1	3	2			1	2	2		1	1	2					1	1	1	1	6			4	3.33
fs	1	1	1		1		1		2	1		2	8	1			1		1	1		3			5	26.67
fv		1		1	1				1	1	4	1	2	4	1			1	1		1	6		1	3	13.33
ht		1	2					2			2	2			5	4			2	2		5	1	1	1	16.67
lc	2		1				1				1				4	1			2	7	1	5	2	2	1	3.33
lf					3	1	1	1	1		1	1	3	1		1	2					11			3	6.67
ls	1	3	2									1	3	2				5		2		9	1		1	16.67
mq				1		1	1			1	1		3	1					4	4		10		2	1	13.33
mt	1					1		1		1	2		2			5		2	4	4		6		1		13.33
pe	2		1				1	1			3	1	2		4				2	4	1	4	1		3	3.33
pp		1	2	2	1	1	2		2		1	2	4	1			1			3	1	5	1			16.67
sm	1		1				2				3		1	1	2	1			3	3	1	7	1	1	2	3.33
ss			1										1		4	2			4	3		3		9	3	30.00
td		2	1		3							5	1	3	1			2				1	2		9	30.00
																					Overall accuracy					**9.73**

Appendix 2.4. Confusion matrix of tree species recognition using summer original spectra with 138 bands classified by linear discriminant analysis

Predicted class

True class	ac	ah	am	bv	cc	ce	cf	cl	ct	dl	dr	fm	fs	fv	ht	lc	lf	ls	mq	mt	pe	pp	sm	ss	td	Accuracy (%)
ac	25					3												2								83.33
ah		25			3																1				1	83.33
am			12		1	1					2	1		1				3	5					4		40.00
bv				30																						100.00
cc		1			13	1	1	3			2	1	1			2		1			2		1	1		43.33
ce	2				4	16		1		1	3	1							1				1			53.33
cf							23							1			6									76.67
cl			1		5			15			1		1			3					1			3		50.00
ct					2		1		21					1	2			1							2	70.00
dl					1		1			20									1	1			2	4		66.67
dr						1					28								1							93.33
fm		1			1	3	1				2	13		2			1	2	2					2		43.33
fs			2					5					19		2	1								1		63.33
fv								1				1		25			2	1								83.33
ht	1					1			3				2	2	20			1								66.67
lc			1		1			1								22				1	3			1		73.33
lf							1			1				1			26					1				86.67
ls		1								1			1	1	1			22	1				1	1		73.33
mq					2	2		2			2	2			1	1			16					2		53.33
mt					2		1						1			3		1		18	1		1	2		60.00
pe		1						2											1		25			1		83.33
pp					2	1				1		2						1	1		3	19				63.33
sm					1	1				1	4												23			76.67
ss					3			4		1	1					5								16		53.33
td		3			2																				25	83.33
																					Overall accuracy					**68.93**

Appendix 2.5. Confusion matrix of tree species recognition using summer first derivatives spectra with 138 bands classified by linear discriminant analysis

Predicted class

True class	ac	ah	am	bv	cc	ce	cf	cl	ct	dl	dr	fm	fs	fv	ht	lc	lf	ls	mq	mt	pe	pp	sm	ss	td	Accuracy (%)
ac	0				2		3			2	2	1						15	2		1		1		1	0.00
ah	1	4	1			1		2			3		1					1		1	7	3	2		3	13.33
am	1		0	2				2	1	1	1			1		2	1	6	5	1	3		3			0.00
bv		1		4		3	1		1		4			4	2	1		2	2	1	1				3	13.33
cc				1	2	1	1	2	1		2	2				1	1	4	2	4	3	1	2			6.67
ce	1	3		1	2	0		1	4		1	1		2		1	1	4	1		2	2	2	1		0.00
cf	1	1	1				1		1			3	3	1			3	6	1	1	3	1	2		1	3.33
cl	2	1	1		1	1	1	0	2		1	1		1		3	1	4	1	2	2	2	1	1	1	0.00
ct		1	1				2		3	2	2		1		1		4	3	1	1	4	1			3	10.00
dl	1	1			7					1	1	1				2	2	1		2	8	1	1	1		3.33
dr		2			1	1	1		2	1	2	1			1	1	3	3	3		2	3	2		1	6.67
fm		1	1		1		2			3	4	1	1	1			3	8				1	2		1	3.33
fs			2		2	1		1	2	1	2	1	6	1	1		1		1	3	2				3	20.00
fv	1		1		1			1	1	1		3		8	1	1	2	6	1			1		1		26.67
ht		1			1		1	1	2	1	1	1	3	3	0		2	11	1			1				0.00
lc	2			3					3		3			2	1	1	2	1	1	3	4			2	2	3.33
lf		2			1			1	1	2	2	3	1	3		1	0	7	2		3			1		0.00
ls			1		1			1	1	3	1		1	3	1			8	1	5	1		1		1	26.67
mq		1	1		6	2		3				1			3		1	3	3		1	1	2	1	1	10.00
mt	1	1	2	1	2	1	1	1	1			1	1	1						3	9		1	1	2	10.00
pe	2		1		2		2		1		1	1	1		1	2	1	1		1	9	1	1		2	30.00
pp		2		1	2	1	2	1							1		1	4			6	6	2		1	20.00
sm		2	2	1	1				2	1				1			3			4	6	2	4		1	13.33
ss		1			1	4			1		1			5			3	3		3	6			1	1	3.33
td	1	2		2	2				2		1			1		1	2	1		1	9	2	2		1	3.33
																					Overall accuracy					**9.07**

Appendix 2.6. Confusion matrix of tree species recognition using summer second derivatives spectra with 138 bands classified by linear discriminant analysis

Predicted class

True class	ac	ah	am	bv	cc	ce	cf	cl	ct	dl	dr	fm	fs	fv	ht	lc	lf	ls	mq	mt	pe	pp	sm	ss	td	Accuracy (%)
ac	7		2	1	1	3	1	1		1		5		1				1	1	1	1		1	2		23.33
ah	3	2			2	1	2	1		1	1							1	1	2	4	8		1		6.67
am	1	3	0	2				1	2	1		3	2	4	1				3	1	1	2	2	1		0.00
bv		2		4		3						1	1	12	1	1	2	1	2							13.33
cc		2		1	1	2		2				1	3	2	2		1			2	3	5	1	2		3.33
ce		3		1		1	1					1		7		1				3	2	5	2	3		3.33
cf	2					1	0	1	2			2	4	2		1			1	5	5	3	1			0.00
cl			1		2	1		1	1	2			2	4				1	3	1	4	1		5	1	3.33
ct	1	2				3			2				3	5	2	1	1			5	2	1		1	1	6.67
dl	2	1			2					0		1	2	2			1		1	2	7	1	4	4		0.00
dr	1	1	1	1		3			1	1	1	1		2	1	1	2	1	4	1		5	1	1		3.33
fm	2	4			1	1		2				0	2	8					3		3	3		1		0.00
fs	2			2	1	2			3				4	2			1	3			4	3	1	2		13.33
fv		1		3		2		1			1	1	1	16	2			1					1			53.33
ht	3	1	1	4			1	1		1			1	10	0			1	1	1	3			1		0.00
lc	2		1	1	2			1	1	1			6	1	1	0				2	4		3	4		0.00
lf		2		3	2	2						2	2	10			1		1	1	1	2		1		3.33
ls		2	2	1		1			3	1			1	4	2			0	1	4	7	1				0.00
mq	1	4		1		1		2			3	2	2	3	2			1	3		2	2		1		10.00
mt	1	1			2	1			1	1			2	3						8	6	2		2		26.67
pe	2	1		1	1		1	2					1	1					1	1	9	3	1	2	3	30.00
pp	1	2		1	2		1	2				2	1	1	1		1		2		5	8				26.67
sm									1				7	2		1	1			4	3	3	6	1	1	20.00
ss		1				3					1		3	6			1	1		5	2	2	2	3		10.00
td	2			1	1	1			1				3	3			1	1		3	3	7	1	1	1	3.33
																					Overall accuracy					**10.40**

Appendix 2.7. Confusion matrix of tree species recognition using autumn original spectra with 138 bands classified by linear discriminant analysis

Predicted class

True class	ac	ah	am	bv	cc	ce	cf	cl	ct	dl	dr	fm	fv	ht	lc	lf	ls	mq	mt	pe	pp	sm	ss	td	Accuracy (%)
ac	23		1		1	3															1			1	76.67
ah		27						1												2					90.00
am			29				1																		96.67
bv				29							1														96.67
cc	2				27						1														90.00
ce	4					24	1													1					80.00
cf		1				1	22									1	1			1		2		1	73.33
cl								28					1										1		93.33
ct						1	2		25	1										1					83.33
dl								1		26									3						86.67
dr				1	4						24											1			80.00
fm											1	29													96.67
fv							3		1				23						1	2					76.67
ht							1						1	26			2								86.67
lc								1							29										96.67
lf																30									100.00
ls							1			3			1	2		1	21					1			70.00
mq	1				3	1												23					2		76.67
mt					1		2			1			2	1			2		21						70.00
pe		2				1	6						1							14	6				46.67
pp		2			1	1	2											1		2	21				70.00
sm					3						2									1		24			80.00
ss						1		2										4		1	1		21		70.00
td		9					2													4				15	50.00
																				Overall accuracy					**80.69**

Appendix 2.8. Confusion matrix of tree species recognition using autumn first derivatives spectra with 138 bands classified by linear discriminant analysis

Predicted class

True class	ac	ah	am	bv	cc	ce	cf	cl	ct	dl	dr	fm	fv	ht	lc	lf	ls	mq	mt	pe	pp	sm	ss	td	Accuracy (%)
ac	5	2	3			4		1		1	1		4				1		1	1	2	1	1	2	16.67
ah	1	3	1			3		4		1		2		1			2		2		3	1		6	10.00
am	3	1	9			1	1		2						1		6			2		3		1	30.00
bv				20	2		1						2	2		2			1						66.67
cc	2	2		1	2			5			2		4		3		1		1		1			6	6.67
ce	6	1	1			3					1	1			4	2		1		2	1	2	3	2	10.00
cf	1	1			1	3	1	1		1		1	1	1	2	3	2			1	1	4	1	4	3.33
cl	4	2	1		1	2		5	1					1	4		1	1	1		1	2	1	2	16.67
ct		1	3		1		1	1	3		5		3	1	1	2	1			1	1	4		1	10.00
dl		1		2	4		1	1	2	4	4			2	3		2		1			2		1	13.33
dr		3			2	2		2	1	1	1		2	2			2		2		1	4		5	3.33
fm				2	5							13		2			1		2		1	3		1	43.33
fv	1		1	3	1				2		1	1	0	4	2	3	5			1	1	3		1	0.00
ht			2	2				1	4		3		4	5		4	3				1	1			16.67
lc	1	4				1		6	4	1		2			3	1	1					3		3	10.00
lf	1					2	1		7				1		1	10		1	1		1	2	2		33.33
ls	1	1	1	2	2	1				1		3	3	4	1	1	5				1	2		1	16.67
mq	2	1			3	2		2				1	1	1		1		5	2		1	1	7		16.67
mt		3		2	2			1		1		4		4	1		1		3		3	3		2	10.00
pe	10	1	3			1	1	1		1					3		1	2		2	1		2	1	6.67
pp	3	3	1		1	2		2	2			1					1			1	7	1	1	4	23.33
sm				1	3	1				2	4				2	2	2		1		3	5		4	16.67
ss	5		1								2	1			1			4			7		9		30.00
td	1	5	3				3	1	1	1				1				1	1	6	1	3		2	6.67
																				Overall accuracy					**17.36**

Appendix 2.9. Confusion matrix of tree species recognition using autumn second derivatives spectra with 138 bands classified by linear discriminant analysis

Predicted class

True class	ac	ah	am	bv	cc	ce	cf	cl	ct	dl	dr	fm	fv	ht	lc	lf	ls	mq	mt	pe	pp	sm	ss	td	Accuracy (%)
ac	5		5				4		1	2			1		4		2	4	1				1		16.67
ah	2	7	3					2		5		1			2		1			1	1	2		3	23.33
am	2	1	10		1	1	2			1					5			1		5				1	33.33
bv	1		1	8		2	3		2	5						1	1		1	2			1	2	26.67
cc	2	2			1	1		3		8	3		1	2	3		1		2			1			3.33
ce			6		1	4				2	1				1		2	5	2	2			2	2	13.33
cf	1	2	5			1	1			5	1			1	4	3			1	1		1	3		3.33
cl	3	3	5					4		8			1		4							1		1	13.33
ct	2			2		1	3	3	2	5			1		2	2				2		2	2	1	6.67
dl	2	1	1	2		1			1	12	8		1	1											40.00
dr	1	1	1	1	1		1	2	3	4	4		2				1	1	2		1			4	13.33
fm					2	1	1		1	2		9	1	2			2		2			1	6		30.00
fv		1	5	2	1	1	1		2	4			0	1	1	1	1	1	2	1		1	1	3	0.00
ht	1		2	1		1	2			7	2			1	1	4		4		1	2		1		3.33
lc	3	2	1		1		1	6	2	3	3				2		1						1	4	6.67
lf			1	1		3			2		1	1		1	1	4	1	1		1	1	2	9		13.33
ls	1	1			2		1			7	2	1	3	2			2	3	1	1			2	1	6.67
mq	1		4			1			2	1	1	5		3				2	1	1	2		6		6.67
mt		2				1	2			5	2	1		7	1				1	2	3		1	2	3.33
pe	5	1	1			2	5	1		1	1	1			4	1	1	1		3				2	10.00
pp	1	1				3		1		1		4					2	1	3	5	4		4		13.33
sm	1			1	1	1				6	1		1	4	1			2	1	1		4	3	2	13.33
ss	2		4							1	1	5	2	1	1	1		1		2	4		5		16.67
td	2	1	5			1	2	2		1	1		1		2				1	7	1			3	10.00
																				Overall accuracy					**13.61**

Appendix 2.10. Confusion matrix of tree species recognition using winter original spectra with 138 bands classified by linear discriminant analysis

Predicted class

True class	ac	ah	am	bv	cc	ce	cf	ct	dl	fm	fv	ht	lc	lf	ls	mq	mt	pe	pp	sm	td	Accuracy (%)
ac	13	1			4		6		2			1						2		1		43.33
ah		24			1													1	4			80.00
am			15			7	1									4			3			50.00
bv			1	25	2		1					1										83.33
cc			1		17	1			6				1			1			1	2		56.67
ce			2			19	2		1		1							1	3	1		63.33
cf		1	3				17		1									2	5	1		56.67
ct				1				27		1		1										90.00
dl	1				2		3		20											4		66.67
fm					1	4	2		1	17	2							2		1		56.67
fv						4		1			20	1						2		2		66.67
ht	2			1		2		1			1	20	2					1				66.67
lc	3			2					4			2	19									63.33
lf														26		4						86.67
ls									1						28			1				93.33
mq		1	1		1				1			1				25						83.33
mt									1	1							25	3				83.33
pe		2			1		1											25	1			83.33
pp		2			2	1	3											2	20			66.67
sm	1				11	2	3		3											10		33.33
td																					30	100.00
																	Overall accuracy					**70.16**

Appendix 2.11. Confusion matrix of tree species recognition using winter first derivatives spectra with 138 bands classified by linear discriminant analysis

Predicted class

True class	ac	ah	am	bv	cc	ce	cf	ct	dl	fm	fv	ht	lc	lf	ls	mq	mt	pe	pp	sm	td	Accuracy (%)
ac	0	1	2	1	3	1	1		1		1	3	3		1			2	2	7	1	0.00
ah		2		1	1		1	1	2			1	2	5	1		7		2	3	1	6.67
am	1		5		4				1	1		3		3	1	1	3	1	5	1		16.67
bv		2	6	0	1	4			1		1	4	3			1	3	2	1	1		0.00
cc	1	3	2	1	2	1			1			6	1	3		1	1		1	3	3	6.67
ce		2	7		2	0	1					8	2				3	2	1	2		0.00
cf	1		4	3	4	2	0		2			4		1	2	1	2		1	3		0.00
ct	1	1	2		1	2		1	3		2	6	5	1	1		1	1		2		3.33
dl	1	1	1		3		2		2	1		4	2				1	4	3	2	3	6.67
fm	1			2	1	3			2	3		7	4		2		1		1	3		10.00
fv		1	1		1	1		1	2	5	0	2	5	1	1		6	1	1	1		0.00
ht		1			2	1				2		16	5							2	1	53.33
lc	3	2	2	1	3		1	2		1	1	3	2	1	2		1			3	2	6.67
lf		1			1						1	1		13	6		2		1	3	1	43.33
ls		1			1	1				1				3	23							76.67
mq		4			2		1	1		1	2	2	3	2	2	0	4	1	3	2		0.00
mt		2		2	1				2	3		1	1	4	2		8	1	1	2		26.67
pe		2	1	1	2		1		7		1	2	2				3	3	3		2	10.00
pp		1	4		2	1			3		2		1	4		1		3	5	2	1	16.67
sm		1	2		3	3				1	1	3	2			1		3	2	4	4	13.33
td		3			1				2	8		2	4	1	3		2		1	1	2	6.67
																	Overall accuracy					**14.44**

Appendix 2.12. Confusion matrix of tree species recognition using winter second derivatives spectra with 138 bands classified by linear discriminant analysis

Predicted class

True class	ac	ah	am	bv	cc	ce	cf	ct	dl	fm	fv	ht	lc	lf	ls	mq	mt	pe	pp	sm	td	Accuracy (%)
ac	2	2		2	2		1	1	4			3	2	2	1	4		2		2		6.67
ah		2		2	2				1	1		4	1		1	3	1	5		7		6.67
am			1	4	3	3			1	2	2	4	4	1		2		2	1			3.33
bv				7						1		1			1	10		9	1			23.33
cc	1	1	1	2	5	2	2		2	1		1	1		1	4		5		1		16.67
ce			3	2	1	7		2		2	2	5		1		1	1	1	1	1		23.33
cf			1		1	4	5					5	3					1	2	7	1	16.67
ct				2				3		9		2					5		1	8		10.00
dl	3		2	5	2		1		3									3		11		10.00
fm				7	1	1		6		6	1					1	5			2		20.00
fv			4	1	1	4		1		5	2	3	2	1			1	3		2		6.67
ht					2	1		3	1	1	3	5	4		4	1		4	1			16.67
lc	1		2		1				1			5	10	4		5					1	33.33
lf		1								2	2		4	15	1	4					1	50.00
ls				2	1						1		3	5	13	3				2		43.33
mq	1	3		1	1	1						2	6	3		12						40.00
mt				5				2		1							21			1		70.00
pe	1			5			2	1				2		1		5		11	1	1		36.67
pp		1			1	4	1	3		2	2	2				3	2	3	1	5		3.33
sm	1		1	3	5	3	2		4				1			2	1	1		6		20.00
td			2				1							1							26	86.67
																	Overall accuracy					**25.87**

Appendix 3.1. Confusion matrix of tree species recognition using spring original spectra with 138 bands classified by neural network

Predicted class

True class	ac	ah	am	bv	cc	ce	cf	cl	ct	dl	dr	fm	fs	fv	ht	lc	lf	ls	mq	mt	pe	pp	sm	ss	td	Accuracy (%)
ac	10	4						6				8				1					1					33.33
ah		26																		4						86.67
am			20				1			2						4				1			1		1	66.67
bv				30																						100.00
cc	1				25			2		1													1			83.33
ce						29															1					96.67
cf	3		1				15			2		3				6										50.00
cl								25			1	1									2				1	83.33
ct				1				3	22						1			1			2					73.33
dl					3			1		9	1	6						2			2		1		5	30.00
dr								1			21	5								1					2	70.00
fm	6	1					1	4				7								6		1		1	3	23.33
fs								3					27													90.00
fv		1						6					1	22												73.33
ht								2							28											93.33
lc																23					7					76.67
lf		2			4			2									20								2	66.67
ls								15		3								12								40.00
mq																			30							100.00
mt	1	1		1	1		2	11		2										10	1					33.33
pe						4															25	1				83.33
pp	2											1										27				90.00
sm																1							29			96.67
ss																				1				25	4	83.33
td								5																	25	83.33
																					Overall accuracy					**72.27**

Appendix 3.2. Confusion matrix of tree species recognition using spring first derivatives spectra with 138 bands classified by neural network

Predicted class

True class	ac	ah	am	bv	cc	ce	cf	cl	ct	dl	dr	fm	fs	fv	ht	lc	lf	ls	mq	mt	pe	pp	sm	ss	td	Accuracy (%)
ac	3	2	5				9									5					3	1		2		10.00
ah		25					3									1				1						83.33
am			8				1	1				4				6					3	4		2	1	26.67
bv				21	1									2		1							1	4		70.00
cc		4			23									1			2									76.67
ce						23															4		3			76.67
cf				1			16											1	1			7		1	3	53.33
cl	1			1				16				1		1			2	4							4	53.33
ct									16					5	1	4		1							3	53.33
dl			1	2			1	1	1	10		1	1	2			1	2		1	5			1		33.33
dr			2				6	1			3	2						6				1	9			10.00
fm	4	4	6			1	3			1		3				1					1	2	2	2		10.00
fs				1	2								24											1	2	80.00
fv				2			1			1			3	19				1							3	63.33
ht									4						25						1					83.33
lc	5							1								17					7					56.67
lf					2								1				26							1		86.67
ls							1						1	3				23					1		1	76.67
mq		1																	23			6				76.67
mt		1		2	2		1	3	2	2						3		1		10		1		2		33.33
pe	6					2	1									1					16	1		2	1	53.33
pp						1													1			27		1		90.00
sm						1												1		1	1		26			86.67
ss								1								1					1			27		90.00
td							3							1		2						1			23	76.67
																					Overall accuracy					**60.40**

Appendix 3.3. Confusion matrix of tree species recognition using spring second derivatives spectra with 138 bands classified by neural network

Predicted class

True class	ac	ah	am	bv	cc	ce	cf	cl	ct	dl	dr	fm	fs	fv	ht	lc	lf	ls	mq	mt	pe	pp	sm	ss	td	Accuracy (%)
ac	0											4								1		13	5	7		0.00
ah		3						1		3		7		1		2			2	2		7	1	1		10.00
am			1													4				5	8	1	4	6	1	3.33
bv				1				2				1	4	10			3	2				3			4	3.33
cc					10							1	2				17									33.33
ce						5																	25			16.67
cf							2			1		4						3		1		15		4		6.67
cl								0						2				10			2	2		1	13	0.00
ct									0				1		5			16		1	4			1	2	0.00
dl			1							11			1				2	3		3	3	1	4		1	36.67
dr											0	1				1				2	3	7	14	2		0.00
fm										1		6								1	5	9	1	7		20.00
fs													23	2			1	1			1				2	76.67
fv				2									2	6	1			14		1		2			2	20.00
ht															27								3			90.00
lc															2	16					4	1	2	3	2	53.33
lf													3				26					1				86.67
ls																		29							1	96.67
mq												2					1		25			2				83.33
mt										4			1		1		2	2		10	7			3		33.33
pe																					17	7	3	3		56.67
pp										1		5									1	23				76.67
sm																				1	1		27	1		90.00
ss			1													1				1	7	1		19		63.33
td								3								1					1	9			16	53.33
																					Overall accuracy					**40.40**

Appendix 3.4. Confusion matrix of tree species recognition using summer original spectra with 138 bands classified by neural network

Predicted class

True class	ac	ah	am	bv	cc	ce	cf	cl	ct	dl	dr	fm	fs	fv	ht	lc	lf	ls	mq	mt	pe	pp	sm	ss	td	Accuracy (%)
ac	30																									100.00
ah		29									1															96.67
am	1		12		2		2		1					4	1				6						1	40.00
bv			1	28										1												93.33
cc	1				18	1	1			3									2					2	2	60.00
ce						30																				100.00
cf			3		3		17			1				2			2		1		1					56.67
cl	1							17		1			2											8	1	56.67
ct			1						21						6				1	1						70.00
dl										16		1		1	3				2		5				2	53.33
dr							2				21														7	70.00
fm							4					7		8					7					2	2	23.33
fs													27							3						90.00
fv									1					27	1									1		90.00
ht									3						25					2						83.33
lc									6						2	10			4	1	2			5		33.33
lf												2					26							2		86.67
ls								3			4				7			13							3	43.33
mq							3							3					21		1			2		70.00
mt				1									2		1				3	22			1			73.33
pe							1														26			3		86.67
pp																						27		1	2	90.00
sm						3					1		1		3								21		1	70.00
ss																					2			26	2	86.67
td								1		1		1		1											26	86.67
																					Overall accuracy					**72.40**

Appendix 3.5. Confusion matrix of tree species recognition using summer first derivatives spectra with 138 bands classified by neural network

Predicted class

True class	ac	ah	am	bv	cc	ce	cf	cl	ct	dl	dr	fm	fs	fv	ht	lc	lf	ls	mq	mt	pe	pp	sm	ss	td	Accuracy (%)
ac	23					3		4																		76.67
ah		21				4					5															70.00
am			15											2		1			2		6				4	50.00
bv				18		1								1			2		7						1	60.00
cc			3		11	1				3	2								1					7	2	36.67
ce		2			1	20		6			1															66.67
cf					2	1	16			1	1			2			4				2				1	53.33
cl								24							2	1								3		80.00
ct						1			16					2	4	6									1	53.33
dl			2		1					15					3						4			4	1	50.00
dr	6	2									22															73.33
fm											1	12		3					10		2	2				40.00
fs			3					4					20		1			1		1						66.67
fv			1	1										23	1	1			3							76.67
ht						1		6			1			1	11			4						5	1	36.67
lc															1	23				2	1			3		76.67
lf				2		2								4		1	19		2							63.33
ls					1	1								1				23		1			2	1		76.67
mq			5	1											1	1	1		12		4	1		3	1	40.00
mt				2	1			2					1		1					18				5		60.00
pe			1		1			1		1					1	3	1				17	1		2	1	56.67
pp												2							1		1	26				86.67
sm						1					1		1										26	1		86.67
ss								1	1	1				1	2	4					1			17	2	56.67
td			2		1			3							3				1		1			1	18	60.00
																					Overall accuracy					**62.13**

Appendix 3.6. Confusion matrix of tree species recognition using summer second derivatives spectra with 138 bands classified by neural network

Predicted class

True class	ac	ah	am	bv	cc	ce	cf	cl	ct	dl	dr	fm	fs	fv	ht	lc	lf	ls	mq	mt	pe	pp	sm	ss	td	Accuracy (%)
ac	14	2				3		2			4			1							1				3	46.67
ah		22			1	4					2														1	73.33
am			9		2									6		1				1	11					30.00
bv				20					3			1			1		3				1	1				66.67
cc		3			15		2			1	1								1		3			1	3	50.00
ce	1	6			3	12				3			1	1					1				2			40.00
cf				2		3	15						1	3			1		1		3	1				50.00
cl					1			10		1	1		1					1	1	8	1			4	1	33.33
ct				2					16					5	2	1		1		2	1					53.33
dl					11					5			1				1			3	7			1	1	16.67
dr	8	6								1	12								1				1		1	40.00
fm												24		1					2			2		1		80.00
fs			2					1					16	2		1		1		7						53.33
fv			1		1				1					23	1				1		1	1				76.67
ht			1		4	1					1		1	1	3			2		5	2			6	3	10.00
lc													1			8			1	11	7			2		26.67
lf				4		2						2			1		20								1	66.67
ls		4							1					2	3			17					1		2	56.67
mq				4			1			1		1		2					9	2	5	1		4		30.00
mt				3	1		1		1							1				20				3		66.67
pe			1		2			1		2	1			6	1	1			7		8					26.67
pp		1					2					6					1		2			18				60.00
sm		3				3												1					23			76.67
ss			1		2			2		1				3			1			2	3			15		50.00
td		1			1			1		2		1	1								3				20	66.67
																					Overall accuracy					**49.87**

Appendix 3.7. Confusion matrix of tree species recognition using autumn original spectra with 138 bands classified by neural network

Predicted class

True class	ac	ah	am	bv	cc	ce	cf	cl	ct	dl	dr	fm	fv	ht	lc	lf	ls	mq	mt	pe	pp	sm	ss	td	Accuracy (%)
ac	28																					1		1	93.33
ah		25	3																					2	83.33
am			29										1												96.67
bv			1	26								3													86.67
cc	2				28																				93.33
ce	5					25																			83.33
cf					2		15		1							6		1		2	1	1	1		50.00
cl								29								1									96.67
ct								1	28														1		93.33
dl									6	21									1			2			70.00
dr											30														100.00
fm												29					1								96.67
fv					1				9				4		3	5			8						13.33
ht														17		4			6				3		56.67
lc								1	9						15	1			1				3		50.00
lf																19				5			6		63.33
ls									4			6			1		17						1	1	56.67
mq	1																	29							96.67
mt														6					23				1		76.67
pe		9																		15	1		4	1	50.00
pp																					28		2		93.33
sm		2			2																	26			86.67
ss																		2					28		93.33
td		1	1		2		2								1	1				3			1	18	60.00
																				Overall accuracy					**76.67**

Appendix 3.8. Confusion matrix of tree species recognition using autumn first derivatives spectra with 138 bands classified by neural network

Predicted class

True class	ac	ah	am	bv	cc	ce	cf	cl	ct	dl	dr	fm	fv	ht	lc	lf	ls	mq	mt	pe	pp	sm	ss	td	Accuracy (%)
ac	17				7		2											1				2		1	56.67
ah		26					3													1					86.67
am			24				6																		80.00
bv				19		1	1					4	2			1	1			1					63.33
cc	2				27															1					90.00
ce	1					25	1									1							1	1	83.33
cf		1		2	2		10						3	3		5				1				3	33.33
cl			1					17	6				1						2	1		2			56.67
ct									10	8			4	2								1		5	33.33
dl									3	15			8							1		1		2	50.00
dr					2	1					24											3			80.00
fm				3			1					17						2		1	6				56.67
fv							4		2	1			13				1		1	2				6	43.33
ht							1					1		20		2			2	1			1	2	66.67
lc									5	1			5		15		1							3	50.00
lf														2		17	4		4	1		1	1		56.67
ls				2		1	3			1		3	3	6			7		1	1				2	23.33
mq		1								1				1	1			14		2	5		2	3	46.67
mt																2	1		27						90.00
pe							3		1				5			1				18	2				60.00
pp								1									1				27		1		90.00
sm											1		8									20	1		66.67
ss																1		1	1				27		90.00
td	1						2						2			1	3		1	1				19	63.33
																				Overall accuracy					**63.19**

Appendix 3.9. Confusion matrix of tree species recognition using autumn second derivatives spectra with 138 bands classified by neural network

Predicted class

True class	ac	ah	am	bv	cc	ce	cf	cl	ct	dl	dr	fm	fv	ht	lc	lf	ls	mq	mt	pe	pp	sm	ss	td	Accuracy (%)
ac	9	2			11						1					1	1			1		4			30.00
ah		16	1		2	6			1				1								1			2	53.33
am			19		1	1	6						1							1				1	63.33
bv				9			4					8	2			1	2				2			2	30.00
cc	1				25			1			1											2			83.33
ce		4	1		1	13		1		1					1		1	2		1	3			1	43.33
cf					2	3	17		2	2										1				3	56.67
cl								24	2				1		1				1					1	80.00
ct						1	2	3	5	5			5	2	1		1		1				1	3	16.67
dl	1	1			1			3	4	12			5			1				1			1		40.00
dr	4				2						19											5			63.33
fm				2								23									4			1	76.67
fv	1		1	1	3	1	1	1					14	1			2		2	2					46.67
ht							5			2				7	1	2	2		3	2	1		3	2	23.33
lc								1					6		19		1		2					1	63.33
lf	1				4		1							1		6	8		4				5		20.00
ls				6			3	1				2	6	5			3		2				2		10.00
mq				1		1	1											12		1	10		1	3	40.00
mt					2		1									1	1		23				2		76.67
pe		4				5	1			2				1						13	1		2	1	43.33
pp		1		1														1			21		1	5	70.00
sm	2							2			2			2								22			73.33
ss	1			1			1					3					1		2		1		19	1	63.33
td	1		1	1	2	1	3						7							2	1			11	36.67
																				Overall accuracy					**50.14**

Appendix 3.10. Confusion matrix of tree species recognition using winter original spectra with 138 bands classified by neural network

True class \ Predicted class	ac	ah	am	bv	cc	ce	cf	ct	dl	fm	fv	ht	lc	lf	ls	mq	mt	pe	pp	sm	td	Accuracy (%)
ac	17	3			1	1	4		2			2										56.67
ah		12			2	1					1						2	2	10			40.00
am			25			2					3											83.33
bv			2	23			4					1										76.67
cc	3	1			17		2		7													56.67
ce		1	1			26											1		1			86.67
cf	3				3		17		1			4	1							1		56.67
ct			1	1				10		1	14	3										33.33
dl	2	1							27													90.00
fm									2	24			1				2		1			80.00
fv			1								29											96.67
ht							1	1				20	7				1					66.67
lc	1						4	1				6	17			1						56.67
lf		2												23		5						76.67
ls															29			1				96.67
mq		1											2			27						90.00
mt									2	2	1		1				23	1				76.67
pe		2								1								22	5			73.33
pp						2						2						3	23			76.67
sm	3																			27		90.00
td																					30	100.00
																	Overall accuracy					**74.29**

Appendix 3.11. Confusion matrix of tree species recognition using winter first derivatives spectra with 138 bands classified by neural network

Predicted class

True class	ac	ah	am	bv	cc	ce	cf	ct	dl	fm	fv	ht	lc	lf	ls	mq	mt	pe	pp	sm	td	Accuracy (%)
ac	5	4	4		10	1	2		1		1	1								1		16.67
ah	1	16			2	3	1				1							2	4			53.33
am			20			2		2			5								1			66.67
bv		1		20			2				6		1									66.67
cc		4			17	1	2	1	4										1			56.67
ce						25	1				3							1				83.33
cf	2		1		4	3	15		1		1	2	1									50.00
ct			2			2		13	1	1	4						2	2	3			43.33
dl		2			3		3	1	18			2								1		60.00
fm								3		15	4							6	2			50.00
fv						1				2	15	1				2		5	4			50.00
ht							2	7			4	15					1	1				50.00
lc								9				3	16					2				53.33
lf														23	1	2		2	2			76.67
ls															25			5				83.33
mq																24	1	3	2			80.00
mt								2	1		5		1				15	6				50.00
pe		1						4		1	2							21	1			70.00
pp			1			10					1							3	15			50.00
sm	1	4																		25		83.33
td																					30	100.00
																	Overall accuracy					**61.59**

Appendix 3.12. Confusion matrix of tree species recognition using winter second derivatives spectra with 138 bands classified by neural network

Predicted class

True class	ac	ah	am	bv	cc	ce	cf	ct	dl	fm	fv	ht	lc	lf	ls	mq	mt	pe	pp	sm	td	Accuracy (%)
ac	14		1		8		1		1		3	2										46.67
ah		16					6	2				1				1		3	1			53.33
am		1	10	2	1		1	1	1	1	6	1						4	1			33.33
bv			4	6	4		6			3	3	2	1							1		20.00
cc	2	1	1		16				5		1	2	1							1		53.33
ce		1	1		5	0					12	2						4	4	1		0.00
cf			1	2	7		13		1				1					5				43.33
ct			1					10		3	7	1	1				4	2	1			33.33
dl					2				25		3											83.33
fm			2	1				1		6	8	6						4	1	1		20.00
fv		1	3					1		7	14							4				46.67
ht		1	1	1	3			1		1		18	4									60.00
lc			1	1				1	4	1		3	15					4				50.00
lf											1			17				1	1		10	56.67
ls		1	4							2	2			1	18	2						60.00
mq		1	2												1	23			2		1	76.67
mt			1					2		1	2	3	1				20					66.67
pe		2	3							1	3							19	2			63.33
pp			5	1	1					4	1						1	9	8			26.67
sm	2				4				3											21		70.00
td										1											29	96.67
																	Overall accuracy					**50.48**

Appendix 4.1. Confusion matrix of tree species recognition of 21 tree species using spring original spectra with 138 bands classified by linear discriminant analysis for seasonal comparison

Predicted class

True class	ac	ah	am	bv	cc	ce	cf	ct	dl	fm	fv	ht	lc	lf	ls	mq	mt	pe	pp	sm	td	Accuracy (%)
ac	20		1			5			1	1								1	1			66.67
ah		27																	1		2	90.00
am	1		21							3		1	2				1	1				70.00
bv				27						2					1							90.00
cc					18				1					10			1					60.00
ce	2		1			23				3							1					76.67
cf						1	21		3	2								1	1	1		70.00
ct								26				3					1					86.67
dl	1					1	1		18						3		3	1		1	1	60.00
fm			1		1	2			1	19								1	5			63.33
fv								1			25				2		1			1		83.33
ht			1							1		28										93.33
lc	1					2				2		2	20					3				66.67
lf					14				2					13	1							43.33
ls									5	3				2	18				1		1	60.00
mq			1				1									28						93.33
mt	2	1		1					6	3						2	14	1				46.67
pe	2					3				2		1	1				1	20				66.67
pp	1					5				2									22			73.33
sm	2					4	1			2							3			18		60.00
td									1	2											27	90.00
																	Overall accuracy					**71.90**

Appendix 4.2. Confusion matrix of tree species recognition of 21 tree species using summer original spectra with 138 bands classified by linear discriminant analysis for seasonal comparison

Predicted class

True class	ac	ah	am	bv	cc	ce	cf	ct	dl	fm	fv	ht	lc	lf	ls	mq	mt	pe	pp	sm	td	Accuracy (%)
ac	26				2					1					1							86.67
ah		22			4	1														3		73.33
am	1		12		2					3	1	2	1		3	5						40.00
bv				30																		100.00
cc		2			7	1	3		5	1		1	1		4	2		2		1		23.33
ce		2			3	16			1	1					1					5	1	53.33
cf		1			2		19		3					2				1		2		63.33
ct					3	1	1	19			1	3			1						1	63.33
dl					1				23	1		1					1			3		76.67
fm			1		4	1			2	14	1			1	1	4			1			46.67
fv								1	2	1	21		1	3					1			70.00
ht	1		1		1					2	1	18			4	1					1	60.00
lc							2						24				1	3				80.00
lf							4		3	1	1			20					1			66.67
ls					1				2			1			25					1		83.33
mq			2		3	1			1			1	4		2	14	1	1				46.67
mt			2		4				1				6			1	15			1		50.00
pe					1											1		24	4			80.00
pp					2	4			1	2					1	1		1	18			60.00
sm			1		2	1	1					1								24		80.00
td		4			2															1	23	76.67
																	Overall accuracy					**65.71**

Appendix 4.3. Confusion matrix of tree species recognition of 21 tree species using autumn original spectra with 138 bands classified by linear discriminant analysis for seasonal comparison

Predicted class

True class	ac	ah	am	bv	cc	ce	cf	ct	dl	fm	fv	ht	lc	lf	ls	mq	mt	pe	pp	sm	td	Accuracy (%)
ac	21		1		2	4													1	1		70.00
ah		25																3	1		1	83.33
am			29				1															96.67
bv				28	2																	93.33
cc	1		1		24		2													2		80.00
ce	5					22	1											1	1			73.33
cf		1				2	20				2			1	1			1		1	1	66.67
ct			1			1	1	20	1		3			1			1			1		66.67
dl							2		17		2						7			2		56.67
fm					1					25					2				2			83.33
fv					1		3	1	1		18				2			2		2		60.00
ht							1				1	25			2			1				83.33
lc	1		1						1				26					1				86.67
lf											1	1		27				1				90.00
ls			1		2		1		1		1	1			20		3					66.67
mq	1	1			2	2										22			2			73.33
mt					1		3		2		1	2		2			19					63.33
pe		1	1				5				1	1						16	5			53.33
pp		2	1		1	1	1				1							1	22			73.33
sm	2				6				2						1					19		63.33
td		6			3		2										1	2	2		14	46.67
																	Overall accuracy					**72.86**

Appendix 5.1. Confusion matrix of tree species recognition using the first eight PC scores of spring data classified by linear discriminant analysis

Predicted class

True class	ac	ah	am	bv	cc	ce	cf	cl	ct	dl	dr	fm	fs	fv	ht	lc	lf	ls	mq	mt	pe	pp	sm	ss	td	Accuracy (%)
ac	7			1			1	1				4										16				23.33
ah		24					1				3	1										1				80.00
am	4	1	25																							83.33
bv				30																						100.00
cc		1			26					1							2									86.67
ce						29															1					96.67
cf	1		1				17					3									1	7				56.67
cl	2	2						24																1	1	80.00
ct									28						1					1						93.33
dl	3				4			4		10		1						4					3		1	33.33
dr											20	10														66.67
fm		4						2				17								1		3		3		56.67
fs										1			20					9								66.67
fv									2					25	3											83.33
ht															27								3			90.00
lc																25					3	2				83.33
lf					6							1					23									76.67
ls								6		4							4	16								53.33
mq																			29			1				96.67
mt	2		1				1	8		2									2	14						46.67
pe						4	2														20	4				66.67
pp	1						1					1										27				90.00
sm	1					4										4				2			19			63.33
ss												2												28		93.33
td		1																							29	96.67
																					Overall accuracy					**74.53**

Appendix 5.2. Confusion matrix of tree species recognition using the first eight PC scores of summer data classified by linear discriminant analysis

Predicted class

True class	ac	ah	am	bv	cc	ce	cf	cl	ct	dl	dr	fm	fs	fv	ht	lc	lf	ls	mq	mt	pe	pp	sm	ss	td	Accuracy (%)
ac	30																									100.00
ah		30																								100.00
am			15		6										1				8							50.00
bv				30																						100.00
cc		2	3		18	2				4														1		60.00
ce						30																				100.00
cf							22			1					1	3			3							73.33
cl		1						28								1										93.33
ct							1		19						2	6				2						63.33
dl					6			1		14			1		5	2			1							46.67
dr		10									20															66.67
fm			1		1					1		16							8		3					53.33
fs													30													100.00
fv							6						3	10		1	1	1						8		33.33
ht					1										24	1				1			3			80.00
lc							4		1					1	8	12								4		40.00
lf			1														29									96.67
ls		8				1		1					9		1			9					1			30.00
mq			1		5							4							19			1				63.33
mt									8				9		1			1		11						36.67
pe					1		1	2		1				3							19	2		1		63.33
pp		2			1					1									2		2	22				73.33
sm						7																	23			76.67
ss		1			2		5	2								2								18		60.00
td		8			3	1																		1	17	56.67
																					Overall accuracy					**68.67**

Appendix 5.3. Confusion matrix of tree species recognition using the first eight PC scores of autumn data classified by linear discriminant analysis

Predicted class

True class	ac	ah	am	bv	cc	ce	cf	cl	ct	dl	dr	fm	fv	ht	lc	lf	ls	mq	mt	pe	pp	sm	ss	td	Accuracy (%)
ac	29				1																				96.67
ah		16					1	3												2				8	53.33
am			29															1							96.67
bv				30																					100.00
cc			1		29																				96.67
ce	9					21																			70.00
cf					1	1	10		2							9				2		2		3	33.33
cl								30																	100.00
ct								2	27	1															90.00
dl								1		19			9		1										63.33
dr		1			4						25														83.33
fm												28				1	1								93.33
fv									4				12		8		4		1					1	40.00
ht													1	18		8			3						60.00
lc								1	8	2			7		12										40.00
lf																15	7			7			1		50.00
ls													3			2	22		2	1					73.33
mq	1																	25		3	1				83.33
mt													4	6		3			16					1	53.33
pe		1					4													24			1		80.00
pp																				3	27				90.00
sm					3																	27			90.00
ss																1		1		5			21	2	70.00
td		1					2						4							2				21	70.00
																				Overall accuracy					**74.03**

Appendix 5.4. Confusion matrix of tree species recognition using the first eight PC scores of winter data classified by linear discriminant analysis

Predicted class

True class	ac	ah	am	bv	cc	ce	cf	ct	dl	fm	fv	ht	lc	lf	ls	mq	mt	pe	pp	sm	td	Accuracy (%)
ac	15	4			3		5													3		50.00
ah		18				5												1	6			60.00
am			26			3					1											86.67
bv			1	27	1			1														90.00
cc	2	10			16		2															53.33
ce		3				22													5			73.33
cf	4	1			3	1	17					4										56.67
ct				1				27									2					90.00
dl	5	2							20			1	2									66.67
fm		1								21								8				70.00
fv		2									25					2		1				83.33
ht		1						1	1			22	4						1			73.33
lc		2					3		2		1	2	17					3				56.67
lf														25		3					2	83.33
ls		2													28							93.33
mq						2										28						93.33
mt									1	1							24	4				80.00
pe		6																24				80.00
pp		1	2			18													9			30.00
sm	2				1															27		90.00
td																					30	100.00
																	Overall accuracy					**74.29**

Appendix 6.1. Confusion matrix of tree species recognition using spring original spectra classified by stepwise linear discriminant analysis (Case2)

Predicted class

True class	ac	ah	am	bv	cc	ce	cf	cl	ct	dl	dr	fm	fs	fv	ht	lc	lf	ls	mq	mt	pe	pp	sm	ss	td	Accuracy (%)
ac	19			1			2	2				3										3				63.33
ah	1	28																							1	93.33
am	1		28													1										93.33
bv				30																						100.00
cc					17					1	2						10									56.67
ce						29	1																			96.67
cf	2						23					3								2						76.67
cl	1							22		5	1														1	73.33
ct									28														2			93.33
dl	3				2	1		4		15								4							1	50.00
dr											28	2														93.33
fm								3				24										2		1		80.00
fs										1			20					9								66.67
fv									2					28												93.33
ht															28								2			93.33
lc																25					4	1				83.33
lf					8								2				19					1				63.33
ls								3		5								22								73.33
mq																			26			4				86.67
mt	3		1				1	4		2									2	12		2	3			40.00
pe						1															27	2				90.00
pp	2					1						3										24				80.00
sm	1										3									10			16			53.33
ss																								30		100.00
td																									30	100.00
																					Overall accuracy					**79.73**

Appendix 6.2. Confusion matrix of tree species recognition using spring first derivatives spectra classified by stepwise linear discriminant analysis (Case2)

Predicted class

True class	ac	ah	am	bv	cc	ce	cf	cl	ct	dl	dr	fm	fs	fv	ht	lc	lf	ls	mq	mt	pe	pp	sm	ss	td	Accuracy (%)
ac	18		2			8		2																		60.00
ah		29																			1					96.67
am	2		24													4										80.00
bv				30																						100.00
cc					23					4							3									76.67
ce	1					27						2														90.00
cf						1	18					2									2	6	1			60.00
cl	5		1	1		1		22																		73.33
ct	1								27						2											90.00
dl						1			1	18	1	1					1	2					5			60.00
dr			6			1					22												1			73.33
fm						3				1		22								1		3				73.33
fs					2					3			19				2	4								63.33
fv														30												100.00
ht															30											100.00
lc						2										25					2	1				83.33
lf					1		1			1							26					1				86.67
ls								2	1	3		1	1	1				21								70.00
mq							1												29							96.67
mt	1			1				1		2									2	23						76.67
pe	1					4		1													22	2				73.33
pp						1	1					1										27				90.00
sm	1					2					1									2			24			80.00
ss																								30		100.00
td			3					2																	25	83.33
																					Overall accuracy					**81.47**

Appendix 6.3. Confusion matrix of tree species recognition using spring second derivatives spectra classified by stepwise linear discriminant analysis (Case2)

Predicted class

True class	ac	ah	am	bv	cc	ce	cf	cl	ct	dl	dr	fm	fs	fv	ht	lc	lf	ls	mq	mt	pe	pp	sm	ss	td	Accuracy (%)
ac	20		1			3		1				1				1					1	2				66.67
ah		29																							1	96.67
am	4		18			1		4				1									1				1	60.00
bv				24			2	2				2														80.00
cc				1	27												2									90.00
ce	2		1			27																				90.00
cf	3		1			1	14			1		3									2	5				46.67
cl	3						1	21							1							3			1	70.00
ct									24					1	1			2			2					80.00
dl			1			1	1			15		1	1	1			4	1		3			1			50.00
dr						1	4	3			14	6											2			46.67
fm	2		2	1		2		8	1	1		11								1		1				36.67
fs										2			23				1	4								76.67
fv									1	3			2	16	2			6								53.33
ht									1						29											96.67
lc	3					3									1	19					3			1		63.33
lf					5		1										24									80.00
ls							1	2		2			1	5				19								63.33
mq				1			1												26			2				86.67
mt				2			5	1		1									2	17	1			1		56.67
pe	7					2	1	3												1	15	1				50.00
pp	4			1		3	3															19				63.33
sm	1					3				1	3									1			21			70.00
ss																					1	1		28		93.33
td	1							1														2			26	86.67
																					Overall accuracy					**70.13**

Appendix 6.4. Confusion matrix of tree species recognition using summer original spectra classified by stepwise linear discriminant analysis (Case2)

Predicted class

True class	ac	ah	am	bv	cc	ce	cf	cl	ct	dl	dr	fm	fs	fv	ht	lc	lf	ls	mq	mt	pe	pp	sm	ss	td	Accuracy (%)
ac	30																									100.00
ah		30																								100.00
am			21		6										1				2							70.00
bv				30																						100.00
cc					19	3		1			1					5				1						63.33
ce					2	24																	4			80.00
cf					1		29																			96.67
cl					5			21					1			3										70.00
ct							6		24																	80.00
dl										21					3	2								4		70.00
dr		2				2					26															86.67
fm					3		1					24							1					1		80.00
fs													26					4								86.67
fv														28				2								93.33
ht			1											1	26								2			86.67
lc					2			1							7	19					1					63.33
lf																	30									100.00
ls						1							6					22						1		73.33
mq			2		4	3													21							70.00
mt					1			3								4				22						73.33
pe		1			1																27	1				90.00
pp		3			2	1															2	22				73.33
sm		1				14																	15			50.00
ss					3											1								26		86.67
td		3				1																			26	86.67
																					Overall accuracy					**81.20**

Appendix 6.5. Confusion matrix of tree species recognition using summer first derivatives spectra classified by stepwise linear discriminant analysis (Case2)

Predicted class

True class	ac	ah	am	bv	cc	ce	cf	cl	ct	dl	dr	fm	fs	fv	ht	lc	lf	ls	mq	mt	pe	pp	sm	ss	td	Accuracy (%)
ac	29					1																				96.67
ah		30																								100.00
am	1		24		2														1					2		80.00
bv				30																						100.00
cc		1			19	3	2				1													4		63.33
ce					4	26																				86.67
cf					1		24										3				1		1			80.00
cl					2			21								1		1			2			3		70.00
ct							2		27						1											90.00
dl										26														4		86.67
dr						6					24															80.00
fm					4	2				1		20					1						1		1	66.67
fs								2					24		2			1							1	80.00
fv														28			1	1								93.33
ht													3	1	20			6								66.67
lc					1											28								1		93.33
lf																	30									100.00
ls						7												22					1			73.33
mq			1		2	1										1			22		1			2		73.33
mt																2				26				2		86.67
pe					1																28	1				93.33
pp		1			2	4															2	21				70.00
sm					1	2					2							2					23			76.67
ss			1		4			2								1				1				21		70.00
td		2			2													1							25	83.33
																					Overall accuracy					**82.40**

Appendix 6.6. Confusion matrix of tree species recognition using summer second derivatives spectra classified by stepwise linear discriminant analysis (Case2)

Predicted class

True class	ac	ah	am	bv	cc	ce	cf	cl	ct	dl	dr	fm	fs	fv	ht	lc	lf	ls	mq	mt	pe	pp	sm	ss	td	Accuracy (%)
ac	23	1				4					2															76.67
ah		28				1					1															93.33
am			19		5										1						2			3		63.33
bv				28										2												93.33
cc	1	4	1		12								1		1				1		2	2		5		40.00
ce		2			1	23					3												1			76.67
cf							26										2				1	1				86.67
cl					2	1		18					2			2			1		2			2		60.00
ct							1		28						1											93.33
dl					1					27														2		90.00
dr	2					8					20															66.67
fm		3			5	1				1	1	14					1		1					3		46.67
fs								7					18		3			2								60.00
fv									1				1	23	1		2	1						1		76.67
ht			2		1								2		21			4								70.00
lc					1											25			1					3		83.33
lf							2					2					26									86.67
ls						6							2					21					1			70.00
mq			1		6					1						1			15		5			1		50.00
mt													1			1				26				2		86.67
pe					1		1	1											1		26					86.67
pp		2			2	3					1								1		1	19		1		63.33
sm		2			1	4					2												21			70.00
ss					8					3	1					3			2	1	2			10		33.33
td		3	1			1												1				1			23	76.67
																					Overall accuracy					**72.00**

Appendix 6.7. Confusion matrix of tree species recognition using autumn original spectra classified by stepwise linear discriminant analysis (Case2)

Predicted class

True class	ac	ah	am	bv	cc	ce	cf	cl	ct	dl	dr	fm	fv	ht	lc	lf	ls	mq	mt	pe	pp	sm	ss	td	Accuracy (%)
ac	26				4																				86.67
ah		28																						2	93.33
am	1		27		1		1																		90.00
bv				30																					100.00
cc					30																				100.00
ce	3					27																			90.00
cf	2		1		2		20		3							2									66.67
cl								30																	100.00
ct							1		27	2															90.00
dl							2			28															93.33
dr											30														100.00
fm												30													100.00
fv									2				19		1		5							3	63.33
ht													2	25		2				1					83.33
lc					1										29										96.67
lf							1									29									96.67
ls							3						1				25		1						83.33
mq	2				1													27							90.00
mt							1						1				3		25						83.33
pe																				28				2	93.33
pp																					30				100.00
sm					4																	26			86.67
ss					1													1					28		93.33
td					1															3				26	86.67
																				Overall accuracy					**90.28**

Appendix 6.8. Confusion matrix of tree species recognition using autumn first derivatives spectra classified by stepwise linear discriminant analysis (Case2)

Predicted class

True class	ac	ah	am	bv	cc	ce	cf	cl	ct	dl	dr	fm	fv	ht	lc	lf	ls	mq	mt	pe	pp	sm	ss	td	Accuracy (%)
ac	27				2																	1			90.00
ah		27																		1				2	90.00
am	1		29																						96.67
bv				30																					100.00
cc	2	1	1		25						1														83.33
ce	5					25																			83.33
cf		1					20						1			3				5					66.67
cl	2				1			26							1										86.67
ct						1	1		27	1															90.00
dl									1	27			1						1						90.00
dr	2				4						24														80.00
fm												28					1				1				93.33
fv							4						24				1			1					80.00
ht													2	27						1					90.00
lc								5							25										83.33
lf																30									100.00
ls					1		3						2	1			22			1					73.33
mq						4												25			1				83.33
mt							1						2	2					25						83.33
pe																				25	1			4	83.33
pp																				3	27				90.00
sm					2																	28			93.33
ss						1												2		1			26		86.67
td		2			1															2				25	83.33
																				Overall accuracy					**86.67**

Appendix 6.9. Confusion matrix of tree species recognition using autumn second derivatives spectra classified by stepwise linear discriminant analysis (Case2)

Predicted class

True class	ac	ah	am	bv	cc	ce	cf	cl	ct	dl	dr	fm	fv	ht	lc	lf	ls	mq	mt	pe	pp	sm	ss	td	Accuracy (%)
ac	22		2		4	1		1																	73.33
ah		25						1												1				3	83.33
am			29		1																				96.67
bv				28			2																		93.33
cc	1				26																			3	86.67
ce	3					27																			90.00
cf							17	1	1	2			2	1		5								1	56.67
cl			1		1			26							2										86.67
ct						1	2		16	9				1					1						53.33
dl							1		1	26									1					1	86.67
dr	1				10						14											5			46.67
fm					1							29													96.67
fv				2	2		4	2		1			15				1			1				2	50.00
ht						2	2		1					24		1									80.00
lc							1	1		1			1		25									1	83.33
lf														1		27			2						90.00
ls							2	1		1			1				22							3	73.33
mq						6												19			2		3		63.33
mt							2		1	1			2	1		2	1		19		1				63.33
pe		1					1													27	1				90.00
pp	1				2													5		3	19				63.33
sm					2	1		1			1											25			83.33
ss						2												6					22		73.33
td		6			3		1						1							4				15	50.00
																				Overall accuracy					**75.56**

Appendix 6.10. Confusion matrix of tree species recognition using winter original spectra classified by stepwise linear discriminant analysis (Case2)

Predicted class

True class	ac	ah	am	bv	cc	ce	cf	ct	dl	fm	fv	ht	lc	lf	ls	mq	mt	pe	pp	sm	td	Accuracy (%)
ac	20				3		7															66.67
ah		29																	1			96.67
am			30																			100.00
bv			1	26	2						1											86.67
cc					26		3													1		86.67
ce						30																100.00
cf							30															100.00
ct				1				26									3					86.67
dl									30													100.00
fm										30												100.00
fv						3					27											90.00
ht										2	1	27										90.00
lc												5	25									83.33
lf														25		4					1	83.33
ls					1										29							96.67
mq						1										29						96.67
mt									4	3							23					76.67
pe																		29	1			96.67
pp						1													29			96.67
sm					3		1		1											25		83.33
td																					30	100.00
																	Overall accuracy					**91.27**

Appendix 6.11. Confusion matrix of tree species recognition using winter first derivatives spectra classified by stepwise linear discriminant analysis (Case2)

Predicted class

True class	ac	ah	am	bv	cc	ce	cf	ct	dl	fm	fv	ht	lc	lf	ls	mq	mt	pe	pp	sm	td	Accuracy (%)
ac	21		1		5		2		1													70.00
ah		29																1				96.67
am			29		1																	96.67
bv			4	20	1		4											1				66.67
cc					25		4		1													83.33
ce						30																100.00
cf			1		2	1	25												1			83.33
ct					1			26		3												86.67
dl					2				27											1		90.00
fm								2		26	2											86.67
fv					1	2		2		1	23							1				76.67
ht				2		1					1	26										86.67
lc	1							1				1	26			1						86.67
lf														27		3						90.00
ls					1										28			1				93.33
mq		1														29						96.67
mt								4		1							25					83.33
pe		4																26				86.67
pp																			30			100.00
sm					3															27		90.00
td																					30	100.00
																	Overall accuracy					**88.10**

Appendix 6.12. Confusion matrix of tree species recognition using winter second derivatives spectra classified by stepwise linear discriminant analysis (Case2)

Predicted class

True class	ac	ah	am	bv	cc	ce	cf	ct	dl	fm	fv	ht	lc	lf	ls	mq	mt	pe	pp	sm	td	Accuracy (%)
ac	21				8		1															70.00
ah		29																	1			96.67
am			26			3													1			86.67
bv	1		1	20		1	3					1						3				66.67
cc	1				25		1		2									1				83.33
ce			3			25	1											1				83.33
cf			1		5	2	21												1			70.00
ct					1			27	1	1												90.00
dl					1		2	1	26													86.67
fm					1	2				23	4											76.67
fv						4		1		3	21							1				70.00
ht				1						2		26	1									86.67
lc								1				3	25			1						83.33
lf														24		6						80.00
ls															29			1				96.67
mq																29			1			96.67
mt								7		1							22					73.33
pe					1		1											28				93.33
pp							1	1											28			93.33
sm					2															28		93.33
td					1																29	96.67
																	Overall accuracy					**84.44**

Appendix 7.1. Confusion matrix of tree species recognition using spring original spectra classified by stepwise linear discriminant analysis (Case3)

Predicted class

True class	ac	ah	am	bv	cc	ce	cf	cl	ct	dl	dr	fm	fs	fv	ht	lc	lf	ls	mq	mt	pe	pp	sm	ss	td	Accuracy (%)
ac	12						2					13										2			1	40.00
ah		28																							2	93.33
am			27													3										90.00
bv			2	28																						93.33
cc					21					1	1						6								1	70.00
ce						28	2																			93.33
cf	2						24					2										2				80.00
cl	3							16		6		2													3	53.33
ct									28														2			93.33
dl	3				2	2		4		11								6		1					1	36.67
dr											27	3														90.00
fm								7				21										2				70.00
fs										4			20					6								66.67
fv									1					29												96.67
ht															28								2			93.33
lc						1	1									24					4					80.00
lf					5								2				22					1				73.33
ls								1		8			1					20								66.67
mq																			26			4				86.67
mt	2		1					2		2									2	18		2	1			60.00
pe						1	1														28					93.33
pp	3											2										25				83.33
sm						1														15	2		12			40.00
ss																								30		100.00
td								1																	29	96.67
																					Overall accuracy					**77.60**

Appendix 7.2. Confusion matrix of tree species recognition using spring first derivatives spectra classified by stepwise linear discriminant analysis (Case3)

Predicted class

True class	ac	ah	am	bv	cc	ce	cf	cl	ct	dl	dr	fm	fs	fv	ht	lc	lf	ls	mq	mt	pe	pp	sm	ss	td	Accuracy (%)
ac	18		5			2		3				1												1		60.00
ah		29																							1	96.67
am	2		28																							93.33
bv				29				1																		96.67
cc					23		1			1							5									76.67
ce	1		1			27						1														90.00
cf	1		1				24					1										3				80.00
cl	5							23																	2	76.67
ct									27						1			2								90.00
dl					2	1	3			13							2	3		6						43.33
dr			8				3	1		1	15	2														50.00
fm	1			1		1	1	2				23								1						76.67
fs										4			21					5								70.00
fv									1					27				2								90.00
ht															30											100.00
lc			1			2										24					3					80.00
lf					1												28					1				93.33
ls							1	1	1	5			1	3				18								60.00
mq			1																27			2				90.00
mt				1			4			5							1		2	16				1		53.33
pe	7					2															21					70.00
pp	3					2	1					3										21				70.00
sm						2	1													2			25			83.33
ss																					1			29		96.67
td	2							1																	27	90.00
																					Overall accuracy					**79.07**

Appendix 7.3. Confusion matrix of tree species recognition using spring second derivatives spectra classified by stepwise linear discriminant analysis (Case3)

Predicted class

True class	ac	ah	am	bv	cc	ce	cf	cl	ct	dl	dr	fm	fs	fv	ht	lc	lf	ls	mq	mt	pe	pp	sm	ss	td	Accuracy (%)
ac	17		4									6									1	2				56.67
ah		29																							1	96.67
am	10		13					3				1				1					1			1		43.33
bv				20			3	2		2		3														66.67
cc				1	17												12									56.67
ce			1			29																				96.67
cf	5						8	3		1		2										7		4		26.67
cl	2			2			1	21	2											1		1				70.00
ct									23				1	2				1		3						76.67
dl					1	1	4			6			2				10	1		4				1		20.00
dr			1				9	1			11	5										1	2			36.67
fm	1					1	1	8			2	14								1		1	1			46.67
fs										9			21													70.00
fv									3	1			3	14				9								46.67
ht						1			1						27						1					90.00
lc	2		3			2										21					2					70.00
lf					5		1			1			3				20									66.67
ls										6			1	8				14			1					46.67
mq																			28			2				93.33
mt				4			3		1										2	19				1		63.33
pe	7					6						1									14	1		1		46.67
pp	3	1		1		1																24				80.00
sm						4	1				2									1	1		21			70.00
ss											1										1			28		93.33
td																					1	7			22	73.33
																					Overall accuracy					**64.13**

Appendix 7.4. Confusion matrix of tree species recognition using summer original spectra classified by stepwise linear discriminant analysis (Case3)

Predicted class

True class	ac	ah	am	bv	cc	ce	cf	cl	ct	dl	dr	fm	fs	fv	ht	lc	lf	ls	mq	mt	pe	pp	sm	ss	td	Accuracy (%)
ac	30																									100.00
ah		30																								100.00
am			25		4														1							83.33
bv				30																						100.00
cc					19	4										6				1						63.33
ce						28																	2			93.33
cf		1			3		22					1		1			2									73.33
cl		1			2	1		24					1			1										80.00
ct							5		24					1												80.00
dl			1							22					4	1								2		73.33
dr											29													1		96.67
fm			2		2		1					20					1		3					1		66.67
fs													23		1			6								76.67
fv													1	27	1			1								90.00
ht			1												27								2			90.00
lc			2		3			2		1					4	16				1				1		53.33
lf																	30									100.00
ls						2							7					20						1		66.67
mq			2		5	2													21							70.00
mt								3								4				23						76.67
pe					1																27	2				90.00
pp					3																1	26				86.67
sm						11							1										18			60.00
ss					3		1																	26		86.67
td		3				1																			26	86.67
																					Overall accuracy					**81.73**

Appendix 7.5. Confusion matrix of tree species recognition using summer first derivatives spectra classified by stepwise linear discriminant analysis (Case3)

Predicted class

True class	ac	ah	am	bv	cc	ce	cf	cl	ct	dl	dr	fm	fs	fv	ht	lc	lf	ls	mq	mt	pe	pp	sm	ss	td	Accuracy (%)
ac	30																									100.00
ah		30																								100.00
am			25		4														1							83.33
bv				30																						100.00
cc		2			17	2					1				1						5			2		56.67
ce					1	27		1			1															90.00
cf					2		24										3				1					80.00
cl					1	1		23													3			2		76.67
ct									29					1												96.67
dl					2					24				2										2		80.00
dr						9					21															70.00
fm			1		2	3						20							3			1				66.67
fs													30													100.00
fv									3					26	1											86.67
ht			1										7	1	19			2								63.33
lc																28				1	1					93.33
lf												4					26									86.67
ls						9					1		5					15								50.00
mq			1		2	2		2											21					2		70.00
mt								3								5				22						73.33
pe																					30					100.00
pp					4	2															3	21				70.00
sm		1			1	14					1												13			43.33
ss			1		4	1		1								2					1			20		66.67
td		3																							27	90.00
																					Overall accuracy					**79.73**

Appendix 7.6. Confusion matrix of tree species recognition using summer second derivatives spectra classified by stepwise linear discriminant analysis (Case3)

Predicted class

True class	ac	ah	am	bv	cc	ce	cf	cl	ct	dl	dr	fm	fs	fv	ht	lc	lf	ls	mq	mt	pe	pp	sm	ss	td	Accuracy (%)
ac	27					2					1															90.00
ah		28				1															1					93.33
am			21		2														2		5					70.00
bv				28					1								1									93.33
cc		6	3		16	1								1					1					2		53.33
ce	2	5			1	21					1															70.00
cf					3		23										3				1					76.67
cl					1	2		21					1			1		1			1			2		70.00
ct		1					1		25					1							1				1	83.33
dl					1					23										2				4		76.67
dr						8					22															73.33
fm		1			8							17							2		1	1				56.67
fs													26		2			2								86.67
fv							1		1				1	23	4											76.67
ht					1								8		20			1								66.67
lc			1					1								23								5		76.67
lf																	30									100.00
ls		1				8							1					20								66.67
mq					2			1											17		5	3		2		56.67
mt							2	4		1			3		1					19						63.33
pe		1			1														1		26	1				86.67
pp		4									1								6			19				63.33
sm		3				11					1												15			50.00
ss					5					2					4	1			1					17		56.67
td		3																							27	90.00
																					Overall accuracy					**73.87**

Appendix 7.7. Confusion matrix of tree species recognition using autumn original spectra classified by stepwise linear discriminant analysis (Case3)

Predicted class

True class	ac	ah	am	bv	cc	ce	cf	cl	ct	dl	dr	fm	fv	ht	lc	lf	ls	mq	mt	pe	pp	sm	ss	td	Accuracy (%)
ac	30																								100.00
ah		24																						6	80.00
am	1		27		1		1																		90.00
bv				30																					100.00
cc	1				29																				96.67
ce	3					27																			90.00
cf					1		21		3							2				2				1	70.00
cl								30																	100.00
ct							1		24	4			1												80.00
dl							2			28															93.33
dr					1						29														96.67
fm												30													100.00
fv					3		2		3				15	1	1	2	2							1	50.00
ht													6	21		2			1						70.00
lc					2										28										93.33
lf																30									100.00
ls							5			1						1	23								76.67
mq	3																	27							90.00
mt							2						2	3			1		21	1					70.00
pe		1																		25				4	83.33
pp																					30				100.00
sm					2																	28			93.33
ss																		1		2			27		90.00
td							1													1				28	93.33
																				Overall accuracy					**87.78**

Appendix 7.8. Confusion matrix of tree species recognition using autumn first derivatives spectra classified by stepwise linear discriminant analysis (Case3)

Predicted class

True class	ac	ah	am	bv	cc	ce	cf	cl	ct	dl	dr	fm	fv	ht	lc	lf	ls	mq	mt	pe	pp	sm	ss	td	Accuracy (%)
ac	29				1																				96.67
ah		26																						4	86.67
am			29		1																				96.67
bv				30																					100.00
cc	1				28																	1			93.33
ce	4					26																			86.67
cf						1	22	1	1	1						3				1					73.33
cl								28							2										93.33
ct							1		24	5															80.00
dl							3		3	24															80.00
dr					4						26														86.67
fm												29					1								96.67
fv					1		2		3				16			1	5			2					53.33
ht							1						1	24		2				2					80.00
lc					1			3							25					1					83.33
lf																30									100.00
ls													6				24								80.00
mq						8												22							73.33
mt										1			3	1					24	1					80.00
pe		1					1													25				3	83.33
pp						1														2	27				90.00
sm					2																	28			93.33
ss						3										2		1					24		80.00
td		1			2															1				26	86.67
																				Overall accuracy					85.55

Appendix 7.9. Confusion matrix of tree species recognition using autumn second derivatives spectra classified by stepwise linear discriminant analysis (Case3)

Predicted class

True class	ac	ah	am	bv	cc	ce	cf	cl	ct	dl	dr	fm	fv	ht	lc	lf	ls	mq	mt	pe	pp	sm	ss	td	Accuracy (%)
ac	27		2		1																				90.00
ah		23																		3				4	76.67
am	1		26		2																			1	86.67
bv			1	20			1					6					1							1	66.67
cc	7				21						1													1	70.00
ce	1				1	27														1					90.00
cf						3	11		1	3						2	3			6	1				36.67
cl	2							24							4										80.00
ct									16	7			2		2				3						53.33
dl									10	18			2												60.00
dr					6						23											1			76.67
fm												26				3	1								86.67
fv					3	1	1		4	1			11	2			5			2					36.67
ht						1	1		1				2	15		9				1					50.00
lc					1			4		1					24										80.00
lf						1							1	2		26									86.67
ls							5			1			2				22								73.33
mq						8												20			2				66.67
mt							3						1	1		3			21	1					70.00
pe		2				3														24				1	80.00
pp	1																	3			26				86.67
sm					9								1									20			66.67
ss						8										1		4					17		56.67
td		2			2		1													1				24	80.00
																				Overall accuracy					**71.11**

Appendix 7.10. Confusion matrix of tree species recognition using winter first derivatives spectra classified by stepwise linear discriminant analysis (Case3). (Note that the confusion matrix classified by stepwise linear discriminant analysis (Case3) using winter original spectra is the same as that classified by stepwise linear discriminant analysis (Case 2) shown in Appendix 6.10)

Predicted class

True class	ac	ah	am	bv	cc	ce	cf	ct	dl	fm	fv	ht	lc	lf	ls	mq	mt	pe	pp	sm	td	Accuracy (%)
ac	17			1	3		9															56.67
ah		29																1				96.67
am			27				1												2			90.00
bv	1			25	1		3															83.33
cc					27		3															90.00
ce			1			29																96.67
cf				2		1	27															90.00
ct								23	1	1							3	1	1			76.67
dl					2		1	2	23			1								1		76.67
fm						1		3		25	1											83.33
fv						5		2		2	20								1			66.67
ht				2						1		27										90.00
lc												4	26									86.67
lf														24		5					1	80.00
ls															29					1		96.67
mq						1										29						96.67
mt								6		1							23					76.67
pe		3																26	1			86.67
pp						1													29			96.67
sm					2		1													27		90.00
td																					30	100.00
																	Overall accuracy					**86.03**

Appendix 7.11. Confusion matrix of tree species recognition using winter second derivatives spectra classified by stepwise linear discriminant analysis (Case3)

Predicted class

True class	ac	ah	am	bv	cc	ce	cf	ct	dl	fm	fv	ht	lc	lf	ls	mq	mt	pe	pp	sm	td	Accuracy (%)
ac	18				2		9												1			60.00
ah		23																4	3			76.67
am			20	6		3													1			66.67
bv	6			15	3	1	4											1				50.00
cc	1				21		5												2	1		70.00
ce			3			27																90.00
cf				4	1	3	22															73.33
ct								17	2								11					56.67
dl					2		2	2	23											1		76.67
fm						1				23	6											76.67
fv				1		4		1		4	18							1	1			60.00
ht				3		1		1		2		22	1									73.33
lc				2				1				3	24									80.00
lf														25	1	3					1	83.33
ls										1					27	2						90.00
mq					1						1					28						93.33
mt								11		1							16	2				53.33
pe		2																23	5			76.67
pp																		4	26			86.67
sm					2		3													25		83.33
td																					30	100.00
																	Overall accuracy					**75.08**

Appendix 8.1. Confusion matrix of tree species recognition using 21 tree species with spring original spectra classified by stepwise linear discriminant analysis for seasonal comparison

Predicted class

True class	ac	ah	am	bv	cc	ce	cf	ct	dl	fm	fv	ht	lc	lf	ls	mq	mt	pe	pp	sm	td	Accuracy (%)
ac	18			1		1	1			8							1					60.00
ah		26																			4	86.67
am			29										1									96.67
bv				30																		100.00
cc					23				2					4							1	76.67
ce						30																100.00
cf	1						26			1									2			86.67
ct								28												2		93.33
dl	3				1	1			13	2				1	6		2			1		43.33
fm										27									3			90.00
fv											30											100.00
ht												30										100.00
lc	1		1										24					4				80.00
lf					5					1				24								80.00
ls									8						22							73.33
mq																29			1			96.67
mt	2			2					4	1						2	19					63.33
pe	3					1												26				86.67
pp	2					1													27			90.00
sm	3					2											7			18		60.00
td																					30	100.00
																	Overall accuracy					**83.97**

Appendix 8.2. Confusion matrix of tree species recognition using 21 tree species with spring first derivatives spectra classified by stepwise linear discriminant analysis for seasonal comparison

Predicted class

True class	ac	ah	am	bv	cc	ce	cf	ct	dl	fm	fv	ht	lc	lf	ls	mq	mt	pe	pp	sm	td	Accuracy (%)
ac	21		6			2				1												70.00
ah		30																				100.00
am	2		28																			93.33
bv	1			29																		96.67
cc					22		1		1					6								73.33
ce	1		1			27				1												90.00
cf	1						25			1									3			83.33
ct								28				1			1							93.33
dl					2	1	5		15					1	3		3					50.00
fm						1	2			27												90.00
fv											25				5							83.33
ht												29	1									96.67
lc						1							25					3	1			83.33
lf														29					1			96.67
ls							1	1	5		4				19							63.33
mq			1													28			1			93.33
mt				4			3		2					1			20					66.67
pe	2					2												25	1			83.33
pp	2					2				3									23			76.67
sm						2	1										1			26		86.67
td	3																				27	90.00
																	Overall accuracy					**83.81**

Appendix 8.3. Confusion matrix of tree species recognition using 21 tree species with spring second derivatives spectra classified by stepwise linear discriminant analysis for seasonal comparison

Predicted class

True class	ac	ah	am	bv	cc	ce	cf	ct	dl	fm	fv	ht	lc	lf	ls	mq	mt	pe	pp	sm	td	Accuracy (%)
ac	15		7			1				2			2					2	1			50.00
ah		30																				100.00
am	9		10							7			3						1			33.33
bv				23	1		1		1	2							2					76.67
cc				2	16									12								53.33
ce						30																100.00
cf	4						13		1	4								2	6			43.33
ct								21			5	1			2		1					70.00
dl					1	2	5		7					12	2		1					23.33
fm	2		1			7	6			10							1		3			33.33
fv								2	2		16	1			9							53.33
ht								2				28										93.33
lc	2		5			3							19					1				63.33
lf				1			2							27								90.00
ls							1	2	5		8			1	12			1				40.00
mq																28			2			93.33
mt				1	3		3	1	3								19					63.33
pe	6					8												14	2			46.67
pp	1					1	2			5									21			70.00
sm						3	1			1							1			24		80.00
td																			8		22	73.33
																	Overall accuracy					**64.29**

Appendix 8.4. Confusion matrix of tree species recognition using 21 tree species with summer original spectra classified by stepwise linear discriminant analysis for seasonal comparison

Predicted class

True class	ac	ah	am	bv	cc	ce	cf	ct	dl	fm	fv	ht	lc	lf	ls	mq	mt	pe	pp	sm	td	Accuracy (%)
ac	29					1																96.67
ah		30																				100.00
am			25		5																	83.33
bv				30																		100.00
cc		2	1		22	2	3															73.33
ce	1					29																96.67
cf					8		18	1			2			1								60.00
ct								27													3	90.00
dl					1				24		1	4										80.00
fm					4				5	20				1								66.67
fv					1		1				28											93.33
ht			1					1			1	23								1	3	76.67
lc					1							1	25				2	1				83.33
lf										1				29								96.67
ls		1				2			2						20						5	66.67
mq			2		6	1										21						70.00
mt					1							1	3			1	22		2			73.33
pe																	5	22	3			73.33
pp					4	2			1										23			76.67
sm		3				8														19		63.33
td		3																			27	90.00
																	Overall accuracy					**81.43**

Appendix 8.5. Confusion matrix of tree species recognition using 21 tree species with summer first derivatives spectra classified by stepwise linear discriminant analysis for seasonal comparison

Predicted class

True class	ac	ah	am	bv	cc	ce	cf	ct	dl	fm	fv	ht	lc	lf	ls	mq	mt	pe	pp	sm	td	Accuracy (%)
ac	29					1																96.67
ah		30																				100.00
am			22		7											1						73.33
bv				30																		100.00
cc		4			18	1	4											3				60.00
ce	1	1			4	24																80.00
cf							29							1								96.67
ct								30														100.00
dl									30													100.00
fm					5	4			2	18						1						60.00
fv											26	1			3							86.67
ht			1								2	20			7							66.67
lc					1								22				1	6				73.33
lf														30								100.00
ls						9									20					1		66.67
mq			1		6	1										21			1			70.00
mt					1								3				26					86.67
pe					1											1		27	1			90.00
pp		1			2	2												2	23			76.67
sm		1				7									1					21		70.00
td		2																			28	93.33
																	Overall accuracy					**83.17**

Appendix 8.6. Confusion matrix of tree species recognition using 21 tree species with summer second derivatives spectra classified by stepwise linear discriminant analysis for seasonal comparison

Predicted class

True class	ac	ah	am	bv	cc	ce	cf	ct	dl	fm	fv	ht	lc	lf	ls	mq	mt	pe	pp	sm	td	Accuracy (%)
ac	27					3																90.00
ah		28				1														1		93.33
am			24		2													3			1	80.00
bv				29										1								96.67
cc	1	3	2		17	4						1				2						56.67
ce	2	2			9	17																56.67
cf		1					28					1										93.33
ct							2	26													2	86.67
dl					4				25							1						83.33
fm		3			6		1			17						3						56.67
fv								3			24	2			1							80.00
ht			2								3	17	1		4		2	1				56.67
lc			1								1		26			1		1				86.67
lf							1							29								96.67
ls					2	6									22							73.33
mq			1		2							1				21		4	1			70.00
mt							2						2				26					86.67
pe									1							3		25	1			83.33
pp		4			1	1				1						6			17			56.67
sm	1				1	9														19		63.33
td		3																1			26	86.67
																	Overall accuracy					**77.78**

Appendix 8.7. Confusion matrix of tree species recognition using 21 tree species with autumn original spectra classified by stepwise linear discriminant analysis for seasonal comparison

Predicted class

True class	ac	ah	am	bv	cc	ce	cf	ct	dl	fm	fv	ht	lc	lf	ls	mq	mt	pe	pp	sm	td	Accuracy (%)
ac	28				2																	93.33
ah		27																			3	90.00
am			28		2																	93.33
bv				30																		100.00
cc	2				28																	93.33
ce	7					23																76.67
cf							23	1			2			1				1		1	1	76.67
ct							1	28	1													93.33
dl									29		1											96.67
fm										29									1			96.67
fv								2			22			3	1						2	73.33
ht							2				2	24		2								80.00
lc					1						1		28									93.33
lf														30								100.00
ls							2		3		3			1	21							70.00
mq	1															24		3	2			80.00
mt							1				5	1					23					76.67
pe		1																26			3	86.67
pp																		1	29			96.67
sm					5															25		83.33
td					1		1											1			27	90.00
																	Overall accuracy					**87.62**

Appendix 8.8. Confusion matrix of tree species recognition using 21 tree species with autumn first derivatives spectra classified by stepwise linear discriminant analysis for seasonal comparison

Predicted class

True class	ac	ah	am	bv	cc	ce	cf	ct	dl	fm	fv	ht	lc	lf	ls	mq	mt	pe	pp	sm	td	Accuracy (%)
ac	29				1																	96.67
ah		25																			5	83.33
am			27		3																	90.00
bv				30																		100.00
cc	1		1		28																	93.33
ce	3					27																90.00
cf					1	1	24	1						2				1				80.00
ct							1	24	5													80.00
dl							3	2	24								1					80.00
fm										28				1	1							93.33
fv					1		2	3			17				5			2				56.67
ht							2				2	22		2			1	1				73.33
lc					1		1						27					1				90.00
lf														30								100.00
ls											7				23							76.67
mq						8										22						73.33
mt											3	1					25	1				83.33
pe		2					1											25			2	83.33
pp						1												2	27			90.00
sm					5															25		83.33
td		1			5																24	80.00
																	Overall accuracy					**84.60**

Appendix 8.9. Confusion matrix of tree species recognition using 21 tree species with autumn second derivatives spectra classified by stepwise linear discriminant analysis for seasonal comparison. (Note that the confusion matrices of the winter data classified by stepwise linear discriminant analysis for seasonal comparison are the same as those in Appendix 6.10, 7.10 and 7.11.)

Predicted class

True class	ac	ah	am	bv	cc	ce	cf	ct	dl	fm	fv	ht	lc	lf	ls	mq	mt	pe	pp	sm	td	Accuracy (%)
ac	23		2		4	1																76.67
ah		25																4			1	83.33
am	2		27		1																	90.00
bv			1	19						6					2						2	63.33
cc	9	1			20																	66.67
ce	1		2		1	25												1				83.33
cf					1	2	15	1			1			1	3			5	1			50.00
ct								13	10		1		2				4					43.33
dl							1	8	19		1						1					63.33
fm				1						26				2	1							86.67
fv	1				1		1	4	1		12	1			5			4				40.00
ht							1	1			3	15		8			1	1				50.00
lc	1				1			2			1		24								1	80.00
lf						1					1	2		25			1					83.33
ls							4	1			2			1	22							73.33
mq						7										21			2			70.00
mt							2					2		4			21	1				70.00
pe		2				2												24			2	80.00
pp	1																		29			96.67
sm					6				1											23		76.67
td	1	2			3													2			22	73.33
																	Overall accuracy					**71.43**

Appendix 9.1. Confusion matrix of tree species recognition using spectral bands in spring "4 bands" band set selected by hierarchical clustering procedures and classified by linear discriminant analysis

Predicted class

True class	ac	ah	am	bv	cc	ce	cf	cl	ct	dl	dr	fm	fs	fv	ht	lc	lf	ls	mq	mt	pe	pp	sm	ss	td	Accuracy (%)
ac	3											4								1		22				10.00
ah	3	1						4					17					4							1	3.33
am	2		21				1	1						4						1						70.00
bv				20										6					4							66.67
cc					21												9									70.00
ce						23															7					76.67
cf	2		1				11			1				1		5						9				36.67
cl	3							2		1		11	4					6				3				6.67
ct				1					25						2	1							1			83.33
dl	8	1			4					0		2	10					4							1	0.00
dr											13	7					4	4						2		43.33
fm	2	1									1	14						3		2		6		1		46.67
fs		10											19					1								63.33
fv							6		2					16					1	1		1	3			53.33
ht						1									10	6				1	4		8			33.33
lc							2		1					1		18					4	4				60.00
lf					7							1					22									73.33
ls		4								2		8	1				7	8								26.67
mq				2															26			2				86.67
mt	4		3				1	2		1		3		4					2	8			2			26.67
pe						4									2						10	13	1			33.33
pp	7						4														1	18				60.00
sm	3					6									2	1				2	3	1	8	4		26.67
ss											4													26		86.67
td		1								1			4					5							19	63.33
																					Overall accuracy					**48.27**

Appendix 9.2. Confusion matrix of tree species recognition using spectral bands in spring "3 edges" band set selected by hierarchical clustering procedures and classified by linear discriminant analysis

Predicted class

True class	ac	ah	am	bv	cc	ce	cf	cl	ct	dl	dr	fm	fs	fv	ht	lc	lf	ls	mq	mt	pe	pp	sm	ss	td	Accuracy (%)
ac	0		1			6				1	1	14									4		1		2	0.00
ah		11	1						6	5			1												6	36.67
am			21				1									4				1		3				70.00
bv		3	1	26																						86.67
cc		3			5				3					11						1					7	16.67
ce						19															1	10				63.33
cf			5				9									3			4		3	6				30.00
cl	1							3	2	4	8	1		2	2		2			3	1		1			10.00
ct		5		8	2				13	2																43.33
dl	5	5			2	1				4			2				5	1			4				1	13.33
dr								1		1	16	3		4	2		2	1								53.33
fm			1			6	1					15			3					3				1		50.00
fs										10			15					4							1	50.00
fv		10	1		2				1					11			2	3								36.67
ht	6							3		2				2	11		1			3				2		36.67
lc			3	1		4	4									15					1	2				50.00
lf	2				4			1		5	5			4	1		4	2		2						13.33
ls										4	6		5				1	14								46.67
mq							4									1			25							83.33
mt	1		2							1	5	1		5	4	1	1		2	6			1			20.00
pe	1		2			5						4									15	2	1			50.00
pp			1			10	5									1					5	8				26.67
sm	6		2					1			4	3			4		1			1	3		4	1		13.33
ss																								30		100.00
td		3			6					2			1												18	60.00
																					Overall accuracy					**42.40**

Appendix 9.3. Confusion matrix of tree species recognition using spectral bands in spring "7 bands" band set selected by hierarchical clustering procedures and classified by linear discriminant analysis

Predicted class

True class	ac	ah	am	bv	cc	ce	cf	cl	ct	dl	dr	fm	fs	fv	ht	lc	lf	ls	mq	mt	pe	pp	sm	ss	td	Accuracy (%)
ac	5	4										2									1	18				16.67
ah	2	28																								93.33
am	1		29																							96.67
bv			1	29																						96.67
cc					21												9									70.00
ce						30																				100.00
cf							19					3								1		7				63.33
cl	2	3						22				1										1			1	73.33
ct									28						2											93.33
dl	1				5	4				7		4					3	5				1				23.33
dr											20	10														66.67
fm											1	23								3		3				76.67
fs										3			20					7								66.67
fv														30												100.00
ht															24						6					80.00
lc																24					5	1				80.00
lf					3							1	2				24									80.00
ls										9			3				4	14								46.67
mq																			27			3				90.00
mt	2		2	1				1		1		2						1	1	18	1					60.00
pe			1			4															24	1				80.00
pp	1						2					2										25				83.33
sm						6					1									1			22			73.33
ss																								30		100.00
td		1								2															27	90.00
																					Overall accuracy					**76.00**

Appendix 9.4. Confusion matrix of tree species recognition using spectral bands in spring "5 red edges" band set selected by hierarchical clustering procedures and classified by linear discriminant analysis

Predicted class

True class	ac	ah	am	bv	cc	ce	cf	cl	ct	dl	dr	fm	fs	fv	ht	lc	lf	ls	mq	mt	pe	pp	sm	ss	td	Accuracy (%)
ac	16		1									8									5					53.33
ah		18		1						5		4								2						60.00
am			23											1		1					5					76.67
bv				24			5												1							80.00
cc					15					1							14									50.00
ce						28															2					93.33
cf	2	4	2	4			9									1					1	7				30.00
cl	2							6				2		4				2		2					12	20.00
ct			1					1	20					3	1	4										66.67
dl	4									6		5					13	2								20.00
dr										3	3	3						1					9	11		10.00
fm	5	2					2	5				8								5				1	2	26.67
fs					1					10			19													63.33
fv		1		2			4		2					10	1					5					5	33.33
ht															30											100.00
lc	2		4			2			8							13					1					43.33
lf					5					3			2				20									66.67
ls								1		7			1					17						1	3	56.67
mq		1		1			2												26							86.67
mt		2			1			1		1		4						1	2	15					3	50.00
pe	4		1			3						1									20	1				66.67
pp	3	1					5					3									3	15				50.00
sm						9					6	2								2		1	10			33.33
ss																		2						28		93.33
td								10		1		6		3											10	33.33
																					Overall accuracy					**54.53**

Appendix 9.5. Confusion matrix of tree species recognition using spectral bands in spring "7 edges" band set selected by hierarchical clustering procedures and classified by linear discriminant analysis

Predicted class

True class	ac	ah	am	bv	cc	ce	cf	cl	ct	dl	dr	fm	fs	fv	ht	lc	lf	ls	mq	mt	pe	pp	sm	ss	td	Accuracy (%)
ac	13					1	5	1				1								2	5				2	43.33
ah	1	19						2		2	1			2											3	63.33
am	2		27													1										90.00
bv				30																						100.00
cc					16					5			2				7									53.33
ce						30																				100.00
cf	4		1				23					1										1				76.67
cl	4							22												2					2	73.33
ct								1	26						2	1										86.67
dl	7									13		2					6	2								43.33
dr	1									6	10	1								2			6	4		33.33
fm	1	1						2				24										2				80.00
fs					1					6			19					4								63.33
fv		1						1	1					24				2		1						80.00
ht															30											100.00
lc			5			1						1				20					2	1				66.67
lf					4								1				25									83.33
ls								1		7		1	1					19							1	63.33
mq							4												26							86.67
mt	1	1					1	1		2							1	1	2	20						66.67
pe	4					2						4									18	2				60.00
pp	1											6									4	19				63.33
sm	4					7					9												10			33.33
ss																								30		100.00
td								2																	28	93.33
																					Overall accuracy					**72.13**

Appendix 9.6. Confusion matrix of tree species recognition using spectral bands in spring "11 bands" band set selected by hierarchical clustering procedures and classified by linear discriminant analysis

Predicted class

True class	ac	ah	am	bv	cc	ce	cf	cl	ct	dl	dr	fm	fs	fv	ht	lc	lf	ls	mq	mt	pe	pp	sm	ss	td	Accuracy (%)
ac	24	2										3										1				80.00
ah	2	28																								93.33
am	1		29																							96.67
bv				30																						100.00
cc					22					1							7									73.33
ce						30																				100.00
cf	1						27					1								1						90.00
cl	4							25																	1	83.33
ct									28						2											93.33
dl	4				1					18		1	1					3		2						60.00
dr								4			21	5														70.00
fm								2				27								1						90.00
fs										2			22					6								73.33
fv														30												100.00
ht															30											100.00
lc			1													24					5					80.00
lf																	29	1								96.67
ls										8		1	1					20								66.67
mq	1																		29							96.67
mt	1	1		1						1							1		2	23						76.67
pe	1					5															23	1				76.67
pp	1					1						4										24				80.00
sm																							30			100.00
ss																								30		100.00
td								2																	28	93.33
																					Overall accuracy					**86.80**

Appendix 9.7. Confusion matrix of tree species recognition using spectral bands in spring "13 bands" band set selected by hierarchical clustering procedures and classified by linear discriminant analysis

Predicted class

True class	ac	ah	am	bv	cc	ce	cf	cl	ct	dl	dr	fm	fs	fv	ht	lc	lf	ls	mq	mt	pe	pp	sm	ss	td	Accuracy (%)
ac	26											3										1				86.67
ah	1	29																								96.67
am			30																							100.00
bv				30																						100.00
cc					23					1							6									76.67
ce						29	1																			96.67
cf	1						27	1				1														90.00
cl	4		1					24																	1	80.00
ct									28						2											93.33
dl	2							1		17		1					3	3		3						56.67
dr											20	10														66.67
fm								2				27										1				90.00
fs										4			21					5								70.00
fv														30												100.00
ht															29	1										96.67
lc																25					5					83.33
lf					3												27									90.00
ls								1		7			1					21								70.00
mq	1						3												26							86.67
mt	1							1		1							1		2	24						80.00
pe						1															29					96.67
pp												2										28				93.33
sm																							30			100.00
ss																								30		100.00
td								4																	26	86.67
																					Overall accuracy					**87.47**

Appendix 9.8. Confusion matrix of tree species recognition using spectral bands in summer "4 bands" band set selected by hierarchical clustering procedures and classified by linear discriminant analysis

Predicted class

True class	ac	ah	am	bv	cc	ce	cf	cl	ct	dl	dr	fm	fs	fv	ht	lc	lf	ls	mq	mt	pe	pp	sm	ss	td	Accuracy (%)
ac	29														1											96.67
ah		26						2			1													1		86.67
am	7		5				5					3							3			7				16.67
bv				28													2									93.33
cc	3				1	1	5			1				2		2			1	1	4	6			3	3.33
ce	2					17														1	2	1	7			56.67
cf	1		7				11					4		3	2				1			1				36.67
cl	1	3						22					2					2								73.33
ct	2								19			1							2	1	1			1	3	63.33
dl	2				3			2		7			2		3						5	6				23.33
dr		6	2				1				10			3					1		2			3	2	33.33
fm	1		2				2					13		2			1		4		2	3				43.33
fs								9					18					3								60.00
fv											1	11	4	4				2			5			1	2	13.33
ht	7				1										1				3	12	2	4				3.33
lc		1			1		5		2		1			2	7	4					4	1			2	13.33
lf				1								2					27									90.00
ls		11						7		1			5		1			5								16.67
mq	2				1		2					6							3			16				10.00
mt						5		4	6				1		3					3			8			10.00
pe	4				2	2	1							2		1					9	7		1	1	30.00
pp	2		1		1		1							1					8		7	8			1	26.67
sm	2					13		1					6					1		3			3		1	10.00
ss		4					1														12			13		43.33
td		3									1			1							8	1		8	8	26.67
																					Overall accuracy					**39.20**

Appendix 9.9. Confusion matrix of tree species recognition using spectral bands in summer "3 edges" band set selected by hierarchical clustering procedures and classified by linear discriminant analysis

Predicted class

True class	ac	ah	am	bv	cc	ce	cf	cl	ct	dl	dr	fm	fs	fv	ht	lc	lf	ls	mq	mt	pe	pp	sm	ss	td	Accuracy (%)
ac	29																					1				96.67
ah		24																					6			80.00
am			21		4						1						4									70.00
bv				29																					1	96.67
cc			1		8	8	8				2					1							2			26.67
ce					2	23				1												3	1			76.67
cf			4		1		12		2	2					2	2	3		1	1						40.00
cl								26		1				1									2			86.67
ct		1							21		3							1		1					3	70.00
dl						6				13				1		5						2		3		43.33
dr		6				1			3		8						6			2			4			26.67
fm	1		2		1	6						9							6			5				30.00
fs		2											16					12								53.33
fv					6	2					5		7	1		1		2		1	2		3			3.33
ht			1		2		7		5		5				2	1				4			3			6.67
lc		2	1		1		6							3	1	10					4		2			33.33
lf			8			1			1			4					14		2							46.67
ls		4						4					1		1			17		1			2			56.67
mq	9		3			9					1	1							5			2				16.67
mt		2	2				4						2	3	3		1	2		9			2			30.00
pe	1	1			1	10	1			1					2	1				1	8		3			26.67
pp	1					9													5			15				50.00
sm		1			1	6	1	1			4					2							8	6		26.67
ss						5		4		10													4	7		23.33
td		4				1					2														23	76.67
																					Overall accuracy					47.73

Appendix 9.10. Confusion matrix of tree species recognition using spectral bands in summer "7 bands" band set selected by hierarchical clustering procedures and classified by linear discriminant analysis

Predicted class

True class	ac	ah	am	bv	cc	ce	cf	cl	ct	dl	dr	fm	fs	fv	ht	lc	lf	ls	mq	mt	pe	pp	sm	ss	td	Accuracy (%)
ac	30																									100.00
ah		29									1															96.67
am			17		4																9					56.67
bv				30																						100.00
cc		1	2		25	1															1					83.33
ce					1	28																	1			93.33
cf			2		3		23							1	1											76.67
cl								24					1								5					80.00
ct									21						9											70.00
dl					1		5			18					1						1	4				60.00
dr		10									20															66.67
fm			2							1		18										8		1		60.00
fs													27			1					2					90.00
fv							1							29												96.67
ht															22					6	1		1			73.33
lc																24				1	4			1		80.00
lf																	30									100.00
ls		6				1							1		2			19					1			63.33
mq			2		4														20		1	3				66.67
mt			1						1				9		1	1				16	1					53.33
pe					1											3					24	2				80.00
pp					2	2													2		1	23				76.67
sm		1				16																	13			43.33
ss					3																3	1		23		76.67
td		10				1																			19	63.33
																					Overall accuracy					**76.27**

Appendix 9.11. Confusion matrix of tree species recognition using spectral bands in summer "5 red edges" band set selected by hierarchical clustering procedures and classified by linear discriminant analysis

Predicted class

True class	ac	ah	am	bv	cc	ce	cf	cl	ct	dl	dr	fm	fs	fv	ht	lc	lf	ls	mq	mt	pe	pp	sm	ss	td	Accuracy (%)
ac	26					4																				86.67
ah		24								6																80.00
am			17						1										4	1	1	6				56.67
bv				23			1		3							1	2									76.67
cc					17	1	1			5				1							3	1			1	56.67
ce	5					24					1															80.00
cf					1		14			6		1					5					3				46.67
cl								18					1		6	1									4	60.00
ct			7	1	1				9					4	2					1	3			2		30.00
dl					3					20				1						2	2			2		66.67
dr	4	11				1				2	11												1			36.67
fm		1			3		3			1		8					2		3			9				26.67
fs								8					22													73.33
fv		1		1	1		5						3	6	1			3			4			5		20.00
ht	2		2					3					1		20										2	66.67
lc																22				1	2			5		73.33
lf				1								2					27									90.00
ls		4				1							6					18							1	60.00
mq				2					4								1		9	2	4	8				30.00
mt				2				10	2						1	2	3		1	6				2	1	20.00
pe									3	1				5					3		15	3				50.00
pp		3			3						1								1		2	20				66.67
sm	4	1				11					4												10			33.33
ss		2						2						6							2	1		17		56.67
td					3	1		5		1				1	7					1					11	36.67
																					Overall accuracy					55.20

Appendix 9.12. Confusion matrix of tree species recognition using spectral bands in summer "7 edges" band set selected by hierarchical clustering procedures and classified by linear discriminant analysis

Predicted class

True class	ac	ah	am	bv	cc	ce	cf	cl	ct	dl	dr	fm	fs	fv	ht	lc	lf	ls	mq	mt	pe	pp	sm	ss	td	Accuracy (%)
ac	30																									100.00
ah		30																								100.00
am			20		6														3	1						66.67
bv				30																						100.00
cc					21	3	4			2																70.00
ce						30																				100.00
cf					1		15			3							7			1	1			2		50.00
cl								27								1								2		90.00
ct			1						22					3	2					2						73.33
dl					1					22									2					5		73.33
dr		11									18												1			60.00
fm					5		1			3		12							7			1		1		40.00
fs													30													100.00
fv					2		5	2		1			4	7			1	3		1				4		23.33
ht			2			1		1							26											86.67
lc														1		24				1				4		80.00
lf																	30									100.00
ls		3				3									7			16							1	53.33
mq					5							1							22			2				73.33
mt					1		1		2				1		6	1	3			12				3		40.00
pe					1		1							2							23	3				76.67
pp					7																	23				76.67
sm		1				11					8												10			33.33
ss					2					1				1										26		86.67
td		1			2	1																			26	86.67
																					Overall accuracy					73.60

Appendix 9.13. Confusion matrix of tree species recognition using spectral bands in summer "11 bands" band set selected by hierarchical clustering procedures and classified by linear discriminant analysis

Predicted class

True class	ac	ah	am	bv	cc	ce	cf	cl	ct	dl	dr	fm	fs	fv	ht	lc	lf	ls	mq	mt	pe	pp	sm	ss	td	Accuracy (%)
ac	30																									100.00
ah		30																								100.00
am			27		1														2							90.00
bv				30																						100.00
cc		3			24	2				1																80.00
ce					1	29																				96.67
cf					2		26										1				1					86.67
cl								29								1										96.67
ct							6		23						1											76.67
dl					2		1			26														1		86.67
dr						4					26															86.67
fm					4					3		20							1					2		66.67
fs													30													100.00
fv														28			1	1								93.33
ht						1									29											96.67
lc								2								23								5		76.67
lf																	30									100.00
ls					2	4									1			23								76.67
mq					4											1			25							83.33
mt								1								4				24				1		80.00
pe					2																26	2				86.67
pp					6	2																22				73.33
sm						5																	25			83.33
ss					3														1					26		86.67
td		4			1	1																			24	80.00
																					Overall accuracy					**87.33**

Appendix 9.14. Confusion matrix of tree species recognition using spectral bands in summer "13 bands" band set selected by hierarchical clustering procedures and classified by linear discriminant analysis

Predicted class

True class	ac	ah	am	bv	cc	ce	cf	cl	ct	dl	dr	fm	fs	fv	ht	lc	lf	ls	mq	mt	pe	pp	sm	ss	td	Accuracy (%)
ac	30																									100.00
ah		28			2																					93.33
am			25		1										2				2							83.33
bv				30																						100.00
cc		2			25	3																				83.33
ce					1	29																				96.67
cf					1		27										1				1					90.00
cl								27								3										90.00
ct							4		26																	86.67
dl										28									1					1		93.33
dr						4					26															86.67
fm			1		5		1					22					1									73.33
fs													30													100.00
fv														27			1	2								90.00
ht						2									28											93.33
lc								2								24								4		80.00
lf												1					29									96.67
ls					1	2					1				1			25								83.33
mq			1		1														28							93.33
mt													1			4				24				1		80.00
pe					1																27	2				90.00
pp					4	2															1	23				76.67
sm						8																	22			73.33
ss					2														1					27		90.00
td		2			1	1																			26	86.67
																					Overall accuracy					**88.40**

Appendix 9.15. Confusion matrix of tree species recognition using spectral bands in autumn "4 bands" band set selected by hierarchical clustering procedures and classified by linear discriminant analysis

Predicted class

True class	ac	ah	am	bv	cc	ce	cf	cl	ct	dl	dr	fm	fv	ht	lc	lf	ls	mq	mt	pe	pp	sm	ss	td	Accuracy (%)
ac	22				5			1		1													1		73.33
ah		4			5			3														1		17	13.33
am			12															1	9	3			5		40.00
bv				29													1								96.67
cc	5	2			14		3			6															46.67
ce	9					18			2														1		60.00
cf	1					1	8		2	1					1	5		4	2	1	1	1	2		26.67
cl	5							17							1							7			56.67
ct	1					3		2	22													2			73.33
dl					6					20			3							1					66.67
dr		9									21														70.00
fm												27					2				1				90.00
fv			1		4	2			2				3	4	4		4						5	1	10.00
ht			5				5			1			2	4		3		1	7	1			1		13.33
lc					3			2	4				2		18								1		60.00
lf			5													6	8	4	1	6					20.00
ls				1			2			1				1		1	19		1	1	1			2	63.33
mq	1															2		18		1	5		2	1	60.00
mt			4											10		5		2	2	7					6.67
pe					3		5						1							13			3	5	43.33
pp																	2	1		1	23		1	2	76.67
sm					1			7		4					2							16			53.33
ss			1			4			1							1		1	3	7			12		40.00
td					2								12							2	2			12	40.00
																				Overall accuracy					**50.00**

Appendix 9.16. Confusion matrix of tree species recognition using spectral bands in autumn "3 edges" band set selected by hierarchical clustering procedures and classified by linear discriminant analysis

Predicted class

True class	ac	ah	am	bv	cc	ce	cf	cl	ct	dl	dr	fm	fv	ht	lc	lf	ls	mq	mt	pe	pp	sm	ss	td	Accuracy (%)
ac	12					2		1													7		8		40.00
ah		4						8					2									2		14	13.33
am			23													5		1		1					76.67
bv				30																					100.00
cc					11		1	1			2	6		1	2						4	2			36.67
ce	10					20																			66.67
cf			5				6		4			3			2	5				2	2		1		20.00
cl					2			27														1			90.00
ct			7				2		9	1		4			4	2						1			30.00
dl		7								20														3	66.67
dr		8			1		2	5	1		9	2			2										30.00
fm		1							10			3	2	3	2				2	6				1	10.00
fv			1						4			5	1	1		2	2		6	2				6	3.33
ht			4				1		1	6		1	2	2	1	6	1			5					6.67
lc					2			1				8		3	8					8					26.67
lf			2		1		2		8							10					7				33.33
ls		2								3		2	4	1			11		5					2	36.67
mq	10																	20							66.67
mt										6			1				9		6	1				7	20.00
pe					10		1					2		3	2	1				6	3	1		1	20.00
pp	2				1											6		1			19		1		63.33
sm		3			6		1	5			4		1		1	1				4		4			13.33
ss						8												1			12		9		30.00
td					1						1						6		4	4				14	46.67
																				Overall accuracy					**39.44**

Appendix 9.17. Confusion matrix of tree species recognition using spectral bands in autumn "7 bands" band set selected by hierarchical clustering procedures and classified by linear discriminant analysis

Predicted class

True class	ac	ah	am	bv	cc	ce	cf	cl	ct	dl	dr	fm	fv	ht	lc	lf	ls	mq	mt	pe	pp	sm	ss	td	Accuracy (%)
ac	28				1																		1		93.33
ah		19						5																6	63.33
am			30																						100.00
bv				30																					100.00
cc	3				27																				90.00
ce	3					27																			90.00
cf					1	1	13						1			9				3		2			43.33
cl					1			28							1										93.33
ct							1		28				1												93.33
dl							2			23			2						2	1					76.67
dr					1						29														96.67
fm												28				2									93.33
fv							1		3				13	1			4		5	2				1	43.33
ht							1						1	19		8				1					63.33
lc								2							24					4					80.00
lf							1									28				1					93.33
ls							1			1			1			1	25			1					83.33
mq	2																	21			7				70.00
mt							3						5	4			4		14						46.67
pe					2															26				2	86.67
pp																		1			29				96.67
sm					4																	26			86.67
ss																		1		10	1		18		60.00
td		3			1															4				22	73.33
																				Overall accuracy					**79.86**

Appendix 9.18. Confusion matrix of tree species recognition using spectral bands in autumn "5 red edges" band set selected by hierarchical clustering procedures and classified by linear discriminant analysis

Predicted class

True class	ac	ah	am	bv	cc	ce	cf	cl	ct	dl	dr	fm	fv	ht	lc	lf	ls	mq	mt	pe	pp	sm	ss	td	Accuracy (%)
ac	24				6																				80.00
ah		23					2			1										4					76.67
am	1		21			2			1				5												70.00
bv			4	8		1						4	1	1		1		3					7		26.67
cc	2				20																	8			66.67
ce	3					27																			90.00
cf	1	1	4		1		5		1	1			4			3	1	1		1	5		1		16.67
cl			1		2			19							3									5	63.33
ct			5					1	17	3			1		2									1	56.67
dl								2		19			1											8	63.33
dr					6						23											1			76.67
fm												28				1					1				93.33
fv			7	1			1		4				7	1			1		2					6	23.33
ht														9			9		1	5	1		5		30.00
lc								10							20										66.67
lf												1				19			4	4	2				63.33
ls										2		6		3	1	1	8		2	1	1		4	1	26.67
mq		1																20		3	6				66.67
mt												2		1		10	2		9	4	1		1		30.00
pe		1					7							1			1			20					66.67
pp																1		2		6	13		8		43.33
sm	2				15						7											6			20.00
ss												3				4	2	5		5	2		9		30.00
td		2						4					8											16	53.33
																				Overall accuracy					**54.17**

Appendix 9.19. Confusion matrix of tree species recognition using spectral bands in autumn "7 edges" band set selected by hierarchical clustering procedures and classified by linear discriminant analysis

Predicted class

True class	ac	ah	am	bv	cc	ce	cf	cl	ct	dl	dr	fm	fv	ht	lc	lf	ls	mq	mt	pe	pp	sm	ss	td	Accuracy (%)
ac	28				2																				93.33
ah		15						1													5			9	50.00
am			28		1				1																93.33
bv				30																					100.00
cc					25						2											3			83.33
ce	6					24																			80.00
cf	1		4		4		10		1							5				3	2				33.33
cl	1				1			28																	93.33
ct			5				2	1	17	3					2										56.67
dl							1			20			2											7	66.67
dr					7						23														76.67
fm												30													100.00
fv			2				3		4				10				1		1					9	33.33
ht							2							8			6		1	12	1				26.67
lc								2	4				3		20									1	66.67
lf							3									27									90.00
ls			1							4		3		1			13		5	2				1	43.33
mq	2					1												26			1				86.67
mt																	3		20	6				1	66.67
pe														1					1	26				2	86.67
pp																				2	27		1		90.00
sm					19						5											6			20.00
ss							1									5		1			4		19		63.33
td								1					10											19	63.33
																				Overall accuracy					69.31

Appendix 9.20. Confusion matrix of tree species recognition using spectral bands in autumn "11 bands" band set selected by hierarchical clustering procedures and classified by linear discriminant analysis

Predicted class

True class	ac	ah	am	bv	cc	ce	cf	cl	ct	dl	dr	fm	fv	ht	lc	lf	ls	mq	mt	pe	pp	sm	ss	td	Accuracy (%)
ac	28				2																				93.33
ah		29																					1		96.67
am			30																						100.00
bv				30																					100.00
cc	3				26																	1			86.67
ce	3					27																			90.00
cf							19		1							8						2			63.33
cl					1			29																	96.67
ct							1		28				1												93.33
dl					1		1			27			1												90.00
dr											30														100.00
fm												30													100.00
fv							1		2				22				2			1				2	73.33
ht							2							24		1				3					80.00
lc					1		1								28										93.33
lf							3									27									90.00
ls										1							26			2				1	86.67
mq	3																	26		1					86.67
mt							2												27	1					90.00
pe																				27				3	90.00
pp																				2	28				93.33
sm					6																	24			80.00
ss																		1		10			19		63.33
td																				1				29	96.67
																				Overall accuracy					**88.89**

Appendix 9.21. Confusion matrix of tree species recognition using spectral bands in autumn "13 bands" band set selected by hierarchical clustering procedures and classified by linear discriminant analysis

Predicted class

True class	ac	ah	am	bv	cc	ce	cf	cl	ct	dl	dr	fm	fv	ht	lc	lf	ls	mq	mt	pe	pp	sm	ss	td	Accuracy (%)
ac	30																								100.00
ah		28						1												1					93.33
am			30																						100.00
bv				30																					100.00
cc	1				29																				96.67
ce	2					28																			93.33
cf							23		1				1			4						1			76.67
cl								30																	100.00
ct							2		28																93.33
dl							4			26															86.67
dr											30														100.00
fm												29								1					96.67
fv					1		3		2				23											1	76.67
ht							2							26					1	1					86.67
lc								2							28										93.33
lf							1									29									96.67
ls							1						3				24			1				1	80.00
mq	1					1												25		3					83.33
mt													2	1					27						90.00
pe																				29				1	96.67
pp																				2	28				93.33
sm					2																	28			93.33
ss								1										1		1	1		26		86.67
td																				2				28	93.33
																				Overall accuracy					**91.94**

Appendix 9.22. Confusion matrix of tree species recognition using spectral bands in winter "4 bands" band set selected by hierarchical clustering procedures and classified by linear discriminant analysis

Predicted class

True class	ac	ah	am	bv	cc	ce	cf	ct	dl	fm	fv	ht	lc	lf	ls	mq	mt	pe	pp	sm	td	Accuracy (%)
ac	9	8			4		2		1			1			1					4		30.00
ah	1	12				3	3			2									9			40.00
am			16								6					3		3	2			53.33
bv				12		4		2			12											40.00
cc	7	3			3		9		3			4	1									10.00
ce		4				10	2						1		1			8	4			33.33
cf	10				1		7					2	9					1				23.33
ct				20				3			4		1				2					10.00
dl	4	7					1		17											1		56.67
fm		7								13		1					6		3			43.33
fv			4			5					20							1				66.67
ht	5	1			1	5			1	2	2	7	1				3	1	1			23.33
lc	2				1	2	2	1	1		3	6	11					1				36.67
lf														25		2		1			2	83.33
ls	1					1							1		20	2				5		66.67
mq						1					1					19		9				63.33
mt			6	1		1			3	8	2		1				6		2			20.00
pe		4				6												13	7			43.33
pp		3	7															3	17			56.67
sm		1							3											26		86.67
td																					30	100.00
																	Overall accuracy					**46.98**

Appendix 9.23. Confusion matrix of tree species recognition using spectral bands in winter "3 edges" band set selected by hierarchical clustering procedures and classified by linear discriminant analysis

Predicted class

True class	ac	ah	am	bv	cc	ce	cf	ct	dl	fm	fv	ht	lc	lf	ls	mq	mt	pe	pp	sm	td	Accuracy (%)
ac	7	3			5	1	2			1									1	10		23.33
ah	5	11					2											2	10			36.67
am			18		1	2		1			7								1			60.00
bv			3	15				12														50.00
cc			3		2	5				2	3		1							14		6.67
ce						20													2	8		66.67
cf	4	2					9				3	4	4						1	3		30.00
ct				15				12				3										40.00
dl		2							20											8		66.67
fm	3								1	14			5							7		46.67
fv			9					1			12					2			6			40.00
ht	5	4					7			1		6	2				3	1		1		20.00
lc	4						5			2		4	10			2	2			1		33.33
lf														26		3					1	86.67
ls						2									24	3					1	80.00
mq						2										28						93.33
mt		5						4				2					17		2			56.67
pe	2	3			1	1	8											4	6	5		13.33
pp		3	2			1					2							5	11	6		36.67
sm	5		1		1		3		1	1								3	2	13		43.33
td																					30	100.00
																	Overall accuracy					**49.05**

Appendix 9.24. Confusion matrix of tree species recognition using spectral bands in winter "7 bands" band set selected by hierarchical clustering procedures and classified by linear discriminant analysis

Predicted class

True class	ac	ah	am	bv	cc	ce	cf	ct	dl	fm	fv	ht	lc	lf	ls	mq	mt	pe	pp	sm	td	Accuracy (%)
ac	10	4			7		4													5		33.33
ah		30																				100.00
am			23																7			76.67
bv		2	1	23							1								3			76.67
cc	13	3			13															1		43.33
ce						24													6			80.00
cf	11						18													1		60.00
ct				4				23				1					2					76.67
dl	5	1					1		20			2	1									66.67
fm										23								7				76.67
fv						1					23							6				76.67
ht	3								1	3		19	1					3				63.33
lc	1								1		2	1	25									83.33
lf														26		3					1	86.67
ls	1														28	1						93.33
mq																29			1			96.67
mt										1	5		2				21	1				70.00
pe																		27	3			90.00
pp			4																26			86.67
sm	6	1			1				1											21		70.00
td																					30	100.00
																	Overall accuracy					**76.51**

Appendix 9.25. Confusion matrix of tree species recognition using spectral bands in winter "5 red edges" band set selected by hierarchical clustering procedures and classified by linear discriminant analysis

Predicted class

True class	ac	ah	am	bv	cc	ce	cf	ct	dl	fm	fv	ht	lc	lf	ls	mq	mt	pe	pp	sm	td	Accuracy (%)
ac	19	1			9		1															63.33
ah		24			1	4													1			80.00
am			13			1		2			3							11				43.33
bv	5		2	9	2		3	9														30.00
cc			1		12	3	7													7		40.00
ce		16	2			11													1			36.67
cf	5				1		18	1	2			3										60.00
ct				7				12		1	7	2					1					40.00
dl					5		7		18													60.00
fm		3								13	1						9		4			43.33
fv		1	1			4					16					2	2	4				53.33
ht	3		2				1	2				12	9				1					40.00
lc				1				3				4	22									73.33
lf														25		4					1	83.33
ls						1									24	5						80.00
mq						1					3					26						86.67
mt		2								10		3				3	11		1			36.67
pe		4	5			4					1							16				53.33
pp		4				5					3								18			60.00
sm	2				7				1											20		66.67
td																					30	100.00
																	Overall accuracy					**58.57**

Appendix 9.26. Confusion matrix of tree species recognition using spectral bands in winter "7 edges" band set selected by hierarchical clustering procedures and classified by linear discriminant analysis

Predicted class

True class	ac	ah	am	bv	cc	ce	cf	ct	dl	fm	fv	ht	lc	lf	ls	mq	mt	pe	pp	sm	td	Accuracy (%)
ac	17				9		3					1										56.67
ah		30																				100.00
am			26			3					1											86.67
bv			4	23				3														76.67
cc					14	3	8													5		46.67
ce						30																100.00
cf	4						24					2										80.00
ct				9				17		1		1					1		1			56.67
dl					5		2		23													76.67
fm										23								5	2			76.67
fv			4			3					17					2			4			56.67
ht	2		1				1				1	20	4					1				66.67
lc						1					1	4	24									80.00
lf														25	1	4						83.33
ls		2								1					27							90.00
mq						2					1					27						90.00
mt		1								6		1					21	1				70.00
pe		4																22	4			73.33
pp						5					1								24			80.00
sm	2				7				1											20		66.67
td																					30	100.00
																	Overall accuracy					**76.83**

Appendix 9.27. Confusion matrix of tree species recognition using spectral bands in winter "11 bands" band set selected by hierarchical clustering procedures and classified by linear discriminant analysis

Predicted class

True class	ac	ah	am	bv	cc	ce	cf	ct	dl	fm	fv	ht	lc	lf	ls	mq	mt	pe	pp	sm	td	Accuracy (%)
ac	17				12		1															56.67
ah		30																				100.00
am			30																			100.00
bv			3	24	2						1											80.00
cc	1				26		3															86.67
ce						30																100.00
cf					1		28					1										93.33
ct				1				26			2						1					86.67
dl					1		6		22			1										73.33
fm										27								3				90.00
fv						3					27											90.00
ht							1				2	23	3					1				76.67
lc	2											3	25									83.33
lf														27		3						90.00
ls		1													29							96.67
mq						1										29						96.67
mt										10		1					19					63.33
pe																		20	10			66.67
pp						2													28			93.33
sm					4				1											25		83.33
td																					30	100.00
																	Overall accuracy					**86.03**

Appendix 9.28. Confusion matrix of tree species recognition using spectral bands in winter "13 bands" band set selected by hierarchical clustering procedures and classified by linear discriminant analysis

Predicted class

True class	ac	ah	am	bv	cc	ce	cf	ct	dl	fm	fv	ht	lc	lf	ls	mq	mt	pe	pp	sm	td	Accuracy (%)
ac	20				8		2															66.67
ah		30																				100.00
am			30																			100.00
bv				28	1						1											93.33
cc					30																	100.00
ce						30																100.00
cf							30															100.00
ct								28		1							1					93.33
dl					2		3		23			1								1		76.67
fm										29								1				96.67
fv						2					28											93.33
ht							2				1	25	1					1				83.33
lc												6	24									80.00
lf														27		3						90.00
ls					1										29							96.67
mq						1										28			1			93.33
mt										9		1					20					66.67
pe		1																23	6			76.67
pp						4													26			86.67
sm					4				1											25		83.33
td																					30	100.00
																	Overall accuracy					**89.37**